Production of alternative fuels by thermochemical conversion of waste materials

Stančin, Hrvoje

FACULTY OF MECHANICAL ENGINEERING AND NAVAL ARCHITECTURE

HRVOJE STANČIN

PRODUCTION OF ALTERNATIVE FUELS BY THERMOCHEMICAL CONVERSION OF WASTE MATERIALS

DOCTORAL THESIS

Zagreb, 2023

FAKULTET STROJARSTVA I BRODOGRADNJE

HRVOJE STANČIN

PROIZVODNJA ALTERNATIVNIH GORIVA TERMOKEMIJSKIM POSTUPCIMA OBRADE OTPADNOGA MATERIJALA

DOKTORSKI RAD

Zagreb, 2023

FACULTY OF MECHANICAL ENGINEERING AND NAVAL ARCHITECTURE

HRVOJE STANČIN

PRODUCTION OF ALTERNATIVE FUELS BY THERMOCHEMICAL CONVERSION OF WASTE MATERIALS

DOCTORAL THESIS

SUPERVISOR:
Prof.dr.sc. NEVEN DUIĆ
Prof.dr.sc. VLADIMIR STREZOV

Zagreb, 2023

Sveučilište u Zagrebu

FAKULTET STROJARSTVA I BRODOGRADNJE

HRVOJE STANČIN

PROIZVODNJA ALTERNATIVNIH GORIVA TERMOKEMIJSKIM POSTUPCIMA OBRADE OTPADNOGA MATERIJALA

DOKTORSKI RAD

Mentor:

Prof.dr.sc. NEVEN DUIĆ

Prof.dr.sc. VLADIMIR STREZOV

Zagreb, 2023

BIBLIOGRAPHY DATA

UDC:

Keywords: *waste management, co-pyrolysis, alternative fuel, product characterisation, synergistic effect, environmental impact assessment*

Scientific area: TECHNICAL SCIENCES

Scientific field: Mechanical engineering

Institution: Faculty of Mechanical Engineering and Naval Architecture

Thesis supervisor: Prof. Neven Duić, PhD

Number of pages: 227

Number of figures: 24

Number of tables: 9

Number of references: 111

Date of examination: 17th July 2023

Thesis defence commission:

Dr. sc. Milan Vujanović, izv. prof.
Dr. sc. Luka Perković, izv. prof.
Assoc.prof. Yijiao Jiang, PhD

Archive: Faculty of Mechanical Engineering and Naval Architecture

TABLE OF CONTENTS

ACKNOWLEDGEMENT

I hereby declare that my Doctoral Thesis is entirely the result of my work and knowledge obtained during my studies, except where otherwise indicated. I have fully cited all used sources and only used the ones given in the list of references

To start, I would like to express my greatest gratitude to the supervisors of this research work, Professor Neven Duić and Professor Vladimir Strezov, for providing me with the opportunity to join their research group and carry out and complete my PhD studies. Their expertise and mentorship greatly helped me grow as a researcher. Even more, their experience and achievements motivated me to continue learning and pursue ambitious goals.

I am very grateful to Dr. Hrvoje Mikulčić, with whom I share a close and fruitful collaboration since Master's degree studies. He introduced me to research work and offered me the opportunity to initiate my PhD studies.

I am extremely grateful to Professor Helena Raclavská and Professor Nebojša Manić, for allowing me to carry out the experimental part of my work in their laboratories. In addition, I am thankful for all the valuable suggestions during the preparation of scientific publications.

I am deeply thankful to Dr. Michal Šafář, who was of great help with experimental work and result analysis. Furthermore, I am very thankful for all discussions and good times I had while staying in the Czech Republic.

I am grateful for the financial support from the International Cotutelle Macquarie University Research Excellence Scholarship (Cotutelle "iMQRES"), Higher Degree Research (HDR) funding from the Faculty of Science and Engineering at Macquarie University.

Many thanks go to the colleagues from PowerLab with whom I shared a lot of memorable moments during the last five years. It was a pleasure. Many thanks also go to the colleagues from MQ Uni for an amazing year and support when the deadline was approaching.

I express gratitude to my friends who followed me throughout this journey and provided me with great support but also unforgettable fun when it was tough.

Special thanks go to my parents, Snježana and Branko, who provided me with love and support and gave me the opportunity to achieve my dreams. Their sacrifices, belief and sometimes unimaginable patience have been of tremendous significance.

Finally, the most immense gratitude goes to my sister Erina, the corner stone throughout all my life. This one is for you, Sis, my source of love and encouragement!

"Yes, there were times, I'm sure you knew
When I bit off more than I could chew
But through it all, when there was doubt
I ate it up and spit it out
I faced it all and I stood tall and did it my way!"

Frank Sinatra, My Way

SUMMARY

Alternative fuels will play a crucial role in the complete decarbonisation of future energy systems based on renewable energy sources, where electricity is not a feasible solution. Therefore, the primary objective of this dissertation was to identify the most promising waste biomass and plastic feedstocks for the co-pyrolysis process with an aim to produce high-quality pyrolysis oil that could be further refined into alternative fuels compatible with existing standards for conventional fuels. This was done by examining the feedstock properties and running a series of experimental investigations. The results showed that sawdust, polystyrene and polypropylene are among the most promising feedstock to be utilised in co-pyrolysis. This evaluation is based on product quantity and quality from an individual and mixture analysis. In addition, the environmental impacts of the process are evaluated by carrying out a life cycle assessment. Finally, the discussion on methodology development for the prediction of product yield is given, which can serve as a base for future research. In summary, gathered observations from carried-out investigations can help better understand process dynamics, which is crucial for further commercialisation.

SAŽETAK

Alternativna goriva imat će ključnu ulogu u tranziciji budućih energetskih sustava baziranima na obnovljivim izvorima energije. Najviše se očekuje tamo gdje električna energija nije održivo rješenje. Stoga je primarni cilj ove disertacije bio identificirati otpadnu biomasu i plastiku sa najviše potencijala za proces ko-pirolize s ciljem proizvodnje visokokvalitetnog ulja koje se može rafinirati u alternativna goriva kompatibilna s postojećim standardima za konvencionalna goriva. To je učinjeno ispitivanjem inicijalnih svojstava sirovine i provođenjem niza eksperimentalnih istraživanja. Rezultati su pokazali da su piljevina, polistiren i polipropilen među sirovinama sa najviše potencijala za korištenje u ko-pirolizi. Ova procjena temelji se na količini i kvaliteti proizvoda dobivenih za individualne uzorke te odabranu mješavinu. Dodatno je provedena analiza utjecaja na okoliš evaluacijom štetnih emisija iz raznih faza procesa. Konačno je prezentirana i metodologija za razvoj modela predviđanja prinosa proizvoda koji može poslužiti kao osnova za buduća istraživanja tog problema. Ukratko, prikupljena zapažanja iz provedenih istraživanja mogu pomoći u boljem razumijevanju dinamike procesa, što je ključno za daljnju industrijalizaciju.

PROŠIRENI SAŽETAK

Energetska tranzicija predstavlja jedan od najvećih izazova danas, s obzirom da fosilna goriva i dalje predstavljaju glavni izvor energije u svim sektorima. Trenutna potrošnja iznosi 53% u proizvodnji električne energije, 66% u industriji te čak 98% u sektoru transporta [1]. Elektrifikacija je primarni cilj za većinu procesa ukoliko se električna energija proizvodi iz obnovljivih izvora energije (OIE). Unatoč tome, električna energija nije održiva opcija za svu vrstu industrijskih procesa ili sva transportna rješenja. Različite vrste alternativnih goriva, tehnologija i procesa, priviknula su istraživački interes posljednjih godina, ali bez uspješne primjene na široj komercijalnoj razini [2]. Jedna od metoda koja pokazuje veliki potencijal za proizvodnju alternativnih goriva je termokemijska pretvorba različite vrste sirovina i otpadnih materijala u vrijedne kemijske spojeve koji se mogu dalje rafinirati u određenu vrstu goriva, ovisno o namjeni. Piroliza i rasplinjavanje su glavni procesi pretvorbe u kojima se dobivaju tekući, plinoviti i pougljenjeni kruti produkti s ciljem daljnjeg korištenja za proizvodnju energije.

S obzirom da se biomasa u raznim formama kontinuirano kroz stoljeća koristi kao izvor energije, njezina svojstva su nadaleko istraživana [3]. Unatoč tomu, današnja biogoriva, imaju znatno lošija svojstva u usporedbi s konvencionalnim fosilnim gorivima. Navedeno implicira da je njihov dekarbonizacijski potencijal ograničen te su potrebne daljnje metode koje mogu unaprijediti njihova svojstva. Jedna od najvećih prednosti već spomenutog termokemijskog postupka proizlazi iz mogućnosti obrade različitih sirovina, uključujući i otpadne materijale [4]. Mogućnost oporabe otpadnih materijala sugerira da se navedeni postupci mogu koristiti ne samo za proizvodnju alternativnog goriva, već i kao metode za gospodarenje otpadom. Navedeno je posebice važno za materijale koji su dostigli svoj reciklabilni potencijal te se nalaze na kraju životnog vijeka [5]. S obzirom na kontinuirani porast proizvodnje otpada i napuštanje prakse odlaganja na otvorene deponije [6], održiva rješenja koja direktno smanjuju masu i volumen imaju značajnu prednost za buduće korištenje na komercijalnoj razini. Iz navedenog može se zaključiti da korištenje otpadnih materijala za proizvodnju alternativnih goriva termokemijskom postupcima može istodobno riješiti probleme gospodarenja otpadom, poboljšati oporabu energije te zamijeniti potrošnju fosilnih goriva.

Biomasa je jedna od rijetkih sirovina koja se istovremeno koristi kao ugljično-neutralno, održivo gorivo te kao sirovina za proizvodnju goriva [7]. Njezina uporaba u procesu izgaranja nadaleko je poznata te se primjenjuje stoljećima. S obzirom na potrebu za daljnjim unapređenjem svojstva biogoriva, istraživački fokus se premjestio prema metodama već

spomenute termokemijske pretvorbe [8]. Unatoč svim istraživačkim naporima, dobivena eksploatacijska svojstva biogoriva ograničena su prirodnom sirovine. Jedan od glavnih problema predstavlja visoki sadržaja kisika, što rezultira nižom ogrjevnom vrijednošću, ali i većom kiselošću te toplinskom nestabilnošću [9]. Kako bi se prevladali ti problemi, istražuje se mogućnost korištenja katalizatora ili zajedničko procesuiranje sa sirovinom bogatom vodikom u formi heterogene mješavine [10]. Upravo je otpadna plastika potencijalna sirovina za zajedničko procesuiranje u formi mješavine s obzirom na udio vodika u strukturi te istovremene probleme sa gospodarenjem otpadom [11].

Gospodarenje otpadom za plastične materijale koji su došli do kraja životnog vijeka i dalje se uglavnom temelji na odlagalištima otpada (49%), dok su mehaničko recikliranje (9%) i energetska oporaba (19%) na prilično niskim razinama. Uz to, gotovo 23% plastičnog otpada nije zbrinuto na prikladan način što rezultira direktnim onečišćenjem tla i voda. Nadalje, pod pojmom plastike podrazumijeva se cijeli spektar polimernih materijala proizvedenih za različite namjene. Više od 460 Mt svježe sirovine koristi se na godišnjoj razini za proizvodnju novih plastičnih proizvoda, što rezultira stvaranjem više od 353 Mt otpada [12]. S obzirom na različite namjene, razlikuju se i procesi proizvodnje te praksa gospodarenja otpadom. U hijerarhiji gospodarenja otpadom koja se temelji na strategiji 4-R (*eng. reduce, reuse, recycle, recovery*), recikliranje prethodi energetskoj oporabi [13]. Stoga se polimerni materijali poput polietilen teraftalata (PET) ili polietilena visoke gustoće (HDPE), koji pokazuju dobar potencijal za mehaničkog recikliranja, ne bi trebali razmatrati za energetsku oporabu sve dok ne dođu do kraja životnog vijeka [14]. S druge strane, polimeri koji se koriste za pakiranje poput polietilena niske gustoće (LDPE), polipropilena (PP) ili polistirena (PS) vrlo su zastupljeni u otpadu, a pritom imaju vrlo nizak potencijal za recikliranje. Nadalje, njihova proizvodnja iz svježe sirovine značajno je jeftinija te s boljim svojstvima od proizvodnje iz reciklata dobivenog mehaničkim ili kemijskim postupcima recikliranjem. Sukladno tomu takvi otpadni materijali predstavljaju idealnu sirovinu za zajedničko procesuiranje sa biomasom [15]. Važno je spomenuti kako gospodarenje otpadom polimera tretiranih raznim aditivima, poput polivinil klorida (PVC) [16], poliuretana (PU) [17] ili miješane plastike (MPW) [18], zahtijevaju posebnu pozornost budući da mogu proizvesti vrlo štetne i otrovne spojeve tokom toplinske dekompozicije, što zahtjeva naknadu obradu dobivenih produkata. Iz navedenog, takvi se materijali čine prikladnijim za kemijsku oporabu ili izravno izgaranje na visokim temperaturama.

Ko-piroliza je u posljednje vrijeme privukla značajnu istraživačku pozornost s obzirom da omogućuje istodobnu proizvodnju visokokvalitetnih alternativnih goriva rješavajući rastući

problem gospodarenja otpadom [19]. Dobiveni proizvodi poput pirolitičkog ulja, sintetskih plinova te pougljenjenog krutog ostatka mogu se dalje koristiti prema potrebi ovisno o dobivenim svojstava te kemijskom sastavu. Najvrjedniji proizvod iz spomenutog procesa je tekuća frakcija dobivena u formi pirolitičkog ulja. Komparativne prednosti pirolitičkih ulja u usporedbi s plinovima ili ugljenom odnose se na zahtjeve za skladištenja i distribuciju, mogućnost primjene te konačnu tržišnu vrijednost [20]. Unatoč tome, kemijskih sastav takvih ulja je izuzetno kompleksan te može sadržavati više stotina različitih spojeva što izravnu upotrebu čini gotovo nemogućom. Unatoč tome, pažljivim odabirom procesnih parametara, sirovine te metoda pred obrade može se značajno poboljšati homogenost proizvedenog ulja te na taj način smanjiti potreba za naknadnim pročišćavanjem [21]. Štoviše, poznavanjem početnog sastava i svojstava sirovine odziv produkata iz procesa može se predvidjeti do određene razine što je izuzetno važno za daljnju industrijalizaciju. Iz navedenog, može se zaključiti da su određene metode pred obrade neizbježne s obzirom da mogu značajno smanjiti potrebu za skupljim metodama naknadnog pročišćavanja.

Za potrebe pirolize i ko-pirolize do sad su istraživane različite vrste sirovina sa različitim istraživačkim ciljevima i fokusom. To ujedno predstavlja i jedan od glavnih problema u procesu industrijalizacije zbog nedostatka dosljednosti u eksperimentalnoj analizi i interpretaciji dobivenih rezultata. Stoga bi sljedeći korak u razvoju procesa trebao biti sužavanje fokusa istraživanja na najpotencijalniju sirovinu koja može značajno povećati prinos te unaprijediti svojstva dobivenog ulja. Nadalje, istraživački napori trebaju biti usmjereni u pronalazak optimalnog sastava mješavine koja može proizvesti visoki udio ugljikovodika te pritom eliminirati većinu neželjenih spojeva sa kisikom u svojem sastavu. Na taj način dobiveno ulje postaje kompatibilno sa konvencionalnim gorivima, što rezultirala manjim troškovima naknadne obrade i rafiniranja. Navedeno se može ostvariti provođenjem niza eksperimentalnih istraživanja na različitim vrstama sirovina. Nadalje, promatranje sinergijskog učinka koji se javlja tijekom interakcije različitih sirovina, važno je za predviđanje prinosa proizvoda iz procesa. Ipak razvijanje modela predviđanja za distribuciju proizvoda na temelju početnih parametara i karakteristika sirovine predstavlja značajan izazov koji zahtjeva dodatne istraživačke napore. Konačno, potrebno je provesti analizu utjecaja na okoliš za navedeni proces kako bi se utvrdila njegova podudarnost sa zahtjevima i ciljevima određenima energetskom tranzicijom. Rezultati takve analize mogu procijeniti prednosti u usporedbi s drugim metodama obrade otpada. Osim toga, takva analiza može identificirati negativne utjecaje procesa, koji bi se mogli zamijeniti održivijim rješenjima, poboljšavajući izglede primijene na široj razini.

CILJEVI I HIPOTEZA ISTRAŽIVANJA

Ciljevi ovog istraživačkog rada su sljedeći:

1. Kvantificirati prinose te distribuciju proizvoda ko-pirolize otpadne biomase i plastičnih materijala ispitivanjem početnih parametara kao što su konačna i neposredna analiza, te istraživanjem sinergijskog efekta koji se javlja tijekom interakcije sirovina, s ciljem smanjenja potreba za provođenjem kontinuiranih eksperimentalnih istraživanja.
2. Procijeniti prihvatljivi udio plastike u smjesi goriva istražujući kemijski sastav, te kinetičke i termodinamičke parametre postupka ko-pirolize koristeći bez-modelske metode kako bi se stekao bolji uvid u interakciju sirovine i utjecaj na kvalitetu bio-ulja.

Hipoteza istraživanja je da se provođenjem niza eksperimentalnih istraživanja može odrediti zadovoljavajući udio biomase i plastike u mješavini za proizvodnju visokokvalitetnih bio-ulja, promatrajući početne parametre materijala, kemijski sastav ulja te kinetiku procesa, s ciljem skaliranja procesa pirolize na industrijsku razinu.

OČEKIVANI REZULTATI I DOPRINOS ISTRAŽIVANJA

1. Model za poboljšano predviđanje prinosa i distribucije proizvoda iz ko-pirolize biomase i otpadne plastike povezivanjem početnih parametara korištenih uzorka i kinetike procesa kako bi se izbjegla potreba za kontinuiranim eksperimentalnim istraživanjima.
2. Određeni prihvatljivi omjeri miješanja biomase i otpadne plastike za proizvodnju visokokvalitetnih bio-ulja, analizom kemijskog sastava te ispitivanjem kinetičkih i termodinamičkih parametara procesa koji će smanjiti potrebu za skupim metodama naknadnog pročišćavanja.
3. Kvantificiranje ugljičnog otiska te potencijal integracije postupka pirolize s obnovljivim izvorima energije, kako bi se dobio bolji uvid u perspektivu procesa na industrijskoj razini.

METODE I POSTUPCI

Kao prvi korak u istraživanju, napravljen je detaljan pregled literature za sva razmatrana alternativna goriva u budućim energetskim sustavima. Analiza je pokazala da istraživački interes za područje značajno raste, a posebice se to odnosi na kemijske spojeve kao što su vodik, amonijak ili alkoholna goriva poput metanola ili etanola. Unatoč tome, navedena alternativna rješenja zahtijevaju razvoj novih sustava za skladištenje, distribuciju i korištenje

što ograničava njihovu upotrebu na komercijalnom nivou. S druge strane, tekuća goriva poput biodizela mogu se lako skladištiti, distribuirati i koristiti u postojećim motorima s unutrašnjim izgaranjem bez značajnih izmjena samog sustava. Međutim, eksploatacijska svojstva biogoriva značajno su slabija od fosilnih zbog visokog udjela kisika u strukturi što rezultira slabijom ogrjevnom vrijednosti te toplinskom nestabilnosti. Istodobno, problem gospodarenja otpadom uglavnom se rješava nisko efikasnim spaljivanjem sa ciljem proizvodnje toplinske i električne energije. Pregledom literature odabrane su termokemijske metode pretvorbe otpadnih materijala, poput pirolize i rasplinjavanja, kao istraživačke metode za proizvodnju visokokvalitetnih alternativnih goriva.

Glavni fokus istraživačkog rada bila su eksperimentalna istraživanja provedena na uzorcima otpadne biomase (piljevine), polistirena, polipropilena te poliuretana. Proces pirolize proveden je na 600 ºC te su ispitani prinosi produkata za individualne uzorke te njihove smjese. U prvom dijelu provedena je ko-piroliza piljevine sastavljene od hrasta, jele i topole s otpadnim PS-om. Udio plastike u smjesi varirao je između 25 i 75%. Analiza je pokazala da se uvođenjem plastike mogu značajno poboljšati svojstva pirolitičkog ulja u usporedbi sa produktima individualnih uzoraka. Dodavanjem 25% PS u smjesu bilo je dovoljno za udvostručenje prinosa tekućine s 31 na 62%. Istovremen je ostvareno smanjenje udjela kisika u konačnim produktima te je ostvaren rast u prinosu aromatskih ugljikovodika. Za smjesu sa 75% PS ostvaren je prinos ulja od gotovo 84%. Međutim, analiza kemijskih spojeva u dobivenom ulju pokazuje da kvaliteta nije nužno poboljšana. Razlog tomu leži u činjenici da se PS razgrađuje na aromatske i policikličke aromatske ugljikovodike (PAH). Iako su aromatski spojevi dobrodošli u sastavu goriva, njihov udio ograničen je ispod 40% zbog problema prilikom izgaranja što rezultira gustim dimom te čađom. Glavni zaključak provedene analiza je da se 25% PS u smjesi s biomasom može smatrati prihvatljivim udjelom.

Ko-pirolize poliuretanske pjene razmatrana je zbog značajnih ograničenja njenog postupka recikliranja. Provedena analiza pokazala je da poliuretanska pjena ima vrlo ograničen potencijal za proces ko-pirolize, osobito ako je namjera proizvodnja goriva. Navedeno proizlazi iz činjenice da većina identificiranih kemijskih spojeva u dobivenom ulju sadrži dušik, te pripada grupi benzenamina, koji ne zadovoljavaju kriterije goriva. Također, PU može samo donekle povećati prinos ulja s obzirom da je razlika za ispitivanje smjese bila manja od 4%. Međutim, analiza plinske frakcije pokazala je značajan udio vodika, što označava rasplinjavanje kao prikladniju opciju za zbrinjavanje ovakve vrste otpada.

Kako bi se prikupile dodatne informacije o samom procesu razgradnje odabranih uzoraka, provedene su termogravimetrijska i kinetička analiza. Cilj ovih metoda bio je istražiti

mehanizme razgradnje te pružiti bolji uvid u dinamiku i međusobnu interakciju materijala tijekom procesa. Promatrani parametri bili su utjecaj brzine zagrijavanja te sastava mješavine na ispitivane termogravimetrijske i kinetičke parametre. Analiza je pokazala da brzina zagrijavanja ima mali utjecaj na konačni udio krutog ostatka iz procesa (~3%). Također, povećanjem brzine zagrijavanja pomiče se temperaturni raspon u kojem se odvija razgradnja neznatno prema višim vrijednostima. Istodobno, sastav mješavine igra presudnu ulogu u samoj kinetici procesa. Kao što se i očekivalo, povećanje udjela PS i PP smanjuje konačnu masu uzorka zbog veće hlapljivosti plastičnih materijala, što omogućuje bolju pretvorbu u tekuće i plinovite produkte. Utjecaj sastava mješavine još je vidljiviji iz analize aktivacijskih energija. U slučaju biomase, aktivacijska energija (E_a) kontinuirano raste tokom procesa, dok se kod uzoraka plastike primjećuje obrnuti trend. U slučaju mješavina, kada udio plastike ne prelazi 50%, E_a može biti čak i niža u usporedbi s pojedinačnim uzorcima između faze isparavanja i promjene mehanizma razgradnje. To bi moglo značiti da interakcija sirovine u prvoj fazi pospješuje ili sprječava razgradnju. Ogromno povećanje E_a koji uslijedi kada se mehanizam razgradnje promijeni s biomase na plastičnu komponentu sugerira da je razgradnja bila spriječena u prvoj fazi. To ujedno znači i da je vrijeme koje oslobođeni hlapljivi spojevi provedu u reaktoru kraće što sugerira mogući pozitivni utjecaj na visoki prirast pirolitičkog ulja.

Na temelju zapažanja prikupljenih u ranijim fazama istraživačkog rada odabrana je mješavina sa 50% piljevine, 25% polistirena i 25% polipropilena. Ovi udjeli su pažljivo odabrani kako bi se povećao prinos pirolitičkog ulja te povećao sadržaj ugljikovodika. Kao glavno zapažanje vrijedi navesti da se sastav smjese pokazao povoljnim za visok prinos ulja s obzirom na udio od 80%, uz 8% plinova i 12% krutog ostatka.. U usporedbi sa kemijskim sastavom ulja iz biomase, vrijedi izdvojiti značajno smanjenje spojeva s kisikom, posebice fenola. U usporedbi s uljem dobivenim iz PS-a, značajno je smanjen udio aromatskih ugljikovodika i PAH-ova. Konačno, u usporedbi s uljem dobivenim iz PP-a, može se uočiti značajno smanjenje alkohola uz održavanje visokog udjela cikličkih i alifatskih ugljikovodika. Ukupni udio ugljikovodika iznosi gotovo 70%, od čega 35% čine alifatski spojevi, dok 32% otpada na aromatske ugljikovodike. Udio aromata, točnije stirena, u granicama je dopuštenog za konvencionalna goriva, uz visoki udio ostalih ugljikovodika. S toga se može zaključiti da je odabrani sastav smjese izuzetno povoljan za proizvodnju alternativnih tekućih goriva.

Konačno za predloženi proces provedena je analiza utjecaja na okoliš. Rezultati su pokazali da ko-piroliza može znatno nadmašiti spaljivanje u smislu smanjenja potencijala globalnog zatopljenja (GWP) te ekotoksičnosti. U usporedbi s odlaganjem otpada, piroliza je

također povoljna za smanjenje ekotoksičnosti te eutrofikacijskog potencijala. Većina emisija povezanih s GWP-om dolazi od potrošnje električne energije za potrebe zagrijavanje pirolitičkog reaktora te za potrebne procese sortiranja i pripreme sirovine, što čini 77% ukupnih CO_2 eq. emisije. Nadalje, analiza osjetljivosti pokazala je da bi se integracijom ko-pirolize s obnovljivim izvorima energije, kao što je fotonapon, moglo dodatno ostavriti smanjenje emisija u gotovo svim kategorijama, a posebice u vezi potencijala globalnog zagrijavanja. Također, analiza osjetljivosti je pokazala da bi prinos proizvoda mogao značajno utjecati na rezultate promatranih kategorija u slučaju smanjenog prinosa pirolitičkog ulja ili nedovoljne kvalitete proizvoda. Stoga se zaključuje da su metode prethodne obrade kao što su sušenje i odvajanje plastike neizbježne. Navedeno proizlazi iz činjenice da se poznavanjem udjela smjese može barem donekle predvidjeti prinos određenih produkata procesa, što direktno utječe na njegovu ekološku, ali i ekonomsku održivost.

KEYWORDS

Waste management

Co-pyrolysis

Product characterisation

Synergistic effect

Alternative fuel

Environmental impact assessment

KLJUČNE RIJEČI

Gospodarenje otpadom

Ko-piroliza

Karakterizacija produkata

Sinergijski efekt

Alternativna goriva

Analiza utjecaja na okoliš

LIST OF ABBREVIATIONS

AD	Anaerobic digestion
AP	Acidification potential
CCU	Carbon capture and utilisation
CHP	Combined heat and power
CLC	Chemical loop combustion
CSP	Concentrating solar power
DAC	Direct air capture
DME	Dimethyl ether
DTG	Derivative thermogravimetric curve
EU	European Union
EV	Electric vehicle
FC	Fuel cell
FET	Freshwater ecotoxicity
FRS	Fossil resource scarcity
FTIR	Fourier transform infrared spectroscopy
FU	Functional unit
GC	Gas chromatography
GC/MS	Gas chromatography/mass spectrometry
GHG	Greenhouse gases
GWP	Global warming potential
HDPE	High-density polyethylene
HTC	Human carcinogenic toxicity
HTNC	Human non-carcinogenic toxicity
ICE	Internal combustion engine
IRENA	International Renewable Energy Agency
KAS	Kissinger-Akahira-Sonuse
LCA	Life cycle assessment
LDPE	Low-density polyethylene
MDA	4,4'-Methylenedianiline
MET	Marine ecotoxicity
MPW	Mixed plastic waste
MSW	Municipal solid waste

OFW	Ozawa-Flynn-Wall
PAH	Polycyclic aromatic hydrocarbons
PE	Polyethylene
PEM	Polymer electrolyte membrane
PEMFC	Proton exchange membrane fuel cell
PET	Polyethylene terephthalate
PP	Polypropylene
PS	Polystyrene
PU	Polyurethane
PUF	Polyurethane foam
PUR	Rigid polyurethane foam
PV	Photovoltaic
PVC	Polyvinyl chloride
RDF	Refuse derived fuel
RE	Renewable energy
RES	Renewable energy sources
SD	Sawdust
SOE	Solid oxide electrolysers
SOFC	Solid oxide fuel cell
SRF	Solid recovered fuel
SS	Sewage sludge
STA	Simultaneous thermal analysis
TET	Terrestrial ecotoxicity
TFEC	Total final energy consumption
TG	Thermogravimetric
TGA	Thermogravimetric analysis
TPES	Total primary energy supply
V2G	Vehicle-2-grid
VM	Volatile matter
VRES	Variable renewable energy sources

NOMENCLATURE

Latin	Description	Unit
A	Pre-exponential factor	s^{-1}
h	Planck constant	J
ΔH	Changes in enthalpy	kJ $kmol^{-1}$
ΔS	Changes in entropy	kJ $kmol^{-1}$
ΔG	Changes in Gibbs energy	kJ $kmol^{-1}$
R	Ideal gas constant	J mol^{-1} K^{-1}
Ea	Activation energy	J mol^{-1}
T	Temperature	ºC
K_B	Boltzmann constant	J K^{-1}
$Y_{cal/the.}$	Experimental or calculated product yield	
$W_{cal/the.}$	Share of feedstock in mixture	
ΔY	Synergy level	

Greek	**Description**	**Unit**
α	Degree of conversion	
β	Heating rate	K min^{-1}

LIST OF FIGURES

LIST OF TABLES

1. INTRODUCTION

The Introduction section starts with a motivation and background analysis of the research topic. Firstly, an extensive literature review is carried out, and the results are published as a scientific paper (PAPER 1). Furthermore, this section is extended with the most recent findings and progress in the field. The research objectives and hypothesis are defined based on the literature review and identified knowledge gap. In addition, scientific contributions that the research aimed to cover are also given.

1.1. Motivation and background analysis

The energy transition represents one of the main challenges today, with fossil fuels still being a major energy source used in all sectors, accounting for 53% in power generation, 66% in industry, and up to 98% in transport [1]. Electrification is the primary goal for most processes if electricity is produced from renewable energy sources (RES). Nevertheless, the remaining gap where electricity is not an option seeks novel and sustainable solutions. Various alternative fuels, novel technologies, and processes have been investigated so far, but without successful deployment on a broader commercial scale [2]. Figure 1 illustrates the potential outlook of future energy systems based on renewables coupled with alternative fuels.

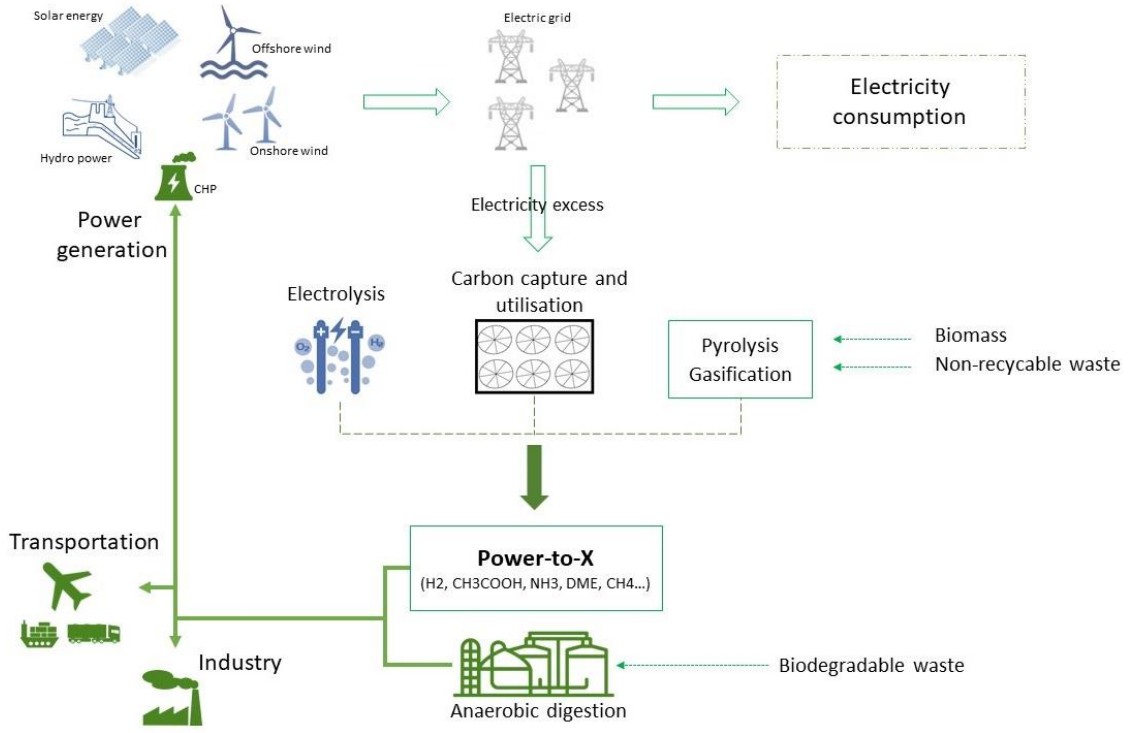

Figure 1 – Potential outlook of future energy systems [2]

As can be seen, the clean production of electricity from RES presents the backbone of the future energy system. Once produced, electricity is directly consumed where needed or can be used to synthesise alternative fuels. Alternative fuels may vary by origin and production process. Still, the common for all of them is that they are produced through a sustainable and clean procedure without the additional emissions of Carbon dioxide (CO_2) [22]. The primary production pathway consists of electricity surplus utilisation to synthesise electrofuels like hydrogen (H_2), ammonia (NH_3), methane (CH_4), etc. This term has lately been introduced to emphasise electricity usage in production and distinguish it from alternative fuels produced through another synthesis route [23]. Alternative fuels can be made in a liquid, gaseous or solid state depending on the production pathway and utilisation goals. Liquid and some gaseous fuels are the most promising solution for the transport sector [24], while solid fuels are likely to be used for stationary needs in power plants [25].

Another promising method to produce alternative fuels is the thermochemical conversion of raw and waste feedstock into valuable chemical compounds that can be further used or refined into fuels. Pyrolysis and gasification are the leading conversion processes where liquid, gaseous and charred products are obtained with an aim for further utilisation for heat and power production. Biomass is one of the most investigated feedstocks for conversion processes since some biofuels are already used commercially [3]. Nevertheless, biofuels nowadays have inferior exploitation properties compared to conventional fossil fuels, implying that their decarbonisation effect is limited and seeks further upgrading methods. In addition, one of the most significant advantages of pyrolysis and gasification is the ability to process various feedstock, including waste materials of different origins [4]. This implies that they could be successfully used not only for alternative fuel production but also as a waste management method to deal with non-recyclable, end-of-life waste [5]. This is especially important due to the ongoing increment of waste generation and the abandoning the practice of landfilling and open dumping [6]. Therefore, using waste materials to produce alternative fuels can simultaneously solve waste management issues, enhance energy recovery, and substitute fossil fuel consumption. A detailed review of all promising alternative fuels considered for future energy systems is given in work by Stančin et al. [2]. Table 1 presents the selected review publications of the most promising alternative fuels considered nowadays, which served as a base for research topic background analysis.

Table 1 - Selected review publications for the most promising alternative fuels [2]

Type of review	Authors	Content
Electrofuels	McDonagh et al. [26] Lehtveer et al. [27]	• Production of electrofuels using curtailed energy from VRES • Higher penetration of VRES might not be sufficient to achieve cost-competitiveness
Hydrogen	Abdalla et al. [28] Parra et al. [29]	• Production, transportation, storage and application challenges • Role of hydrogen for deep system decarbonization
Ammonia	Giddey et al. [30] Valera-Medina et al. [31]	• Sustainable synthesis and transport application • Highlights of previous research regarding utilization of Ammonia as a viable energy vector for power applications
Biodiesel/Biomass	Shukla and Kumar [32] Bajwa et al. [33] Perkins et al. [34] Widjaya et al. [35] Sher et al. [36]	• Review on alternative biofuels • Review on solid densified biomass products • Fast pyrolysis for the production of liquid biofuels • Biomass gasification • Thermal and kinetic analysis of six different biomass fuels for power generation
Alcohol derived fuels	Verhelst et al. [37] Svanberg et al. [38] Çelebi and Ayday [39] Awad et al. [40]	• Methanol as an IC engine fuel • Methanol for shipping • Review on light alcohol fuels • Alcohol and ether alternative fuels
Non-recyclable waste	Makarichi et al. [41] Al-Salem et al. [42] Hassan et al. [43]	• Review on waste incineration • Pyrolysis of waste plastics • Co-pyrolysis of biomass and plastics

Biomass is one of the rare feedstocks simultaneously being used as a carbon-neutral, sustainable fuel and a feedstock for fuel production [7]. Its utilisation in the combustion process is well known and used throughout centuries, while recently, the focus has shifted toward thermochemical conversion methods since they can significantly enhance derived biofuel properties [8]. Nevertheless, exploitation properties of such fuels are limited due to the nature of the feedstock and high oxygen content, which results in lower heating value, higher acidity, and thermal instability [9]. Catalysts or co-processing with hydrogen-rich feedstock have been introduced to overcome these problems as a potential solution to enhance derived product

quality and quantity. Waste plastics are potential hydrogen-rich feedstock that can greatly enhance biofuel properties [11].

Waste management of plastics that have reached their end-of-life stage is still primarily based on landfilling (49%), while mechanical recycling (9%) and energy recovery (19%) are at low rates. In addition, almost 23% of plastic waste is mismanaged, resulting in significant leakages and overall land and water pollution. Furthermore, the term plastics encompasses the family of polymer materials produced for various purposes nowadays, accounting for more than 460 Mt of virgin-grade products and generating more than 353 Mt of waste annually [12]. Since the application differs, the production process and waste management practice also differ. In the waste management hierarchy based on 4R (reduce, reuse, recycle, recover), recycling is preferred over energy recovery [13]. Therefore, polymers like polyethylene terephthalate (PET) or high-density polyethylene (HDPE), which exhibit good mechanical recycling potential, should be only considered for energy recovery once they reach the end-of-life stage [14]. On the other hand, packaging plastics like low-density polyethylene (LDPE), polypropylene (PP) or polystyrene (PS) are very abundant in waste streams while having meagre recycling potential. Furthermore, their production from virgin-grade feedstock is cheaper with better properties than production from recyclates obtained through mechanical or chemical recycling. Therefore, such waste materials represent the ideal biomass co-processing feedstock [15]. Finally, waste management of polymers treated with various additives in production stages, like polyvinyl chloride (PVC) [16], polyurethanes (PU) [17] or mixed plastics waste (MPW) [18], requires special attention since they can yield some very harmful and toxic compounds. Due to the high requirements for after-processing methods, they seem more suitable for chemical recovery or direct combustion at high temperatures than for thermo-chemical conversion.

Co-pyrolysis recently gained significant research attention since it allows the simultaneous production of high-quality alternative fuels while dealing with the rising waste management problem [19]. Pyrolytic products like oils, gases, and char can be further utilised based on derived properties and chemical composition. The most valuable product from such process is the liquid fraction obtained as pyrolytic oil. The comparative advantages of pyrolytic oils compared to gases or char are related to storage and distribution logistics, number of applications and market value [20]. Nevertheless, the chemistry of pyrolysis oils is exceptionally complicated since they could be composed of hundredths of species, making direct utilisation almost impossible. Regardless, chemical analysis of pyrolysis oil from experimental investigations shows that derived properties are of higher quality from co-

pyrolysis compared to individual pyrolysis of examined feedstock [44]. Zhang et al. [45] co-pyrolysed pine sawdust and plastics (PE, PP, and PS) at 600 ºC to maximise the yield of aromatics and olefins. The best result is achieved in the case of a PE/sawdust mixture with a ratio of 4:1. In this case yield of aromatics and olefins could be enhanced by 36% and 35%, respectively. Lu et al. [46] confirmed that feedstock interaction during co-pyrolysis can greatly reduce the oxygen content in pyrolysis oil, increasing heating value and thermal stability. Hassan et al. [47] co-pyrolysed torrefied biomass with PS, showing that the aromatic content of derived pyrolysis oil is greatly increased by introducing PS at the expense of oxygenated compounds. Moreover, the study gives a potential mechanism for the formation of major aromatic hydrocarbons. Özsin and Pütün [48] investigated the co-pyrolysis of biomass with different plastics, focusing on synergistic effect and product yield. The study concludes that the major driver for the synergistic effect is the biomass-plastic ratio in the fuel blend, while the influence of other parameters is less pronounced. Ephraim et al. [49] analysed the synergistic effect and product yield from pine wood co-pyrolysis with PS and PVC. The difference in experimental and theoretical yield is observed for all investigated mixtures, but with the opposite trends. This implies that product yield depends on the feedstock type, and some materials, like PVC, are not favourable for high liquid yield. Kai et al. [50] co-pyrolysed corn stalk and HDPE observed the strongest synergistic effect for small plastic content (<20%). Liu et al. [51] performed catalytic pyrolysis over the pine sawdust, finding that the addition of a catalyst has a limited impact on product distribution. At the same time, it might promote secondary reactions at higher temperatures to increase the gas yield. This is only a minor number of conducted studies in the field. Some additional interesting studies also used during this research work can be found here [9], [52], [53].

Thermal degradation and kinetic analysis of individual biomass and plastic samples are widely investigated in the literature, while extensive research on co-pyrolysis kinetics has recently emerged. Biomass was in research focus for a long time since it was already used commercially. Due to the complex structure and the presence of various extractives and minerals, it is especially interesting to investigate the decomposition kinetics of waste biomass like sawdust. Alam et al. [54] co-pyrolyzed the bamboo sawdust with LDPE observing that the increment of heating rates shifts the position of the peak temperatures and broadens the range of degradation mechanism. Luo et al. [55] investigated the decomposition mechanism of beech sawdust to determine conversion ranges and activation energies. Analysing the changes in activation energies, three stages of the degradation mechanism have been identified following the change in conversion rate. Zhang et al. [56] used wood sawdust, confirming the three stages

of decomposition, with the active pyrolysis stage as the most intensified. The main biomass structure components, cellulose and hemicellulose, are decomposed in this area. Han et al. [57] analysed the kinetic behaviour of pine sawdust mixtures with PP, LDPE, HDPE, and PVC. The most important observation is that plastics soften at a lower temperature but without decomposition. Softening hinders heat and mass transfer, preventing the complete release of volatiles and resulting in lower conversion rates for biomass fraction in the mixture. Suriapparao et al. [58] used microwave-assisted co-pyrolysis of PP and PS with various biomass to investigate the plastic influence on bio-oil quality. An increment of bio-oil is noticed, but without explaining the volatiles interaction and influence on final product distribution. Burra and Gupta [59] investigated the kinetics of pinewood with plastic wastes. The most interesting observation is that even built of monomer units, PP requires two pseudo components for the modelling process. Furthermore, the highest synergistic effect was observed for a mixture with a low share of PP. Stančin et al. [60] investigated the kinetics and thermodynamics parameters from the sawdust and polyurethane mixtures co-pyrolysis at different heating rates. The results show that Friedman's method gives the most accurate data regarding the activation energy (Ea). In addition, interesting results are observed regarding polyurethane decomposition, which exhibits quite similar behaviour to biomass samples rather than plastics. This results in overlapping the decomposition areas, suggesting significant potential for volatile interaction.

Environmental impact assessment is an essential tool in determining the associated emissions of the proposed process. Even though biomass-related emissions can be considered neutral in the utilisation stage, increased deforestation and land use can negatively impact the environment. Moreover, biofuel production has environmental impacts, especially in the pre-treatment and drying stages, which should be addressed [61]. On the other hand, waste management of end-of-life plastics causes tremendous environmental burdens and threatens human health. Current treatment methods rely either on incineration (42%) or landfilling (23%), while mechanical recycling accounts just for 34% [62]. Since alternative fuel production from co-pyrolysis requires significant energy and material input, greenhouse gases and pollutant emissions are inevitable. Therefore, it is necessary to quantify these impacts from the process, and life cycle assessment (LCA) is the most comprehensive tool to achieve that. Up to now, LCA has been carried out for different types of biomass and plastic thermochemical conversion methods. Nevertheless, comparing the results is often very difficult since different system boundaries, functional units, or impact assessment methods are applied. Global warming potential (GWP) expressed in kg CO_2 eq. is the only impact category common for all

studies, which can be used to compare the results to some extent. This is because emissions used to calculate GWP are similar to all assessment methods and consist of CO_2, CH_4, nitrous oxide (N_2O), and various hydrochlorofluorocarbons (HCFC) [63]. Gahane et al. [64] carried out a review of LCA for biomass pyrolysis. In the scope of the study, different types of biomass feedstock, energy sources, pre-treatment and utilisation methods are considered. The study concluded that biofuel production and utilisation emissions are lower than fossil fuels, and biofuels can be considered a sustainable alternative. Fan et al. [65] compared biofuel production emissions from raw and waste biomass. The lowest emissions are associated when the pyrolysis oil is produced from waste wood since it enters the system free of burdens from harvesting and cultivation processes. Nevertheless, waste wood comes with higher collection and transportation impacts due to the lower product density. The main observation is that pyrolysis oil could save between 77-99% of GHG emissions if used as a fossil fuel substitute. Vienesecu et al. [66] emphasised that emissions from the process could be three times higher compared to conventional fuels if poor fuel quality is achieved.

Antelava et al. [67] carried out a detailed review of LCA studies related to the waste treatment of plastics. The main problem observed for mechanical recycling is associated with the uncertainty of product quality. Therefore, even though mechanical recycling is the preferred option, the quality of recyclate often constrains the complete replacement of virgin material. Jeswani et al. [15] studied the LCA of chemical recycling for mixed plastic waste (MPW). Pyrolysis as a chemical recycling method was found to have about 50% lower GWP than energy recovery in the form of incineration. Nevertheless, the rest of the impact categories, such as acidification and eutrophication potential, perform worse. Some studies found that landfilling is a better option than thermal treatment from the perspective of GWP but worse for the rest of the impact categories [68], [69]. Mechanical recycling often shows the most neutral environmental impacts. However, the quality of recyclate must be at least 80% of that of virgin material to be considered as an adequate replacement [70].

Finally, a limited number of studies focus on the LCA of co-pyrolysis. In fact, only Neha et al. [71] assessed co-pyrolysis as a waste treatment method. In their research, food waste and LDPE were co-pyrolysed, concluding that process outperforms landfilling or open dumping several times in terms of GWP. Due to the high moisture content of food waste (>70%), the drying requirements are significant, accounting for almost 57% of total energy demand. The energy required to carry out the pyrolysis process is also high and responsible for an additional 33% of total energy consumption. Biomass drying and pyrolysis are found to be the main

contributors to the environmental impacts and should be carefully observed when planning the process.

1.2. Knowledge gap analysis

Up to now, various feedstocks have been investigated in the pyrolysis and co-pyrolysis process with different aims and research focus. This diverse research focuses also presents one of the major drawbacks of scaling up the process on an industrial level due to the missing consistency in experimental analysis and results interpretation. Therefore, the next step in process development should be narrowing the research focus on the most prominent feedstock for high liquid yield. Moreover, research attempts should find the optimal feedstock share in a co-pyrolysis mixture that can give high hydrocarbon content while eliminating most unwanted compounds, making the pyrolysis oil compatible with conventional fuels. This would immediately enhance the exploitation properties of derived oil, resulting in lower after-treatment and refinement costs.

Experimental investigations can reveal the most promising feedstock and process parameters for further deployment on a commercial level. Based on the results from the individual analysis, mixture composition can be prepared in a way to promote the yield of preferred chemical compounds found in conventional liquid fuels. Furthermore, by observing the synergistic effect that occurs during the feedstock interaction, product yield can be predicted to some extent. Developing a prediction model for product distribution based on initial feedstock parameters and characteristics is the final step in the commercialisation process. A life cycle assessment (LCA) can be deployed to understand the environmental impact of the process. Results from such analysis can evaluate the benefits compared to other waste treatment methods. In addition, LCA analysis can identify the negative impacts of the process, which could be substituted by more sustainable solutions, enhancing process outlook and chances to be deployed on a broader scale.

1.3. Objectives and hypothesis of research

The objectives of this thesis are to:

- To quantify the co-pyrolysis product yields and distribution of waste biomass and end-of-life plastics materials by examining the parameters, such as ultimate and proximate analysis, and by investigating the synergistic effect that occurs during the feedstock interaction, to reduce the need for continuous experimental investigations.

- To estimate the acceptable plastic content in the fuel mixture by investigating the chemical composition, and kinetic and thermodynamic parameters of the co-pyrolysis process using model-free analysis methods to gain enhanced insights into the feedstock interaction and the influence on the bio-oil quality.

The research hypothesis is that by conducting the series of experimental investigations it is possible to determine the acceptable mixing ratio of biomass-plastic fuel blends and pyrolysis process parameters for the production of high-quality bio-oils by observing the feedstock parameters, bio-oil chemical composition and process kinetics to improve the scalability of the process on an industrial level.

1.4. Scientific contribution

The expected results and contribution of this research are the following:

- Enhanced prediction of product yield and distribution from the co-pyrolysis of biomass and waste plastics by establishing correlations between the feedstock parameters and process kinetics to avoid the need for continuous experimental investigations.
- Determined eligible mixing ratios of biomass and waste plastics for the production of high-quality bio-oils by analysing the chemical composition of derived bio-oil and examining the process kinetic and thermodynamic parameters which will reduce the need for expensive after-treatment methods.
- Carried out environmental footprint analysis and potential integration of pyrolysis procedure with the renewable energy sources to provide a better insight on process scalability on an industrial level.

2. MATERIALS AND METHODS

This chapter gives a detailed overview of used materials and methods. Since the experimental investigations were carried out on three different experimental set-ups, there might be slight differences in the pre-treatment methods or operating conditions. Nevertheless, these differences are considered during the planning stage of experiments, and parameters are selected to minimise or have a negligible effect on results.

2.1. Materials used in experimental investigations

Feedstock used in the scope of this dissertation was collected as waste materials. They were selected based on the observations from the literature review with an aim to produce high quantity and quality pyrolysis oil. Sawdust is chosen as one of the most abundant by-products of the wood industry. In addition, forestry residues like wood shavings, chips, bark, slender twigs, and similar also represent potential feedstock for the pyrolysis process if moisture and ash contents are low with the high volatile matter [34]. PS, PP, and PU are selected from the family of plastic materials for in-depth analysis and evaluation of the potential for the pyrolysis process. PS and PP are widely used as packaging materials with limited recycling potential. High volatile matter and hydrogen content, coupled with a meagre share of ash, moisture, and oxygen in their structure, marks them as the ideal feedstock to enhance bio-oil properties [58]. On the other hand, PU is selected due to their structural differences compared to conventional plastics, which makes their mechanical recycling almost impossible [72]. At the same time, their thermal degradation mechanism is very similar to biomass feedstock, raising research interest in their potential co-processing to produce alternative fuels.

2.1.1. Sample preparation

Before subjecting to experimental investigations, samples were shredded, sieved, and dried. Particle sizes were <0.125 mm for SD and <0.45 mm for plastics obtained through sieving to ensure satisfactory mixture homogeneity. Drying was carried out in a vacuum oven at 70 ºC for at least three hours to remove moisture. Samples were prepared for individual investigation, but also in the form of biomass-plastic mixtures with varying plastic content of 25%, 50%, and 75%. For the final assessment, and based on previous findings, a blend with 50% SD, 25% PS and 25% PP is prepared. These shares are considered the most promising for the high yield of pyrolysis oil with dominant hydrocarbon content.

Analysis was performed according to the standard procedure to determine the elemental composition of the samples [73]. Elemental (ultimate) and proximate analyses were carried out whenever new feedstock was used in experimental investigations. The ultimate analysis was carried out for raw samples and the charred residue collected from 600 ºC. Proximate analysis was carried out on 1±0.010 g of samples to determine the share of volatile matter (VM) [74], moisture [75], and ash content [76]. Additionally, fixed carbon (FC) was calculated by the difference.

2.2. Equipment and methods used in experimental investigations

The pyrolysis experiments were carried out in two types of reactors. In both cases, the samples were heated from room temperature to 600 ºC at a heating rate of 10 ºC/min. Samples masses and carrier gas flow rate were determined by reactor geometry. Moreover, since non-condensable volatiles are the products of greatest interest, the carrier gas flow rate was selected to be sufficient in removing volatiles from the reaction zone, preventing secondary crackings and yield of gases.

2.2.1. Fixed bed reactor

This set-up design consists of a stainless-steel fixed bed reactor with a condensation flask to collect condensable volatiles and directly integrated with a gas chromatograph to analyse the non-condensable gases. The temperature was controlled by a PID controller with K-type thermocouples to measure and control the temperature inside the reactor. Nitrogen was used as a carrier gas with an 80 ml/min flow rate. The schematic view of the experimental setup is given in Figure 2, while detailed explanations are presented in work by Hlavsova et al. [77]. The initial sample masses were approximately 2 g. The solid yield was calculated by weighing masses before and after experiments. The yield of the gaseous fraction was calculated at N_2 free-vol.% basis, and it is based on the obtained volume fractions from gas chromatography (GC) and individual gas densities. Condensable gases are purged from the reactor and cooled down using a condensation flask filled with ice. The yield of pyrolysis oil is calculated by the difference between initial mass and solid and gas yield. Obtained oil is further diluted with dichloromethane and stored in a freezer before being subjected to gas chromatography-mass spectrometry (GC/MS) analysis to identify chemical composition. Analysis was done by injecting 1 µl of sample in a split ratio 1:10 into chromatograph Agilent 7890 A equipped with an HP 5ms column (60 m x 0.25 mm x 0.25 µm). The injector temperature was set at 250 ºC,

with helium as carrier gas with a constant 1 ml/min flow. The organic compounds were separated using the following programme: 48 ºC with a retention time of 2.5 min, followed by heating up to 280 ºC at 5 ºC/min with a retention time of 0.5 min. The mass spectrometric analysis was performed in the range m/z= 35-650. The compounds identification is carried out using internal standards and library and comparison with literature.

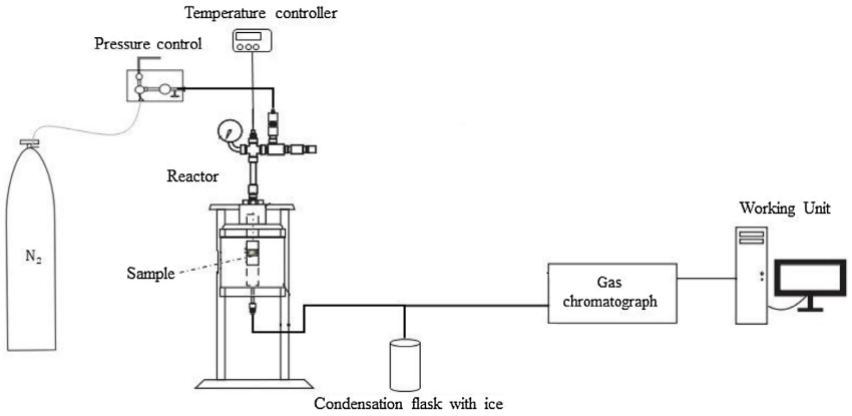

Figure 2 - Schematic view of the used fixed-bed reactor [78]

2.2.2. Infrared furnace

An infrared furnace with a glass tube was used for the experimental investigations of individual SD, PS, and PP samples and their blend with 50% SD, 25% PS, and 25% PP. This experimental setup was used to produce liquid and char fractions, while a separate micro-GC unit was used to analyse the evolution of gases. Figure 3 presents the schematic view of the experimental set-up, while detailed explanations are given in Strezov et al. [79].

In addition to 600 ºC, pyrolysis oils were also collected at 500 ºC to investigate the temperature influence on oil quality. Nitrogen was used as a carrier gas at a 10 ml/min flow rate. Initial sample masses varied due to their densities being 825, 950, 1250 and 1400 mg for SD, mixture, PP and PS, respectively. The liquid fraction was collected at the end of the tube, diluted with dichloromethane and stored in the freezer before being subjected to gas chromatography-mass spectrometry (GC/MS) to determine chemical composition. The liquid yield was calculated by the difference between initial mass and solid and gas yields. Before GC/MS analysis, pyrolysis oils were dehydrated with sodium sulfite (anhydrous) to remove moisture content and filtrated using washed silica gel to remove impurities. To remove organic compounds, silica gel was previously baked at 450 ºC between 24-48h.

Spectral analysis was carried out by Agilent Technologies 5977A MSD with an integrated 7890B GC system equipped with an HP 5 ms column (30 m x 250 μm x 0.25 μm). The samples were injected at 300 ºC in splitless mode with helium as carrier gas at a constant 1 ml/min flow

rate. The organic compounds were separated by the oven programme starting at 40 ºC with a retention time of 2 min, heating at 4 ºC/min to 300 ºC and holding up time of 45 min. The transfer line temperature was set at 300 ºC, with quadrupole and ion-source temperatures of 150 and 250 ºC, respectively. The organic compounds were identified and quantified by internal standards of the Agilent Qualitative software database and through comparison with literature.

The gas characterisation was conducted using Agilent Technologies 490 micro-GC. Column 1 consisted of 5 m PBQ + 10m MS5A, while column 2 was 10 m PPU. Samples with 100 mg mass were pyrolysed from room temperature to 1000 ºC at a heating rate of 10 ºC/min. Helium was used as a carrier gas with a 50 ml/min flow. Before entering the chromatograph, gases were cooled in an ice bath to ensure that only non-condensable gases passed through. The gas yield was calculated on a He-free basis.

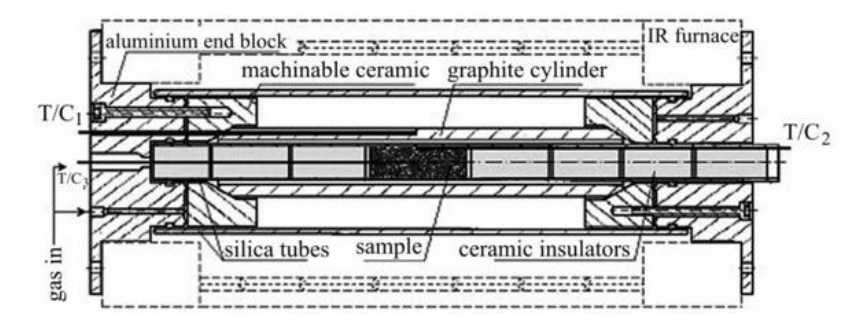

Figure 3 - Illustration of infrared furnace used for three-component mixture analysis [79]

2.2.3. Solid residue characterisation

Fourier Transform Infrared Spectroscopy (FTIR) was performed for the raw samples and charred residue collected at 600 and 1000 ºC. Samples were investigated individually and in the form of mixtures. Nicolet 6700 FT-IR was used to determine the spectral compositions from 4000 to 500 cm^{-1} wavenumber. The results were compared with the internal software spectra database (OMNIC Spectra) and related literature.

2.3. Thermogravimetric and kinetic analysis

This section presents the methods used for thermogravimetric and kinetic analysis. In general, thermogravimetric analysis (TGA) is carried out first to determine the sample's decomposition mechanism. In this work, TGA is carried out for all investigated samples and their mixtures. Values obtained from TGA analysis are further used for the kinetic and thermodynamic study. However, kinetic and thermodynamic parameters are assessed for all

individual samples and only two-component sawdust-plastic mixtures. The three-component mixture, selected as the most promising one, is subjected to thermal analysis.

2.3.1. Thermogravimetric and thermal analysis

Thermogravimetric analyses (TGA) of the individual and final proposed mixture were carried out on Mettler Toledo TGA/DSC 1 STARe system instrument. Samples with an initial mass of about 11 mg were heated from room temperature to 1000 ºC at a heating rate of 10 ºC/min under an inert atmosphere. Nitrogen was used as carrier gas with a 20 ml/min flow. Results were used to determine the sample decomposition mechanism and final masses of solid residue.

Thermal analysis was carried out in an infrared furnace by heating the samples from room temperature to 1000 ºC at a constant heating rate of 10 ºC/min. Samples masses were 1 g ± 0.15 g. Nitrogen was used to ensure an inert atmosphere with a 5 ml/min flow rate. The experimental setup and calculation methods are described in the work by Strezov et al. [79]. Besides determining the nature of reactions, results were also used to determine the final temperature for pyrolysis, considering the temperature lag between the samples' surface and centre.

2.3.2. Kinetic and thermodynamic analysis

The prepared samples are conducted to the Simultaneous Thermal Analysis (STA), which provides data for TGA and DTA simultaneously on the same sample. The NETZSCH STA 445 F5 Jupiter system was used for STA measurements under the following conditions:

- sample mass: 10 ± 0.5 mg.
- temperature range: from room temperature to 800 °C.
- heating rates: β = 5, 10 and 20 °C/min.
- the carrier gas: pure argon with a total gas flow rate of 70 mL/min.

The first step in the kinetic analysis is a calculation of activation energies (E_a). Model-free methods are used to calculate activation energies due to the heterogeneity of the mixtures, which may result in the misidentification of the appropriate kinetic model. Besides, model-free methods allow the analysis of activation energy as a function of conversion rate, giving better insight into process dynamics. This is especially important in the case of multi-component mixtures where shifts in decomposition mechanism are inevitable. Four model-free

isoconversional methods are used in the scope of this work: Friedman (Eq. 1), Kissinger-Akahira-Sonuse (Eq. 2), Ozawa-Flynn-Wall (Eq. 3), and Starink (Eq. 4).

$$\ln(\beta \frac{d\alpha}{dT}) = \ln[Af(\alpha)] - \frac{Ea}{RT} \quad \text{Eq. 1}$$

$$\ln(\frac{\beta}{T^2}) = \ln\left[\frac{AR}{EaG(\alpha)}\right] - \frac{Ea}{RT} \quad \text{Eq. 2}$$

$$\ln \beta = \left[\frac{0.0048 * AEa}{RG(\alpha)}\right] - 1.052(\frac{Ea}{RT}) \quad \text{Eq. 3}$$

$$\ln(\frac{\beta}{T^{1.92}}) = C_s - 1.0008\frac{Ea}{RT} \quad \text{Eq. 4}$$

In the equations mentioned above, α represents the degree of conversion, β is the heating rate, T is the temperature A, E_a, and R are the pre-exponential coefficient, the activation energy, and the universal gas constant, respectively. Thermodynamic parameters, including the pre-exponential factor, are calculated using the following equations 5-8:

- Pre-exponential factor (A) $$A = \frac{\beta * Ea * \exp(\frac{Ea}{R * T_m})}{R * T_m^2} \quad \text{Eq. 5}$$
- Changes of enthalpy (ΔH) $$\Delta H = Ea - RT_\alpha \quad \text{Eq. 6}$$
- Changes in entropy (ΔS) $$\Delta S = \frac{\Delta H - \Delta G}{T_m} \quad \text{Eq. 7}$$
- Changes of free Gibbs energy (ΔG) $$\Delta G = Ea + R * T_m * \ln(\frac{K_B * T_m}{h * A}) \quad \text{Eq. 8}$$

Where K_B represents the Boltzmann constant (1.381×10^{23} J/K), h Plank constant (6.626×10^{34} Js), T_m DTG peak temperature, and T_α the temperature at the degree of conversion α [80].

2.4. Evaluation of the synergistic effect

This section describes the methodology used to evaluate the synergistic effect that occurs during the feedstock interaction, which can be crucial for product yield and distribution. In addition, a brief overview of materials and methods used to develop a methodology for predicting product yield is given.

2.4.1. Synergistic effect analysis

The synergistic effect is the main driver for product distribution from the co-pyrolysis of biomass and waste plastics [81]. To determine the level of synergy, experimental results are compared to the theoretical values. Theoretical values (Y_{cal}) are calculated using the following Eq. 9:

$$Y_{cal}=W_{SD}Y_{SD}+W_{Plast}Y_{Plast} \quad \text{Eq. 9}$$

Where $W_{SD/Plast}$ stands for proportions of each component in investigated mixtures, and $Y_{SD/Plast}$ presents the values obtained from the individual pyrolysis [82]. The existence and level of synergy are determined by the difference between experimentally obtained values and calculated ones using Eq. 10. According to [43], it can be stated that synergy exists when the difference between the experimental and calculated values is positive.

$$\Delta Y=Y_{exp}-Y_{cal} \quad \text{Eq. 10}$$

2.4.2. Methodology for prediction model development

Materials and methods used to develop a methodology for predicting product yield are mostly taken from the available literature and coupled with the observations from conducted experimental investigations. The main limitation observed while analysing literature is related to the reliability and repeatability of presented results. Different process conditions, feedstock types and investigation objectives make the comparison and, consequently, usage of derived results very complicated. Furthermore, most of the consulted studies only present part of the required input data. Comprehensive analyses that would examine initial feedstock properties and their relation to final product yield and distribution are often missing. Consequently, this results in a limited database and developed prediction models are only accurate in some narrow range of process conditions. The most significant progress in modelling and predicting the product yield is achieved in the field of biomass gasification [83].

On the other hand, modelling the thermochemical conversion of two different types of feedstocks is still in the emerging phase. Developed models for homogenous feedstock are not applicable in this case since they completely ignore the other constituent in the mixture. Even more, such models do not consider feedstock and volatile interaction during the process, which implies that the synergistic effect is completely neglected. Since the synergistic effect is one of the main drivers for the product yield from the thermal degradation of multi-component mixtures, its inclusion in the modelling process is inevitable.

2.5. Life cycle assessment (LCA)

The LCA is used to assess the environmental impacts of the proposed procedure. The system boundaries are set from feedstock collection in the form of waste materials to the production of pyrolysis oil as the final step. This implies that oil refining and upgrading are not considered, and no credits or burdens are assessed for oil utilisation. As the main product, pyrolysis oil is evaluated with all environmental impacts, while credits are received for producing by-products that can substitute fossil fuels elsewhere. Synthetic gas (syngas) is used internally to provide heat, while char is sent to the market as a coal substitute. The functional unit used for impact assessment is 1 t of the pyrolysis oil produced. The model of the proposed system is given in Figure 4. As shown, co-pyrolysis is preceded by several processes related to feedstock transport and pre-treatment. Input waste flows are free of production or cultivation burdens, but there are environmental impacts derived from their collection. Biomass, preferably in waste forms like sawdust or shavings, is collected and transported from the sawmill or source of origin to a hypothetical co-pyrolysis plant, where it is dried and shredded to a particle size below 2 mm. The plastic stream starts with waste collection in the form of mixed plastic waste transported to the separation plant. MPW is further separated on monomer fractions where non-recyclable components are diverted from landfilling or incineration to a pyrolysis plant. Before mixing with sawdust, plastic is shredded to the same particle size to ensure the homogeneity of the mixture. The prepared mixture is then introduced to the pyrolysis reactor and heated to 600 ºC under an inert atmosphere, where liquid, gaseous and solid charred products are obtained.

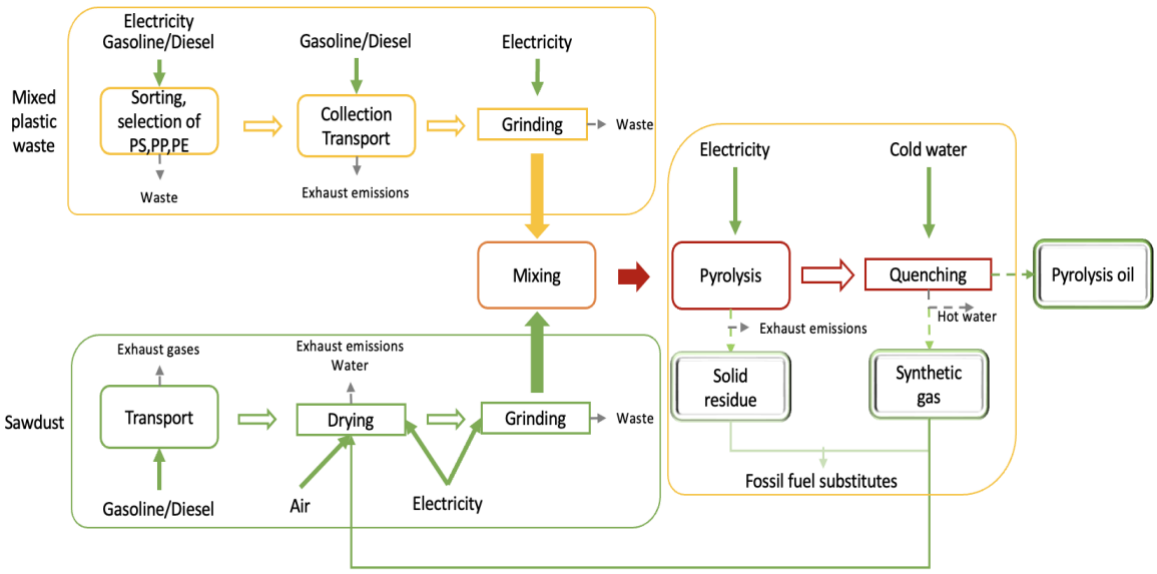

Figure 4 - Proposed system model for LCA analysis

The ecoinvent 3.8 database [84] is used as inventory data, while additional literature is consulted for further information about specific consumptions and flows for processes inside the system. Impact assessment is carried out in OpenLCA 1.11. [85] using the ReCiPe Midpoint 2016 (H) method. As a functional unit, the 1 t of pyrolysis oil is assessed using the consequential approach. This implies that the environmental impacts present the comparison between pyrolysis and incineration or landfilling from the perspective of waste materials utilisation. Altogether 18 impact categories are assessed, of which nine are widely discussed. The rest of the impact categories are briefly mentioned since their impact is primarily neutral. The global warming potential (GWP) expressed in kg CO_2 eq. is used to compare the results with similar studies. The rest of discussed categories include human carcinogenic toxicity (HTC), human non-carcinogenic toxicity (HTNC), freshwater ecotoxicity (FET), marine ecotoxicity (MET), terrestrial ecotoxicity (TET), all expressed in kg 1,4-DCB. Additionally, fossil resource scarcity (FRS) in kg oil eq., acidification potential (AP) in SO_2 eq., and fine particulate matter formation expressed in kg $PM_{2.5}$ eq. are briefly discussed.

3. SELECTED RESULTS

In this chapter, selected results from research work are presented. Figures and tables are directly taken from published papers and appropriately referenced where necessary. The most important observations are briefly discussed here, while extensive analysis can be found in published papers (PAPER 1-4). Additional results regarding the experimental investigation and environmental assessment that have not yet been published are discussed more detailly.

3.1. Elemental and proximate analysis of considered feedstock

Elemental and proximate analysis was the first step in evaluating the feedstock suitability for the considered process. From the elemental perspective, it is of special interest to observe the share of carbon (C) and hydrogen (H), while volatile matter (VM) and ash content are crucial proximate parameters. The results from the samples used in this research are summarised in Table 2. The sulphur is only detected in traces (0.1%) for SD, PS, and PP, and its therefore not included in the table to maintain better visibility. Since the experimental investigations were conducted on the same type of feedstock but taken from different sources, ultimate and proximate analyses were conducted twice. To emphasise the difference, numeration is introduced.

Table 2 - Results from ultimate and proximate analysis

Sample	C	H	O	N	VM	FC	Ash	Moisture
	%							
SD	47.3	6.0	44.8	2.5	73.0	18.3	1.3	7.4
PS	89.6	8.2	0.9		98.4	0.2	1.3	
PUR	63.9	6.5	17.0	6.7	82.0	9.5	5.8	2.7
PP	85.5	12.4	1.9	0.1	98.7		1.0	0.3
SD_2	46.2	6.4	47.4		87.9	2.2	0.6	9.3
PS_2	90.9	7.8	1.3		99.6		0.1	0.3
PP_2	81.9	14.6	3.5		96.3	0.7	2.5	0.6
Mix	62.9	8.6	28.5		93.9	0.2	1.1	4.8

From Table 2, it is interesting to observe that the results from elemental analysis of SD samples are very similar even though the type of biomass differentiates. A mixture of oak, fir and beech was used for the SD sample, while SD_2 consisted only of *pine radiata*. Yet, this difference is obvious in the case of VM and moisture content. SD_2 sample has almost a 10% higher share of VM and almost twice higher share of moisture. This suggests that SD_2 could

be very favourable for liquid yield. The share of ash is 1.3% in the case of SD composed of different types of biomass, while homogenous SD_2 has only 0.6%.

Polystyrene is known for its high C and H content, extreme volatility (>98%) and low share of ash (1-2%). Similarly, high hydrocarbon content is founded in polypropylene materials. The difference compared to PS is in the share of hydrogen, which is often above 10% for PP, while slightly lower values are observed in the case of PS.

Polyurethane exhibits the values between these found for sawdust or PS/PP samples. The share of carbon is significantly higher than in SD yet pronouncedly lower than in PS or PP. A notable share of nitrogen is also observed (6.7%) as a consequence of the synthesis process and usage of flame retardants due to the application requirements [86]. Besides, the 17% of oxygen content was calculated by the difference, emphasising the structural difference to conventional polymers.

Finally, the mixture (Mix) comprising 50% SD_2, 25% PS, and 25% PP was analysed. The share of carbon was in the range between those found for individual samples (63%), while the share of hydrogen (8.6%) was higher compared to individual SD_2 and PS_2 but still comparably lower to PP_2. Besides, almost 29% of oxygen is calculated by the difference. Even more interesting is to analyse the results from the proximate analysis. The mixture was found to be highly volatile, with VM accounting for almost 94%. This is a very encouraging observation that suggests a high liquid yield might be obtained. In addition, only 1.1% of ash content implies that most of the sample will decompose to volatiles that will either condense to pyrolysis oil or will be collected as non-condensable gases.

3.2. Selected results from co-pyrolysis of waste materials

The pyrolysis of individual samples and co-pyrolysis of two-component biomass-plastic mixtures was the first step in the research work. This section presents the observations regarding the product yield, chemical composition of obtained pyrolysis oil, and their further utilisation possibilities. In addition, a brief discussion is given regarding the potential application of obtained by-products.

3.2.1. Co-pyrolysis of two-component biomass-plastic mixtures

Preliminary co-pyrolysis experiments have been conducted on two types of biomass-plastic mixtures. Firstly, PS has been co-pyrolysed in mixture blends with SD, with varying content between 25 and 75%. As can be seen in Figure 5, the liquid yield from individual

samples greatly differs. Almost 50% of derived products from SD pyrolysis are non-condensable gases, while liquid (bio-oil) yield is only 31.5%, with 20.5% solid residue. On the other hand, the liquid yield from PS pyrolysis is remarkably 96%, with only 3.1% of solid residue and an almost negligible share of gases (<1%). Based on results from the individual analysis, it was assumed that PS could greatly enhance the oil yield if co-pyrolysed with sawdust. Only a small introduction of PS (25%) to the mixture doubled the liquid yield (62.3%) compared to individual SD pyrolysis. Further increment of PS increases the liquid yield to 73 and 84% for mixtures with 50 and 75% of PS. The increased liquid yield was exclusively at the expense of gaseous fraction. The yield of gases from the mixture dramatically decreases with the introduction of PS, accounting for only 17% of the mixture with 25% PS. Further increment of plastic content decreases the share of gases to 11 and 6%. PS have a very small share of solid residue; therefore, most of the residue from mixture pyrolysis is due to the SD component. Consequently, as the share of PS in the mixture increase, the share of solid residue decreases. The observed solid residue is 20.7% for the SD-dominant blend, which is halved to only 10% for the blend where PS is a major constituent. Observations from product yield analysis suggested that PS is a very promising feedstock for co-pyrolysis, and only a slight introduction of it to the mixture can greatly enhance the liquid yield. The chemical characterisation of derived pyrolysis oil is done to determine the acceptable share of PS in a mixture blend that can be used for the production of alternative fuels.

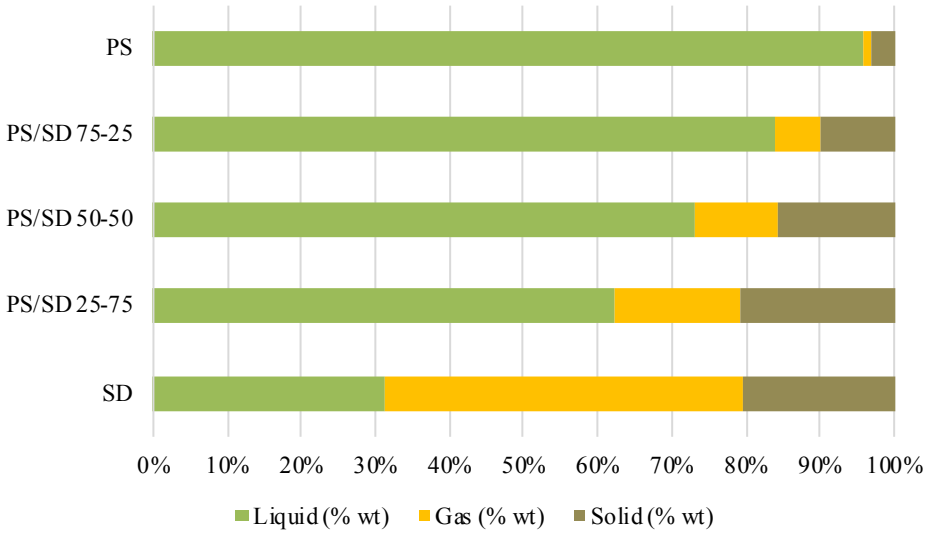

Figure 5 - Product yield from SD-PS co-pyrolysis [78]

The detailed characterisation and discussion of identified chemical compounds are presented and published in PAPER 2. SD-derived oil or bio-oil expresses very heterogenous structures with different organic species, of which most are present in traces. In total, 43

compounds are present with a share higher than 1%, and they represent 80% of the bio-oil composition. Most of the compounds have attached oxygen atoms in their structure and belong to the family of phenols, ketones, aldehydes, acids, alcohols or sugars. The hydrocarbon content of bio-oil is poorly 13%, with styrene, toluene and 2-phenyl tetralin as the most significant identified compounds. On the other hand, the PS-derived oil has a more homogenous structure, where the nine most prominent compounds account for 82% of the total yield. The following compounds are found with the highest share: styrene, α-methylstyrene, 1,3,5-triphenyl cyclohexane, and 2-phenyl tetralin. They are all hydrocarbons, and most of them belong to the aromatic group with a benzene-attached ring.

Similarly to the product yield, the small introduction of PS to a mixture blend (25%) greatly changed the yield of identified compounds in the oil. The most important outcome of feedstock interaction is almost complete removal of oxygenated compounds. Phenols are only visible representative of SD found in mixture-derived oils, and their share decreases from 3 to only 1% with the increment of plastic content. Even more, the identified compounds in derived oils mostly belong to the family of aromatic hydrocarbons, containing benzene rings inside their structure. Since the share of aromatics is limited to 40% in conventional fuels [87], it is clear that the share of PS should also be limited in mixture blends. Besides, the increment of PS content promotes the formation and yield of PAHs, which represent a threat to human health. Finally, the conducted investigation showed that utilisation of PS in co-pyrolysis mixtures greatly enhances the quality of obtained pyrolysis oil compared to bio-oil from individual sawdust. Nevertheless, due to the nature of derived chemical species, its share in mixture blend should be limited to some extent. The identified chemical compounds from mixtures co-pyrolysis are given in Table 3.

Table 3 - Selected compounds from SD-PS co-pyrolysis [78]

Chemical compound	**PS/SD 25-75%** Share [%]	**PS/SD 50-50%** Share [%]	**PS/SD 75-25%** Share [%]
α-Methylstyrene	4.82	7.69	8.33
1,2-Diphenylcyclopropane	2.24	3.23	4.04
Benzene, 1,1'-(1,3-propanediyl) bis-	3.65	6.46	7.98
benzene, 1,1',1"-[5-methyl-1-pentene-1,3,5-triyl] tris-	5.10	0.90	0.61
Cyclohexane, 1,3,5-triphenyl-	19.97	8.99	11.70
Cyclopentane, methyl-	3.44	1.18	0.73
Ethylbenzene	7.25	11.28	8.76
Naphthalene, 1,2,3,4-tetrahydro-2-phenyl-	5.95	7.32	8.73
Styrene	27.38	23.40	15.21
Toluene	1.12	5.70	8.15
Sum of selected compounds	80.91	76.15	74.25
Compounds with share below 0.5%	19.09	23.85	25.75

Figure 6 presents the product distribution from the co-pyrolysis of SD with rigid polyurethane foam (PUR). Chemical structure and composition are greatly different in the case of PUR compared to the rest of the plastics (Table 2). Consequently, the product distribution from thermal degradation pronouncedly differs as well. The liquid is the most abundant fraction, with almost doubled values (61.2%) compared to bio-oil (31.4%). Nevertheless, this is still much lower compared to PS. Besides, the share of solid residue (22.1%) and a gaseous fraction (16.7%) is significant, implying that the production of liquid fuels from such feedstock has serious constraints. This is even more evident when the analysis is extended to the product yield from PUR-containing mixtures. Introducing the PUR to the mixture blend increased the liquid yield to 48.4% at the expense of non-condensable gases, whose share is halved (24.2%). The share of solid residue is also increased to 27.4%, which is higher compared to individual analysis of both samples. Nevertheless, further increment of PUR content has an almost negligible effect on product distribution. As can be seen from Figure 6, mixtures with 50 and 75% of PUR have similar product distribution compared to the mixture with only 25% of PUR content. This suggests that PUR can somewhat enhance liquid yield, but a high share of gases and solid residue is inevitable due to the building blocks.

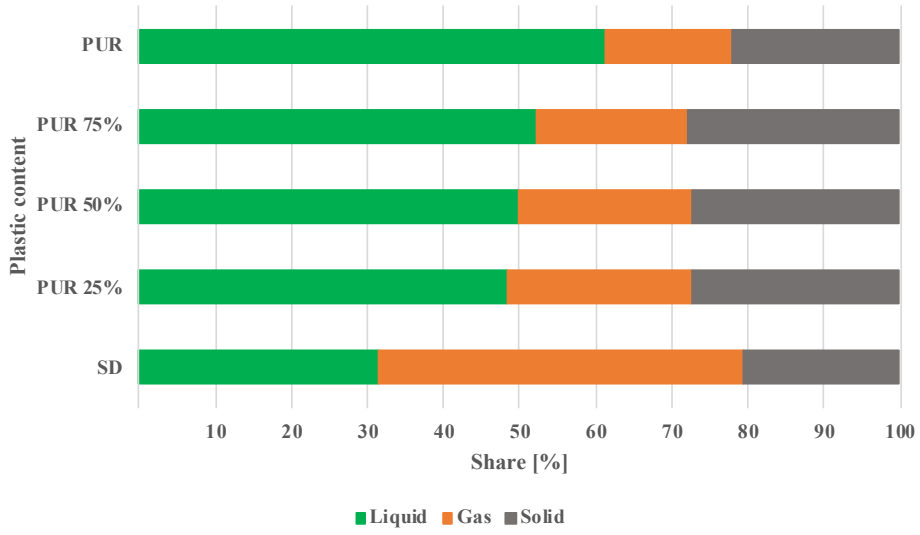

Figure 6 - Product yield from SD-PUR co-pyrolysis [88]

Even more, the chemical characterisation of liquids suggests minimal utilisation possibilities of such oil for fuel purposes (Figure 7). Altogether, 94 chemical species are identified in PUR-derived oil, while eight of them are responsible for 75% of the total liquid

yield. Benzenamines are the major organic group found in PUR-derived oil, responsible for 72% of identified compounds. Additionally, the share of aromatic hydrocarbons is 8%, while phenols and alcohols account for 6% each. Benzenamines are valuable chemicals that can be used to synthesise new chemicals, but their utilisation as an alternative fuel is not compatible with the existing standards for conventional fuels. Hence, the analysis of the mixture's oils is crucial to confirm above mentioned statement. The share of benzenamines varies between 42 and 75% for mixtures with 25 and 75% of PUR content, respectively. Phenols are the second most abundant organic groups, also found in oils from individual samples. Their share is reduced with the increment of plastic content, but it is not completely removed since they are structural compounds of the PUR building block. Similarly, alcohols are detected in all derived oils, and their share is more-less stable and independent from the PUR content in the mixture. Since benzenamines have a nitrogen atom in their structure, while phenols and alcohols contain oxygen atoms, it can be stated that PUR is not an appropriate feedstock for liquid fuel production. The presence of nitrogen in the fuel can cause the formation of NO_X emissions, while oxygenated compounds reduce heating value and cause thermal instability. Detailed chemical characterisation and discussion are given in PAPER 3.

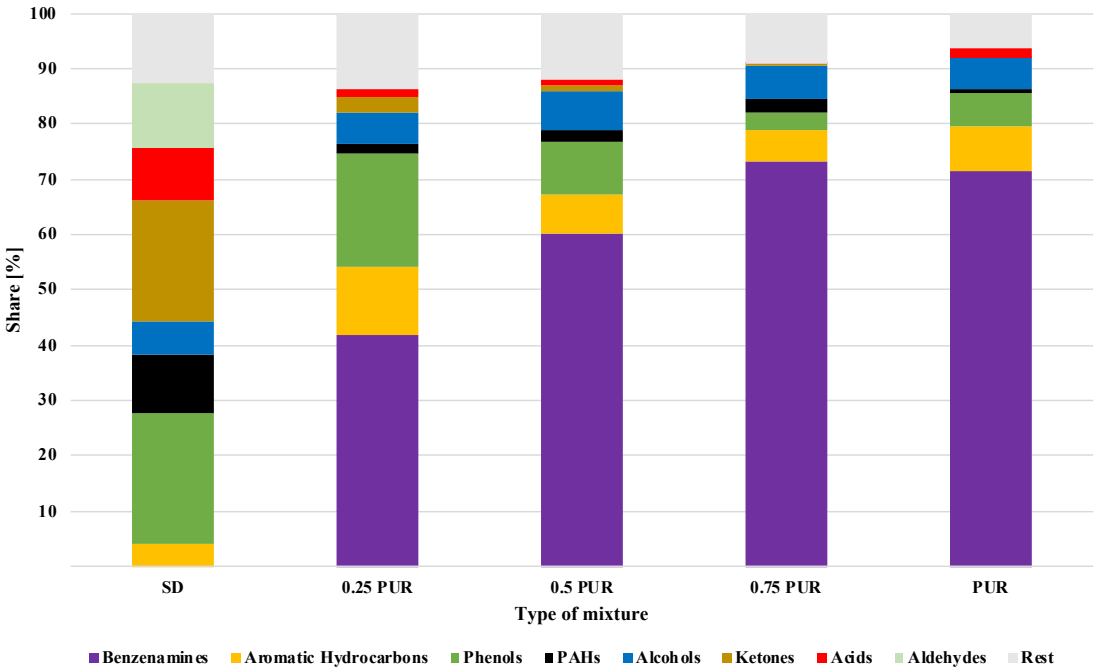

Figure 7 - Identified organic groups in derived pyrolysis oil from SD-PUR co-pyrolysis [88]

3.2.2. Co-pyrolysis of a three-component biomass-plastic mixture

Based on the observations from previous experimental results and the literature, a three-component mixture is selected to be utilised in co-pyrolysis with the aim to maximise high-quality liquid yield. The proposed composition consisted of 50% pine sawdust, 25% PS and 25% PP. Sawdust is the principal constituent of a mixture blend that gives carbon neutrality to produced oil. PS is selected to maximise the liquid yield and give aromatic content, while PP is chosen to increase the share of aliphatic hydrocarbons in derived oil. The product yield for individual samples and their mixture is given in Figure 8. Individually, the liquid yields are 98, 76, and 50% for PS, PP and pine SD, respectively. As expected, a high liquid yield is also achieved in the case of the mixtures, with almost 81%. In addition, approximately 7% of gases are collected, and solid residue at the end of the process is about 12%. The observed distribution of pyrolysis products suggests that the proposed mixture could be very favourable for producing alternative liquid fuels. Nevertheless, to confirm this statement, it is necessary to carry out chemical characterisation.

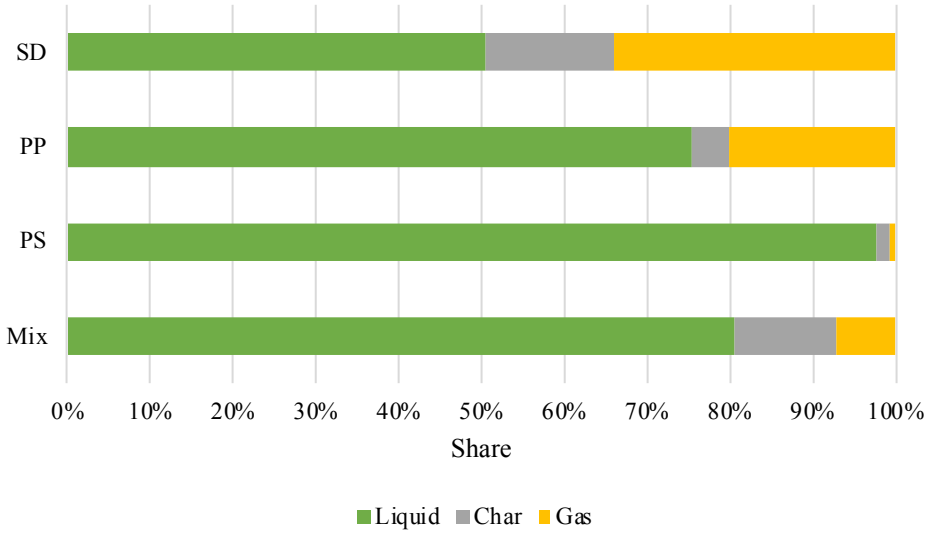

Figure 8 - Product yield from SD-PS-PP co-pyrolysis

Analysis of the mixture's pyrolysis oil showed that hydrocarbon content is almost 70%. Aromatics account for 32.1%, while cyclic and linear hydrocarbons share is 30.3 and 4.6%, respectively. The remaining 2.6% of hydrocarbons are PAHs. The identified organic groups in derived pyrolysis oils from all investigated samples are presented in Table 4. As can be seen, the achieved hydrocarbon content and division on aromatics and aliphatics are in line with conventional fuel standards. The most significant compounds identified in pyrolysis oil are styrene (20%), 1-propene, 3-(2-cyclopentenyl)-2-methyl-1,1-diphenyl (14.6%), and 2-

Isopropyl-5-methyl-1-heptanol (7.1%). In addition, it should be emphasised that mixture composition reduced the yield of 2-phenyl tetralin to only 2.2%, which is a significant reduction compared to individual PS pyrolysis. Even more, such low yield is a great outcome of the co-pyrolysis and feedstock interaction since 2-phenyl tetralin is quite often found in derived pyrolysis oil of different feedstock types. Compounds with the most significant yield from the co-pyrolysis mixture are presented in Table 5. As can be seen, the oil composition also depends on the final temperature. With the temperature increment, compounds with higher C-number tend to decrease in share. Nevertheless, their secondary cracking reduces oil homogeneity since more compounds with lower C-number are produced.

Table 4 - Identified organic groups in pyrolysis oil from proposed mixture

Temperature [°C]	Mix		PS		PP		SD	
	500	600	500	600	500	600	500	600
Aromatic hydrocarbons	38.0%	32.1%	72.0%	74.6%				
Cyclic hydrocarbons	28.4%	30.3%	0.2%	0.4%	36.8%	34.4%	3.0%	3.5%
Sulfoxides			1.7%	0.3%			1.1%	3.5%
Alcohols	10.8%	12.4%			38.3%	35.4%	9.1%	1.6%
Linear hydrocarbons	5.1%	4.6%	1.4%	4.8%	10.8%	11.3%		
Ester/Acid	0.7%	3.6%					1.8%	1.4%
PAHs	3.6%	2.6%	20.5%	18.0%				2.3%
Other oxygenated compounds	1.4%	1.4%			5.2%	6.4%	5.4%	0.3%
N_2-containing compounds	0.9%	0.7%					33.5%	2.5%
Silanes					1.2%	0.8%		
Polysaccharides							1.4%	
Phenols							32.4%	71.8%
Ketones							5.4%	3.7%
Furans							0.6%	0.1%

The potential drawback of oil utilisation might be in a relatively higher share of alcohols (12.4%) and acids (3.6%). The complete reduction of alcohols is complex since they are often used as additives in plastic production. For illustration, alcohols were the second most abundant organic group from PP pyrolysis, accounting for 35% of the oil composition. On the other hand, the yield of acids is often promoted when the feedstock is not cleaned from organic impurities before being introduced to the reactor. The catalytic co-pyrolysis might be beneficial for the complete removal of oxygenated compounds, even though to which extent remains questionable. Finally, it can be stated that the chemical characterisation of oil composition confirms the significant potential for liquid fuel production from the proposed mixture.

Table 5 - Most prominent compounds identified in mix-derived oil

Compound	Formula	Share [%]	
		500 ºC	600 ºC
Styrene	C_8H_8	29.2%	20.2%
1-propene, 3-(2-cyclopentenyl)-2-methyl-1,1-diphenyl	$C_{21}H_{22}$	19.3%	14.6%
2-Isopropyl-5-methyl-1-heptanol	$C_{11}H_{24}O$	6.6%	7.1%
1R,2c,3t,4t-Tetramethyl-cyclohexane	$C_{10}H_{20}$	4.1%	5.8%
Benzene, 1,3-dimethyl-	C_8H_{10}	2.8%	3.6%
Benzene, 1,1'-(1,3-propanediyl)bis-	$C_{15}H_{16}$	2.5%	3.5%
.alpha.-Methylstyrene	C_9H_{10}	2.1%	2.6%
1-Decanol, 2-hexyl-	$C_{16}H_{34}O$	1.7%	2.4%
Cyclohexane, 1,2,3,5-tetraisopropyl-	$C_{18}H_{36}$		2.4%
Naphthalene, 1,2,3,4-tetrahydro-2-phenyl-	$C_{16}H_{16}$	3.6%	2.2%
Carbonic acid, eicosyl vinyl ester	$C_{23}H_{44}O_3$		2.0%
3-Heptene, 2,6-dimethyl-	C_9H_{18}	1.8%	1.7%
1,7-Dimethyl-4-(1-methylethyl)cyclodecane	$C_{15}H_{30}$		1.7%
Cyclohexane, 1,2,3,4,5,6-hexaethyl-	$C_{18}H_{36}$	2.0%	1.2%

3.2.3. Process by-products analysis

Gas yield from the individual samples varies significantly in terms of cumulative volumetric yields and composition. Gases started to evolve slightly below 500 ºC, with the maximum amount noted at 1000 ºC. The highest yield of 974 ml/g is observed for SD at 1000 ºC (Figure 9). If the co-pyrolysis temperature is 600 ºC, the gas yield would be around 450 ml/g. PP also yields a significant amount of gases, which is also observed in the literature [89]. At 600 ºC, 183 ml/g of gases is collected, further increasing to almost 500 ml/g at 1000 ºC. The high gas yield from these two samples shows that most volatiles are converted to non-condensable gases, which might comprise liquid yield. On the other hand, the gas yield from PS is almost negligible. At 600 ºC, gases account for less than 10 ml/g, while at 1000 ºC, only 27 ml/g is collected. Consequently, this shows that pyrolysis can convert volatiles from PS to valuable liquids, as preferred. Even though SD and PP compose 75% of the mix, the gas yield of the mixture is several times lower than their individual analyses. At 600 ºC, only 47 ml/g of gases are evolved, which is further increased to 135 ml/g at 1000 ºC. This implies that feedstock interaction and the introduction of PS greatly influence volatile conversion and favour liquid yield at the expense of gases.

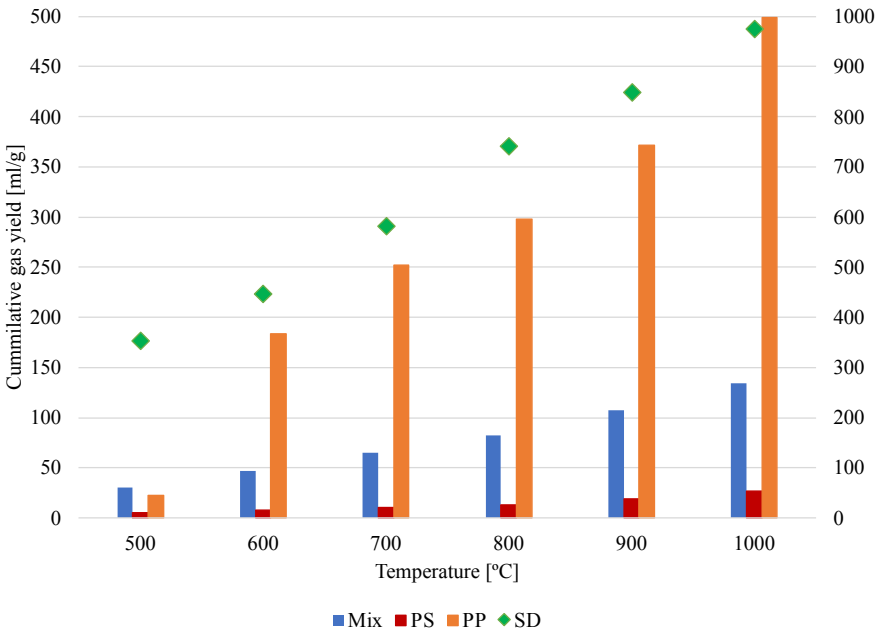

Figure 9 - Cumulative gas yield

The gas composition differs among the investigated samples. At 600 ºC, the pyrolysis gas from sawdust is composed mainly of carbon monoxide (CO) and carbon dioxide (CO_2), combined accounting for 83% of volume share (Figure 10a). The rest is comprised of methane (13%), hydrogen (2%), and higher hydrocarbons (2%). With the further temperature increment, the share of CO and CO_2 declines while the percentage of hydrogen notably increases. At the final temperature of 1000 ºC, gas is composed of CO (31%), CO_2 (25%), and CH_4 (13%), while hydrogen accounts for almost 30%. Ethane and ethylene are present with a nearly negligible 2% combined.

A significantly different composition is observed for PP (Figure 10b). At 600 ºC, a representative amount of gases is collected, composed of light hydrocarbons (89%). The combined yield of CO and CO_2 is almost negligible throughout the process, ranging between an initial 6% and 13% at the final temperature. At the final temperature, a significant share of light hydrocarbons is converted to methane (32%) and hydrogen (24%). Nevertheless, the percentage of hydrocarbons is still respective, with 17% noted for ethane and 14% for ethylene.

Since PS generally yields a small amount of gases, its composition is not of great interest. At 600 ºC, the gas yield is below 10 ml/g, with hydrogen (32%) and methane (24%) as the main constituents (Figure 10c). With further temperature increments, the share of hydrogen is significantly increasing at the expense of light hydrocarbon gases. At a final temperature of 1000 ºC, it accounts for almost 70% of the total gas yield. For quantitative comparison, at 1000 ºC, hydrogen yield is approximately at the same levels as in the case of SD at 600 ºC.

Finally, the composition of the gases from mixtures expresses similar trends to individual SD sample (Figure 10d). At 600 ºC, CO and CO_2 account for 84% of gas composition. Methane brings an additional 11%, while the rest are hydrogen and hydrocarbons. With temperature increment, the share of hydrogen increases at the expense of hydrocarbons, but also because of tar cracking at high temperatures. At 1000 ºC, hydrogen is the principal constituent of the gas composition with 32%, followed by CO_2 (31%) and CO (29%). The share of methane is reduced to only 6%, while ethane and ethylene are responsible for 1% each.

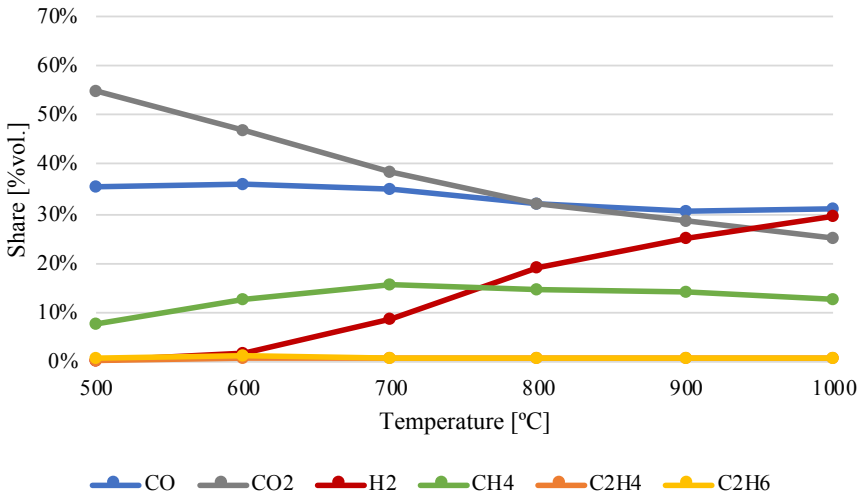

a) Sawdust

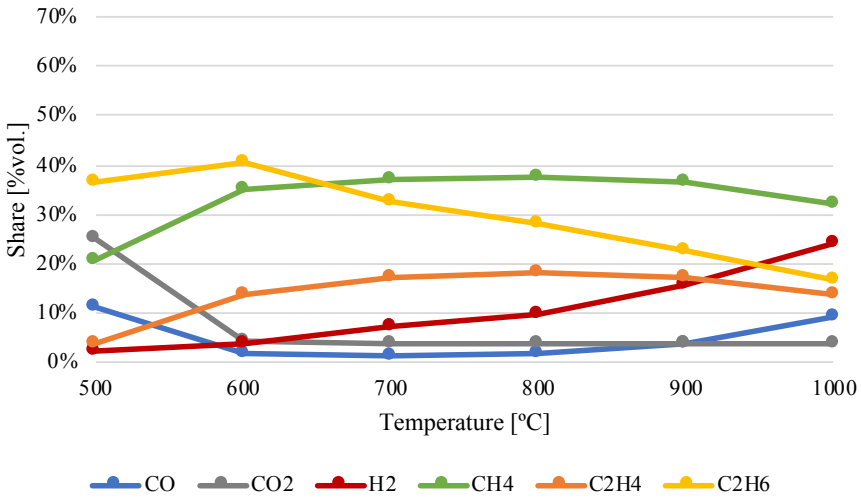

b) PP

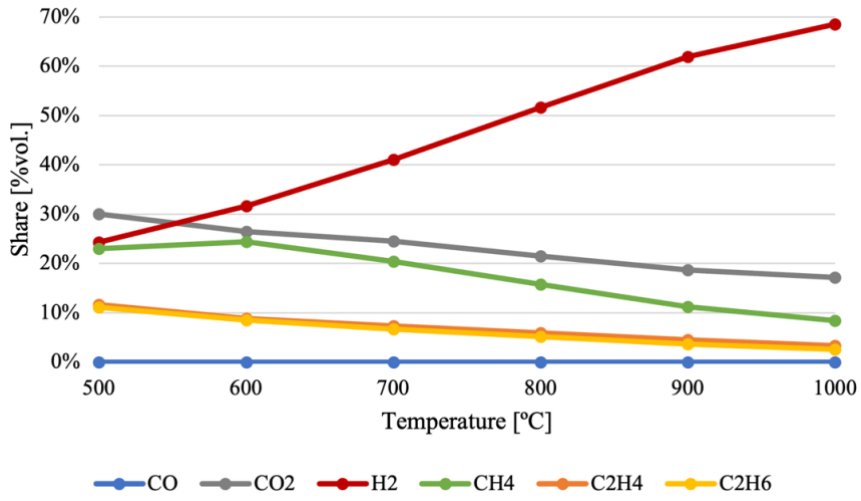

c) PS

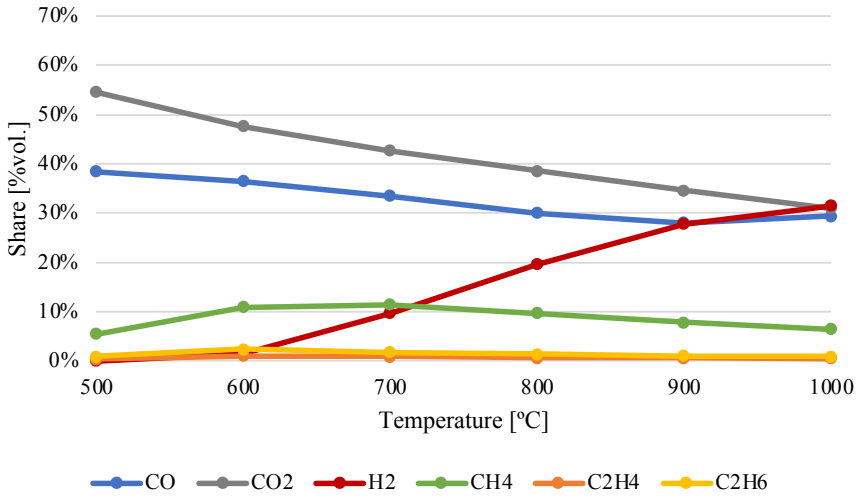

d) Mixture

Figure 10 - Composition of obtained pyrolysis gases

Spectra analysis of char samples collected from 600 and 1000 ºC reveals which organic groups remain are still present in the solid residue. This can be used as a preliminary assessment for char further potential application. It should be emphasised that char yield from plastics is minimal. Therefore, most of the volatiles are expected to be converted into liquid and gases, and only a minor share remains in the solid residue. Results from FTIR analysis are presented in Figure 11. Besides the char analysis, raw samples were subjected to FTIR to set the benchmark for comparison. In the case of PP char from 600 ºC, few peaks can be identified, starting at 2956 cm^{-1} with the stretching of a methyl group, reported for a raw sample as well. Furthermore, intense stretching can be observed at 1016 cm^{-1} again, corresponding to the inorganic group with silica content. It should be mentioned that the peak at 671 cm^{-1}, also found in PP's spectra with talc, suggests the presence of the inorganics once again. Temperature

increment to 1000 ºC completely degrades the sample and ensures that most organics are converted into volatiles. Between 1070 and 850 cm^{-1}, the rocking of remaining C-H bonds is noted.

PS completely degrades almost without solid residue, and char traces can be collected from the tube wall and the FTIR spectra for the char collected for both temperatures corresponds to that of a solid carbon.

Analysis of char fraction from SD is the most important due to the highest yield of solid residue. Compared to the raw sample, there are no peaks above 1600 cm^{-1} in the case of char from 600 or 1000 ºC, implying complete conversion of oxygenated compounds into volatiles at this range. In the case of char from 600 ºC, notable bending is noted at 1573 cm^{-1} indicating the presence of aromatic hydrocarbons and benzene rings. Similar to the raw sample at 1157 cm^{-1}, deformations of C-H and C-O bonds are noted suggesting presence of lignin compounds [90]. This can be confirmed when observing spectra from 1000 ºC, where this peak is not seen. The 600 ºC is sufficient to degrade cellulose and hemicellulose, but some of the lignin component remains. Only further temperature increments can completely degrade biomass so that no specific organic group can be identified. It should be mentioned that several additional peaks can be seen in char spectra from 600 ºC in the range between 865-500 cm^{-1}, corresponding most probably to hydrocarbons.

Analysis of mixture char shows similar observations. At 600 ºC, most compounds are degraded and converted into volatiles. Slight bending of aromatic rings can be seen at 1575 cm^{-1}. Similar to individual PP sample, intense stretching occurs at 1018 cm^{-1}. The peak absorbance is pronouncedly lower than individual PP since the share of PP in the mixture is only 25%. Even though this peak seems to be the most prominent in char at 600 ºC. Moreover, similar to individual SD at 600 ºC, several peaks are observed between 867-670 cm^{-1}, suggesting the presence of hydrocarbons. Finally, in the case of mixtures char from 1000 ºC, the vast majority of organic compounds are completely degraded and there are almost no clear peaks to identify the remaining compounds. The only pronounced peak is at 1070 cm^{-1}, representing the deformations in C-O-C bonds.

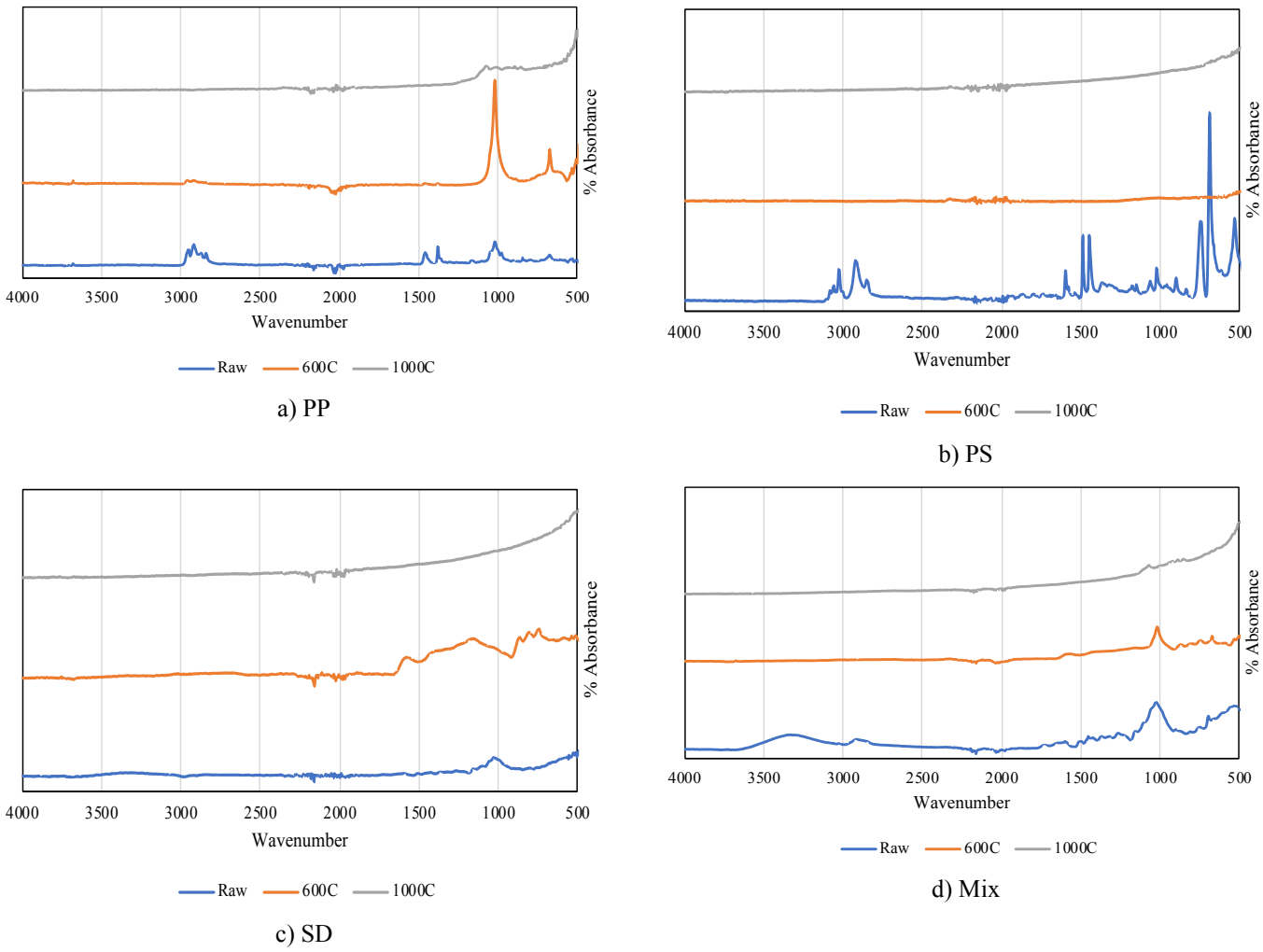

Figure 11 - FTIR spectra from investigated raw and charred samples

3.2.4. Comparison with other studies and summary of main observations

The results obtained from 3.2.2 were further compared to related studies from the literature to draw conclusions from a critical perspective. Suriapparao et al. [58] investigated the co-pyrolysis of PS and PP with different types of biomass, including mixed wood sawdust. Results from the ultimate and proximate analysis show similarities, as well as product yield for SD and PS, while in the case of PP main difference is in the oil yield. This study reports almost 15% higher oil yield, which is unsurprising since the PP can be produced in various forms depending on the application. Regarding the mixtures with biomass-plastic ratio 1:1, oil yield was 60% in the PS case, with a notable gas share of 27%. In the case of PP-SD, oil yield was only 30%, with almost 54% of gases. PS-derived oils were mostly composed of monoaromatics and polycyclic aromatic hydrocarbons. On the other hand, PP oils were composed of aliphatics, PAHs, and various oxygenated compounds with a lower share. The low oil yield for PP and rubberwood seed co-pyrolysis was also reported in a study by Izzatie et al. [91], with only 37%

noted at 550 ºC. Simultaneously, the gas yield was between 40-70% in the temperature range of 450-600 ºC. Nguyen et al. [92] co-pyrolysed PS and pine SD showing a great reduction of oxygenated and acetic compounds with a simultaneous increase in heating value. Nevertheless, the used temperature of 500 ºC seems to be slightly too low due to higher char yield. The reduction of oxygenated compounds with only a slight introduction of PS to mixed wood SD was also confirmed in a study by Stančin et al. [78]. Furthermore, this study shows that only 25% of PS in the mixture will greatly enhance aromatic selectivity. Nisar et al. [93] showed that the polymers recovered from mixed waste should be pre-treated to avoid a higher yield of oxygenated compounds, especially acids. Finally, Li et al. [89] investigated the gasification potential of PS and PP, obtaining very limited gas yield without using CO_2 as a gasification agent. This suggests that PS and PP might be more appropriate for pyrolysis than gasification.

3.3. Results from thermogravimetric and kinetic analysis

This section reveals results from the thermogravimetric, thermal and kinetic analyses of investigated samples. The main focus is on the results from the thermogravimetric and thermal analysis of mixtures with 50% SD_2, 25% PS, and 25% PP. Additionally, results from the kinetic and thermodynamic analysis of two-component biomass-plastic mixtures are discussed. The aim of such analysis was to determine the decomposition mechanism, the influence of the heating rate and mixture composition on process dynamics and calculate kinetic and thermodynamic parameters. Observations from this analysis are useful for a better understanding of feedstock interaction and process dynamics.

3.3.1. Thermogravimetric and thermal analysis of a proposed three-component mixture

Thermogravimetric analysis is typically applied as a preliminary experimental method to determine the decomposition mechanism of the sample. Plastic samples, such as PS and PP, have been widely investigated [59], [91], [93], and results from their analysis are mostly very similar among the studies. This is because polymer materials are built from monomer units which decompose simultaneously in a very narrow temperature range [93]. Discrepancies can occur if plastic is heavily treated with additives in the production stage or due to some external impurities collected during the exploitation stage. Plastic samples used in this study have degradation mechanisms already reported in the literature and corresponding to the results from

their proximate analysis (Table 2). Since the share of ash and FC is initially low, the remaining solid residue at the end of the process is also expected to be low.

PS starts to decompose at around 350 ºC with a very steep mass loss in a single step. At 450 ºC, decomposition is finished, with a final mass residue of only 1.1%. Similarly, PP decomposition starts at a slightly higher temperature of 400 ºC and continues until 490 ºC, where most of the sample is already decomposed, resulting in a final mass of 3.7%.

Biomass decomposition exhibits a more complicated degradation mechanism than plastic samples. It consists of three structural constituents: cellulose, hemicellulose and lignin, which are degraded in different temperature ranges. In addition, even the same kind of biomass could express different degradation mechanisms because of ash or moisture contents. This is especially evident when it comes to ash content, which is a consequence of the mineral presence and related to the type of soil where biomass was grown [94]. The SD used in this study starts with moisture evaporation until ~200 ºC with a mass loss of about 7%. This step is immediately followed by the most intensive stage of degradation, where mostly cellulose and hemicellulose are decomposed. Between 200 and 400 ºC, most of the initial sample mass has deteriorated, and the residue is only 23% of the initial mass. Further heating results in additional mass loss, even though degradation intensity slows down. At 500 ºC remaining mass is around 18.5%, which is further reduced to 15.5% at 600 ºC. At the end of the process, the mass residue is only 12% of the initial mass. Between 600 and 1000 ºC, only 3% of the sample mass is decomposed, suggesting that selected SD could be a promising feedstock for pyrolysis since most of the sample is decomposed when reaching 600 ºC.

For the degradation of the biomass and plastic mixture, similar to the individual SD, moisture evaporation starts immediately at the beginning of the process and goes up to 130 ºC with a total mass loss of approximately 4%. Mass loss is slightly less pronounced than individual SD but corresponds to moisture content from the proximate analysis. The primary decomposition step starts at around 250 ºC with cellulose and hemicellulose degradation and continues up to approximately 400 ºC. Even though this area correlates with individual SD degradation mechanism, the introduction of plastics reduces the intensity of decomposition and shifts toward slightly higher temperatures. At approximately 400 ºC, where 60% of the mass is left, the degradation mechanism shifts due to initiated plastic degradation. From individual samples, it was visible that plastic degradation is very intense and in a narrow temperature range. The same is noticed for the mixture, even though the degradation intensity is lower than for individual plastics, probably due to charred residue from the previous stage, which interferes with heat transfer. By reaching 500 ºC, most of the sample is already decomposed,

and the remaining mass is only 13.2%. Further temperature increments have almost negligible effects on final mass. At 600 ºC, solid residue accounts for 12% of initial mass, which can be only reduced to 10% if the sample is heated up to 1000 ºC. TG curves for investigated samples are given in Figure 12.

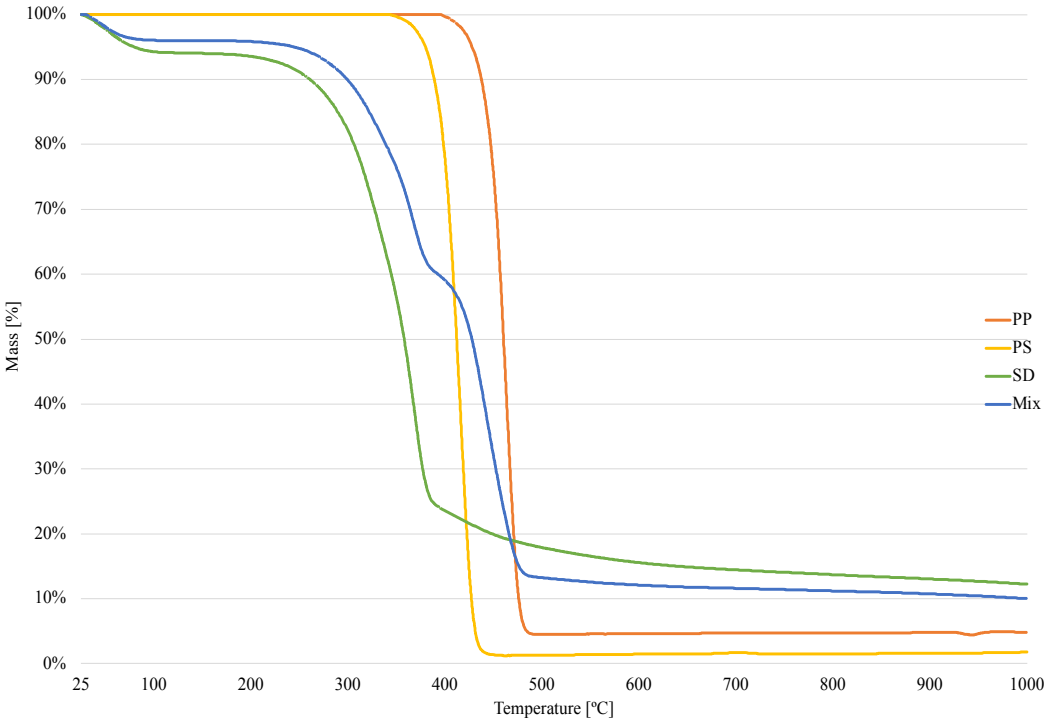

Figure 12 - TG curves of individual samples and mixture

The thermal analysis results are complementary to the results from TGA and are presented in Figure 13. Between 100 and 200 ºC, the endothermic peaks indicating moisture evaporation can be noticed for all samples except for PS. In the case of SD, this peak is related to the evaporation of strongly bound water. PP showed a pronounced peak, which can be attributed to the melting of the PP fibres without mass loss, which occurs at 170 ºC [95]. The primary decomposition stage for PP starts around 400 ºC, even though changes in specific heat can be observed already at 300 ºC when vaporisation is initiated. By 500 ºC, the sample is completely decomposed, and specific heat is reduced to only 0.5 MJ/m^3. At around 250 ºC, slight fluctuations in specific heat can be observed for SD and mixture. Since cellulose, hemicellulose and lignin are decomposed in this range, this is expected. At 500 ºC, the specific heat for SD becomes constant, indicating that the main decomposition phase is completed. Biomass decomposition generally consists of endothermic peaks in the early stages when moisture is evaporated (100-150 ºC) and at the beginning of cellulose and lignin decomposition (320-360 ºC). Slight exothermic reactions are observed between these areas, already reported in the

literature [96]. On the other hand, in the case of the mixture, specific heat sharply increases to almost double values before reaching 400 ºC since the plastic components decompose immediately after the SD is carbonised. When comparing the results, it is clear that this sharp increase is a consequence of PS presence. Individually, PS undergoes significant and intensified changes in a very narrow temperature range where specific heat dramatically fluctuates. Between 400 and 450 ºC, a tremendous increase in specific heat is noticed, with a peak at 431 ºC. Shortly after the decomposition, specific heat drops back to a similar level as the other samples. Finally, it is important to observe that the decomposition of all samples is mainly completed at 500 ºC, which indicates that for the maximised yield of volatiles, there is no need to heat the sample further.

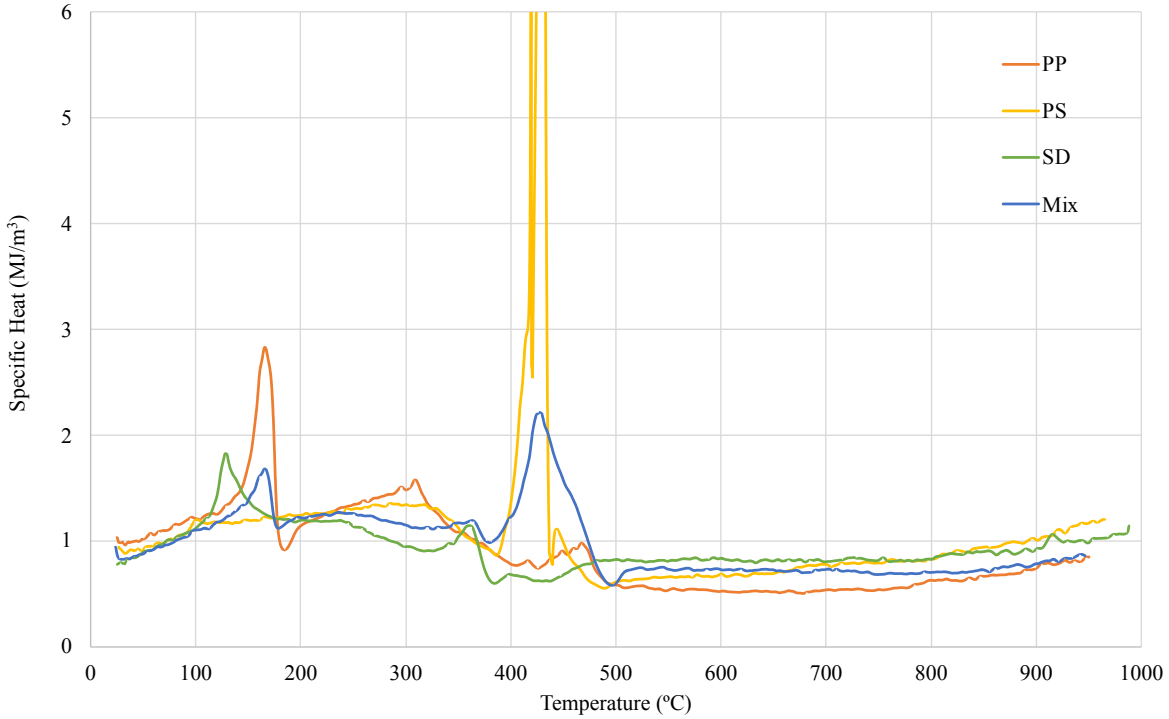

Figure 13 - Specific heat of investigated samples

3.3.2. Thermogravimetric and kinetic analysis of two-component biomass-plastic mixtures

The thermal degradation of mixtures with PS and PP is presented in Figure 14 and Figure 15, respectively. It is observed from TG curves that the samples with 25 and 50% plastic content express two stages of degradation. The first stage, up to 400 °C, is primarily due to the decomposition of the biomass component, while the second stage represents plastic decomposition. Besides, for the mixtures with 25% of plastics, it can be noted small evaporation step below 100 °C accounted for less than 5% mass loss. The influence of the

heating rate on this first stage is just slightly visible for investigated mixtures of both plastic materials. In the case of PS-containing mixtures (Figure 14), increment of heating rates shifted the temperatures of the first peaks for approximately 5 °C with each increment of the rate, from 345 °C for 5 °C/min to 355 °C for 20 and 30 °C/min. Similar behaviour is also noted for PP (Figure 14), with exactly the same positions as the first peaks. This implies that at this temperature range, only sawdust is decomposed. It should be noted that the increment of plastic content greatly reduces the intensity of the first peak. Even though this is expected, the reduction is quite pronounced for the mixtures with an equal share of both feedstocks, suggesting that plastics may hinder the complete sawdust decomposition in the first stage. This phenomenon was already reported by Han et al. and here confirmed for both investigated plastics [97]. This might directly affect the final product yield and distribution in the pyrolysis process but should be examined more. The end of the first stage is at about 375 °C for the case of 5 and 10 °C/min, while for higher heating rates of 20 and 30 °C/min, the end temperature is increased to 390 °C. As expected, the mixtures where sawdust is the main compound have a higher mass loss in this first stage due to the decomposition of cellulose and hemicellulose. Almost half of the mass sample is decomposed in the first stage. As the share of the plastic fraction increases, the mass loss decreases. Therefore, for the mixtures with an equal share of both feedstocks, the remaining masses at the end of the first stages are between 70-75%. Further increment of plastic content to 75% of the mixture composition reduces mass loss even more, and the remaining mass is up to 80%. It should be emphasised that the heating rate has a limited influence on mass loss in the first stage. A slow heating rate of 5°C/min ensures better heat transfer and release of volatiles. Therefore, the mass losses are more pronounced in this case. Nevertheless, the differences between the slowest and fastest heating rates are less than 10% in sample mass. Finally, it can be stated that the decomposition mechanism of the first stage is more influenced by the mixture composition rather than the heating rate [98]. The TG and DTG curves clearly show that fast-heating rates of 20 and 30 °C/min express almost identical behaviour. The only visible stand-out is noted for 5 °C/min, even though this influence also disappears as the share of plastics increases.

The second stage follows up immediately after the completion of the first one. In the case of PP-derived mixtures, the lag between the two stages of degradation is slightly more pronounced, especially for the mixture with 25% of PP (plateau in Figure 15a). The second stage almost overlaps with the first one for PS-containing mixtures, which can be expected since the onset temperature for individual PS degradation is 375 °C. Consequently, the second peak corresponding to plastic decomposition appears earlier in the case of PS than PP. The

main degradation step of the second stage for PS-containing mixtures occurs between 420 and 430 °C and increases with the increment of the heating rate. The sawdust has a limited influence on the position of the second peak since it is just slightly shifted to higher temperatures compared to individual PS analysis. The end of the second stage is slightly above 450 °C, similar to individual PS decomposition, which confirms that the influence of SD on the second stage is limited. Nevertheless, the influence of the mixture composition is a crucial parameter for the final mass. A mixture with 25% of PS has a quite high final mass of residue, which accounts for the 25% of the initial mass. This is even higher than the results from individual SD analysis, where approximately 20% of the final mass was observed. Further increment of the PS reduces the final mass below 20%, with only minor differences observed between applied heating rates. Generally, the heating rate has a moderate influence on the second stage of degradation. While the impact on final mass is almost negligible, the intensity and the position of the second peak are highly dependent on this parameter. An increment of the heating rate shifts the peak positions and end temperatures to higher values, broadening the range in which decomposition occurs. Besides, the degradation intensity is considerably higher with high heating rates, suggesting that most volatiles are released in the narrow temperature range shortly before the process completes. Due to that fact, the residence time of volatiles released in the second stage is reduced, which might benefit the yield of condensable products obtained as bio-oil [99].

For the PP-containing mixtures, the second peak's position corresponds to the peak from individual PP decomposition. There are no visible differences among the investigated mixtures, which means that PP decomposition dominates in this stage. This is also supported by the fact that the mixtures with a higher portion of PP have a broader range in which decomposition occurs, similar to individual analysis. Nevertheless, there are pronounced differences in terms of applied heating rates. An increment of heating rate firstly shifts the temperature of the second peak to higher values but also broadens the range in which decomposition takes place. This difference between the slowest and fastest applied heating rate can be up to 40 °C in terms of ending temperature. Since both investigated parameters, heating rate and mixture composition, have a notable impact on the second stage, the differences between final masses are more pronounced. The mixture with 25% sawdust has a final residue of 20%, similar to individual SD. This is further reduced by incrementing plastic content to 15 and 10%, respectively. It is interesting to notice that in the case of a mixture with 75% of PP, the lowest final mass (5%) is noted for the heating rates of 10 and 20 °C/min, while almost 10% is observed for 5 °C/min.

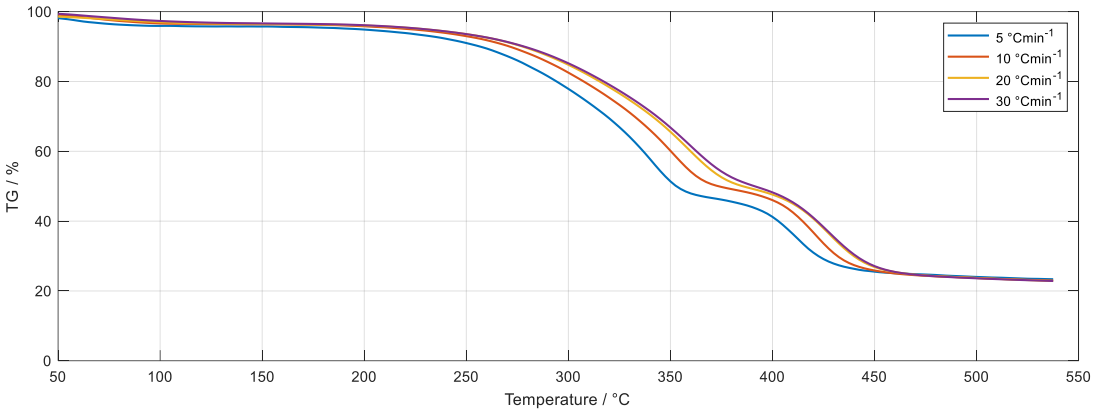

a) 25% PS

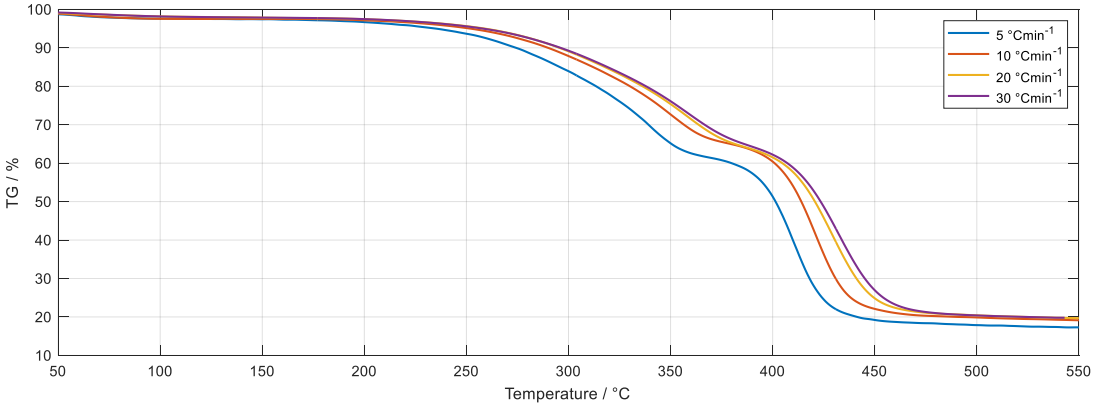

b) 50% PS

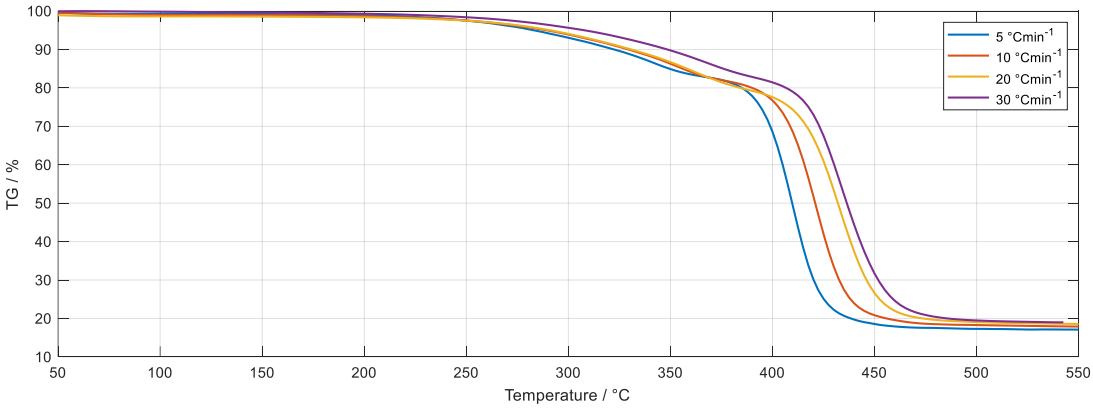

c) 75% PS

Figure 14 - TG curve for SD-PS mixtures

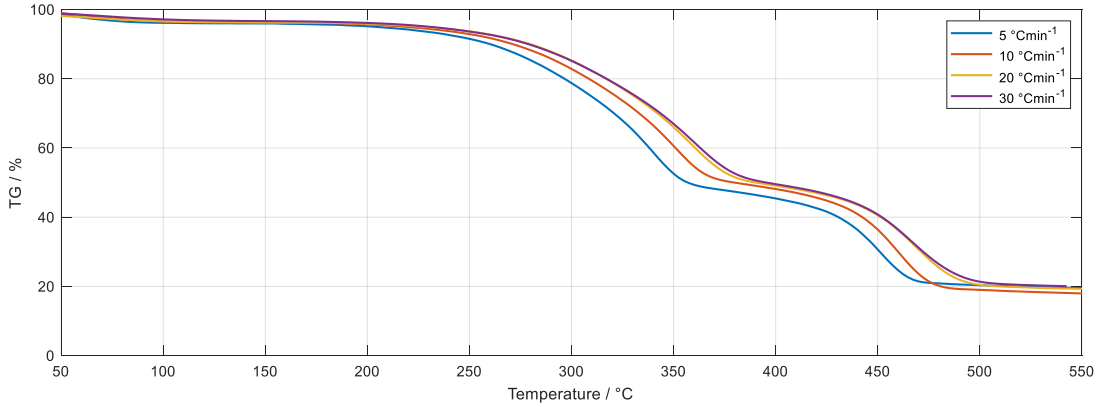

a) 25% PP

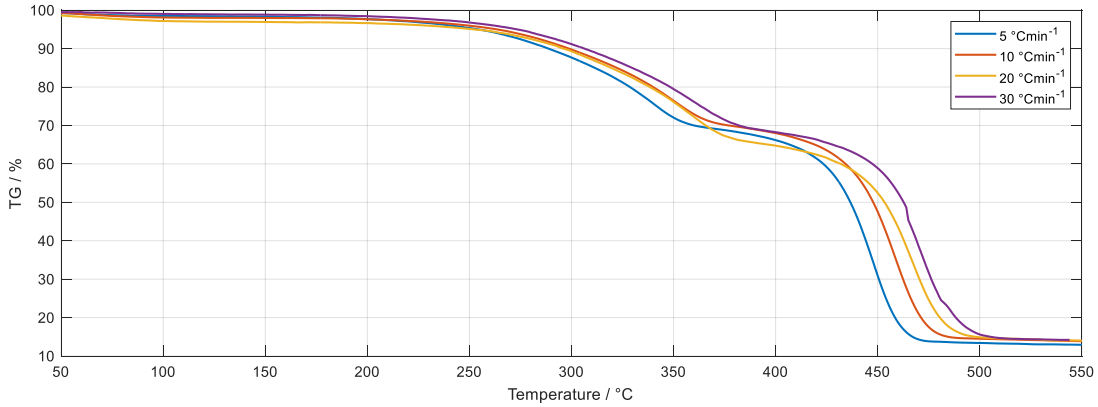

b) 50% PP

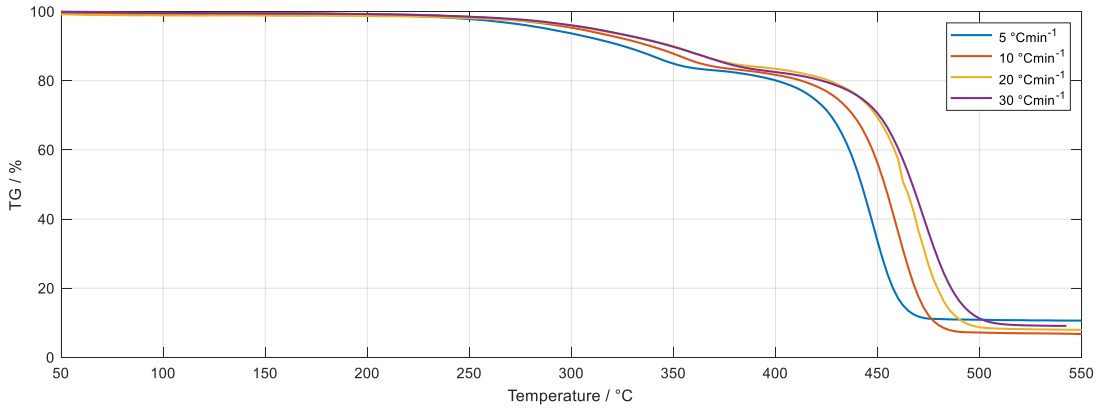

c) 75% PP

Figure 15 - TG curves for SD-PP mixtures

Thermogravimetric analysis is also conducted for sawdust-PUR mixtures, and the results are presented in PAPER 4. Nevertheless, since the comprehensive analysis showed that PUR is not a suitable feedstock for co-pyrolysis, they won't be discussed in detail here. Even though, observations which are derived from this work could be very valuable in finding an appropriate method for waste management of polyurethanes.

3.3.3. Kinetic and thermodynamic analysis of selected feedstock

Similarly to the previous section, the analysis of kinetic and thermodynamic parameters for sawdust co-pyrolysis with PS and PP are presented here, while the results from SD-PUR analysis can be found in published work.

Results for all investigated mixtures and methods are summarised in Figure 16. The mean activation energies reported for the SD sample are 241 kJ/mol for Friedmann and around 229 kJ/mol for other used methods. Nevertheless, mean activation energies don't give a good overview of the process since values are greatly dependable on the conversion range (α). Hence, the division of SD decomposition based on conversion ranges is the following: the first stage (α=0.05-0.45), the second stage (α=0.45-0.7), and the final stage (α=0.7-0.85). In the first stage, the E_a sharply increase as a consequence of moisture evaporation. After this point, values are gradually increasing until reaching α=0.5. In this area, most of the cellulose and hemicellulose are decomposed. Between α=0.5-0.8, the values remain constant. This corresponds to the TG curve, where a linear decrease in mass is observed because of lignin decomposition. After α=0.8, values are dramatically increasing again, which is expected since, at that point, most of the sample is already decomposed, and the remaining share requires significant energy input.

While E_a values are increasing throughout the SD decomposition, a complete reversal trend is observed for plastic samples. In the case of PS, the highest values (~290 kJ/mol) are noted at the beginning of the process for α=0.1. As the decomposition proceeds, values are gradually decreasing to the final value of approximately 220 kJ/mol at α=0.9. For the PP, the initial E_a is slightly lower than PS, about 280 kJ/mol. When degradation starts, a minor increment in E_a is seen at α=0.2, which is then immediately followed up by a continuous linear decrease to the final value of 200 kJ/mol.

The activation energies from investigated mixtures show interesting behaviour. For the mixtures where SD is the dominant constituent (75% share), the introduction of plastics increases the E_a at the beginning of the process. This suggests that plastic presence influences moisture evaporation in a way that more energy is required to initiate the process. Constant values for E_a are then observed until reaching α=0.6. At this point, the decomposition mechanism shifts from biomass to plastic feedstock, sharply decreasing values to even lower than those reported for individual samples. This is followed up by a sharp increase in E_a for α=0.7-0.9, which implies that biomass decomposition was hindered in the previous stage, resulting in a tremendous increase in energy demand at the end of the process.

Similar trends for the mixtures with equal shares of both constituents are observed for the first stage of decomposition. The introduction of plastics increases the E_a to initiate the decomposition process, which is followed up by constant values until reaching the point at which the decomposition mechanism shifts. The difference between PS and PP containing feedstock is at which point this shift happens. In the case of PS, this happens at α=0.4, while for the PP, this is at α=0.3. Before reaching this point, activation energies are decreasing, similar to mixtures with 25% of plastic content. Once again, the shift in the decomposition mechanism requires tremendous energy input, resulting in a dramatic increase in E_a. This increment seems to be more pronounced for the mixture with PS since differences in E_a, in this case, are almost 200 kJ/mol, compared to 100 kJ/mol for the PP mixture. In the second stage, the activation energy slowly decreases, which is completely opposite to the mixtures with 25% of plastics and more similar to individual PS and PP behaviour. Nevertheless, the reported values for E_a are higher than in individual samples, which is a direct consequence of feedstock interaction during the process.

For the mixtures where plastic is the dominant constituent with a 75% share, reported values of activation energies to have almost identical behaviour as individual plastic samples, therefore, they won't be discussed further.

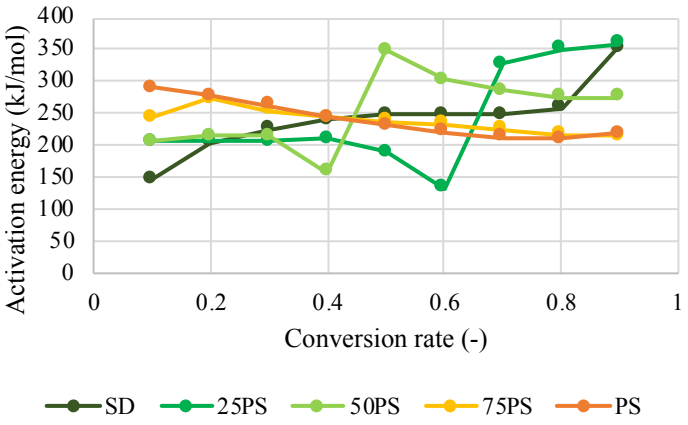

a) Friedman

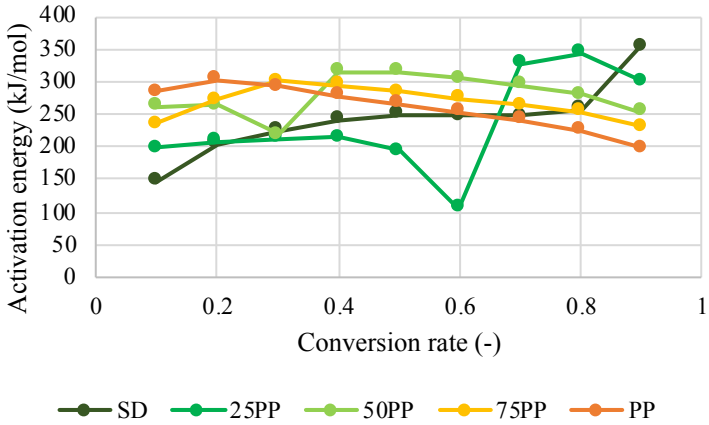

b) Friedman

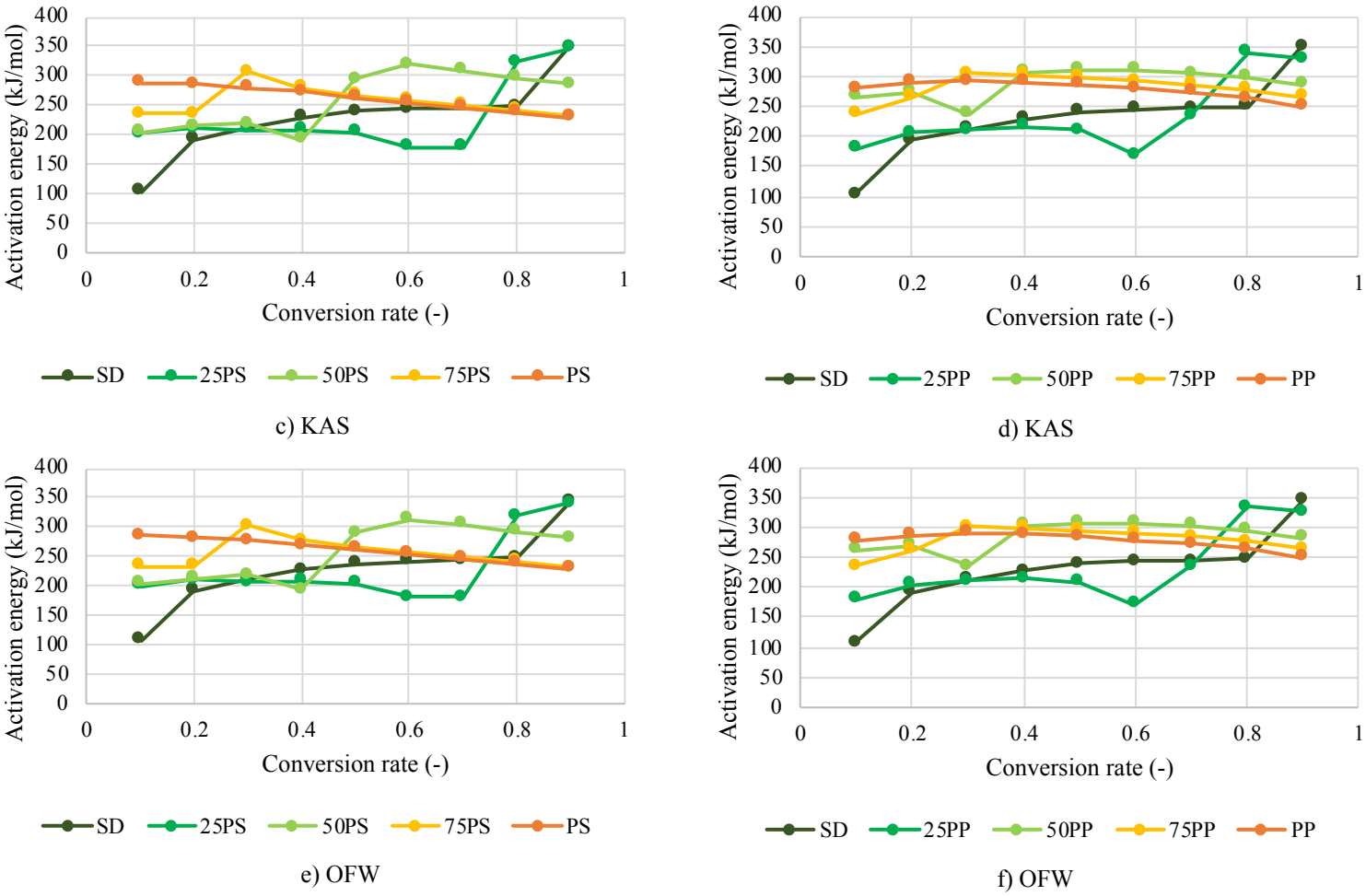

Figure 16 - Calculated activation energies for PS-containing mixtures left (a, c, e), and PP-containing mixtures right (b, d, f)

Thermodynamic parameters are calculated using apparent Friedman's activation energies; therefore, the curve trendlines are more less like those presented in Figure 16.

The analysis of the pre-exponential factors (Figure 17a) and b)) shows that all investigated samples express high reactivity immediately at the beginning of the process ($A>10^{10}$ s^{-1}). In the case of SD, they are increasing as the conversion proceeds and are between 10^{13} and 10^{27}. At the same time, plastics have high values at the beginning of the process ($1.8x10^{20}$, and $7.6x10^{17}$ s^{-1} for PS and PP, respectively), but this reactivity fades away as conversion goes on. The pre-exponential factors for mixtures show very similar behaviour to activation energies. The step increment is noticed after the decomposition mechanism shift, implying the samples' high reactivity. Since the values continue to increase in the second stage, released volatiles from the SD degradation in the first stage, coupled with the volatiles released in this stage, are frequently colliding inside the reactor. This steep increment in reactivity suggests that plastic hinders sawdust decomposition in the previous stage, which reflects in high volatile interaction in the second stage.

The changes in enthalpy (Figure 17c) and d)) are firmly following the activation energy trendline. From the thermodynamic perspective, this implies that minor introduction of plastic might reduce the required energy needed to initiate the process, but this will inevitably result in hindered decomposition in the first stage and a dramatic increase in energy demand in the second stage.

Changes in entropy give information about the level of order inside the system Figure 17e) and f)). Higher entropy also implies higher reactivity of the system. As expected, the highest level of disorder for analysed mixtures occurs after the change of decomposition mechanism. Therefore, it can be stated that interaction between biomass and plastic-derived compounds can only happen in the second stage of decomposition. In this stage, temperatures are sufficient to initiate plastic decomposition and support the complete decomposition of the solid and volatile products obtained in the previous step.

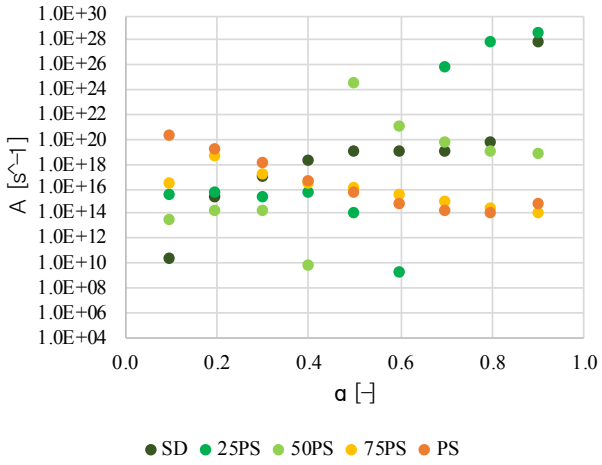

a)

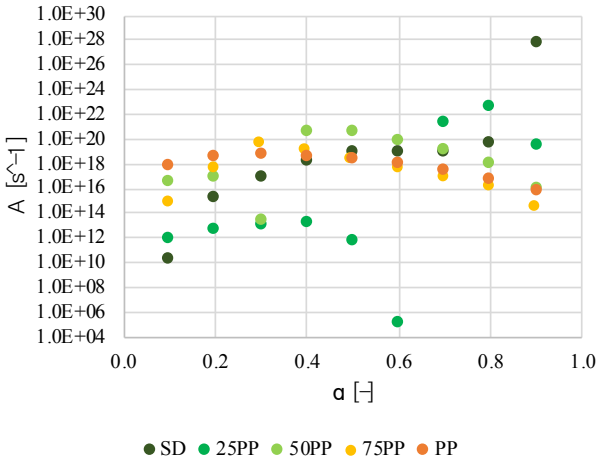

b)

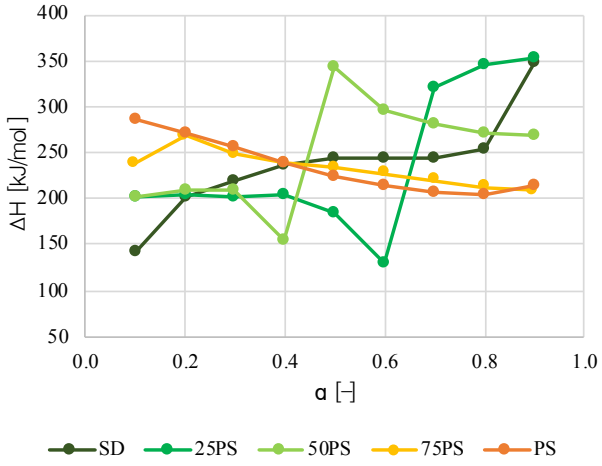

c)

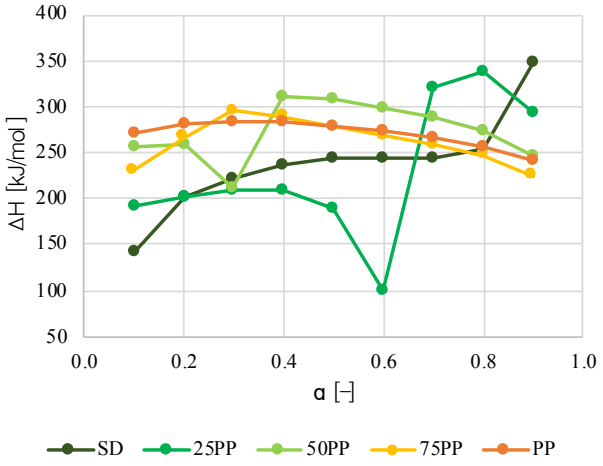

d)

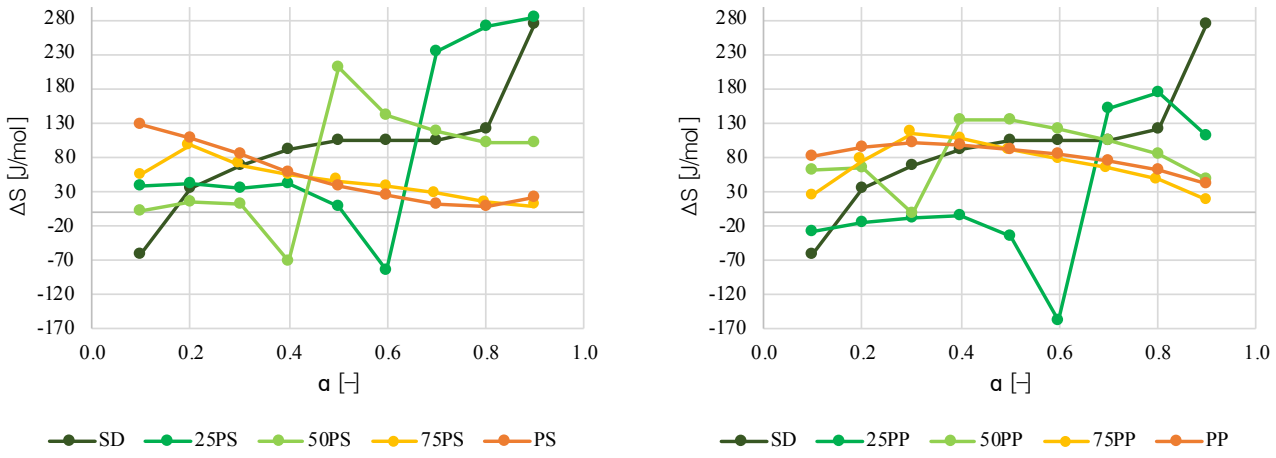

e) f)

Figure 17 – Selected thermodynamic parameters (a-b) pre-exponential factor, (c-d) changes in enthalpy, (e-f) changes in entropy

3.4. Results from the evaluation of the synergistic effect and prediction model development

This section presents the observations from the evaluation of the synergistic effect. Moreover, these observations are further discussed from the perspective of how they can be utilised to develop a methodology or model for predicting product yield.

3.4.1. Evaluation of the synergistic effect

The analysis of the synergistic effect starts with its evaluation for two-component mixtures (Table 6). In both cases, for PS and PUR-containing mixtures, the highest level of synergy is observed for a liquid fraction for mixtures with 25% of plastic content. In the case of mixtures with 25% PS, the positive synergy level of almost 15% is calculated entirely at the expense of gaseous fraction (-19.3%). The yield of solid residue is slightly higher than expected but still below 5%. As the plastic content increase in the mixture, the synergistic effect fades away. Interestingly, this trade-off between liquid and gas fractions follows the linear trend. With each increment of plastic content for 25%, the level of synergy for both liquid and gas fractions decrease by approximately 5%. Even more interesting is to observe that this trend is noted in both cases for PS and PUR, even though the results from the rest of the analysis greatly differ. The main difference, in this case, can only be observed for the yield of solid fraction. With the increment of PS content in the mixture, the level of synergistic effect fades away, and values approach what is theoretically expected. In the case of PUR, the level of synergy is constant

for a solid fraction and accounts for approximately 6%. Besides, for the mixture with 75% of PUR, an even lower yield of liquid fraction is observed than was calculated.

Table 6 - Evaluation of the synergistic effect for two-component mixtures

Sample	Liquid fraction			Gas fraction			Solid fraction		
	Cal.	Exp.	ΔY	Cal.	Exp.	ΔY	Cal.	Exp.	ΔY
SD	-	31.3	-		48.1	-	-	20.5	-
0.25 PS	47.5	62.3	14.8	36.3	17.0	-19.3	16.2	20.7	4.5
0.5 PS	63.7	73.2	9.5	24.5	11.1	-13.4	11.8	15.7	3.9
0.75 PS	79.8	83.8	4.0	12.7	6.1	-6.6	7.4	10.0	2.6
PS	-	96.0	-		0.9	-	-	3.1	-
0.25 PUR	38.9	48.5	9.6	40.3	24.2	-16.1	20.9	27.4	6.5
0.5 PUR	46.3	49.9	3.6	32.4	22.7	-9.7	21.3	27.4	6.1
0.75 PUR	53.8	52.1	-1.7	24.6	20.1	-4.5	21.7	27.8	6.2
PUR	-	61.2	-	-	16.7	-	-	22.1	-

There are some very interesting observations from the evaluation of synergistic effect for three-component mixtures. Since plastic accounts for 50% of the mixture composition, but each plastic constituent is present with 25% of the share, it was of great interest to see how this will reflect on the synergistic effect. As can be seen in Table 7, the highest positive synergy is achieved for liquid yield (12.2%). Once again, this trade-off was completely on the expanse of the gas fraction. The yield of the solid fraction was just slightly higher than expected (~3%). Positive synergy for liquid yield is higher than the values observed in Table 6 for mixtures with 50% of plastics. This is a very interesting observation suggesting that the level of synergy could be manipulated by the selection of a multi-component mixture. Nevertheless, the influence and role of biomass content for the synergistic effect remains unknown and should be investigated more. This is especially due to the fact that there are a wide variety of different biomass types which have a different elemental and structural composition which directly reflects the product distribution.

Table 7 - Evaluation of synergistic effect for the three-component mixture

Sample	Liquid fraction			Gas fraction			Solid fraction		
	Cal.	Exp.	ΔY	Cal.	Exp.	ΔY	Cal.	Exp.	ΔY
PS_2	-	97.8	-	-	0.8	-	-	1.5	-
PP_2	-	75.5	-	-	19.9	-	-	4.6	-
SD_2	-	50.4	-	-	34.0	-	-	20.6	-
Mix	68.5	80.7	12.2	22.2	7.1	-15.1	9.3	12.1	2.8

3.4.2. Discussion on methodology for the prediction model development

Prediction of the product yield from the thermochemical conversion processes has recently emerged as a very interesting research topic. Most of the attempts have been made for biomass due to general higher research attention [100]–[102]. Nevertheless, the complex structure of biomass samples most often results in limited application potential for the developed models since they are mostly applicable to the feedstock they are developed for. Changes in biomass type can show great discrepancies between predicted and actual values. Consequently, the prediction of product yield from co-processing is even harder. Besides the inaccuracy of individual models, the feedstock interaction that results in a synergistic effect only increases the uncertainties.

The most important parameters for product yield and which requires special attention are the following:

- Type of the feedstock with their elemental and structural composition
- Pyrolysis temperature that affects the extent and rate of the pyrolysis reactions
- Heating rate which influences the reaction kinetics and degradation mechanism
- Residence time with direct impact on the extent of the conversion and the degree of secondary reactions
- Feedstock particle size that influences heat and mass transfer rates during the process
- Catalysts which can promote specific pyrolysis reactions and selectivity toward preferred chemical compounds
- Reactor type with their geometries

It is important to note that the effect of these input parameters can be interdependent and greatly vary depending on the specific feedstock and pyrolysis conditions used. Nevertheless, for co-pyrolysis, the type of feedstock seems to be a critical factor for yield, but also product quality [103].

Firstly, it is important to discuss the structural composition of considered feedstock and how they affect the product yield. For biomass, the chemical composition can vary widely depending on the type of biomass and its origin. It typically consists of three main pseudo-components: cellulose, hemicellulose, and lignin. Besides, various minerals, proteins or fats can be found depending on the soil type and cultivation conditions. Cellulose and hemicellulose are carbohydrates that are composed of glucose and other sugar units, while lignin is a complex aromatic polymer that provides structural support to the plant cell walls. Biomass feedstocks

that are rich in cellulose and hemicellulose can produce more bio-oil with higher oxygen content, while feedstocks that are rich in lignin can produce more char with higher carbon content [100].

On the other hand, the chemical composition of plastics can also vary widely depending on the production process and utilisation purposes. Plastics are generally composed of long-chain polymers made up of repeating units of monomers (i.e. ethylene, propylene, styrene) with additives such as plasticisers, stabilisers, and pigments. In general, plastics are characterised by highly volatile matter that favours the yield of liquids and gases from pyrolysis. As can be seen, the level of structural complexity greatly differs between biomass and plastics. Therefore, it is necessary to know the initial structure of feedstock due to its direct influence on product selectivity [104].

Even more important seems to be to know the initial ultimate and proximate parameters of the samples. The ultimate analysis provides information about the feedstock's elemental composition and involves determining the feedstock's carbon, hydrogen, nitrogen, sulphur, and oxygen contents. The information obtained from the ultimate analysis can be used to predict product yields in different ways. For example, the carbon and hydrogen contents of the feedstock can be used to calculate the theoretical heating value and assume the hydrocarbon content of derived products. The presence of nitrogen and sulphur is generally not welcomed since it lowers the exploitations properties of obtained products. The oxygen content of the feedstock is particularly important in co-pyrolysis, as it can affect the trade-off between final products. Higher oxygen share will result in higher oxygen-containing compounds in derived oils, but even more, it will result in a high yield of carbon dioxide and monoxide in the gaseous fraction. Furthermore, the elemental composition will directly influence the compound's selectivity and quality inside the obtained products, while its influence on product distribution itself is limited. This is supported by the fact that elements detected in the initial sample composition are later observed in all obtained products. This implies that they will be distributed to all pyrolytic products with random mechanisms rather than following some pathway. This is confirmed by carried out experiments.

Simultaneously, the proximate analysis could be an important tool in the prediction of product yield from co-pyrolysis because it provides information about the key components that directly reflect on product distribution. Such analysis typically involves the determination of the moisture, ash, volatile matter, and fixed carbon contents of the feedstock. The moisture content of the feedstock is important because it affects the heating value and the pyrolysis temperature required to achieve the desired product yields. Excessive moisture in the feedstock

can also lead to incomplete pyrolysis and low product yields. Ash content noted at the beginning of the process will surely result in solid residue at the end. In the meantime, it can serve as a catalyst for secondary crackings of volatiles and their conversion toward lower carbon numbers. The volatile matter of the feedstock is the most important parameter for the yield of liquid and gaseous fractions. High volatile matter content results in a high share of liquids and non-condensable gases. Like ash content, the fixed carbon also affects the char produced at the end of the process and high fixed carbon results with high solid residue [105].

To most convenient way to use results from ultimate and proximate analysis could be through their incorporation into a statistical model by using the input parameters as independent variables. Nevertheless, a significant problem, in this case, represents the lack of reliable data in the literature that could be used for required statistical analysis. Process conditions such as temperature, heating rate, and residence time often significantly vary between experimental investigations. This means that even though different process conditions have been investigated, the available data for each of them are quite limited. This results that the proposed models having a very limited application scale [106]. Most efforts have been given to develop empirical models that use experimental data to develop mathematical equations among input variables. Statistical analysis, such as regression analysis or artificial neural networks, can then be applied to establish correlations between input parameters [107]. Some of the commonly used empirical models can be additive, multiplicative, statistical or artificial neural networks. The additive model assumes that the product yield from the co-pyrolysis of biomass and plastic feedstock is equal to the sum of the product yields from individual pyrolysis processes, and there is no interaction between feedstock during co-pyrolysis. The multiplicative model, on the other hand, assumes that the feedstock interacts during the process and that product yield is equal to the product of the product yield from individual pyrolysis processes. This model assumes that there is a synergistic effect, but it doesn't quantify its influence. Statistical models use regression analysis to develop mathematical equations and correlations between input parameters, such as the type and composition of the biomass and plastic feedstocks, the pyrolysis conditions, and the reactor type. Finally, artificial neural networks use machine learning techniques to learn from experimental data and develop complex nonlinear relationships between the input parameters and the product yield.

Since experimental investigations show that feedstock does interact during the process, the additive model can be discharged from further analysis. Artificial neural networks require extensive input data but also significant computational resources and proficiency, which makes

them complicated to run. Finally, multiplicative and statistical models are showing the most perspective to be developed anytime soon.

In the case of the multiplicative models, it is necessary to find a way hot to include synergistic effect into the equation. It is known that the synergistic effect can be higher under certain conditions, such as lower pyrolysis temperatures, longer residence times, complementary properties of the waste materials, like differences in their thermal stability, reactivity, and composition, and finally, optimal mixing ratio. The mixing ratio seems to be the most influential parameter based on experimental investigations, and even though it may vary on the type and composition of the mixture, it is best to balance the amounts of the waste materials to achieve the highest synergistic effect (Table 6 and Table 7).

The statistical model for the prediction of product yield uses regression analysis to develop a mathematical equation and correlations between input parameters. The regression analysis involves fitting a mathematical equation to a set of experimental data by minimising the sum of the squared differences between the predicted and actual product yield values. The resulting equation can then be used to predict the product yield for new sets of input parameters. The accuracy of the statistical model depends on the quality of the experimental data used to develop the model and the choice of input parameters. Some general steps for developing a statistical model consist of the following activities:

- Experimental data collection for different input parameters, such as the type and composition of the feedstock, pyrolysis conditions, and reactor type. The product yield is measured and recorded for each experiment.
- Data pre-processing by removing outliers, missing values, and other anomalies that can affect the accuracy of the model.
- Model selection based on the nature of the experimental data and assumptions. Linear, polynomial or stepwise regression are some of the commonly used regression models.
- Model fitting with experimental data using a regression algorithm, such as least squares. The algorithm estimates the coefficients of the model equation that best fit the experimental data.
- Model validation where the accuracy is evaluated using statistical measures such as the coefficient of determination (R-squared) or root mean squared error (RMSE). The model is also validated using independent experimental data to ensure its reliability.

Nevertheless, all models are developed and validated on specific types of feedstock and process conditions and, when applied elsewhere, show notable differences between predicted

and experimental yield. The lack of reliable experimental data and its dispersion over a wide range of observed parameters makes the development of the universal model for the prediction of product yield almost impossible. During this research, a significant amount of experimental data is collected and analysed from the perspective of prediction model development. Nevertheless, coupling these data with the literature showed significant constraints due to the different process conditions. Therefore, developing a reliable prediction model did not give reliable results. To overcome such problems in future work, several recommendations are drawn that can help tailor methodology for the prediction of product yield that could be applied to a different type of feedstock:

- Firstly, knowing the initial parameters from the ultimate and proximate analysis, as well as the structural composition of the sample, is an absolute necessity. Based on a wide range of experimental data, mathematical correlations should be established. Instead of aiming to achieve a high statistical agreement for one type of feedstock, research should focus on achieving a satisfactory level for a wide range of feedstock, even if accuracy is slightly compromised.
- Secondly, by narrowing the research focus to temperatures between 500 and 600 ºC, the influence of this parameter could be greatly reduced, which would help in developing the universal model. Experimental investigation in this research showed that in the case of co-pyrolysis, the influence of the heating rate is limited since the mixture composition plays a dominant role in product dynamics. In addition, the analysis of the synergistic effect showed that this influence is the strongest for a lower share of plastic content inside the mixture. All this suggests that the research focus should shift toward the investigation of mixture blends with different types of feedstocks and a share of plastics up to 50% while maintaining the same process conditions.
- The final step in developing a prediction model should be coupling the results from the initial ultimate and proximate analysis with the final synergistic effect analysis. First, it is needed to achieve high accuracy and statistical agreement for independently developed correlations between the results from ultimate and proximate analysis and final product yield for individual samples. Secondly, since the feedstock interacts during the co-pyrolysis, this will lead to the occurrence of a synergistic effect, which consequently affects product distribution. Therefore, by conducting a series of experimental investigations, appropriate correlations should be established between the

share of plastic content and the level of synergy. Again, with high accuracy and repeatability. Once when established correlations give a could prediction for the product yield from the individual sample analysis, they could be used to calculate theoretical product yield. This theoretical yield can further be used to calculate the theoretical yield of products from co-pyrolysis. Finally, at this point, a calculated level of synergy from established correlations could be introduced, giving the approximate values for product yield from the process.

3.5. Selected results from Life cycle assessment (LCA) analysis

In the scope of the work, three scenarios are considered based on the current waste management methods used to deal with end-of-life plastic waste. This implies that mechanical recycling is not considered, and pyrolysis is evaluated as an alternative to incineration or landfilling. Each scenario represents a specific country: S1 - Germany, S2 - Croatia and S3 - Australia, but the results are comparable to other countries with the same end-of-life treatment methods. Table 8 summarises the assessed scenarios alongside waste management methods currently used to deal with waste plastics. The values for S1 and S2 scenarios are taken from the ecoinvent database [108], while for the S3 are taken from national strategic documents [109], [110] due to the lack of data in the database. As shown, the S1 scenario is vastly dominated by incineration, while S2 and S3 scenarios are based on landfilling with the difference if they are sanitary or unsanitary. Open dump, in the case of S3, represents a waste plastic leakage to the environment based on [111].

Table 8 - Analysed scenarios in scope of LCA analysis

Scenario	S1 DE	S2 HR	S3 AU
Treatment method		**[%]**	
Incineration	99	1	1
Sanitary landfill	0.5	27	80
Unsanitary landfill		70	10
Open burning	0.5	2	
Open dump			9

3.5.1. Life cycle assessment of proposed co-pyrolysis process

Global warming potential is one of the most important categories when discussing environmental impacts. As shown in Table 9, the greatest savings of CO_2 eq. are in the case of scenario S1 (-574 kg CO_2 eq.). At the same time, S2 and S3 have almost identical values and

positive contributions to this impact category (~400 kg CO_2 eq.). The reason behind the GWP reduction in scenario S1 is due to avoided incineration of waste plastics, which would emit emissions into the air. In the case of S2 and S3 scenarios, waste streams are mostly diverted from sanitary and unsanitary landfills, and credits for this are considerably lower compared to S1. In such cases, received credits are insufficient to compensate for the rest of the process burdens, and overall values are positive.

Table 9 - Summary of environmental impact assessment category

Impact category	Reference unit	S1 DE	S2 HR	S3 AU
Global warming potential	kg CO_2 eq.	-547.0	408.5	394.9
Freshwater ecotoxicity	kg 1,4-DCB eq.	-9.9	-80.1	-84.1
Terrestrial ecotoxicity		2410.2	3823.3	3762.7
Human carcinogenic toxicity		99.8	30.6	40.3
Human non-carcinogenic toxicity		814.3	-2862.9	-2498.0
Marine ecotoxicity		-23.3	-115.9	-122.4
Fossil resource scarcity	kg oil eq.	270.9	153.5	109.2
Fine particulate matter formation	kg $PM_{2.5}$ eq.	3.2	0.5	0.5
Freshwater eutrophication	kg P eq.	1.2	-0.3	-0.1
Marine eutrophication	kg N eq.	0.1	-0.2	-0.1
Terrestrial acidification	kg SO_2 eq.	6.2	1.3	1.3
Ozone formation, Human health	kg NOx eq.	2.9	0.9	0.9
Ozone formation, Terrestrial ecosystems		3.0	0.9	1.0
Ionizing radiation	kBq Co-60 eq.	62.3	13.1	13.7
Land use	m^2a crop eq.	1001.3	700.5	674.2
Mineral resource scarcity	kg Cu eq.	2.1	1.8	1.6
Stratospheric ozone depletion	kg CFC11 eq.	0.0	0.0	0.0
Water consumption	m^3	189.3	158.0	157.0

Results of the toxicity impact categories expressed in kg 1,4-DCB eq. significantly differ between the three considered cases. The proposed process reduces freshwater and marine ecotoxicity, especially when the waste is diverted from landfills (S2-S3). The credits received for avoided landfilling are several times higher than for avoided incineration. In the case of freshwater toxicity, avoided emissions are around 80 kg 1,4-DCB eq. for scenarios S2-S3, compared to 10 kg 1,4-DCB eq. in the case of S1. Credits are even higher in the case of marine toxicity, with savings of more than 115 kg 1,4-DCB eq. for S2-S3, while only 23 kg of

emissions are prevented for S1. Some credits are received for char fraction sent to market, around 11 and 8 kg 1,4-DCB eq. for marine and freshwater ecotoxicity, respectively.

Human carcinogenic impact (HTC) is mainly associated with the sawdust drying process and the combustion of synthetic gas to provide heat. Emissions are not directly related to the combustion itself but to the background process for delivering air for the combustion (27.03 kg 1,4-DCB eq). Similarly, water used for cooling comes with substantial burdens, but most are associated with the distribution network development rather than the pyrolysis process. The HTC is higher in the case of S1 (99.8 kg 1,4-DCB eq.) compared to other scenarios (30.6 and 40.3 for S2 and S3, respectively). This is because avoided incineration requires higher input of fossil fuels to compensate for lost electricity and heat production. Increased demand for fossil fuels consequently requires more mining operations, resulting in rising environmental burdens. Char fraction, which can be sent to market as a lignite substitute, saves around 15% of the emissions related to HTC.

Human non-carcinogenic toxicity shows the most significant differences between scenarios. The S2 and S3 scenarios show a remarkable reduction of emissions associated with HTNC, 2862.9 and 2498 kg 1,4-DCB eq. On the other hand, for the S1 scenario, the process generates significant emissions (814 kg 1,4-DCB eq.) For all scenarios, around 300 kg 1,4 DCB eq. is saved since char is used as a coal substitute which prevents mining operations. Additional credits of 37 kg 1,4-DCB eq. are associated with synthetic gas sent to market.

Terrestrial ecotoxicity (TET) is the category with the highest impact in terms of absolute values. There are several reasons behind these. Firstly, when comparing the results between scenarios, it is noticeable that the treatment methods play an essential role. Avoided incineration brings tremendously higher credits than avoided landfilling, especially in the case of waste PP. Avoided waste plastic landfilling also brings some credits, but not nearly enough to compensate for process burdens. Moreover, significant burdens associated with TET come from sawdust stream flows and feedstock transport to the processing unit. Almost 2000 kg 1,4-DCB eq. is related to the drying process with burdens associated with the production of compression equipment used for air supply. Furthermore, sawdust is heavily burdened with emissions related to various processing techniques like slab, siding, chopping, suction and similar. Finally, significant emissions come from the transport sector due to break wear emissions of copper and antimony to the air. This is the only impact category where the transport sector plays a significant role in environmental impacts.

Regarding fossil resource scarcity, all scenarios generate environmental burdens. Nevertheless, it should be emphasised again that produced pyrolysis oil could substitute

conventional naphtha, which would get significant credits, which are still not given in this case due to system boundaries. In general, most of the burdens in this category come from the consumption of fossil fuels to produce the electricity required for the process. In the case of S1, avoided incineration requires higher input of other fuels to satisfy heat and electricity production, therefore, burdens are even higher in this case (270.9, compared to 153.5 and 109.2 kg oil eq. for S2 and S3). About 33 kg of oil eq. is saved for sending the char to the coal market.

The process has a minor or neutral environmental impact for the rest of the impact categories. For terrestrial acidification, it can be observed how avoided incineration increases SO_2 eq. emissions since higher fossil fuel inputs are required to produce electricity and heat. Land use and water consumption have a notable impact. Land use is associated with forestry activities, unrelated to the pyrolysis itself, but it is present here as a background process for acquiring sawdust. Even though system boundaries are set up at feedstock acquisition as the first step, some background processes are inevitable when using a consequential approach. Water used for cooling and condensing volatiles also has a significant impact. Still, this parameter would greatly depend on the cooling system, which is closely related to the reactor design and, as such, may vary greatly.

3.5.2. Life cycle assessment of pre-treatment processes

Figure 18 presents the global warming potential for each process preceding pyrolysis. Environmental impacts from waste streams present cumulative credits or burdens gained through the pre-treatment process for each feedstock separately. They merge into a single flow in the mixing process which is then subjected to pyrolysis in the next step.

It can be seen from Figure 18 that the diversion of plastic waste from current waste treatment methods, like incineration or landfilling, brings immediate GWP credit to the proposed process. As already discussed, avoiding incineration is beneficial for reducing GWP due to avoiding direct emissions of CO_2 to the air. Therefore, emissions savings are several times higher in the case of S1, compared to S2 and S3, where pyrolysis prevents methane leakage from landfills. On the other hand, sawdust utilisation comes with burdens associated with forestry and post-processing actions. The sawdust pre-treatment increases GWP until the grinding stage with the same rate for all analysed scenarios. Nevertheless, in the grinding step, a slight reduction is noticed in the case of S1, while a small increment occurs for the rest. This depends on the treatment method for dust collected at this stage, but the overall impact is limited since grinding is considered efficient, with minimal losses. Nevertheless, it should be

mentioned that sawdust initially comes with a very low GWP of only 34 kg CO_2 eq., confirming the hypothesis about its carbon neutrality. Before mixing, when all pre-treatment methods are performed, the GWP of the sawdust stream is between 141 and a maximum of 175 kg CO_2 eq. for S1 and S2, respectively.

After the mixing stage, the S1 scenario negatively contributes to GWP, while S2 and S3 express positive values. The primary reason for this is because credits for using waste plastics are insufficient to cover the burdens from the sawdust side. Furthermore, the electricity mix used to power up the process plays an important role, and electricity consumption is the primary source of environmental burdens associated directly with pyrolysis.

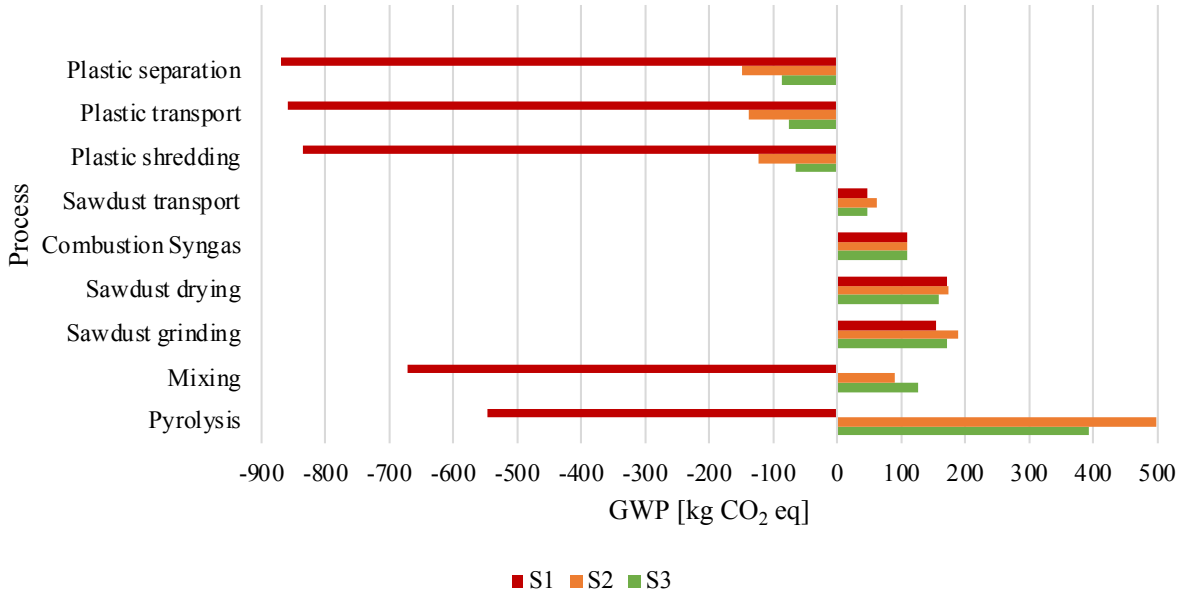

Figure 18 - Global warming potential of separate processes

Environmental impacts from electricity are associated with emissions directly emitted to the environment from power plants and the background processes required to produce equipment. Electricity consumption is several times lower for pre-treatment processes compared to pyrolysis itself. Consequently, GWP associated with electricity consumption is several times higher in the case of pyrolysis than for the rest of the processes together. The GWP from electricity consumption varies between very low 67 kg CO_2 eq. for S1 to high values in the case of S3 and S2 with 272 and 334 kg CO_2 eq., respectively. All emissions from the electricity sector are based on ecoinvent electricity mixes for selected countries using consequential system modelling. Plastic separation accounts for approximately 7% of the emissions associated with GWP. Sawdust drying with the combustion of synthetic gas has negligible electricity consumption. Sawdust and plastic grinding processes together contribute to additional 6-7% kg CO_2 eq. Mixing has only slightly higher values, accounting for about

8%, while the remaining 77% of the emissions associated with electricity consumption come from pyrolysis and reactor heating. The results are summarised in Figure 19. The rest of the impact categories have a similar share of emissions for the pre-treatment processes.

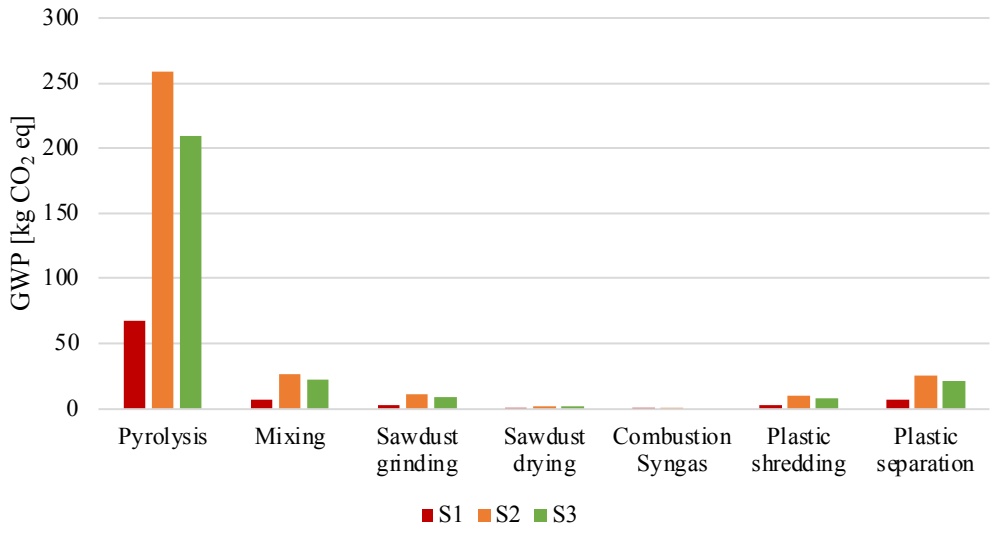

Figure 19 - Global warming potential associated with electricity consumption

Feedstock transport, for both SD and plastics, brings some burdens to the process. Since the transport distance and market are assumed to be the same for all scenarios (S1-S3), values do not differentiate between them. Global warming potentials for this process are 14 and 11 kg CO_2 eq. for SD and plastics, respectively. Slightly higher values in the case of the SD are due to the significant moisture content, which is later removed with the drying process. Nevertheless, mass loss in the drying stage indicates that the initial feedstock requirement is higher for the sawdust stream than the plastic, resulting in higher transport emissions.

3.5.3. Waste flow analysis

Plastic consists of two separate waste streams for PS and PP. Their utilisation in pyrolysis comes with either credits or burdens, depending on which treatment methods they are diverted from. Simultaneously, waste sawdust comes to the process with burdens. Nevertheless, these burdens are several times lower than the plastic counterparts for most impact categories, implying that plastics utilisation in the process is the major source or sink of the emissions.

Global warming potential is significantly reduced by using both PP and PS in all scenarios (Figure 20). The biggest savings are achieved for avoided incineration (S1) of waste PS and PP with -541 and -410 kg CO_2 eq., respectively. A comparison of scenarios S2 and S3 shows that diverting waste plastics from unsanitary landfills brings slightly bigger credits than

sanitary ones. Once again, more considerable savings are achieved for waste PS. On the other hand, sawdust positively impacts this category due to the background processes related to forestry activities, and emissions are about 48 kg CO_2 eq. Treatment of plastic impurities from separation and grinding increases GWP, especially if treated by incineration. In general, dust from biomass grinding has a negligible impact on all categories.

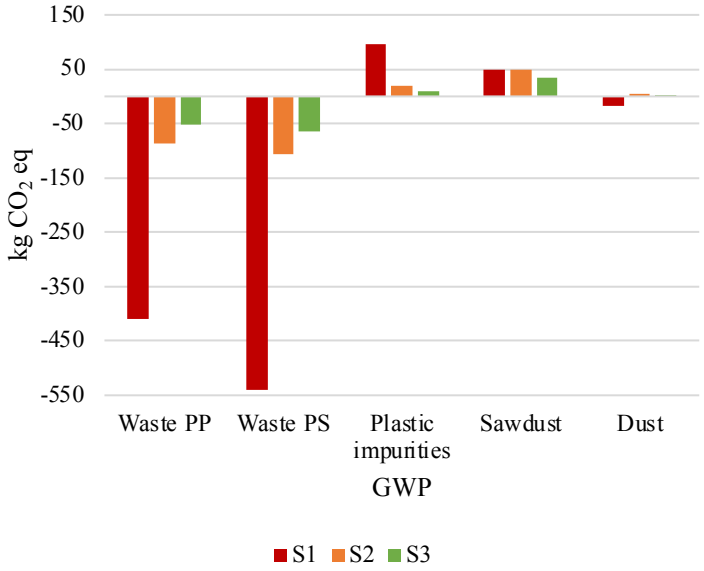

Figure 20 – Global warming potential of waste flows

Regarding human toxicity categories, the results are quite the opposite (Figure 21), and the biggest differences are observed in S1. The main source of carcinogenic emissions from the incineration of plastics is chromium VI emissions into the water. Chromium VI, or hexavalent chromium, is used as a pigment in ink, dyes, paints and plastics. In Figure 21a, waste PP has a slightly bigger impact than waste PS, even though values are very similar at 37.8 and 36.1 kg 1,4-DCB eq., respectively. Treatment of plastic impurities in S1 by incineration brings some credits (6.6 kg 1,4-DCB eq.). Landfilling, either sanitary or unsanitary, negatively impacts the carcinogenic impact category. In both S2 and S3 cases, diverting the plastic wastes from landfills brings negligible credits to the process of only 1 kg avoided 1,4-DCB eq. emissions. In this case, emissions are primarily associated with arsenic and chromium leaking into the groundwater.

Sawdust does not have a visible impact on human toxicity categories. The carcinogenic impact is 0.2 kg 1,4-DCB eq., while around 21 kg 1,4-DCB eq. is noted in the case of non-carcinogenic toxicity. Nevertheless, in Figure 21b, it can be seen that the non-carcinogenic toxicity potential for waste plastics, associated with zinc and vanadium emission to the water, is enormous. This is especially evident in the case of waste PS, in which utilisation brings

substantial credits for pyrolysis. The highest emissions savings are achieved in S2, where ~2400 kg 1,4-DCB eq. is saved, compared to 2200 kg 1,4-DCB eq. in S3. The utilisation of waste PP in pyrolysis instead of landfilling brings notable savings of 969 and 930 kg 1,4-DCB eq., for S2 and S3, respectively. Nevertheless, incineration might be better than pyrolysis regarding HTNC emissions (Figure 21b). For the S1, emissions associated with using waste PS and PP are 479 and 328 kg 1,4-DCB eq., respectively. From plastic impurities treatment, it can be seen that incineration reduces non-carcinogenic toxicity slightly better than pyrolysis, while landfilling increases emissions drastically (~400 kg 1,4-DCB eq.).

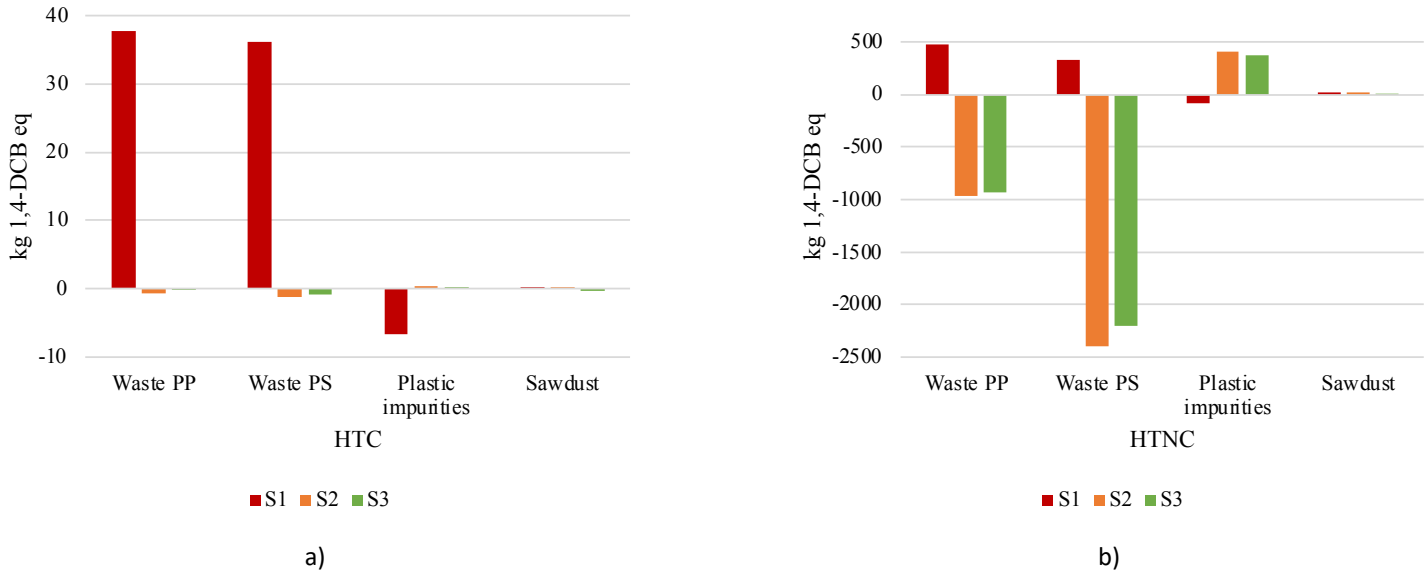

Figure 21 - Human carcinogenic (a) and non-carcinogenic (b) toxicity

Ecotoxicity categories presented in Figure 22 are primarily associated with zinc emissions to the air. For the waste PP, vanadium is also emitted. Zinc is used as a heat stabilizer in plastic production, as a coating material in the metal industry, in rubber production and other applications. This is important because zinc emissions are found almost in all processes, from waste treatment and electricity production to feedstock transport.

The same trends and similar values are obtained for the marine (Figure 22a) and freshwater (Figure 22b) ecotoxicities. For MET, diverting waste PP from current treatment methods to pyrolysis saves between 63 and 87 kg 1,4-DCB eq. On the other hand, diverting waste PS from incineration brings only slight credits to the process (15 kg 1,4-DCB eq.), but diverting waste PS from landfills brings tremendous credits of almost 100 kg 1,4-DCB eq. for scenarios S2 and S3. Treatment of plastic impurities from separation and grinding burdens the process, especially if waste is landfilled (S2-S3).

Regarding the FET, waste PP saves between 43 to 62 kg 1,4-DCB eq., while waste PS brings an additional 10 and 70 kg 1,4-DCB eq. Similarly to MET, avoided landfilling brings

bigger credits than avoided incineration. Sawdust has a negligible impact on these two ecotoxicity categories.

Terrestrial ecotoxicity shows different values and trends between the analysed scenarios and the other two ecotoxicity categories. In Figure 22c, obtained values for waste PP greatly differ. In S1, more than 2000 kg 1,4-DCB eq. is saved if waste PP is pyrolysed rather than incinerated. Compared to unsanitary (S2) and sanitary (S3) landfilling, pyrolysis saves almost 300 and 40 kg 1,4-DCB eq., respectively. All these savings are achieved due to the prevented emissions of vanadium into the air. Simultaneously, the impacts of waste PS show even more interesting results. For the S1, waste PS does not reduce emissions but increases for almost 300 kg 1,4-DCB eq. If unsanitary landfilling is prevented, about 136 kg 1,4-DCB eq. are saved, while only 17 kg of emissions is prevented in the case of sanitary landfilling. Landfill emissions from waste PS are due to the release of mercury in the air, while vanadium and, to a lower extent, cadmium is responsible for PP emissions. When it comes to sawdust, tremendous emissions of 722 kg of 1,4-DCB eq. are observed (Figure 22c). High contributions come from the slab and siding process, but the market for transport is the most significant generator of emissions. Biomass feedstock is generally transported several times between chopping and final processing, which requires continuous usage of transport services, resulting in zinc and antimony emissions from break-wearing to the air. This category is similar to the analysed scenarios since they use the same transport markets. This is the only environmental impact category where sawdust impacts exceed waste plastics.

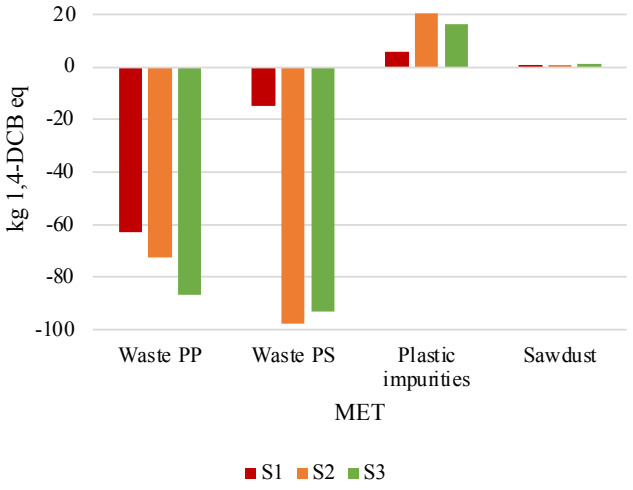

a)

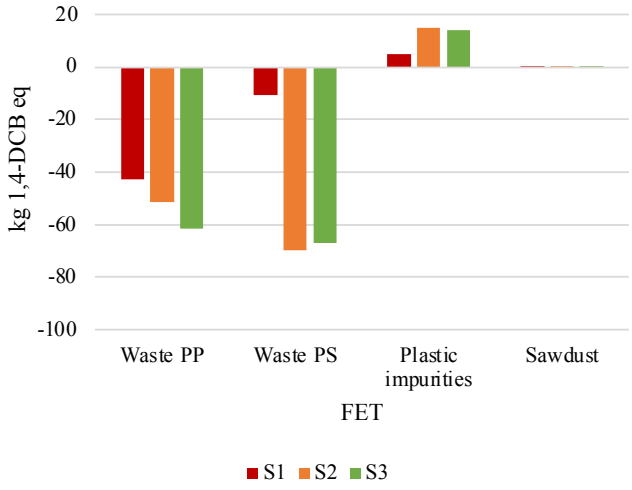

b)

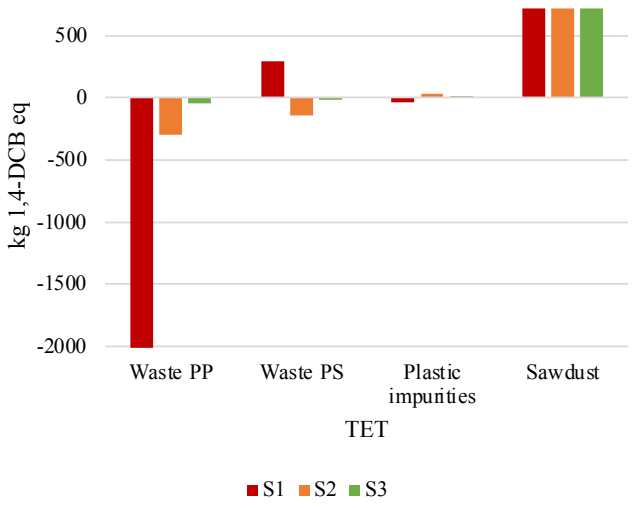

c)

Figure 22 - Ecotoxicity impact categories marine (a), freshwater (b), terrestrial (c)

3.5.4. Sensitivity analysis

Additional scenarios are built to carry out sensitivity analysis. Varying parameters were electricity mix and product yield. Results are presented in percent of changes to allow easier orientation.

Electricity mix

Two additional scenarios are made to investigate the electricity mix influence and the potential emission reductions by powering the process entirely with renewables. Scenarios S4 and S5 represent the variation of scenarios S1 and S3. All flows are kept the same, except the electricity, where the market group for electricity is wholly substituted by electricity production from a solar tower power plant of 20 MW. In the case of S4, the provider is selected for the rest of the world, while for S5 provider is dedicated to Australia. Figure 23 represents the impact categories of most significant concern. For scenario S4, analysed impact categories show emission reductions of up to 10% compared to S1. The limited impact is because, in S1, 76% of electricity already comes from renewable wind production. Marine and freshwater ecotoxicity express almost 100 and 200% reduction, respectively. On the other hand, GWP is reduced by only 10%, or an additional 60 kg CO_2 eq., and avoided emissions are now more than 600 kg CO_2 eq. It is worth mentioning that TET is reduced by almost 25% but still accounts for 1780 kg 1,4-DCB eq.

In the Australian case, the emission reduction is much more pronounced. In S5, solar energy needs to substitute almost 70% of fossil fuels, primarily natural gas and coal, compared to the electricity mix in S3. Since a high share of fossil fuels is substituted, emissions are more

significantly reduced (Figure 23). The most considerable emission reductions are achieved in fossil resource scarcity (68%) and GWP (61%), even though the overall GWP of the process is still positive with ~155 kg CO_2 eq. Notable reductions are also seen in AP by 41% to only 0.8 kg SO_2 eq. and HTC, where the decrease is 25% from 40.3 to 30.3 kg 1,4-DCB eq. The rest of the impact categories have emission reductions of around 10%.

For both scenarios, the introduction of solar energy reduced the environmental impacts. In case when fossil fuels are substituted (S5), the reduction can be large. Solar energy can bring only small further savings if the electricity mix already consists of a high share of renewables, like wind in S4.

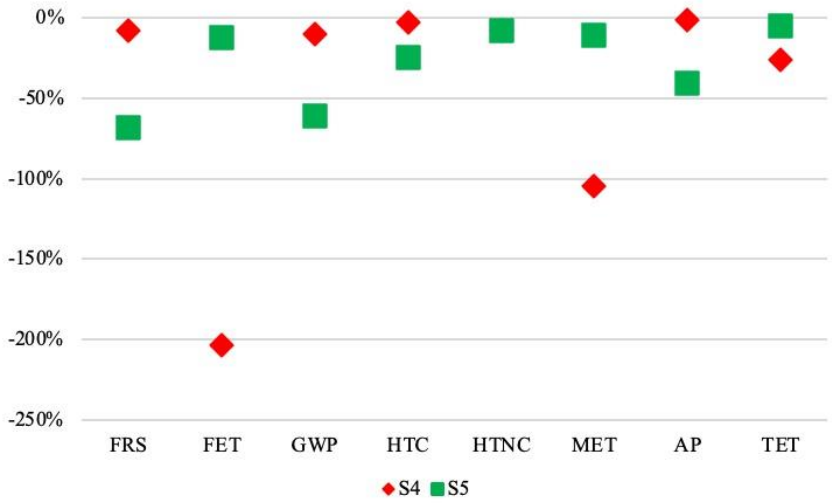

Figure 23 - Sensitivity analysis – electricity mix

Product yield

Two additional scenarios, S6 and S7, are also created here, representing the variation of S1 and S3 (Figure 24). In these cases, it was assumed that pyrolysis oil yield was halved to only 403 kg, while new masses for char and gas fractions are 367 and 230 kg, respectively. The new mass of char and syngas fraction is calculated by the difference and maintaining the same ratio between them. Since the yield of products depends on process conditions and feedstock quality, it is assumed that due to some impurities or feedstock composition, the yield of products might vary, also affecting the environmental impacts. Figure 24 shows that product variation has more influence on environmental impacts than the electricity mix. The low liquid yield would cause a 100% increase in GWP for S7, while a more than 100% reduction occurs for S6. This is because low liquid yield requires more feedstock initially to meet production requirements. As a result, more plastic waste is diverted from incineration (S6), consequently reducing the emissions. In the case of S7, more feedstock demands more electricity from fossil fuels to power the process, thus doubling its emissions. Significant reduction is noticed in the

case of TET for both scenarios. This results from a substantial char fraction sent to market as a coal substitute, reducing the need for background mine operations. In general, high char yield is beneficial in reducing the demand for coal and associated emissions with coal mining. If credits were given to pyrolysis oil for substituting petroleum products in the first place, a change in yield would likely result in worsened environmental impacts.

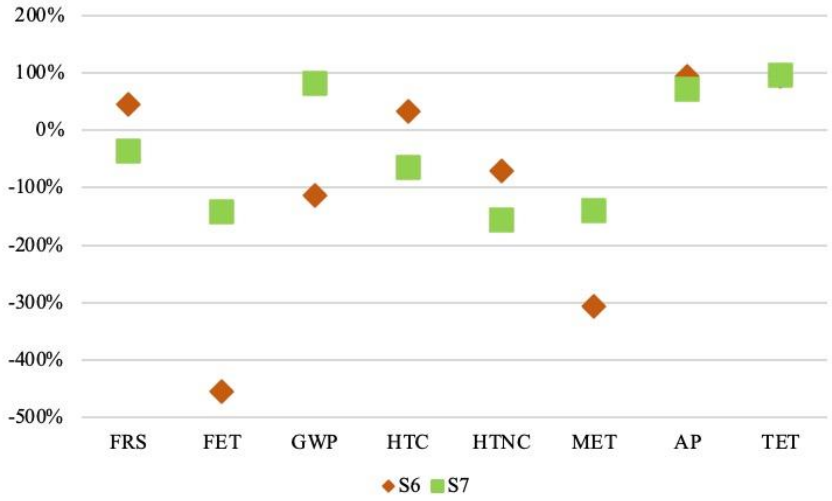

Figure 24 - Sensitivity analysis - product yield

4. CONCLUSIONS AND FUTURE WORK

4.1. Key findings

Alternative fuels are inevitable in future energy systems, especially in transport and industry sectors, where electricity isn't a suitable solution. Fuels that can be utilised within the existing infrastructure and without significant modifications are preferred with greater potential to be deployed on a commercial scale. Up to now, significant research efforts have been given to develop suitable alternatives; however, full-scale deployment is still lacking. This thesis examines several waste materials that could be utilised in the thermochemical conversion processes with an aim to produce alternative fuels. The presented results and conclusions are based on an in-depth literature review, experimental investigations, and environmental assessment of the procedure. Valuable observations are discussed throughout chapters and can be used for further process development and scaling up on a commercial level.

Firstly, detailed literature review is given for all considered alternative fuels in future energy systems. A systematic review is carried out by analysing and selecting relevant scientific publications indexed in citation databases. Results showed that alternative fuels are gaining more and more research attention due to their crucial role in decarbonising high-energy intensive processes. Chemicals like hydrogen, ammonia or alcohol-derived fuels like methanol have been widely investigated as potential solutions. Nevertheless, all of them require either the development of dedicated storage and distribution systems or the development of dedicated utilisation technologies like fuel cells which limits their enrolment on a full scale. On the other hand, liquid fuel like biodiesel can easily be stored, distributed, and utilised in existing internal combustion engines without significant modifications. Biofuels are already deployed commercially, accounting for approximately 10% of total energy consumption, even though the vast majority is solid biomass inefficiently combusted in household stoves. Such practice raises serious sustainability concerns since future consumption is expected to increase. Therefore, novel biofuel production methods are necessary, focusing on waste biomass like sawdust, forestry and agricultural residues. However, due to the biomass nature, which has a high share of oxygen within their structures, derived fuel properties will always lag behind

fossil fuels regarding heating values. This implies that in order to substitute fossil fuels, they have to be consumed at a higher rate, only deepening sustainability issues.

At the same time, waste management and disposal of end-of-life materials are still seeking for innovative solutions that could increase the recycling rates and enhance energy recovery where mechanical recycling isn't a viable option. Nowadays, incineration is the only energy recovery option used to process waste with an aim to produce heat and electricity from recovered embodied energy. Nevertheless, waste is often incinerated without appropriate treatment, resulting in a lower-efficiency process. In general, energy production from biofuels and waste continuously increases but at a slow pace due to the abovementioned drawbacks for both feedstocks. Between 2000 and 2019, their consumption for energy production increased from 36.7 to only 43.4 EJ.

Thermochemical conversion processes like pyrolysis and gasification seem to be very promising methods to process biomass and plastic feedstock with an aim to produce high-quality alternative fuels. Derived products are collected in liquid, gaseous and char form and can be easily utilised within existing technologies after refinement. Finally, co-processing biomass and plastic feedstock in fuel mixtures can enhance bio-fuel properties, making the product more competitive to fossil fuels and other alternatives. Based on the literature review, co-pyrolysis of sawdust with polystyrene, polypropylene, and polyurethane is selected as the feedstock of interest for further research investigations.

Experimental investigations are carried out for individual samples and their respective mixtures to investigate the product yield and composition and the decomposition process kinetics. Firstly, the co-pyrolysis of a sawdust mixture composed of oak, fir and poplar wood with waste PS was carried out at 600 ºC. The plastic content in the mixture varied between 25 and 75%. The analysis shows that adding plastic can significantly enhance the derived product properties compared to individual sawdust pyrolysis. Only 25% of PS in the mixture was enough to double the liquid yield from 31 to 62% while simultaneously reducing the share of oxygenated compounds and promoting the yield of aromatic hydrocarbons. A mixture with 75% of PS expressed the highest liquid yield of almost 84%. Nevertheless, the analysis of identified compounds in the mixtures shows that oil quality is not necessarily enhanced. This is because PS decomposes on aromatic and polycyclic aromatic hydrocarbons. While aromatics are welcomed in fuel composition, their share is restricted to below 40% due to the combustion process's problems with released smoke and particles. On the other hand, PAHs pose a threat to human health and are not preferred in fuels. Therefore, the analysis suggested that 25% of PS in the mixture with biomass could be considered an acceptable share. Furthermore, this

work suggested introducing PP to sawdust and PS mixture to enhance the selectivity toward aliphatic hydrocarbons, which would further increase oil quality.

In the scope of the thesis, the co-pyrolysis potential of polyurethane foam was investigated due to its recycling limitations, marking it as a potential feedstock for thermochemical conversion. The results show that polyurethane foam has limited potential to be utilised in co-pyrolysis, especially if the intention is to produce fuel-quality grade oil. This is derived from the fact that most of the identified compounds from PU decomposition are nitrogen-containing, like benzenamines, that do not meet fuel criteria but seem more appropriate for chemical synthesis. In addition, PU can increase liquid yield only to some extent since the difference between the mixtures with 25 and 75% of PU content was less than 4%. On the other hand, gas fraction from PU decomposition consists mainly of hydrogen, which marks gasification as the more suitable option for end-of-life treatment.

Additionally, thermogravimetric, kinetic and thermodynamic analyses were carried out to investigate the decomposition mechanisms and gather better insight into process dynamics and feedstock interaction during the process. The primary goal of these investigations was to investigate the influence of the heating rate and mixture composition on investigated thermogravimetric and kinetic parameters. The analysis showed that the heating rate has a low impact on feedstock decomposition since only slight differences are observed in the yield of solid residue (~3%). Additionally, an increment in the heating rate shifts the temperature range where decomposition takes place slightly toward higher values. Simultaneously, the analysis showed that mixture composition plays a crucial role in decomposition kinetics. Firstly, as expected, an increment of PS and PP content reduces the final mass of the mixture residue due to the higher volatile matter of plastic materials, allowing better conversion to volatiles. Even more, it is interesting to observe the values for activation energies. In the case of SD, activation energy continuously increases with the increment of conversion rate, while a reverse trend is observed for plastic samples. At the beginning of the process, sawdust E_a is two to three times lower than plastics. When conversion reaches 50%, the values are at a similar level. After that point, activation energies for plastics decrease until the end of the process. At the same time, in the case of sawdust, the steady increment is followed up by a tremendous jump at the end when less than 20% of the initial sample mass is left. In the case of the analysis of the mixture, very interesting results are observed. For the mixtures where plastic share does not exceed 50%, E_a can be even lower compared to individual samples between the evaporation stage and the change of decomposition mechanism. This could imply that feedstock interaction in the first stage can either promote or hinder degradation. Nevertheless, the tremendous increase in

E_a observed once when the decomposition mechanism switches from sawdust to plastic samples suggests that degradation was hindered in the first stage. To understand the consequence of such feedstock interaction on product distribution, synergistic effect analysis should also be considered. Since high synergy levels in liquid yield are noted for a mixture with 25 and 50% of PS, it can be stated that hindering sample degradation in the first stage helps in better yield of liquid products due to the limited time for their secondary cracking and conversion into light, non-condensable volatiles.

Important observations are collected from the comprehensive experimental investigation of sawdust, PS, PP, and their mixture, which is considered promising for co-pyrolysis. Based on the previous findings, blending shares were 50% sawdust, 25% PS, and 25% PP. These shares are carefully selected to maximise the oil yield and enhance its hydrocarbon content. There are several main findings observed in this work. Firstly, the mixture composition is favourable for high liquid yield since more than 80% is reported, with the solid residue accounting for approximately 12% and the rest being a gaseous fraction. Moreover, oil quality is greatly improved compared to individual pyrolysis of samples. Compared to SD-derived oil, the most remarkable results are achieved in reducing the yield of oxygenated compounds, especially phenols, which are the leading organic group in bio-oils. Compared to PS-derived oil, significant improvement is achieved in reducing the yield of aromatics and PAHs. These reductions are especially important since their presence in fuels can cause severe environmental and health consequences. Finally, compared to PP-derived oil, a notable reduction of alcohol yield can be observed while maintaining high hydrocarbon content with cyclic and linear hydrocarbons. Therefore, selected feedstock and mixture composition is exceptionally favourable for the production of alternative liquid fuels. The hydrocarbon content of derived oil is almost 70%, with 35% aliphatics and 32% aromatic hydrocarbons. The share of aromatics, more precisely styrene, is sufficient to meet conventional fuel requirements. On the other hand, the share of aliphatics could be further improved by increasing the share of PP in the mixture.

Finally, the Life cycle assessment (LCA) was carried out for the proposed process. Besides the product quality, the justification for the co-pyrolysis is associated with environmental impacts and the fact that each feedstock enters the process with embodied emissions. These emissions could either bring credits or burdens to observed environmental impact categories. Most sawdust emissions are associated with high-energy requirements for feedstock pre-treatment and, to some extent, initial cultivation and processing activities. On the other hand, emissions associated with waste plastics result from their end-of-life treatment methods. The

assessment showed that co-pyrolysis could significantly outperform incineration in terms of global warming potential (GWP) and freshwater and marine ecotoxicities. Nevertheless, the negative impacts on human carcinogenic and non-carcinogenic toxicities, terrestrial ecotoxicity and acidification potential are observed. Compared to landfilling, pyrolysis is favourable for reducing human non-carcinogenic toxicity, freshwater and marine ecotoxicity, and eutrophication potential. Nevertheless, it is much worse in terms of GWP due to associated activities with energy production for the process requirements. Most emissions associated with GWP come from electricity consumption to power up the reactor and pre-treatment processes, accounting for 77% of total CO_2 eq. emissions. Sensitivity analysis showed that integrating co-pyrolysis with renewables like solar energy can significantly reduce environmental impacts in almost all categories, especially related to GWP. Furthermore, sensitivity analysis showed that product yield could significantly impact environmental categories in case of reduced oil yield or insufficient product quality to substitute fossil fuels. Therefore, pre-treatment methods like drying and plastic separation are inevitable because they ensure that product yield and quality will be in the expected range.

4.2. Limitations and future directions

The main limitation of this research work is that it does not investigate upgrading requirements and direct utilisation possibilities of the obtained pyrolysis oil. Therefore, future work should focus on the refinement procedure, which would give final remarks regarding the oil quality and suitability to be used as a petroleum substitute. Additionally, large-scale experiments are necessary to confirm observations from lab-scale investigations. Finally, the continuous operation of a pyrolysis reactor is one of the challenging tasks and should be investigated more.

Uncertainties about product yield from the process represent one of the greatest challenges. Product distribution reflects utilisation possibilities, environmental impacts, and economic viability. Therefore, developing a method to predict product yield based on initial sample characteristics is of significant interest. Kinetic analysis and a better understanding of the synergistic effect could be effective tools in these attempts.

Finally, collecting measurement data for process requirements and emissions could give more reliable results regarding the environmental impacts of the proposed process. This also implies the inclusion of emissions from pyrolysis oil refinement and usage in internal combustion engines. Integrating process with renewable energy sources is the final step that

would make the derived product carbon neutral and, therefore, fully acceptable in future energy systems.

5. REFERENCES

[1] IEA, “Key World Energy Statistics 2021,” 2021.

[2] H. Stančin, H. Mikulčić, X. Wang, and N. Duić, “A review on alternative fuels in future energy system,” *Renewable and Sustainable Energy Reviews*, vol. 128, 2020, doi: 10.1016/j.rser.2020.109927.

[3] M. v. Rodionova, A. M. Bozieva, S. K. Zharmukhamedov, Y. K. Leong, J. Chi-Wei Lan, A. Veziroglu, T. N. Veziroglu, T. Tomo, J. S. Chang, and S. I. Allakhverdiev, “A comprehensive review on lignocellulosic biomass biorefinery for sustainable biofuel production,” *Int J Hydrogen Energy*, vol. 47, no. 3, pp. 1481–1498, Jan. 2022, doi: 10.1016/J.IJHYDENE.2021.10.122.

[4] S. Mariyam, M. Shahbaz, T. Al-Ansari, H. R. Mackey, and G. McKay, “A critical review on co-gasification and co-pyrolysis for gas production,” *Renewable and Sustainable Energy Reviews*, vol. 161, p. 112349, Jun. 2022, doi: 10.1016/J.RSER.2022.112349.

[5] D. Porshnov, P. Lund, and J. Byrne, “Evolution of pyrolysis and gasification as waste to energy tools for low carbon economy,” *Wiley Interdiscip Rev Energy Environ*, vol. 11, no. 1, p. e421, Jan. 2022, doi: 10.1002/WENE.421.

[6] A. Reichel, “Diverting waste from landfill - Effectiveness of waste-management policies in the European Union,” 1999.

[7] S. Douvartzides, N. D. Charisiou, W. Wang, V. G. Papadakis, K. Polychronopoulou, and M. A. Goula, “Catalytic fast pyrolysis of agricultural residues and dedicated energy crops for the production of high energy density transportation biofuels. Part I: Chemical pathways and bio-oil upgrading,” *Renew Energy*, vol. 185, pp. 483–505, Feb. 2022, doi: 10.1016/J.RENENE.2021.12.083.

[8] S. Jha, S. Nanda, B. Acharya, and A. K. Dalai, “A Review of Thermochemical Conversion of Waste Biomass to Biofuels,” *Energies (Basel)*, vol. 15, no. 17, Sep. 2022, doi: 10.3390/EN15176352.

[9] X. Hu and M. Gholizadeh, “Biomass pyrolysis: A review of the process development and challenges from initial researches up to the commercialisation stage,” *Journal of Energy Chemistry*, vol. 39. Elsevier B.V., pp. 109–143, Dec. 01, 2019. doi: 10.1016/j.jechem.2019.01.024.

[10] X. Zhang, H. Lei, S. Chen, and J. Wu, “Catalytic co-pyrolysis of lignocellulosic biomass with polymers: A critical review,” *Green Chemistry*, vol. 18, no. 15. Royal Society of Chemistry, pp. 4145–4169, 2016. doi: 10.1039/c6gc00911e.

[11] M. H. M. Ahmed, N. Batalha, H. M. D. Mahmudul, G. Perkins, and M. Konarova, “A review on advanced catalytic co-pyrolysis of biomass and hydrogen-rich feedstock: Insights into synergistic effect, catalyst development and reaction mechanism,” *Bioresource Technology*, vol. 310. Elsevier Ltd, Aug. 01, 2020. doi: 10.1016/j.biortech.2020.123457.

[12] “Global Plastics Outlook,” *Global Plastics Outlook*, Feb. 2022, doi: 10.1787/DE747AEF-EN.

[13] J. Kirchherr, D. Reike, and M. Hekkert, “Conceptualizing the Circular Economy: An Analysis of 114 Definitions,” *SSRN Electronic Journal*, Sep. 2017, doi: 10.2139/SSRN.3037579.

[14] Z. O. G. Schyns and M. P. Shaver, “Mechanical Recycling of Packaging Plastics: A Review,” *Macromolecular Rapid Communications*, vol. 42, no. 3. Wiley-VCH Verlag, Feb. 01, 2021. doi: 10.1002/marc.202000415.

[15] H. Jeswani, C. Krüger, M. Russ, M. Horlacher, F. Antony, S. Hann, and A. Azapagic, “Life cycle environmental impacts of chemical recycling via pyrolysis of mixed plastic waste in comparison with mechanical recycling and energy recovery,” *Science of the Total Environment*, vol. 769, May 2021, doi: 10.1016/j.scitotenv.2020.144483.

[16] W. Li, Z. Bai, T. Zhang, Y. Jia, Y. Hou, J. Chen, Z. Guo, L. Kong, J. Bai, and W. Li, “Comparative study on pyrolysis behaviors and chlorine release of pure PVC polymer and commercial PVC plastics,” *Fuel*, vol. 340, p. 127555, May 2023, doi: 10.1016/J.FUEL.2023.127555.

[17] Y. Nishiyama, S. Kumagai, S. Motokucho, T. Kameda, Y. Saito, A. Watanabe, H. Nakatani, and T. Yoshioka, “Temperature-dependent pyrolysis behavior of polyurethane elastomers with different hard- and soft-segment compositions,” *J Anal Appl Pyrolysis*, vol. 145, no. October 2019, p. 104754, 2020, doi: 10.1016/j.jaap.2019.104754.

[18] I. Kremer, T. Tomić, Z. Katančić, M. Erceg, S. Papuga, J. Parlov Vuković, and D. R. Schneider, “Catalytic pyrolysis and kinetic study of real-world waste plastics: multi-layered and mixed resin types of plastics,” *Clean Technol Environ Policy*, vol. 24, no. 2, pp. 677–693, Mar. 2022, doi: 10.1007/S10098-021-02196-8.

[19] Z. Wang, K. G. Burra, T. Lei, and A. K. Gupta, “Co-pyrolysis of waste plastic and solid biomass for synergistic production of biofuels and chemicals-A review,” *Progress in Energy and Combustion Science*, vol. 84. Elsevier Ltd, May 01, 2021. doi: 10.1016/j.pecs.2020.100899.

[20] Energy and Natural Resources, “Pyrolysis Oil Market | Global Industry Report, 2031.” https://www.transparencymarketresearch.com/pyrolysis-oil-market.html (accessed Mar. 09, 2023).

[21] X. Zhang, H. Lei, L. Zhu, M. Qian, X. Zhu, J. Wu, and S. Chen, “Enhancement of jet fuel range alkanes from co-feeding of lignocellulosic biomass with plastics via tandem catalytic conversions,” *Appl Energy*, vol. 173, pp. 418–430, Jul. 2016, doi: 10.1016/j.apenergy.2016.04.071.

[22] I. Ridjan, B. V. Mathiesen, and D. Connolly, “Terminology used for renewable liquid and gaseous fuels based on the conversion of electricity: A review,” *J Clean Prod*, vol. 112, pp. 3709–3720, 2016, doi: 10.1016/j.jclepro.2015.05.117.

[23] S. Brynolf, M. Taljegard, M. Grahn, and J. Hansson, “Electrofuels for the transport sector: A review of production costs,” *Renewable and Sustainable Energy Reviews*, vol. 81, no. July 2016, pp. 1887–1905, 2018, doi: 10.1016/j.rser.2017.05.288.

[24] A. Sharma and V. Strezov, “Life cycle environmental and economic impact assessment of alternative transport fuels and power-train technologies,” *Energy*, vol. 133, pp. 1132–1141, 2017, doi: 10.1016/j.energy.2017.04.160.

[25] D. S. Bajwa, T. Peterson, N. Sharma, J. Shojaeiarani, and S. G. Bajwa, “A review of densified solid biomass for energy production,” *Renewable and Sustainable Energy Reviews*, vol. 96, no. June, pp. 296–305, 2018, doi: 10.1016/j.rser.2018.07.040.

[26] S. McDonagh, P. Deane, K. Rajendran, and J. D. Murphy, “Are electrofuels a sustainable transport fuel? Analysis of the effect of controls on carbon, curtailment, and cost of hydrogen,” *Appl Energy*, vol. 247, pp. 716–730, Aug. 2019, doi: 10.1016/J.APENERGY.2019.04.060.

[27] M. Lehtveer, S. Brynolf, and M. Grahn, “What Future for Electrofuels in Transport? Analysis of Cost Competitiveness in Global Climate Mitigation,” *Environ Sci Technol*, vol. 53, no. 3, pp. 1690–1697, Feb. 2019, doi: 10.1021/ACS.EST.8B05243/SUPPL_FILE/ES8B05243_SI_002.XLSX.

[28] T. A. Tasneem Abdalla, T. A. Tasneem Abdalla, Q. Wang, Q. Wang, T. Xiaoqiang, and T. Xiaoqiang, “The Study on Dual Fuel Spray and Characteristics of Combustion of

Diesel, Natural Gas and Dual Fuel," *Journal of Energy Conservation*, vol. 1, no. 1, pp. 14–30, Jun. 2018, doi: 10.14302/issn.2642-3146.jec-18-2135.

[29] D. Parra, L. Valverde, F. J. Pino, and M. K. Patel, "A review on the role, cost and value of hydrogen energy systems for deep decarbonisation," *Renewable and Sustainable Energy Reviews*, vol. 101, pp. 279–294, Mar. 2019, doi: 10.1016/J.RSER.2018.11.010.

[30] S. Giddey, S. P. S. Badwal, C. Munnings, and M. Dolan, "Ammonia as a Renewable Energy Transportation Media," *ACS Sustain Chem Eng*, vol. 5, no. 11, pp. 10231–10239, 2017, doi: 10.1021/acssuschemeng.7b02219.

[31] A. Valera-Medina, H. Xiao, M. Owwn-Jones, W. I. F. David, and P. J. Bowen, "Ammonia for power," *Prog Energy Combust Sci*, vol. under revi, pp. 63–102, 2018, doi: 10.1016/j.pecs.2018.07.001.

[32] "Environmental Concerns and Sustainable Development," *Environmental Concerns and Sustainable Development*, 2020, doi: 10.1007/978-981-13-6358-0.

[33] D. S. Bajwa, T. Peterson, N. Sharma, J. Shojaeiarani, and S. G. Bajwa, "A review of densified solid biomass for energy production," *Renewable and Sustainable Energy Reviews*, vol. 96, pp. 296–305, Nov. 2018, doi: 10.1016/J.RSER.2018.07.040.

[34] G. Perkins, T. Bhaskar, and M. Konarova, "Process development status of fast pyrolysis technologies for the manufacture of renewable transport fuels from biomass," *Renewable and Sustainable Energy Reviews*, vol. 90, pp. 292–315, Jul. 2018, doi: 10.1016/J.RSER.2018.03.048.

[35] E. R. Widjaya, G. Chen, L. Bowtell, and C. Hills, "Gasification of non-woody biomass: A literature review," *Renewable and Sustainable Energy Reviews*, vol. 89, pp. 184–193, Jun. 2018, doi: 10.1016/J.RSER.2018.03.023.

[36] F. Sher, A. Yaqoob, F. Saeed, S. Zhang, Z. Jahan, and J. J. Klemeš, "Torrefied biomass fuels as a renewable alternative to coal in co-firing for power generation," *Energy*, vol. 209, Oct. 2020, doi: 10.1016/j.energy.2020.118444.

[37] S. Verhelst, J. W. Turner, L. Sileghem, and J. Vancoillie, "Methanol as a fuel for internal combustion engines," *Prog Energy Combust Sci*, vol. 70, pp. 43–88, Jan. 2019, doi: 10.1016/J.PECS.2018.10.001.

[38] M. Svanberg, J. Ellis, J. Lundgren, and I. Landälv, "Renewable methanol as a fuel for the shipping industry," *Renewable and Sustainable Energy Reviews*, vol. 94, pp. 1217–1228, Oct. 2018, doi: 10.1016/J.RSER.2018.06.058.

[39] Y. Çelebi and H. Aydın, "An overview on the light alcohol fuels in diesel engines," *Fuel*, vol. 236, pp. 890–911, Jan. 2019, doi: 10.1016/J.FUEL.2018.08.138.

[40] O. I. Awad, R. Mamat, O. M. Ali, N. A. C. Sidik, T. Yusaf, K. Kadirgama, and M. Kettner, “Alcohol and ether as alternative fuels in spark ignition engine: A review,” *Renewable and Sustainable Energy Reviews*, vol. 82, pp. 2586–2605, Feb. 2018, doi: 10.1016/J.RSER.2017.09.074.

[41] L. Makarichi, W. Jutidamrongphan, and K. anan Techato, “The evolution of waste-to-energy incineration: A review,” *Renewable and Sustainable Energy Reviews*, vol. 91, pp. 812–821, Aug. 2018, doi: 10.1016/J.RSER.2018.04.088.

[42] S. M. Al-Salem, A. Antelava, A. Constantinou, G. Manos, and A. Dutta, “A review on thermal and catalytic pyrolysis of plastic solid waste (PSW),” *Journal of Environmental Management*, vol. 197. Academic Press, pp. 177–198, Jul. 15, 2017. doi: 10.1016/j.jenvman.2017.03.084.

[43] H. Hassan, J. K. Lim, and B. H. Hameed, “Recent progress on biomass co-pyrolysis conversion into high-quality bio-oil,” *Bioresource Technology*, vol. 221. Elsevier Ltd, pp. 645–655, Dec. 01, 2016. doi: 10.1016/j.biortech.2016.09.026.

[44] A. O. Oyedun, T. Gebreegziabher, D. K. S. Ng, and C. W. Hui, “Mixed-waste pyrolysis of biomass and plastics waste – A modelling approach to reduce energy usage,” *Energy*, vol. 75, pp. 127–135, Oct. 2014, doi: 10.1016/J.ENERGY.2014.05.063.

[45] H. Zhang, J. Nie, R. Xiao, B. Jin, C. Dong, and G. Xiao, “Catalytic Co-pyrolysis of Biomass and Di ff erent Plastics (Polyethylene , Polypropylene , and Polystyrene) To Improve Hydrocarbon Yield in a Fluidized-Bed Reactor,” 2014.

[46] P. Lu, Q. Huang, A. C. (Thanos) Bourtsalas, Y. Chi, and J. Yan, “Synergistic effects on char and oil produced by the co-pyrolysis of pine wood, polyethylene and polyvinyl chloride,” *Fuel*, vol. 230, pp. 359–367, Oct. 2018, doi: 10.1016/J.FUEL.2018.05.072.

[47] E. B. Hassan, I. Elsayed, and A. Eseyin, “Production high yields of aromatic hydrocarbons through catalytic fast pyrolysis of torrefied wood and polystyrene,” *Fuel*, vol. 174, pp. 317–324, Jun. 2016, doi: 10.1016/J.FUEL.2016.02.031.

[48] G. Özsin and A. E. Pütün, “A comparative study on co-pyrolysis of lignocellulosic biomass with polyethylene terephthalate, polystyrene, and polyvinyl chloride: Synergistic effects and product characteristics,” *J Clean Prod*, vol. 205, pp. 1127–1138, Dec. 2018, doi: 10.1016/J.JCLEPRO.2018.09.134.

[49] A. Ephraim, D. Pham Minh, D. Lebonnois, C. Peregrina, P. Sharrock, and A. Nzihou, “Co-pyrolysis of wood and plastics: Influence of plastic type and content on product yield, gas composition and quality,” *Fuel*, vol. 231, pp. 110–117, Nov. 2018, doi: 10.1016/J.FUEL.2018.04.140.

[50] X. Kai, T. Yang, S. Shen, and R. Li, "TG-FTIR-MS study of synergistic effects during co-pyrolysis of corn stalk and high-density polyethylene (HDPE)," *Energy Convers Manag*, vol. 181, pp. 202–213, Feb. 2019, doi: 10.1016/J.ENCONMAN.2018.11.065.

[51] P. Liu, Y. Wang, Z. Zhou, H. Yuan, and T. Zheng, "Gas fuel production derived from pine sawdust pyrolysis catalyzed on alumina," *Asia-Pacific Journal of Chemical Engineering*, vol. 15, no. 4, p. e2456, Jul. 2020, doi: 10.1002/APJ.2456.

[52] J. Chattopadhyay, T. S. Pathak, R. Srivastava, and A. C. Singh, "Catalytic co-pyrolysis of paper biomass and plastic mixtures (HDPE (high density polyethylene), PP (polypropylene) and PET (polyethylene terephthalate)) and product analysis," *Energy*, vol. 103, pp. 513–521, May 2016, doi: 10.1016/J.ENERGY.2016.03.015.

[53] X. Jin, J. H. Lee, and J. W. Choi, "Catalytic co-pyrolysis of woody biomass with waste plastics: Effects of HZSM-5 and pyrolysis temperature on producing high-value pyrolytic products and reducing wax formation," *Energy*, vol. 239, Jan. 2022, doi: 10.1016/j.energy.2021.121739.

[54] M. Alam, A. Bhavanam, A. Jana, J. kumar S. Viroja, and N. R. Peela, "Co-pyrolysis of bamboo sawdust and plastic: Synergistic effects and kinetics," *Renew Energy*, vol. 149, pp. 1133–1145, Apr. 2020, doi: 10.1016/j.renene.2019.10.103.

[55] L. Luo, X. Guo, Z. Zhang, M. Chai, M. M. Rahman, X. Zhang, and J. Cai, "Insight into Pyrolysis Kinetics of Lignocellulosic Biomass: Isoconversional Kinetic Analysis by the Modified Friedman Method," *Energy and Fuels*, vol. 34, no. 4, pp. 4874–4881, Apr. 2020, doi: 10.1021/acs.energyfuels.0c00275.

[56] Y. Zhang, J. Hu, X. Cheng, and M. H. Tahir, "Pyrolysis characteristics, kinetics, and biochar of fermented pine sawdust–based waste," *Environmental Science and Pollution Research*, 2023, doi: 10.1007/s11356-022-25084-0.

[57] B. Han, Y. Chen, Y. Wu, D. Hua, Z. Chen, W. Feng, M. Yang, and Q. Xie, "Co-pyrolysis behaviors and kinetics of plastics-biomass blends through thermogravimetric analysis," *J Therm Anal Calorim*, vol. 115, no. 1, pp. 227–235, Jan. 2014, doi: 10.1007/S10973-013-3228-7/FIGURES/7.

[58] D. V. Suriapparao, B. Boruah, D. Raja, and R. Vinu, "Microwave assisted co-pyrolysis of biomasses with polypropylene and polystyrene for high quality bio-oil production," *Fuel Processing Technology*, vol. 175, pp. 64–75, Jun. 2018, doi: 10.1016/j.fuproc.2018.02.019.

[59] K. G. Burra and A. K. Gupta, “Kinetics of synergistic effects in co-pyrolysis of biomass with plastic wastes,” *Appl Energy*, vol. 220, pp. 408–418, Jun. 2018, doi: 10.1016/j.apenergy.2018.03.117.

[60] H. Stančin, H. Mikulčić, N. Manić, D. Stojiljiković, M. Vujanović, X. Wang, and N. Duić, “Thermogravimetric and kinetic analysis of biomass and polyurethane foam mixtures Co-Pyrolysis,” *Energy*, vol. 237, Dec. 2021, doi: 10.1016/j.energy.2021.121592.

[61] D. Iribarren, J. F. Peters, and J. Dufour, “Life cycle assessment of transportation fuels from biomass pyrolysis,” *Fuel*, vol. 97, pp. 812–821, Jul. 2012, doi: 10.1016/j.fuel.2012.02.053.

[62] PlascticsEurope, “Plastics-the Facts 2021 An analysis of European plastics production, demand and waste data.”

[63] “LCA Measure - Global Warming Potential (GWP) – LCA Measure Details.” https://calculatelca.com/static-content/software/impact-estimator/help-files/introduction/summary_measure_details_global_warming_potential.html (accessed Mar. 24, 2023).

[64] D. Gahane, D. Biswal, and S. A. Mandavgane, “Life Cycle Assessment of Biomass Pyrolysis,” *Bioenergy Research*, vol. 15, no. 3. Springer, pp. 1387–1406, Sep. 01, 2022. doi: 10.1007/s12155-022-10390-9.

[65] Y. Van Fan, R. R. Tan, and J. J. Klemeš, “A system analysis tool for sustainable biomass utilisation considering the Emissions-Cost Nexus,” *Energy Convers Manag*, vol. 210, Apr. 2020, doi: 10.1016/j.enconman.2020.112701.

[66] D. N. Vienescu, J. Wang, A. Le Gresley, and J. D. Nixon, “A life cycle assessment of options for producing synthetic fuel via pyrolysis,” *Bioresour Technol*, vol. 249, pp. 626–634, Feb. 2018, doi: 10.1016/j.biortech.2017.10.069.

[67] A. Antelava, S. Damilos, S. Hafeez, G. Manos, S. M. Al-Salem, B. K. Sharma, K. Kohli, and A. Constantinou, “Plastic Solid Waste (PSW) in the Context of Life Cycle Assessment (LCA) and Sustainable Management,” *Environ Manage*, vol. 64, no. 2, pp. 230–244, Aug. 2019, doi: 10.1007/s00267-019-01178-3.

[68] O. Eriksson and O. Finnveden, “Plastic waste as a fuel-CO 2-neutral or not?,” 2009, doi: 10.1039/b908135f.

[69] A. Demetrious and E. Crossin, “Life cycle assessment of paper and plastic packaging waste in landfill, incineration, and gasification-pyrolysis,” *J Mater Cycles Waste*

Manag, vol. 21, no. 4, pp. 850–860, Jul. 2019, doi: 10.1007/S10163-019-00842-4/TABLES/7.

[70] D. Lazarevic, E. Aoustin, N. Buclet, and N. Brandt, "Plastic waste management in the context of a European recycling society: Comparing results and uncertainties in a life cycle perspective," *Resour Conserv Recycl*, vol. 55, no. 2, pp. 246–259, Dec. 2010, doi: 10.1016/J.RESCONREC.2010.09.014.

[71] S. Neha, K. Prasanna Kumar Ramesh, and N. Remya, "Techno-economic analysis and life cycle assessment of microwave co-pyrolysis of food waste and low-density polyethylene," *Sustainable Energy Technologies and Assessments*, vol. 52, Aug. 2022, doi: 10.1016/j.seta.2022.102356.

[72] D. Simón, A. M. Borreguero, A. de Lucas, and J. F. Rodríguez, "Recycling of polyurethanes from laboratory to industry, a journey towards the sustainability," *Waste Management*, vol. 76, pp. 147–171, Jun. 2018, doi: 10.1016/J.WASMAN.2018.03.041.

[73] "Macquarie University - Elemental Microanalysis Service." https://www.mq.edu.au/research/research-centres-groups-and-facilities/secure-planet/facilities/chemical-analysis-facility/elemental-microanalysis-service (accessed Feb. 24, 2023).

[74] "ISO - ISO 562:1981 - Hard coal and coke — Determination of volatile matter content." https://www.iso.org/standard/4652.html (accessed Feb. 22, 2023).

[75] "ASTM D 2867 : 2004 Standard Test Methods for Moisture in Activate." https://infostore.saiglobal.com/en-us/standards/astm-d-2867-2004-143767_saig_astm_astm_319038/ (accessed Feb. 22, 2023).

[76] "ASTM D2866 : Standard Test Method for Total Ash Content of Activated Carbon." https://global.ihs.com/doc_detail.cfm?document_name=ASTM%20D2866&item_s_key=00017015 (accessed Feb. 22, 2023).

[77] A. Hlavsová, A. Corsaro, H. Raclavská, D. Juchelková, H. Škrobánková, and J. Frydrych, "Syngas production from pyrolysis of nine composts obtained from nonhybrid and hybrid perennial grasses," *Scientific World Journal*, vol. 2014, 2014, doi: 10.1155/2014/723092.

[78] H. Stančin, M. Šafář, J. Růžičková, H. Mikulčić, H. Raclavská, X. Wang, and N. Duić, "Co-pyrolysis and synergistic effect analysis of biomass sawdust and polystyrene mixtures for production of high-quality bio-oils," *Process Safety and Environmental Protection*, vol. 145, pp. 1–11, Jan. 2021, doi: 10.1016/j.psep.2020.07.023.

[79] V. Strezov, J. A. Lucas, and L. Strezov, “Computer aided thermal analysis,” *J Therm Anal Calorim*, vol. 72, no. 3, pp. 907–918, Nov. 2004, doi: 10.1023/A:1025030618161.

[80] X. Yuan, T. He, H. Cao, and Q. Yuan, “Cattle manure pyrolysis process: Kinetic and thermodynamic analysis with isoconversional methods,” *Renew Energy*, vol. 107, pp. 489–496, 2017, doi: 10.1016/j.renene.2017.02.026.

[81] K. R. G. Burra, X. Liu, Z. Wang, J. Li, D. Che, and A. K. Gupta, “Quantifying the sources of synergistic effects in co-pyrolysis of pinewood and polystyrene,” *Appl Energy*, vol. 302, Nov. 2021, doi: 10.1016/j.apenergy.2021.117562.

[82] A. Ephraim, D. Pham Minh, D. Lebonnois, C. Peregrina, P. Sharrock, and A. Nzihou, “Co-pyrolysis of wood and plastics: Influence of plastic type and content on product yield, gas composition and quality,” *Fuel*, vol. 231, no. April, pp. 110–117, 2018, doi: 10.1016/j.fuel.2018.04.140.

[83] M. Ajorloo, M. Ghodrat, J. Scott, and V. Strezov, “Modelling and statistical analysis of plastic biomass mixture co-gasification,” *Energy*, vol. 256, p. 124638, Oct. 2022, doi: 10.1016/J.ENERGY.2022.124638.

[84] “ecoinvent v3.8 - ecoinvent.” https://ecoinvent.org/the-ecoinvent-database/data-releases/ecoinvent-3-8/ (accessed Jan. 02, 2023).

[85] A. Ciroth, “ICT for environment in life cycle applications openLCA - A new open source software for Life Cycle Assessment,” *International Journal of Life Cycle Assessment*, vol. 12, no. 4, pp. 209–210, 2007, doi: 10.1065/LCA2007.06.337.

[86] H. Stančin, J. Růžičková, H. Mikulčić, H. Raclavská, M. Kucbel, X. Wang, and N. Duić, “Experimental analysis of waste polyurethane from household appliances and its utilization possibilities,” *J Environ Manage*, vol. 243, no. May, pp. 105–115, 2019, doi: 10.1016/j.jenvman.2019.04.112.

[87] R. K. Mishra, S. M. Chistie, S. U. Naik, and P. Kumar, “Thermocatalytic co-pyrolysis of waste biomass and plastics: Studies of physicochemical properties, kinetics behaviour, and characterization of liquid product,” *Journal of the Energy Institute*, vol. 105, pp. 192–202, Dec. 2022, doi: 10.1016/j.joei.2022.09.003.

[88] H. Stančin, M. Šafář, J. Růžičková, H. Mikulčić, H. Raclavská, X. Wang, and N. Duić, “Influence of plastic content on synergistic effect and bio-oil quality from the co-pyrolysis of waste rigid polyurethane foam and sawdust mixture,” *Renew Energy*, vol. 196, pp. 1218–1228, Aug. 2022, doi: 10.1016/J.RENENE.2022.07.047.

[89] J. Li, X. Ye, K. G. Burra, W. Lu, Z. Wang, X. Liu, and A. K. Gupta, "Synergistic effects during co-pyrolysis and co-gasification of polypropylene and polystyrene," *Appl Energy*, vol. 336, Apr. 2023, doi: 10.1016/j.apenergy.2023.120750.

[90] H. Yang, R. Yan, H. Chen, D. H. Lee, and C. Zheng, "Characteristics of hemicellulose, cellulose and lignin pyrolysis," *Fuel*, vol. 86, no. 12–13, pp. 1781–1788, Aug. 2007, doi: 10.1016/j.fuel.2006.12.013.

[91] N. I. Izzatie, M. H. Basha, Y. Uemura, M. S. M. Hashim, M. Afendi, and M. A. F. Mazlan, "Co-pyrolysis of rubberwood sawdust (RWS) and polypropylene (PP) in a fixed bed pyrolyzer," *Journal of Mechanical Engineering and Sciences*, vol. 13, no. 1, pp. 4636–4647, Mar. 2019, doi: 10.15282/jmes.13.1.2019.20.0390.

[92] Q. van Nguyen, Y. S. Choi, S. K. Choi, Y. W. Jeong, and Y. S. Kwon, "Improvement of bio-crude oil properties via co-pyrolysis of pine sawdust and waste polystyrene foam," *J Environ Manage*, vol. 237, pp. 24–29, May 2019, doi: 10.1016/j.jenvman.2019.02.039.

[93] J. Nisar, G. Ali, A. Shah, M. Iqbal, R. A. Khan, Sirajuddin, F. Anwar, R. Ullah, and M. S. Akhter, "Fuel production from waste polystyrene via pyrolysis: Kinetics and products distribution," *Waste Management*, vol. 88, pp. 236–247, Apr. 2019, doi: 10.1016/j.wasman.2019.03.035.

[94] S. v. Vassilev, D. Baxter, L. K. Andersen, and C. G. Vassileva, "An overview of the chemical composition of biomass," *Fuel*, vol. 89, no. 5, pp. 913–933, May 2010, doi: 10.1016/J.FUEL.2009.10.022.

[95] "Polypropylene Fibre Preventing the Occurrence of Spalling | Encyclopedia MDPI." https://encyclopedia.pub/item/revision/d9eafe60d0601e96dfd689f8ccd5bf7b (accessed Feb. 22, 2023).

[96] V. Strezov, B. Moghtaderi, and J. A. Lucas, "THERMAL STUDY OF DECOMPOSITION OF SELECTED BIOMASS SAMPLES," 2003.

[97] B. Han, Y. Chen, Y. Wu, D. Hua, Z. Chen, W. Feng, M. Yang, and Q. Xie, "Co-pyrolysis behaviors and kinetics of plastics-biomass blends through thermogravimetric analysis," *J Therm Anal Calorim*, vol. 115, no. 1, pp. 227–235, Jan. 2014, doi: 10.1007/s10973-013-3228-7.

[98] K. Slopiecka, P. Bartocci, and F. Fantozzi, "Thermogravimetric analysis and kinetic study of poplar wood pyrolysis," *Appl Energy*, vol. 97, pp. 491–497, 2012, doi: 10.1016/j.apenergy.2011.12.056.

[99] F. Abnisa and W. M. A. Wan Daud, “A review on co-pyrolysis of biomass: An optional technique to obtain a high-grade pyrolysis oil,” *Energy Convers Manag*, vol. 87, pp. 71–85, Nov. 2014, doi: 10.1016/j.enconman.2014.07.007.

[100] Z. Kaczor, Z. Buliński, and S. Werle, “Modelling approaches to waste biomass pyrolysis: a review,” *Renew Energy*, vol. 159, pp. 427–443, Oct. 2020, doi: 10.1016/J.RENENE.2020.05.110.

[101] A. Hai, G. Bharath, M. F. A. Patah, W. M. A. W. Daud, R. K., P. L. Show, and F. Banat, “Machine learning models for the prediction of total yield and specific surface area of biochar derived from agricultural biomass by pyrolysis,” *Environ Technol Innov*, vol. 30, p. 103071, May 2023, doi: 10.1016/J.ETI.2023.103071.

[102] M. Khan, Z. Ullah, O. Mašek, S. Raza Naqvi, and M. Nouman Aslam Khan, “Artificial neural networks for the prediction of biochar yield: A comparative study of metaheuristic algorithms,” *Bioresour Technol*, vol. 355, p. 127215, Jul. 2022, doi: 10.1016/J.BIORTECH.2022.127215.

[103] X. Zhu, Y. Li, and X. Wang, “Machine learning prediction of biochar yield and carbon contents in biochar based on biomass characteristics and pyrolysis conditions,” *Bioresour Technol*, vol. 288, p. 121527, Sep. 2019, doi: 10.1016/J.BIORTECH.2019.121527.

[104] R. E. Harmon, G. Sribala, L. J. Broadbelt, and A. K. Burnham, “Insight into Polyethylene and Polypropylene Pyrolysis: Global and Mechanistic Models,” *Energy and Fuels*, vol. 35, no. 8, pp. 6765–6775, Apr. 2021, doi: 10.1021/ACS.ENERGYFUELS.1C00342.

[105] Y. Li, R. Gupta, and S. You, “Machine learning assisted prediction of biochar yield and composition via pyrolysis of biomass,” *Bioresour Technol*, vol. 359, p. 127511, Sep. 2022, doi: 10.1016/J.BIORTECH.2022.127511.

[106] D. Ying Ying Tang, K. Wayne Chew, H. Y. Ting, Y. H. Sia, F. G. Gentili, Y. K. Park, F. Banat, A. B. Culaba, Z. Ma, and P. Loke Show, “Application of regression and artificial neural network analysis of Red-Green-Blue image components in prediction of chlorophyll content in microalgae,” *Bioresour Technol*, vol. 370, p. 128503, Feb. 2023, doi: 10.1016/J.BIORTECH.2022.128503.

[107] R. A. U. Nabi, M. Y. Naz, S. Shukrullah, M. Ghamkhar, N. U. Rehman, M. Irfan, A. O. Alqarni, S. Legutko, I. Kruszelnicka, D. Ginter-Kramarczyk, M. Ochowiak, S. Włodarczak, A. Krupińska, and M. Matuszak, “Analysis of Statistically Predicted Rate

Constants for Pyrolysis of High-Density Plastic Using R Software," *Materials 2022, Vol. 15, Page 5910*, vol. 15, no. 17, p. 5910, Aug. 2022, doi: 10.3390/MA15175910.

[108] "Home - ecoinvent." https://ecoinvent.org/ (accessed Jan. 02, 2023).

[109] J. Pickin, C. Wardle, K. O'farrell, P. Nyunt, S. Donovan, and B. Grant, "Final National Waste Report 2020," 2020.

[110] Schandl H, King S, Walton A, Kaksonen AH, Tapsuwan S, and Baynes TM, *Circular economy roadmap for plastics, glass, paper and tyres*. CSIRO, Australia, 2020.

[111] S. Black, K. Harwood, S. Lees, K. Kuhanandan, J. Clements, K. Dickson, P. Mijer, L. le Miere, J. Guo, D. Kheng, V. Rathod, and K. Lees, "PLASTIC REVOLUTION TO REALITY A roadmap to halve Australia's single-use plastic litter 2020," 2020. [Online]. Available: www.wwf.org.au

6. CURRICULUM VITAE

HRVOJE STANČIN, mag.ing.mech. was born on the 17th of September 1993 in Varaždin, Croatia. After finishing high school "Gymnasium Fran Galović" in Koprivnica in 2012, as one of the best students in his generation, he enrolled at the Faculty of Mechanical Engineering and Naval Architecture (FMENA), University of Zagreb, Croatia. He finished his undergraduate studies in mechanical engineering in 2016 and his graduate studies in 2018. During graduate studies, he spent one semester at Vysoka Škola Banska-Technicka Univerzita Ostrava, Czech Republic, in the scope of Erasmus+ programme, where he worked on research for the purposes of his Master's Thesis. After completing his studies, he got employed at the Faculty of Mechanical Engineering and Naval Architecture, University of Zagreb, at the Department of Power, Energy and Environmental Engineering as a project assistant, working on an EU-funded project in field of blue energy. At the end of 2019, he started his PhD studies, while continuing to work on EU-funded projects as a member of the PowerLab group and SDEWES Centre. At the end of 2020, he initiated the Cotutelle doctoral programme at the University of Zagreb and Macquarie University, Sydney, Australia. In the scope of this agreement, he spent one year in Australia, working on his research at the Faculty of Science and Engineering, Department of Earth and Environmental Sciences.

He attended sevral international scientific conferences and has been a part of the local organising committee of the international SDEWES conferences in 2019 and 2021. He is the author of ten scientific papers published in renowned (CC/SCI indexed) journals. His current Scopus h-index is 7 with over 300 citations. He serves as a reviewer for Renewable and Sustainable Energy Reviews, Journal of Cleaner Production, Fuel, Energy, Energy Conversion and Management, Cleaner Chemical Engineering, Journal of Environmental Management, Thermal Science, and JSDEWES.

He is a profound English speaker and uses German and Czech language passively.

List of published scientific journal papers:

[1] H. Stančin, V. Strezov, H. Mikulčić, "Life cycle assessment of alternative fuel production by co-pyrolysis of waste biomass and plastics"; *Journal of Cleaner Production,* vol. 414, Aug. 2023, doi: 10.1016/j.jclepro.2023.137676

[2] H. Stančin, H. Mikulčić, X. Wang, N. Duić, "A review on alternative fuels in future energy system"; *Renewable and Sustainable Energy Reviews*, vol. 128, 2020, doi: 10.1016/j.rser.2020.109927

[3] H. Stančin, M. Šafář, J. Růžičková, H. Mikulčić, H. Raclavská, X. Wang, N. Duić, "Co-pyrolysis and synergistic effect analysis of biomass sawdust and polystyrene mixtures for production of high-quality bio-oils"; *Process Safety and Environmental Protection*, vol. 145, pp. 1–11, Jan. 2021, doi: 10.1016/j.psep.2020.07.023

[4] H. Stančin, M. Šafář, J. Růžičková, H. Mikulčić, H. Raclavská, X. Wang, N. Duić, "Influence of plastic content on synergistic effect and bio-oil quality from the co-pyrolysis of waste rigid polyurethane foam and sawdust mixture"; *Renew Energy*, vol. 196, pp. 1218–1228, Aug. 2022, doi: 10.1016/J.RENENE.2022.07.047

[5] H. Stančin, H. Mikulčić, N. Manić, D. Stojiljiković, M. Vujanović, X. Wang, and N. Duić, "Thermogravimetric and kinetic analysis of biomass and polyurethane foam mixtures Co-Pyrolysis"; *Energy*, vol. 237, Dec. 2021, doi: 10.1016/j.energy.2021.121592

[6] Stančin, Hrvoje; Růžičková, Jana; Mikulčić, Hrvoje; Raclavská, Helena; Kucbel, Marek; Wang, Xuebin; Duić, Neven, "Experimental analysis of waste polyurethane from household appliances and its utilization possibilities"; *Journal of environmental management*, vol: 243, 2019; doi: 10.1016/j.jenvman.2019.04.112

[7] Hrvoje Stančin, Antun Pfeifer, Christoforos Perakis, Nikolaos Stefanatos, Marko Damasiotis, Stefano Magaudda, Federica Di Pietrantonio, Hrvoje Mikulčić, "Blue Energy Spearheading the Energy Transition: The Case of Crete"; *Frontiers in Energy Research*, 2022, (10, 868334); https://doi.org/10.3389/fenrg.2022.868334

[8] Mikulcic, H; Jin, QM; Stancin, H; Wang, XB; Li, SS; Tan, HZ; Duic, N.; "Thermogravimetric Analysis Investigation of Polyurethane Plastic Thermal Properties Under Different Atmospheric Conditions"; *Journal Of Sustainable Development Of Energy, Water, and Environment Systems (JSDEWES)*; Volume: 7 Issue: 2 doi: 10.13044/j.sdewes.d6.0254

[9] Wang, X; Ma, D; Jin, Q; Deng, S; Stančin, H; Tan, H; Mikulčić, H.; "Synergistic effects of biomass and polyurethane co-pyrolysis on the yield, reactivity, and heating value of biochar at high temperatures"; *Fuel Processing Technology*, Vol. 194, November 2019; doi:10.1016/j.fuproc.2019.10612

[10] Group of authors in the scope of project collaboration https://www.frontiersin.org/articles/10.3389/fenrg.2022.939961/full ; „Integrating Blue Energy in Maritime Spatial Planning of Mediterranean Regions"; *Frontiers in Energy Research*, 2022; doi:10.3389/fenrg.2022.939961

7. SUMMARY OF PAPERS

PAPER 1

Stančin, Hrvoje; Mikulčić, Hrvoje; Wang, Xuebin; Duić, Neven: **A Review on Alternative Fuels in Future Energy System**; *Renewable and Sustainable Energy Reviews*; *128 (2020); https://doi.org/10.1016/j.rser.2020.109927*

Transition and decarbonization of the energy sector require the utilization of new technologies and energy sources. Higher penetration of intermittent renewable energy sources implies the installation of energy storage, to store electricity excess and enhanced system efficiency. These electricity surpluses that will occur more often in the future energy system could be effectively utilized for the production of alternative fuels. Most of the alternative fuels that are considered for future applications are already known chemicals or products, nowadays used for other purposes. Another great advantage of some alternative fuels lies in their possibilities to act as an energy carrier. This feature might be crucial while discussing their utilization potential and further development. Fuels which can simultaneously be used for power generation and as an energy carrier will have a more important role in the future and are likely to be utilized on a greater scale. Renewable energy source like biomass, on the other hand, is already widely used, and their role in the future system is not questionable. Even though significant increment in biomass consumption raises serious concerns about its sustainability, and seeks for new approaches. In this work, the authors tried to review alternative fuel characteristics, alongside their utilization and production opportunities. To come up with the optimal solutions, the authors compared various proposed alternative fuels, alongside their advantages and drawbacks with an aim to find the most appropriate role for each fuel.

Hrvoje Stančin - writing original manuscript, review and editing; visualisation, conceptualisation; methodology. Hrvoje Mikulčić - writing original manuscript, review and editing, methodology. Xuebin Wang - review and editing, formal analysis, supervision. Neven Duić – supervision.

PAPER 2

Stančin, Hrvoje; Šafář, Michal; Růžičková, Jana; Mikulčić, Hrvoje; Raclavská, Helena; Wang, Xuebin; Duić, Neven: **Co-Pyrolysis and Synergistic Effect Analysis of Biomass Sawdust and Polystyrene Mixtures for Production of High-quality Bio-oils**; *Process Safety and Environmental Protection; 145 (2021);* https://doi.org/10.1016/j.psep.2020.07.023

Usage of traditional biomass raises serious concerns regarding its sustainability due to the inefficient combustion in household stoves and potential over-usage if the intention is to replace fossil fuels in power plants. Co-pyrolysis of biomass feedstock with different waste materials, especially plastics, might be a promising alternative for sustainable usage of enhanced biofuels. Even more, co-pyrolysis can help to integrate waste management schemes into the power production sector. Plastics materials have properties similar to those of fossil fuels in terms of heating value and the absence of oxygenated compounds; therefore, they could significantly improve the properties of biomass products, especially bio-oils. Especially interesting for this method is polystyrene (PS) since it yields a high share of liquid fraction, which is the most valuable pyrolytic product. In this work, co-pyrolysis was performed for a mixture of waste biomass sawdust (oak, poplar and fir wood) and waste polystyrene from dairy product packaging. Pyrolysis was carried out for sawdust and polystyrene alone, and their respective fuel blends (PS/SD 25-75%, PS/SD 50-50%, PS/SD 75-25%) from room temperature to 600°C with a retention time of half an hour. The highest yield of liquid fraction was noticed for mixtures with 75% of PS, while the lowest one was for blends with 25% of PS, with a yield of 83.86% and 62.33%, respectively. Additionally, the mass spectrometric analysis was carried out to determine the chemical composition of the obtained oil.

Hrvoje Stančin - writing original manuscript, review and editing; visualisation, conceptualisation; methodology, experimental analysis. Michal Šafar - experimental analysis, results analysis. Jana Ružičkova - results analysis. Hrvoje Mikulčić - methodology, visualisation. Helena Raclavska - supervision, methodology, results analysis, conceptualisation. Xuebin Wang - supervision. Neven Duić - supervision

PAPER 3

Stančin, Hrvoje; Šafář, Michal; Růžičková, Jana; Mikulčić, Hrvoje; Raclavská, Helena; Wang, Xuebin; Duić, Neven: **Influence of plastic content on synergistic effect and bio-oil quality from the co-pyrolysis of waste rigid polyurethane foam and sawdust mixture;** *Renewable Energy; 196 (2022);* https://doi.org/10.1016/j.renene.2022.07.047

Current disposal of end-of-life plastics by landfilling or incineration raises serious environmental concerns, simultaneously representing an irretrievable loss of valuable resources. Especially this is evident for materials that have a complex structure, like polyurethane foams. In this work, co-pyrolysis with sawdust was carried out to analyze and evaluate the product quality for further utilization as alternative fuels. The introduction of polyurethane increased the oil yield but in a limited range since no significant difference was observed between the mixture with 25 and 75% of polyurethane content. In addition, the chemical analysis showed that small addition of polyurethane is sufficient to eliminate most of the oxygenated compounds derived from sawdust. Nevertheless, the obtained liquid products are mostly benzenamines that do not meet the criteria for fuel composition. Analysis of the synergistic effect shows that the strongest impact is visible for a small branch of plastic content where liquid yield was promoted at the expense of gas. With a further increment of plastic content, this effect fades away, except for the solid residue which remains constant. Finally, a brief analysis of the gaseous fraction showed that obtained products are preferred in syngas composition, with notable hydrogen yield as the most valuable constituent.

Hrvoje Stančin - writing original manuscript, review and editing; visualisation, conceptualisation; methodology, experimental analysis. Michal Šafar - experimental analysis, results analysis. Jana Ružičkova - results analysis. Hrvoje Mikulčić - methodology, visualisation. Helena Raclavska - supervision, methodology, results analysis, conceptualisation. Xuebin Wang - supervision. Neven Duić - supervision

PAPER 4

Stančin, Hrvoje, Mikulčić, Hrvoje; Manić, Nebojša; Stojiljković, Dragoslava; Vujanović, Milan; Wang, Xuebin; Duić, Neven: **Thermogravimetric and Kinetic Analysis of Biomass and Polyurethane Foam Mixtures Co-Pyrolysis**; *Energy*; *237 (2021);* https://doi.org/10.1016/j.energy.2021.121592

Alternative fuels are crucial for the decarbonisation of high-energy demanding processes. The utilisation of waste materials to produce alternative fuels is especially interesting since, the co-pyrolysis of waste plastics and biomass was lately introduced as promising method since the synergistic effect might enhance the product properties compared to those from individual pyrolysis. Furthermore, the utilisation of waste biomass, like sawdust, is interesting since it does not influence the sustainability of biomass consumption, and even more, it avoids the usage of raw feedstock. Thermogravimetric analysis is performed to determine the thermal

degradation behaviour and kinetic parameters of investigated mixtures to find the most appropriate utilisation method. Co-pyrolysis was conducted for three mixtures with the following biomass/polyurethane ratios: 75-25 %, 50-50 %, 25-75 %, over a temperature range of 30-800 °C, at three heating rates 5, 10 and 20 °C/min, under an inert atmosphere. Obtained results were subjected to comprehensive kinetic analysis to determine effective activation energy using the isoconversional model-free methods and provide a detailed analysis of the samples' thermal degradation process. This work aimed to identify the main thermal decomposition stages during co-pyrolysis of biomass and polyurethane mixtures and provide the mixture composition's influence on the considered thermochemical conversion process.

Hrvoje Stančin - writing original manuscript, review and editing; visualisation, conceptualisation; methodology, experimental analysis. Hrvoje Mikulčić - writing and editing, methodology. Nebojša Manić - supervision, writing and editing, results analysis, experimental work. Dragoslava Stojiljković . methodology, conceptualisation, experimental work. Milan Vujanović - methodology, visualisation. Xuebin Wang and Neven Duić - supervision.

PAPER 5

Stančin, Hrvoje, Mikulčić, Hrvoje; Manić, Nebojša; Stojiljković, Dragoslava; Vujanović, Milan; Duić, Neven; **Thermogravimetric and Kinetic Analysis of Waste Biomass and Plastic Mixtures***; JSDEWES (under revision)*

Thermogravimetric and kinetic analysis of biomass and plastic co-pyrolysis can provide valuable inputs for a better understanding of decomposition mechanisms. Such inputs are important for selecting the appropriate process conditions but can also be helpful for process modelling. This work investigates the properties of heterogenous sawdust in a mixture with polypropylene and polystyrene. Thermogravimetric analysis is conducted to determine the decomposition mechanism and kinetic parameters of investigated mixtures and to derive appropriate conclusions regarding their further utilization potential. Co-pyrolysis was performed on mixtures with the following biomass/plastic ratios: 75-25%, 50-50%, 25-75%, over a temperature range of 30-550 °C, at four heating rates 5, 10, 20, and 30 °C/min, with pure argon as a carrier gas. Obtained results were then subjected to comprehensive kinetic and thermodynamic analysis. The primary goal was to determine effective activation energies using model-free methods, pre-exponential factors, and elementary thermodynamic parameters such as changes in enthalpy, entropy, and free Gibbs energy. Finally, the influence of the heating rate and mixture composition was extensively investigated by analyzing calculated parameters.

Hrvoje Stančin - writing original manuscript, review and editing; visualisation, conceptualisation; methodology, experimental analysis. Hrvoje Mikulčić - writing and editing, methodology. Nebojša Manić - supervision, writing and editing, results analysis, experimental work. Dragoslava Stojiljković - methodology, conceptualisation, experimental work. Milan Vujanović - methodology, visualisation. Neven Duić - supervision.

PAPER 6

Stančin, Hrvoje; Strezov, Vladimir; **Co-pyrolysis of three-component biomass-plastic mixture for alternative fuel production***; Energy and Fuels (under revision)*

Thermochemical conversion of waste materials recently gained significant attention since it opens the opportunity for the simultaneous production of alternative fuels while tackling issues related to waste management. Co-pyrolysis of waste biomass and plastics is very promising since the demand for feedstock can be satisfied from different streams, while obtained products have higher value properties. In this work, detailed experimental analysis and product characterisation is performed for three individual samples (pine sawdust, polypropylene, polystyrene) and their respective mixtures with 50% of sawdust, and 50% of plastics equally divided between polypropylene and polystyrene. Results showed that feedstock interaction during co-pyrolysis generally enhances the product properties compared to individual pyrolysis. In the case of pyrolysis oil, a high yield of almost 80% is obtained, with hydrocarbons as the most prominent constituents. Higher than theoretically expected liquid yield is achieved at the expense of gaseous fraction. Since sawdust is the primary source of gases, the mixture's gas composition was weakly affected by the introduction of plastics. Finally, the synergistic effect that occurs between biomass and plastics moderately impacts solid residue, which is slightly increased compared to theoretical values. It can be stated that introducing plastics greatly improves the properties of pyrolytic products, especially when aiming to maximise high-quality liquid yield.

Hrvoje Stančin - writing original manuscript, visualisation, conceptualisation, methodology, data collection, experimental work. Vladimir Strezov - writing original manuscript, methodology, results analysis, supervision.

PAPER 7

Stančin, Hrvoje; Strezov, Vladimir; Mikulčić, Hrvoje; **Life cycle assessment of alternative fuel production by co-pyrolysis of waste biomass and plastics**; *Journal of Cleaner Production; 414 (2023);* https://doi.org/10.1016/j.jclepro.2023.137676

In the scope of energy transition and overall decarbonisation, various alternative fuels are investigated as potential substitutes for conventional fossil fuels. Co-pyrolysis has emerged as a potential solution for production of alternative fuels, while dealing with waste management issues, due to its ability to process different feedstocks. Biomass-derived fuels, with all their constraints, are already used on a commercial scale. Simultaneously, significant efforts are given to scale up fuel production from the thermal treatment of waste plastics. The fuel must be produced sustainably with minimal environmental impacts to be considered an alternative. This study presents the life cycle assessment (LCA) of waste biomass and plastic materials, co-pyrolysed with an aim to produce pyrolysis oil that could be used as a petroleum substitute. Moreover, the environmental impacts from the co-pyrolysis are compared to incineration and landfilling, which are today mostly used to deal with end-of-life plastics. The LCA is carried out in openLCA software using ReCiPe Midpoint 2016 method. Results show that co-pyrolysis mostly reduces emissions associated with environmental impacts, even though this greatly depends on the treatment method used to divert the feedstock. Furthermore, most process emissions are associated with electricity consumption, therefore, integration of plastic processing with renewable energy sources can further reduce the environmental impacts. Finally, the products derived from the process should be of high quality with minimal after-treatment requirements to effectively substitute fossil fuels.

Hrvoje Stančin - writing original manuscript, visualisation, conceptualisation, methodology, data collection, experimental work, simulation. Vladimir Strezov - writing original manuscript, methodology, results analysis, supervision. Hrvoje Mikulčić - writing original manuscript and paper submission.

PAPER 1

Renewable and Sustainable Energy Reviews 128 (2020) 109927

Contents lists available at ScienceDirect

Renewable and Sustainable Energy Reviews

journal homepage: http://www.elsevier.com/locate/rser

A review on alternative fuels in future energy system

H. Stančin [a,*], H. Mikulčić [a,b], X. Wang [b,**], N. Duić [a]

[a] University of Zagreb, Faculty of Mechanical Engineering and Naval Architecture, Croatia
[b] MOE Key Laboratory of Thermo-Fluid Science and Engineering, Xi'an Jiaotong University, Xi'an, Shaanxi, 710049, China

ARTICLE INFO

Keywords:
Alternative fuel
Smart energy system
Variable renewable energy source
Electrolysis
Carbon capture
Pyrolysis
Hydrogen
Biofuel

ABSTRACT

Transition and decarbonization of the energy sector require the utilisation of new technologies and energy sources. Higher penetration of intermittent renewable energy sources implies the installation of energy storage, to store electricity excess and enhanced system efficiency. These electricity surpluses that will occur more often in the future energy system could be effectively utilized for the production of alternative fuels. Most of the alternative fuels that are considered for future applications are already known chemicals or products, nowadays used for other purposes. Another great advantage of some alternative fuels lies in their possibilities to act as an energy carrier. This feature might be crucial while discussing their utilisation potential and further development. Fuels which can simultaneously be used for power generation and as an energy carrier will have a more important role in the future and are likely to be utilized on a greater scale. Renewable energy source like biomass, on the other hand, is already widely used, and their role in the future system is not questionable. Even though significant increment in biomass consumption raises serious concerns about its sustainability, and seeks for new approaches. In this work, the authors tried to review alternative fuel characteristics, alongside their utilisation and production opportunities. To come up with the optimal solutions, the authors compared various proposed alternative fuels, alongside their advantages and drawbacks with an aim to find the most appropriate role for each fuel.

1. Introduction

The transition toward a 100% Renewable Energy System is a complex process with different technical and economic challenges. In order to achieve predetermined goals, several steps should be carried out simultaneously, including increment of energy efficiency, savings in primary energy consumption, and finally, deployment of variable renewable energy sources (VRES) [1]. A high share of intermittent renewables like wind and solar in the electricity mix consequently affects the grid stability and requires the flexible operation of conventional, baseload power plants [2]. Moreover, a higher share of VRES indicates that the periods with an excess or lack of electricity production will be more often; therefore, it is necessary to include short- and long-term energy storage [3]. Fig. 1 illustrates the penetration of VRES into the power system for the case of the European Union (EU28). It is known that about 30% of VRES can be balanced by the grid. Up to 80% of VRES can be integrated using demand response technologies like vehicle-to-gird (V2G), thermal storages, and other types of short-term storage. To integrate 100% of VRES, long-term energy storages are a necessity. Hydropower and biomass are renewable energy sources, suitable for flexible operation in a decarbonized energy system. Nevertheless, these resources may be scarce in some countries or geographical regions, and even more, their over-usage to fill the remaining gap of 20% may be unsustainable [4]. Lately, the chemical conversion of electricity surplus into some form of alternative fuel (Power-to-X) is introduced as a promising solution since they can act as an energy source or carrier, but also as long term energy storage [5].

Alternative fuels may vary by its origin and production process, but the common for all of them is that they are produced through the sustainable and clean procedure, without the additional emissions of Carbon dioxide (CO_2) [6]. There are two main pathways for the synthesis of alternative fuels: direct utilisation of electricity surplus and thermochemical conversion of raw feedstock. For the former one, the term electrofuels has lately been introduced to clearly emphasize the production route and usage of electricity [7]. Electrofuels are carbon-neutral fuels synthesized from the VRES electricity surplus in a

* Corresponding author.
** Corresponding author.
E-mail addresses: hrvoje.stancin@fsb.hr (H. Stančin), hrvoje.mikulcic@fsb.hr (H. Mikulčić), wxb005@mail.xjtu.edu.cn (X. Wang), neven.duic@fsb.hr (N. Duić).

https://doi.org/10.1016/j.rser.2020.109927
Received 29 December 2019; Received in revised form 7 May 2020; Accepted 14 May 2020

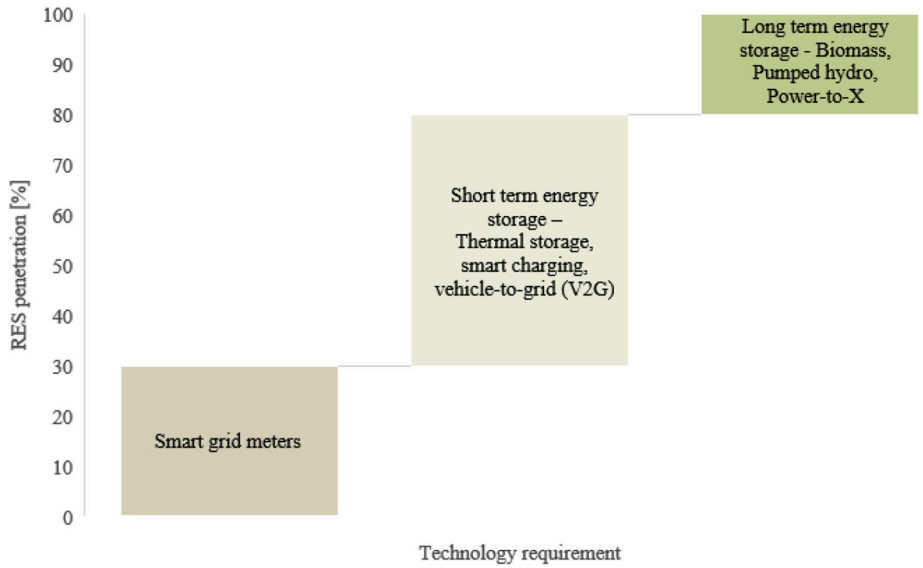

Fig. 1. Integration of Renewable Energy Sources into Electrical Grid [4].

gas, or liquid form, and carbon neutrality is achieved by closing the loop in a way that used CO_2 is captured from the exhaust gases or directly from the air [8]. In addition, electrolysis which is a crucial technology for the synthesis of electrofuels can be operated in a flexible mode in accordance with the production of the renewables, increasing the overall system efficiency and simultaneously allowing higher penetration of VRES [9]. The basic synthesis components of electrofuels are Hydrogen (H_2) and CO_2; therefore production targets are synthetic hydrocarbon gases like methane (CH_4) or butane, or in liquid form alcohol fuels like methanol (CH_3OH) [10]. Another, aforementioned, pathway for the synthesis of alternative fuels is through the thermochemical conversion of a raw feedstock into useful gaseous or liquid fuels [11]. These processes are widely investigated nowadays since they can convert different waste materials or raw feedstock into valuable alternative fuels or chemicals. The main challenge for broader application of thermo-chemical conversion is to couple synthesis process with VRES and lower the production costs. On the other hand, the main advantage of alternative fuels is derived from the fact that once produced; they can easily be stored and distributed where needed [12]. Fig. 2 presents potential pathways for the clean synthesis and utilisation of alternative fuels in future energy systems.

Alternative fuels can be synthesized in a liquid, gaseous or solid

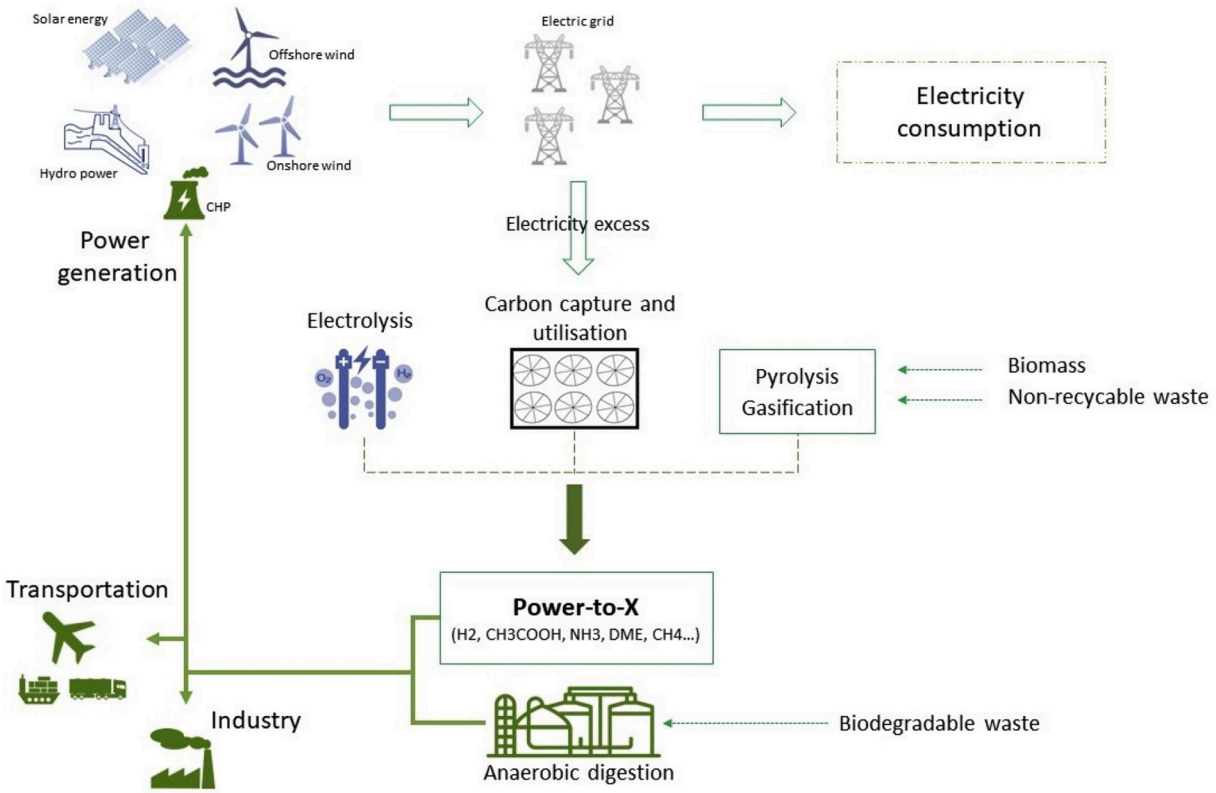

Fig. 2. Production pathway for Alternative Fuels synthesis using VRES.

Table 1
Recent review papers on various alternative fuels.

Type of review	Authors	Content
Electrofuels	McDonagh et al. [18]	• Production of electrofuels using curtailed energy from VRES
	Lehtveer et al. [19]	• Higher penetration of VRES might not be sufficient enough to achieve cost-competitiveness
Hydrogen	Abdalla et al. [20]	• Production, transportation, storage and application challenges
	Parra et al. [21]	• Role of hydrogen for deep system decarbonization
Ammonia	Giddey et al. [23]	• Sustainable synthesis and transport application
	Valera-Medina et al. [22]	• Highlights of previous research regarding utilisation of Ammonia as a viable energy vector for power applications
Biodiesel/Biomass	Chandra Bhan, Lata Verma, and Jiwan Singh [32]	• Review on alternative biofuels
	Bajwa et al. [14]	• Review on solid densified biomass products
	Perkins et al. [25]	• Fast pyrolysis for the production of liquid biofuels
	Widjaya et al. [26]	• Biomass gasification
	Sher et al. [33]	• Thermal and kinetic analysis of six different biomass fuels for power generation
Alcohol derived fuels	Verhelst et al. [34]	• Methanol as an IC engine fuel
	Svanberg et al. [28]	• Methanol for shipping
	Çelebi and Ayday [27]	• Review on light alcohol fuels
	Awad et al. [35]	• Alcohol and ether alternative fuels
Non-recyclable waste	Makarichi et al. [29]	• Review on waste incineration
	Al-Salem et al. [30]	• Pyrolysis of waste plastics
	Hassan et al. [31]	• Co-pyrolysis of biomass and plastics

phase, depending on the application needs and production processes. Liquid and some gaseous fuels are the most promising solution for the transport sector [13], while solid fuels are likely to be used for stationary needs in power plants [14]. Additionally, fuels that might be utilized in more than one form, and simultaneously being used as an energy carrier or storage will be deployed on a greater scale. To maximise fuel and overall system efficiency, cross-sectoral integration is mandatory [15]. This implies, combined heat and power (CHP) production, but even more, deeper integration of transport and industry within the power generation sector [16]. Cogeneration plants have notably higher efficiency compared to conventional power plants; therefore, they are preferred in the future energy system. Moreover, waste heat can be utilized for district heating or industrial purposes, or directly for the production of alternative fuels. Term alternative fuels will be used for all considered fuels in this review, including electrofuels, to avoid potential confusion.

The majority of alternative fuels still haven't reached the commercial scale of application due to the limitations in production or consumption processes and technologies. Mainly, this is related to a high energy penalty which fuels need to undergo during the life-cycle or the economic viability of the production process itself [13]. At the moment, biomass is the only one commercially used, while its consumption is expected to increase even more. Other alternative fuels like hydrogen, ammonia, methanol, biodiesel, biogas, waste-derived fuels, etc. still haven't reached commercial maturity, and their current consumption is almost negligible [17]. Table 1 presents recent reviews on considered alternative fuels with a brief description of the main objectives. McDonagh et al. [18] analysed the cost and efficiency of electrofuels production using curtailed energy when VRES penetration is between 40 and 60%. It was shown that up to 56% more could be achieved in production with approximately similar cost reduction. Lehtveer et al. [19] analysed the cost-competitiveness of electrofuels in future energy systems, showing that they are unlikely to become feasible even with higher penetration of VRES. Abdalla et al. [20] and Parra et al. [21] reviewed the role of hydrogen for deeper system decarbonization, concluding that pronouncedly more needs to be done by policymaking to boost up the broader deployment of hydrogen as an alternative fuel. Valera-Medina et al. [22] and Giddey et al. [23] evaluated the role of ammonia in the future energy system. They find that ammonia might have an important role as energy storage or carrier. Biodiesel and biomass were widely investigated over the years as a carbon-neutral energy source. Lately, the research focus was shifted to the solutions that could significantly improve the properties of biofuels and enhance their efficiency. The utilisation of waste biomass feedstock [24] through thermochemical conversion processes such as pyrolysis [25] or gasification [26] could significantly improve the sustainability of biomass consumption. Various alcohol derived fuels are widely investigated as a potential substitute for IC engines [27]. Especially interesting is the methanol, as the simplest alcohol, which has great potential for utilisation in the shipping sector [28]. Finally, non-recyclable waste could be effectively utilized as a feedstock for fuel production overcoming the problems related to waste incineration [29]. Waste plastic materials are lately investigated for fuel production [30], especially to improve the properties of bio-oils through co-pyrolysis processes [31]. The list of alternative fuels is extensive, and this paper covers mainly the most promising at the moment.

This review paper aims to present and analyse the most prominent alternative energy sources, which are nowadays widely investigated as a potential alternative fuel, and energy carriers or storage. Up to now, various alternatives fuels have been investigated and detailed reviews have been carried out as summarised in Table 1. Nevertheless, comprehensive review which would summarise and evaluate considered alternatives with their advantages and drawbacks, as well as the prospective for greater deployment is widely missing. In addition, alternative fuels are often compared in competitive way, promoting the usage of one fuel for all applications. In this work, the authors analysed the most prominent chemicals, biofuels and alcohol derived fuels with a goal to find a complementary role for each of them in future energy systems. Finding a complementary role is especially important to continue with the research in a way which would maximise application potential of each considered fuel.

2. Materials and methods

The research method is based on a three-step procedure, consisting of (i) systematic literature review and information synthesis, (ii) grouping of studies by selecting the most prospective and promising solutions and (iii) assessment of accuracy and topic relevance. The literature search was done by searching scientific databases Scopus and Web of Science. Fig. 3 presents a flowchart of how the literature review was done. Firstly, the scientific databases were searched for general terms like alternative fuels, synthetic fuels and electrofuels by keywords, abstract and title. The great number of publications can be found when these terms are searched, and most of the studies are not directly relevant to the topic

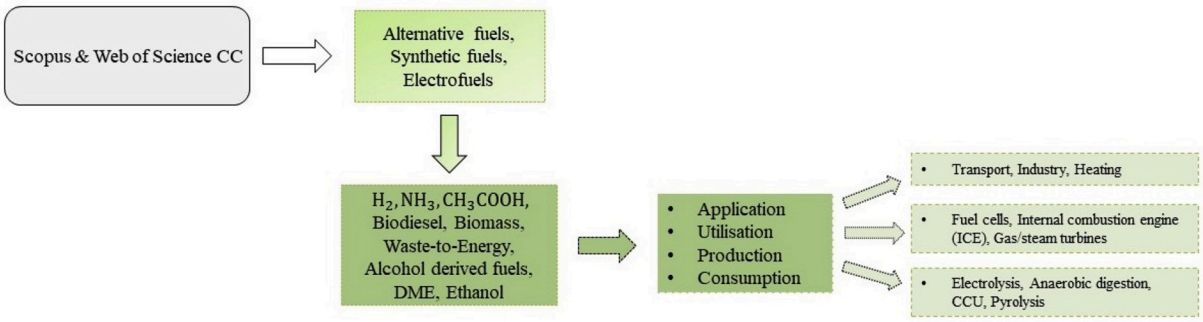

Fig. 3. Flowchart of used methodology for literature review.

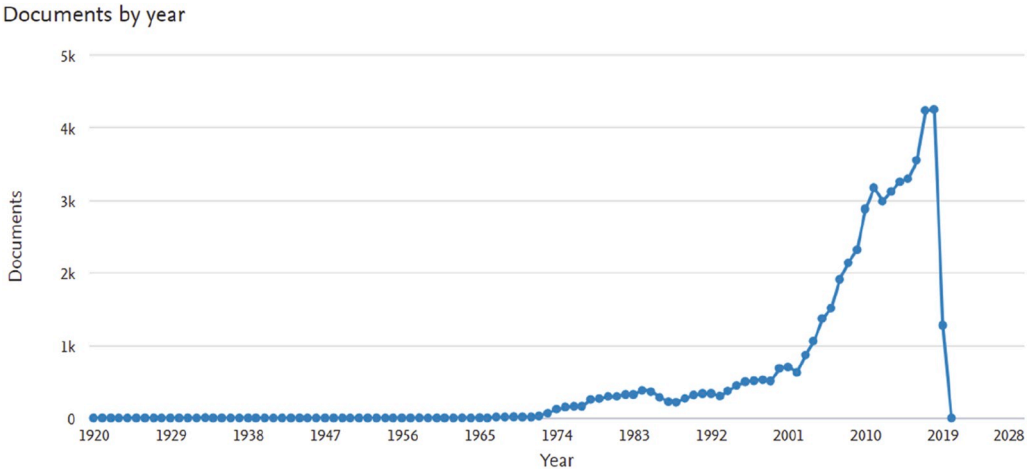

Fig. 4. Number of publications for alternative fuels in the Scopus database [36].

and objectives of this work. Therefore, additional refinement related to the field of energy was applied, narrowing the results to approximately 5000 recent studies which were marked as promising by scanning the title, and keywords. Based on the obtained and synthesized results from the last 5 years, the most promising alternative fuels are selected. This selection was based on the research activity and a number of available publications. Each fuel was additionally investigated and reviewed regarding the application needs, utilisation technologies and production routes.

Fig. 4 presents the number of publications per year that can be found in the Scopus database regarding alternative fuels. From the figure, it can be seen that alternative fuels are gaining research momentum since the 2000s.

3. Review of alternative fuels and utilisation possibilities

To present current and future energy demand, "Global Energy Transformation: A roadmap to 2050" 2018, by International Renewable Energy Agency (IRENA) was used [17].

3.1. Overview of current and future energy demand

According to the IRENA roadmap, the share of renewable energy in total primary energy supply (TPES) was 15% in 2015. This should be increased by two-thirds of overall consumption to meet goals for 2050, while TPES should remain at nowadays level. In 2017, the share of all renewable sources (RES) in the power sector was 25%, with an aim to increase this share to 85% by 2050. This will ensure that electricity from RES accounts for 60% of total renewable energy (RE) in TPES. In a reference case for 2015, electricity accounts for about 20% of total final energy consumption (TFEC), while the rest are other sources, mainly fossil fuels. To meet projected goals, more than 13 000 new, renewable gigawatts needs to be installed. The major increment is expected from VRES, wind and solar photovoltaic (PV) energy, where most new capacities will be installed. The high share of VRES indicates more periods with excess or lack of electricity production, requiring some form of energy storage. Synthesis of alternative fuels from electricity surplus can offer multiple benefits, especially in terms of transport and industry, where very little has been done so far. In 2015, the share of renewable energy in the transport sector was around 4%, while this is expected to increase to 58% by 2050. The most are expected from electric vehicles (EV), especially for light-duty transport; while decarbonization of aviation, shipping, and high-duty vehicles seeks for different solutions. This gap may be filled with high-energy density alternative fuels like hydrogen, advanced biofuels or electrofuels. Transition and decarbonization of an industry sector will be a particularly challenging task. The share of renewable energy for the industry was approximately 14% in 2015, with biomass and renewable electricity equally represented. Electrification of the low-temperature processes will significantly contribute to decarbonization of the sector, while high-temperature processes require the introduction of alternative fuels. Besides biomass, a higher contribution is expected from emerging alternative fuels like hydrogen, enhanced bioenergy and similar. The overall share of renewable energy in the industry is expected to be 60% of TFEC in 2050 [17]. Fig. 5 illustrates the current and predicted renewable energy and electricity consumption according to the IRENA scenario. Current and expected share of renewable energy is on the left, while the share of electricity is on the right side for each sector. In case of power generation, the number refers only to share of renewable energy.

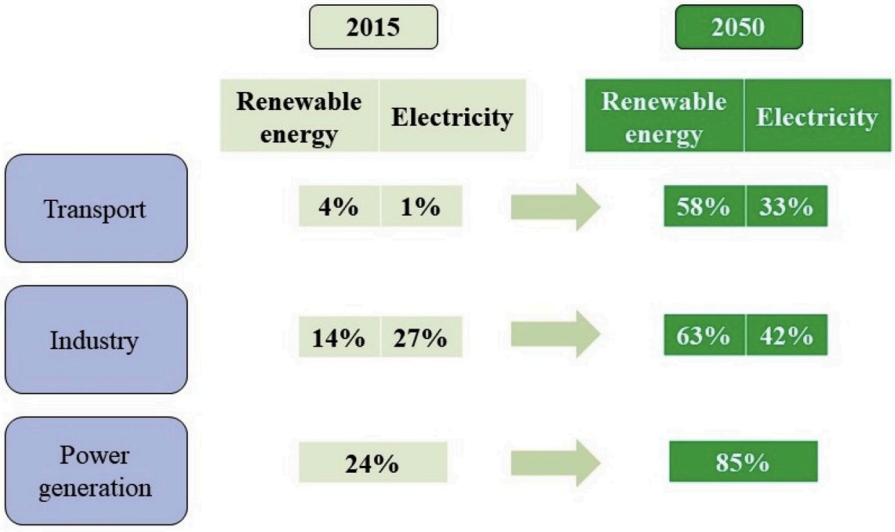

Fig. 5. Current and predicted renewable energy and electricity consumption by the sector [17].

3.2. Alternative fuels

3.2.1. Hydrogen

Hydrogen is the cleanest known energy source that can be produced from various energy sources like fossil fuels, nuclear energy or VRES [20]. Currently, hydrogen is widely used as rocket fuel in the aerospace sector [37], as a refining material for the petrochemical industry as well as in multiple other industrial processes [38]. Almost 50% of hydrogen is globally used only for the production of Ammonia (NH3) [39]. When used as a fuel, hydrogen oxidation releases only water and heat, without additional emissions (Equation (1)). Even though hydrogen is the most abundant chemical element in the universe, its natural, elemental occurrence on earth is seldom. Nevertheless, hydrogen can be found in various hydrocarbons, water or synthesized chemicals.

$$2H_2(g) + O_2(g) \rightarrow 2H_2O(g) + heat \quad (1)$$

One of the biggest advantages lies in high energy density which varies between 120 and 142 MJ/kg [40]. High energy density coupled with the maturity of production processes promotes hydrogen as potential seasonal storage in the future energy, as well as the alternative fuel [21]. Fuel cells look like the most promising solution for hydrogen utilisation for both portable and stationary use [41]. Nevertheless, due to the low volumetric energy content, the efficient application requires liquefication at −253 °C, or compression to 700 bars. Both processes are highly energy-intensive, resulting in energy losses around 10% for compression, and about 40% for liquefaction [39]. In addition, high flammability requires cautious handling procedures and raises several safety issues. Materials used for hydrogen storages must not react with hydrogen in any form and simultaneously serve as an excellent heat insulator [41]. In addition, problems with a hydrogen distribution network are even greater, and it is estimated that new infrastructure would costs over several billion dollars in the coming decades [39]. Even though serious issues are ahead of hydrogen utilisation as a fuel, strong strategic pushback by policymakers and notable research efforts, presume that hydrogen will have a role in the future. To overcome existing problems and open the path for broader application, an appropriate distribution network needs to be developed, and cost-competitive production from renewables should be met.

3.2.2. Ammonia

Ammonia (NH_3) is an entirely carbon-free chemical compound widely used as a fertilizer, which recently gained significant attention as a potential energy carrier or alternative fuel [23]. Ammonia is nowadays widely used chemical and its production accounts for approximately 200 million tons yearly. Currently, the primary feedstock for the synthesis via the Haber-Bosch process are fossil fuels like natural gas, coal, and oil as well as nitrogen from the air [22]. Ammonia is at room temperature, and 10 bar pressure in the liquid phase and its storing is quite easy with already developed distribution infrastructure. The energy density of ammonia is around 22.5 MJ/kg, with one of the highest gravimetric hydrogen densities (17.8 wt%), making it an ideal energy carrier for hydrogen fuel [23]. Sustainable usage of ammonia implies that electricity surplus from VRES is utilized for electrolysis and production of hydrogen, which is then synthesized with the nitrogen from the air. Where needed ammonia is once again converted to the hydrogen and then utilized for power generation [23]. Even though this process is highly energy-intensive and results with a significant energy penalty, the procedure is quite easy, and infrastructure is already in place [42]. Moreover, ammonia can be effectively used as energy storage since its price is more competitive than storing pure hydrogen. According to the study, storing hydrogen in the form of ammonia for 182 days costs 0.54 $/kg$H_2$, compared to the 14.95 $/kg$H_2$ if the pure hydrogen is stored [43]. There are already existing storage facilities in Qatar that use ammonia for storing hydrogen [44]. If the ammonia is solely used as a fuel, its energy content is equal to H_2 energy content. Complete ammonia oxidation is clean since the products are nitrogen, water and release heat (Equation (2)).

$$4NH_3 + 3O_2 \rightarrow 2N_2 + 6H_20 + heat \quad (2)$$

The main problem of using ammonia is its high toxicity and hazardous nature. Ammonia is a colourless gas with a sharp odour, lighter than air, and it can cause serious health issues. In the liquid phase, ammonia is strongly corrosive, especially if mixed with water [45]. Moreover, incomplete combustion of ammonia leads to the formation of pollutant NO_X emissions. Issues related to the direct application of ammonia in IC engines or gas turbines are related to the high ignition temperature (~650 °C), and comparably lower energy density than gasoline which requires engine modifications [23]. Moreover, ammonia has low burning velocity and often needs additives like H_2, CH_4, or diesel to be ignited. Direct application in fuel cells is only feasible for solid oxide fuel cells (SOFCs) due to the high working temperatures, where ammonia could be cracked and utilized through hydrogen [42]. The utilisation of ammonia as fuel has several concerns; nevertheless, the International Environmental Agency (IEA) classified ammonia as a potential energy carrier and remarkable efforts are conducted globally to establish clean production.

3.2.3. Biodiesel

Biodiesel consists of monoalkyl esters; a long chain of fatty acid oils derived from renewable lipid sources such as non-edible vegetables, lignocellulose biomass or animal fats [46]. There are four generations of biodiesel, even though only two of them reached commercial scale. The 1st generation biodiesel was firstly introduced biofuel, produced from food crops like corn, sugar cane, wheat, and vegetable oils. The second generation is produced from energy crops and non-edible vegetables, waste oils and lignocellulose feedstock. It is important to emphasize that biodiesel can only be produced sustainably if production does not compete with the food supply chain. The 3rd and 4th generations of biodiesel are still emerging, and they include algal biomass and genetically modified microorganisms, respectively [47]. Up to know, biodiesel was successfully applied for the transport sector in fuel blends with conventional oil. There are two standards for biodiesel production, for the EU (EN14214) and for the U.S. (ASTM 6751) [48]. The calorific value of biodiesel is between 38 and 45 MJ/kg, which is comparable to conventional diesel [49]. Problems with biodiesel are mainly related to its higher viscosity and density resulting with fuel injection problems. For this reason, biodiesel is blended with diesel to improve cold start and fuel intake. In addition, lower energy density implies slightly higher fuel consumption [50]. On the other side, the performance of biodiesel in conventional IC engines is quite remarkable [51]. The reduction of pollutant emissions can be up to 78%, depending on the fuel quality and blend ratio [52]. Particularly, biodiesel combustion decreases the formation of Carbon monoxide (CO), CO_2, particulate matter (PM), and unburned hydrocarbons emissions, while NO_X emissions are slightly higher [53]. It was shown that engine performance could be increased by 3% when 20% of biodiesel was mixed with gasoline [54]. Currently, biodiesel is produced through transesterification, where feedstock is mixed with methanol or ethanol [49]. Pyrolysis might be a new potential method for the production of high-quality biodiesel fuels from the various feedstock [55]. The yield of bio-oil in such a process is up to 75%, with a heating value between 36 and 42 MJ/kg depending on the feedstock type, while the process is carried out on mild temperatures between 400 and 600 °C, with the feedstock that contains low moisture content [25]. The interesting research topic is upgrading the bio-oils through the co-pyrolysis process with waste materials to improve quality and fuel properties [56].

3.2.4. Alcohol derived fuels

Alcohol derived fuels like methanol, ethanol, and Dimethyl Ether (DME), have already been successfully deployed for internal combustion engines (ICE). Due to the application limitations, alcohol fuels are often introduced in fuel blends where it shares does not exceed 20% [53]. This review covers methanol as the simplest form of alcohol, ethanol as the commercially used fuel, and DME as the prominent fuel to be used in IC engines in the future.

3.2.5. Methanol

Methanol, known as methyl or wood alcohol is one of the simplest alcohols which oxides as a clean fuel when produced with recycled CO_2 (Equation (3)) [57]. Currently, the primary market for the methanol is the chemical industry, even though significant efforts are given for utilisation as an automotive fuel as well (around 20 million tons/yearly for fuel blends) [34]. At the standard room temperature and pressure, methanol is in a liquid state, which makes it easier for handling and distribution. Nowadays it is mainly produced from catalytic conversion of carbon monoxide and hydrogen from natural gas, or from the gasification of coal. To be used in the future decarbonized energy system, the production process must shift toward cleaner solutions like Power-to-Liquid, which involves CO_2 capture technologies and electrolysis of water [58]. The alternative solution includes the biomass-to-energy approach where bio-methanol is produced [59], or solar production [60]. If the sustainable and cost-effective production is met, there are no further technical barriers for greater usage of methanol as a fuel, especially in the shipping sector [34]. Methanol has been widely shipped over the globe, which encouraged investigations for its utilisation as a fuel. Tanks and IC engines can easily be modified, while several refilling stations have already been installed [28]. Toxicity and high corrosion potential (higher than gasoline), as well as the swelling and shrinking of polymers, represents the main drawback of its utilisation [61]. Besides, methanol energy density is halved compared to conventional marine fuels, which makes it unsuitable for long voyages [62]. Lower energy density implies multiple refilling or the installation of additional tanks. Fuel blend of methanol and diesel can reduce NO_X emission by 30%, while methanol can increase overall engine performance and efficiency [34]. Up to know methanol was used in existing IC engines, while specific methanol engines are under development for smaller vessels, road and commuter ferries [61]. Methanol can also be utilized in the fuel cells, even though this produces relatively lower voltage and has poor conversion efficiency [63]. It should be mentioned that if methanol is not produced from renewable sources, the GHG cycle is even higher than conventional heavy fuel oils. Methanol is also investigated as a potential hydrogen carrier in Power-to-X systems, due to the fact that is it the simplest form of electrofuels [64].

$$2\,CH_3OH + 3\,O_2 \rightarrow 2\,CO_2 + 4\,H_2O \quad (3)$$

3.2.6. Ethanol

Ethanol or ethyl alcohol is the simple form of alcohol, commonly produced from the fermentation of biological matter. Today, a tremendous amount of ethanol is used for the medical application, as well as for the production of alcoholic beverages. Efforts to utilize ethanol for the IC engine started in the 1930s in the USA, with an even greater increase following the oil crises in the 1970s. In that period, significant importance ethanol gained in Brazil, where a national program for the production of alcohol fuels was established alongside subsidies for blending conventional fuels with ethanol. As a result, around 20% of the cars in Brazil are operated solely on ethanol, while the rest can have ethanol share up to 20%. The heating value of ethanol is around 27 MJ/kg, which is pronouncedly lower compared to gasoline (44 MJ/kg) and requires the installation of bigger storage tanks [65]. Besides, oxygen content in ethanol is around 35%wt., followed up by high latent heat of vaporization, indicating problems with a cold start. Ethanol oxidation releases CO_2, H_2O, and heat, as presented in Equation (4). Since the fuel is produced from biological feedstock and crops, CO_2 emissions might be considered neutral [66]. Nevertheless, if higher consumption of such fuel is expected in the future, problems with sustainability may arise due to over usage of biomass feedstock. Another drawback of ethanol combustion in IC engines is related to uncomplete combustion where significant amounts of formaldehyde emissions are released, which promotes the formation of ground-level ozone. The performance of an engine ran on ethanol fuel blend is satisfactory with efficiency similar to those powered by gasoline. Simultaneously, the reduction of CO_2 emissions could be up to 20% when "well to tank" is calculated [67]. Finally, in dedicated modified engines, ethanol performance is pronouncedly better, especially if a comparison is carried out for fuel blends or standard engines [68].

$$C_2H_5OH + 3\,O_2 \rightarrow 2\,CO_2 + 3\,H_2O \quad (4)$$

3.2.7. Dimethyl ether (DME)

Dimethyl ether is the simplest ether widely used as a precursor for the synthesis of a wide variety of organic chemicals. Lately, blending the DME with fossil fuels for spark-ignited engines has been proposed as an interesting method for the enhancement of combustion properties and improvement of engine thermal efficiency [69]. The DME can be produced in a two-stage process where firstly methanol is produced from methane steam reforming and then dehydrated to DME [70]. Sustainable production could be achieved if syngas is obtained from biomass gasification or methanol is produced using CCU technologies and

electrolysis [71]. The DME is a non-toxic and non-carcinogenic compound with very low global depletion potential, which makes it an ideal substitute for fossil fuels in IC engines. In addition, the DME burns with a visible blue flame, and it has a sweet odour which is an important safety issue. It has the highest heating value of alcohol derived fuels (~29 MJ/kg), and cetane number similar to that of diesel (55–60), which marked him as a potential diesel substitute [72]. The main advantages of the DME utilisation as a fuel are the following: decreased emissions of NO_X, hydrocarbons, CO and complete absence of soot and SO_X emissions. Significantly reduced pollutant emissions promote the DME as a potential solution for the substitution of diesel fuel in IC engines [73]. A major drawback for wider application is related to comparably lower heating value, which implies the installation of bigger storage tanks. In addition, lover viscosity results with significant injection and leakage problems, demanding a new, dedicated fuel delivery system [74].

3.2.8. Biomass

Biomass is one of the few energy sources, simultaneously used as a fuel and feedstock for fuel production [75]. In 2010, total biomass consumption reached 56 EJ/yr, mainly for residential and building heating and cooking in individual, poorly efficient stoves. In addition, biomass is used as a fuel for cogeneration (CHP) power plants (4.5 EJ/yr), and also in industry and transport sector with the cumulative consumption of approximately 13 EJ/yr. It is expected that inefficient stoves will be replaced by 2050 with modern ones, and biomass will remain an important energy source in rural areas. In the future, demand for the biomass is expected to double by 2030 from nowadays levels to approximately 108 EJ/yr. The increase is expected in all sectors, and it is estimated to be ~31 EJ/yr in transport, and ~21 EJ/yr for the industry. The remaining 56 EJ/yr is foreseen for power generation and heating (individual and district heating) [75]. Traditional biomass (i.e. firewood) which is now widely used, strives for new approaches in order to find more appropriate solutions to enhance the sustainability of its consumption [76]. Firstly, the usage of traditional biomass for heating and cooking in rural areas should be minimized and replaced by electricity. Furthermore, the usage of traditional biomass with low exploitation properties should be abandoned, while the research focus should shift toward enhanced biofuels [11]. Such biofuels have improved combustion properties, easier are for handling and distribution, and finally, can be produced from waste biomass residues. Waste biomass sources like agricultural waste, sawdust, tree shavings, cutters, and wooden chips, are bulky by-products of some other industrial activity, but most importantly they could be efficiently utilized in forms of densified fuels. The most prominent solutions are pellets, briquettes, and cubes. Densified, solid fuels share similar characteristics in terms of density (450–750 kg/m^3), moisture content (8–12%), and heating value (15–21 MJ/kg). The difference is that pellets are mainly used for heating stoves and individual boilers, while briquettes are used for industrial applications [77]. The main advantage of densified fuels over traditional biomass is in the lower moisture content (up to 40%), which enhance overall combustion performance up to 40–68%, depending on the wood type [78]. The promising solutions for upgrading the biofuels could be the pyrolysis [79] or gasification [26]. Obtained product are high-quality biochars, bio-oils, and syngas. Biochar can be used as an environmentally friendly soil fertilizer, bio-oils can be further refined for biodiesel, while syngas can be utilized in gas turbines. Biomass pyrolysis occurs in the temperature range between 300 and 600 °C, in the absence of oxygen, while gasification is carried out between 800 and 1000 °C with controlled air and oxygen content [26]. Some catalysts are used to enhance the selection of product yield [79]. Lately, microalgae are examined for the production of biogas, composed of typical syngas compounds (CO, CO_2, CH_4, H_2O, H_2) with a calorific value between 10 and 35 MJ/kg [80]. Even though the cultivation of algae still didn't reach commercial applications due to the production costs, the idea looks promising since they are not competing with food production. Finally, biomass can be upgraded through co-pyrolysis with waste materials in order to enhance the synergistic effects of individual components and to obtain high-quality products [81]. More on this will be discussed later.

3.2.9. Non-recyclable waste

Firstly, it needs to be stated that Waste-to-energy should be the last measure in waste management systems. Prior to energy recovery, reusing and recycling are preferable, while waste incineration should be applied for the non-recyclable waste only. Currently, a widely used energy recovery method is waste incineration for cogeneration of electricity and heat [29]. Waste is used in the form of solid recovered fuel (SRF), refuse-derived fuel (RDF) or through direct combustion of municipal solid waste (MSW) [29]. Since the waste generation is inevitable and will be generated at higher rates in the future, sustainable solutions for waste management practice is necessary. Thermochemical conversion is a highly efficient method for reduction of mass and volume, but higher SO_X, NO_X and other pollutant emissions raise serious environmental concerns [82]. Decreasing NO_X emissions is especially important since they are a source of multiple health issues [83]. Thermo-chemical treatment of waste is lately introduced as a method to deal with waste materials that reached recycling potential, or their recycling is economically inefficient (low-quality plastics, composite materials, end-of-life plastics). Such materials might be used as feedstock to improve the exploitation properties of biomass or MSW [84]. It was shown that plastics could significantly enhance biomass properties through a synergistic effect when optimal fuel blend is pyrolyzed [85]. In addition, various waste, like rubber [86], MSW [87], or sewage sludge [88] have been co-pyrolyzed with biomass, and again it was shown that fuel blends products (liquid, gas, char) are noticeably upgraded compared to the individual pyrolysis [89]. Using non-recycling waste to upgrade biomass properties offers several benefits. Firstly, over usage of biomass could be prevented since the feedstock needs are partially satisfied with waste. Secondly, the waste management sector can be effectively integrated into the energy system in order to find an appropriate and sustainable disposal solution [90]. Finally, obtained products of high quality can be further utilized where appropriate (bio-liquids for biodiesel, syngas for steam generators). General characteristics of waste fuels could not be provided since the composition of waste significantly varies over the regions and countries, but also over time. This is one of the main drawbacks of waste utilisation as a fuel since the multiple investigations should be continuously carried out to determine the waste composition, characteristics, and appropriate pre-treatment methods. Furthermore, exhaust gases may contain toxic and harmful compounds that require complicated and expensive after treatment [91]. Nevertheless, since the generation of waste is inevitable in the future, sustainable solutions for its disposal should be found. Energy recovery seems the most promising and cost-effective solution, even though public acceptance of this method is still mostly missing. In further chapter to avoid confusion, when implying to energy recovery of non-recyclable waste, "waste fuel" expression will be used.

3.3. Form of utilisation (solid/liquid/gaseous fuels)

Form of utilisation implies the state of matter in which fuel could be utilized. The most of considered alternative fuels might be utilized in more than one state, with the different efficiencies. This section briefly discusses the possible form of utilisation for considered fuel alongside their advantages and drawbacks.

Solid fuels are nowadays widely used for stationary purposes in power plants, or for satisfying high-energy demand in industrial processes [92]. Solid alternative fuels might have an especially important role in the decarbonization of heavy industry, currently dependable on fossil fuels [93]. Alternative solid fuels, like biomass or waste-derived fuels, could be an adequate substitution for fossil fuels without significant infrastructure modifications [94]. Besides space and dry conditions, no additional requirements are needed. Application of solid fuels for the

power generation will most likely be in CHP power plants (i.e. district heating), while notable consumption of biomass is expected to remain in rural areas as well [76]. Biomass is already used in the form of densified fuels like firewood, wood chips, pellets, briquettes for heat and power production on a commercial scale [95]. In addition, biomass is often used in fuel blends to decrease GHG emissions of fossil fuels like coal [96]. To achieve sustainability in biomass consumption, new approaches and utilisation technique are necessary. This includes gasification, pyrolysis, and anaerobic digestion of raw biomass with an aim to enhance the properties of derived products. Similar to biomass, waste is also already used as an energy source [97]. Nevertheless, current waste management practice relies on unsustainable methods, where waste is incinerated in CHP power plants or cement kilns without appropriate pre-treatment [93]. This implies that the pre-selection process, where valuable materials would be recovered is skipped, resulting in economic losses as well [98].

Liquid fuels like gasoline, diesel, and heavy oils are conventionally used in IC engines for all types of transport (road vehicles, shipping, aviation) [99]. Even though it is expected that electric vehicles (EVs) will dominate the future transport sector, additional alternative fuels are needed as well [100]. This is due to the fact that heavy, cargo vehicles need high-density fuels for a drive, or propulsion [101]. In addition, battery capacities are still not enough for long-range voyages since they demand multiple charging stops. This becomes a severe issue for overseas transport since multiple stops for charging are unpractical and time-consuming [40]. Alternative fuels that can be utilized in the liquid state are biodiesel and ethanol on a commercial scale, and methanol and DME in the concept proof stage [46]. Pyrolysis oil could also be utilized in a liquid state, even though more research is required to find an appropriate application and production procedure. Finally, hydrogen and ammonia, as potential transport fuels are both facing storage problems when liquified. While ammonia is strongly toxic and usage raises safety concerns; cryogenic technology is necessary to liquefy hydrogen below the critical point of −252 °C, resulting with high energy penalty [22].

Gaseous fuels are important transition fuel, while their importance will increase even more since they can be used in a flexible ramping mode. This is especially important for grid balancing once when a high share of VRES is achieved [102]. Gaseous fuels are utilized in gas turbines or steam boilers, preferably in the CHP cycle with high efficiency [103]. Syngas and biogas are the most prominent alternative fuels to be used for stationary applications like CHP [104]. They are obtained through conventional gasification [105], pyrolysis [106] or anaerobic digestion [107]. The main component of gas fuel is methane, while a notable portion of CO, CO_2, H_2, and higher hydrocarbons are obtained as well [108]. The main drawback of such fuels is inconstant and lower heating value (10–35 MJ/kg) compared to natural gas (19–21 MJ/kg) [109]. On the other hand, hydrogen is the most prominent gaseous fuel to be used for mobile applications, and it is already utilized for automotive purposes, using fuel cell technology [110]. In addition, a lot is expected from hydrogen as a fuel in aviation, heavy-duty vehicles and long-range shipping. Even though hydrogen needs to be compressed to 700 bars, this is still a more appropriate and practical solution for the commercial application then cryogenic liquefication [111]. Used storages are made entirely from composite materials (IV carbon-composite technology) which endures high pressures, and deformation in case of crushing [20]. Lastly, if ammonia is going to be utilized as a fuel, most likely, it will be in the gaseous state [23]. In the gas phase, ammonia can be co-fired with similar gas fuels to improve combustion performance and to overcome problems related to liquid ammonia. Fig. 6 presents the potential application and utilisation technologies for considered alternative fuels. As it was already mentioned, some fuels might be utilized in more than one form and in different technologies. Nevertheless, the efficiency of utilisation in each technology is pronouncedly different, requiring additional insights and research to find the most appropriate solution. More on this will be discussed in the next section.

3.4. *Utilisation technologies*

This section aims to present the efficiency of considered alternative

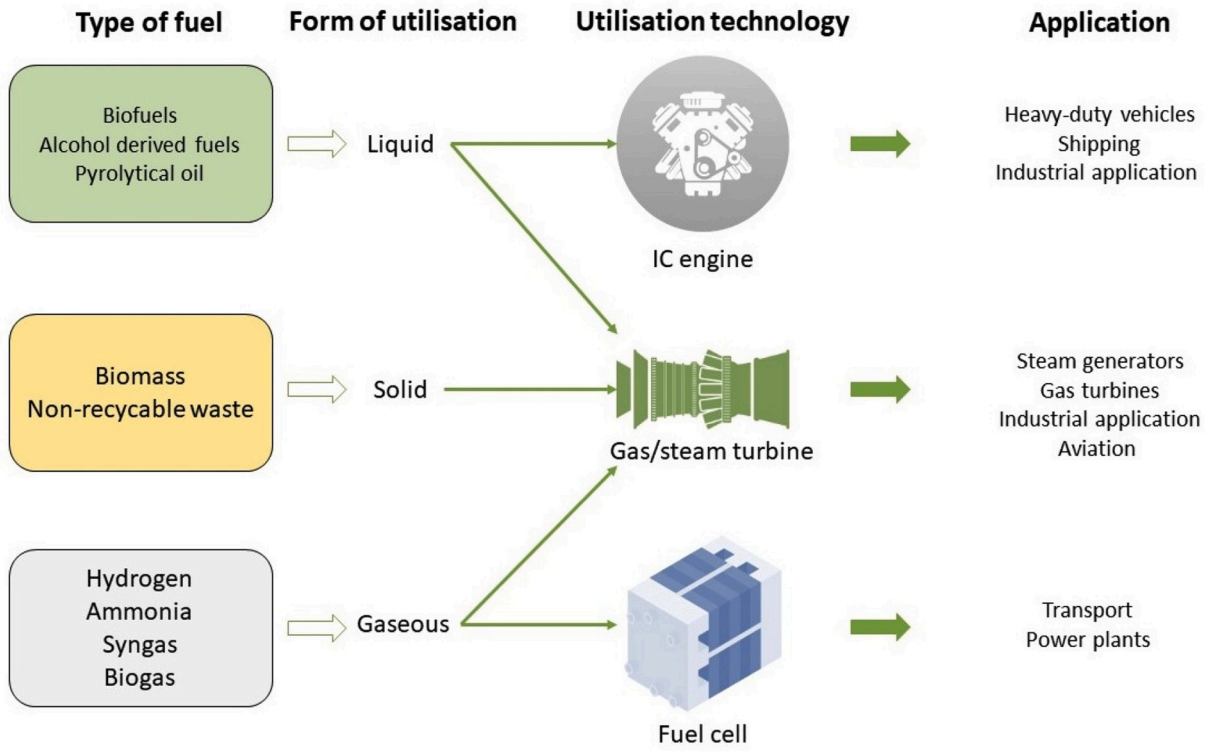

Fig. 6. Form and Technology utilisation perspectives for Alternative Fuels.

fuels demonstrated on commercial or research scale. Majority of considered alternative fuels were tested for all presented technologies with different success. Technologies and alternative fuels that are used commercially are discussed briefly, while more attention is given to the emerging ones.

3.4.1. Fuel cells (FCs)

Fuel cells become widely discussed and investigated technology when hydrogen was introduced as a potential alternative fuel. Proton-Exchange Membrane Fuel Cell (PEMFC) and Solid Oxide Fuel Cell (SOFC) are the most attractive and investigated nowadays [40]. Hydrogen utilisation in fuel cells has gone farthest, and it is already commercially available, with the Toyota Mirai as a notable example of a hydrogen-powered vehicle [112]. Fuel cells are also foreseen for other types of transport, including shipping and aviation sectors [110]. They are relatively small in size, and therefore ideal for portable applications. For the hydrogen case, both fuel cells show a similar efficiency of approximately 50–60% depending on the fuel purity. While PEMFCs seems like a logical solution for portable applications due to the low operating temperature (up to 100 °C), the SOFCs could be the solution for stationary use. High working temperatures (500–1000 °C) of SOFCs requires longer start-up time, therefore more practical application for this technology is in power plants. The efficiency of compressed hydrogen used in PEMFC with all loses is about 40% [9]. Methanol can also be utilized in PEMFC, without reforming, making a new subgroup of proton-exchange fuel cells, called direct methanol fuel cells (DMFC). Operating conditions of these FCs are relatively similar to those of PEMFC, while conversion efficiency varies between 13 and 29% [63]. Ammonia is the last alternative fuel tested with fuel cell technology. Due to the high operating temperature of SOFCs, ammonia can be directly utilized without reforming, with the efficiency between 39 and 50% [22]. Highest efficiency is achieved when ammonia is used for stationary CHP production directly without reforming. If ammonia is used as a vehicle fuel, PEMFC is required due to the lower operating temperature, implying that ammonia is used as an energy carrier, and before being introduced to FCs needs to be reformed to pure hydrogen, which results with significant energy penalty. In the end, the net efficiency for the best-case scenario is between 11 and 19% [23].

3.4.2. Internal combustion engines (IC engines)

Biodiesel is the only fuel utilized in the conventional IC engine on a commercial scale. In addition, biodiesel can be used solely as a fuel or in blends with the conventional diesel. When the bottom one is applied, the share of biodiesel is indicated with factor “B" and the respective share (i.e. B20, indicates that share of biodiesel is 20%, while rest is diesel) [52]. The share of biodiesel in the fuel mix is limited by the engine itself, quality of fuel, and requirements that need to be satisfied. The especially important criterion is fuel quality which mainly depends on the feedstock used for the production, and it is determined based on fuel viscosity, flash point, calorific value, and specific density [54]. Quality can be controlled during the production process by appropriate pre-treatment methods and processes parameter manipulation (temperature, pressure, or used catalyst) [113]. The overall performance of the engine can be enhanced, while concentrations of exhaust emissions may vary. Even though it can be stated that the overall reduction of GHG emission can be achieved when biodiesel is blended with conventional diesel, this strongly depends on operating conditions. While NO_X emissions in most cases are decreased, CO and CO_2 emissions seem to be slightly increased [114]. Nevertheless, it is expected that biodiesel will be used in the future for IC engines since it has been proven in the operating environment, and it is widely discussed as a potential fuel for the aviation sector in the form of bio-jet fuel [115]. Usage of methanol for IC engines has been discussed for a long time with some actual examples of implementation. The problem of methanol deployment for IC engines is related to its high corrosive potential, which requires engine modifications [116]. Finally, methanol has lower energy content compared to petroleum fuels which imply a need for larger tanks. Nevertheless, simple production procedures, coupled with the increased engine performance and efficiency, opens the possibility to use methanol in the shipping sector as a partial substitution for fossil fuels. This is supported by the fact that methanol can reduce NO_X emission by up to 30%, which is a remarkable success for the shipping sector [28]. Ammonia was tested for IC engine applications as well [110]. The main problem of using ammonia in the IC engine is related to the high burning temperatures, which require the addition of some other fuel like diesel to enhance the start-up process [117]. These problems are prevailing when spark-ignition engines are used [23]. Generally, when ammonia is used as fuel for the IC engine, it must be in conjunction with some other conventional fuel to ease the start of the combustion process. Relatively low reactivity followed by high auto-ignition temperature and low flame velocity limits the application of ammonia solely as a fuel. Achieved overall efficiency of ammonia combustion in IC engines is between 35 and 40% [22]. The advantage of using ammonia in the IC engine is derived from the fact that high octane numbers (~130) can reduce knocking and improve combustion properties. The main issue related to ammonia application in IC engines is in fact that potentially higher NO_X emission can occur if there is incomplete combustion.

3.4.3. Gas and steam turbines

Biomass is already used in the CHP cycle, and its consumption will only increase [114]. The great advantage of biomass is that it can easily be introduced to existing power plants where can be combusted solely or in fuel blends with fossil fuels. Even though the efficiency is slightly lower, a remarkable reduction of pollutant emissions in exhaust gases might be achieved, especially in terms of NO_X, SO_X, and particulate matter emissions [118]. Furthermore, emitted CO_2 can be considered neutral since it was consumed during plant life. If there is high moisture content (i.e. firewood), combustion efficiency is notably lower due to the fact that a considerable amount of energy is used for vaporization [119]. Lately, significant efforts are noticed in the research, to achieve synergistic effects of biomass and other types of solid fuel in order to enhance fuel quality and properties [120]. Such fuel blends (i.e. biomass-plastics) could be effectively applied in power plants since the treatment systems for exhaust gases are already in place [121]. Biogas and syngas, as the products of biomass upgrading, can be utilized in gas turbines for the combined cycle as well [122]. The quality of biogas obtained from anaerobic digestion (AD) depends on feedstock type, but even more on production conditions [123]. More on AD will be discussed in the following section. Syngas is, on the other hand, derived from biomass gasification (800–1000 °C) or pyrolysis (300–600 °C) and again, slight shifts in the temperature region significantly affect its composition [26]. This is directly reflected in its calorific value and consequently, overall efficiency. When obtained gaseous fuels have a higher share of hydrocarbons and hydrogen, combustion characteristics are better, and efficiency is higher [124]. If gaseous fuels are synthesized from renewables, emitted CO_2 can be considered carbon neutral. In order to decrease the share of CO_2 in biogas composition, a further upgrade is required. This implies amine scrubbing for CO_2 removal or co-pyrolysis of biomass with high calorific waste on high temperatures, to increase hydrocarbon content [125]. The utilisation of biogas in power plants has a significant drawback since it may cause acidification and eutrophication several times higher compared to fossil fuels [126].

Waste incineration is a long-time used practice for energy recovery of waste materials. Solid waste is introduced to the power plant where it is burned at high temperatures between 750 and 1100 °C [98]. Because of the feedstock content, exhaust gas contains various pollutants like SO_X, NO_X, CO_X, Polycyclic Aromatic Hydrocarbons (PAHs) and heavy metals. This requires complicated and expensive treatment of flue gases, and it is considered as a major drawback. Nevertheless, stringent control emissions make this process quite effective for waste management, simultaneously producing heat and electricity with an efficiency of up to 80% [127]. Hydrogen and ammonia could also be utilized in gas turbines,

Table 2
Summary of main fuel characteristics.

Type of fuel	Chemicals			Biofuels		Waste
	H_2	NH_3	Alcohol derived fuels	Biodiesel	Biomass	Syngas/biogas	
Calorific Value (MJ/kg)	120–140	22.5	~19 (Methanol) ~27 (Ethanol) ~29 (DME)	38–45	15–21	10-35 Syngas 15-22 Biogas	Vary
Feedstock and production	Electrolysis, Biomass and waste gasification	H_2 (electrolysis) + N_2 (air separation)	Biomass, CO_2 (CCU), H_2 (electrolysis)	Energy crops, waste oils, lignocellulosic plants	Sawdust, agricultural waste, tree shavings and cutters and similar	Biomass, non-recyclable waste, biodegradable waste	MSW, RDF, SRF, non-recyclable waste, sewage sludge
Combustion products	H_2O, Heat	H_2O, N_2 Heat	CO_2, H_2O	CO, CO_2, NO_X	CO_2	CO_2, CO, NO_X	CO_2, NO_X, SO_X, various pollutants
Utilisation efficiency							
Fuel cell	50–60% (PEMFC/SOFC)	11–19% (SOFC)	13–29% (DMFC)	–	–	–	–
IC engine	–	35–40%	Up to 40% (depends on the type of engine)	Varies	–	–	–
Gas and heat turbines	–	55–60%	–	–	Up to 80% (CHP), Electricity production; 30–34% dry biomass, 45% co-firing		Up to 80% (CHP); only electricity ~22%

even though seldom work was done in this field. Ammonia was used in various fuel blends and achieved efficiency in combined cycle with gas turbines is between 55 and 60% [23]. Problems reported with the application of ammonia for IC engines are similar in this case as well. Direct combustion of hydrogen in gas turbines have a severe drawback related to its high reactivity which results in high burning temperatures, flame speed and similar. Therefore, hydrogen utilisation in gas turbines requires the development of dedicated technology [128]. Table 2 summaries all presented alternative fuels with their main characteristics such as calorific value, feedstock for production and derived combustion products. Between the considered alternative fuels, hydrogen has the highest calorific value without emission of greenhouse gases. Moreover, it can be produced from the completely clean procedure, if the electrolysis is powered by renewable energy sources. Ammonia and alcohol derived fuels, express the most disadvantaged characteristics required to meet fuel specifications. They have the lowest calorific values, and incomplete combustion might result in even higher emissions.

4. Production pathways

This section aims to present essential technologies and processes for the synthesis of considered alternative fuels. Water electrolysis might be a key technology for fuel synthesis, since it can be driven in flexible mode, allowing higher penetration of VRES. Even more, clean hydrogen is inevitable for the production of other forms of alternative fuels as well.

4.1. Sustainable methods for clean production of alternative fuels

4.1.1. Hydrogen production

Hydrogen production from fossil fuels is a known procedure where natural gas or coal is used as a feedstock. Today, hydrogen is most often produced from steam reforming of methane, while it can be produced from partial or autothermal oxidation or gasification as well [20]. Nevertheless, production from fossil fuels is not possible in the future decarbonised energy system, and procedure must shift toward sustainable solutions. Production from renewable energy sources implies pyrolysis or gasification of biomass [26] or water electrolysis from the electricity surplus from VRES [129].

One of the most prospective ways to produce clean hydrogen is water electrolysis (Equation (5)). Notable research efforts are conducted to bring this procedure on a commercial scale, and even though this accounts for only 4% of today's production, perspective is bright [129]. There are several types of electrolysers, divided by the nature of electrolyte they use. The most prominent ones are Polymer Electrolyte Membrane (PEM) electrolyser, alkaline electrolyser, and Solid Oxide Electrolysers (SOE) [129]. Electrolysers have the capacity to produce hydrogen with high purity (99.999 vol%) with the efficiency of between 70 and 85% [130]. Process efficiency mainly depends on the load factor of renewables and electrolyser efficiency itself. Since the water is carbon-free, and technology reached the maturity stage, the last step for broader deployment of electrolysis is the economic competitiveness of the procedure. At the moment, production costs of hydrogen from electrolysis (~$3/kg) are double than those from natural gas reforming ($1.2.-1.5/kg) [20]. Since the electricity is the main driver of electrolysis production costs, once when higher penetration of VRES is achieved, this procedure would be entirely competitive to steam reforming of fossil fuels. This is especially important in the future energy system, where it will be more periods with electricity surpluses, which can be effectively utilized for electrolysis. This would ensure grid stability, avoidance of production curtailment, and more importantly, clean production of hydrogen [128]. Furthermore, hydrogen can be directly produced from solar, nuclear or waste heat utilisation from industrial processes. If the hydrogen is produced directly from solar energy, concentrating solar power (CSP) seems like the optimal solution since higher temperatures are required [21]. Production using nuclear energy implies the integration of waste heat for high-temperature electrolysis,

even though this requires further research efforts [131].

$$2\,H_2O \rightarrow 2\,H_2 + O_2 \quad (5)$$

Technological maturity implies that clean hydrogen production could be completely viable once when a higher share of VRES is integrated since this will cause a further reduction of electricity costs which are the main driver for full commercialization and broader application.

4.1.2. Ammonia synthesis

The main constituents for ammonia synthesis are H_2 and nitrogen (N_2) via the Haber-Bosch process. Hydrogen is most often obtained from the reformation of natural gas, which accounts between 1 and 2% of the annual energy demand [45]. The Haber-Bosch process is energetically demanding and kinetically complex. It is important to emphasize that Haber-Bosch production of ammonia operates as a continuous process whereby each pass through the reactor converts only about 15% of the N_2 and H_2 to NH_3, yet with continuous recycling and overall conversion rates are around 97% [132]. This recycling implies that intermittency of VRES is not a severe problem since the feedstocks can be produced when there is electricity excess and stored for later use. Some types of "green" ammonia synthesis processes have been demonstrated in America, Australia, Africa, Canada, Germany, the Middle East, Norway, and the United Kingdom [133]. Moreover, a small-scale solar ammonia facility has been operating for a few years at Pinehurst Farm in Iowa. The ammonia thus produced is used as a fertilizer and as a fuel for tractors [134].

Switching to clean production implies the electrolysis and air separation, which can be entirely powered by VRES. Cryogenic air separation provides N_2, used for ammonia production and oxygen, which has other valuable applications. To maintain a fully green process, and avoid CO_2 emissions, the electrolyser should be powered by electricity surplus from the grid or by direct renewable solar energy installed in situ [22]. If the direct solar energy is used, due to the low solar conversion efficiency (~16%), the overall primary energy input increases, from 16.4 MJ/kg-NH_3 of methane to 236.7 MJ/kg-NH_3 of solar energy. Low efficiency leads to higher production costs due to higher energy demands. In the best-case scenario, 27.2 MJ of solar electricity displaces 16.4 MJ of natural gas, required to manufacture the same amount of ammonia (1 kg) [45]. Nevertheless, in regions endowed with wind and solar resources and with a high share of VRES, green ammonia could be competitive. In these ideal locations, the cost of solar and wind electricity is predicted in the range of $30/MWh, which translates into a cost-competitive $2/kg of H_2 from water electrolysis. In other words, if solar electricity is available, usage for ammonia production is suboptimal at least until the electricity mix becomes nearly 100% renewable [43].

4.1.3. Methanol synthesis

An innovative trend becoming increasingly evident in the scientific literature is the use of light to drive or assist chemical reactions and processes to produce clean methanol. The prospect of using solar energy, CO_2 and water to synthesize methanol could lead to an economically viable technology, capable of replacing fossil fuel heavy industry with a renewably sourced alternative [59]. There are different ways to produce light-assisted chemical products, including direct utilisation to convert CO_2 and water through solar thermochemistry, photochemistry, or photoelectrochemistry. Another potential solution is the gasification of biomass feedstock to produce syngas [64]. Solar concentrators in conjunction with complementary focusing elements, intensify the sunlight incident on the biomass gasification reactor. The temperatures thereby achieved should be sufficient to affect biomass gasification (~850 °C) without the need for external heating. Again, similar to ammonia, the low efficiency of solar-to-power technology is considerable constraint affecting overall processes efficiency. Therefore, an interesting solution might be coupling hydrogen from electrolysis and integration with CCU technologies utilising electricity surpluses from the grid [60]. An excellent example of sustainable and clean methanol production is in Reykjavik, Iceland. This industrial facility commissioned in 2007, annually produces 4000 metric tonnes of methanol made from captured CO_2 and H_2. This corresponds to 5500 MT of recycled CO_2 per year. The location of the facility allows utilisation of geothermal steam from the 75 MW_{el} Orka's Svartsengi power station to provide renewable heat and electricity., while captured CO_2 accounts for about 10% of total annual power plant emissions. Electricity is mainly used to power alkaline water electrolysis to produce H_2, which in turn reduces CO_2 in the presence of a catalyst, in a process operating at 250 °C and 5–10 MPa [129].

4.1.4. Anaerobic digestion

The anaerobic digestion is a process that includes four biometabolism steps (hydrolysis, acidogenesis, acetogenesis, and methanogenesis) in which biodegradable waste is converted into valuable biogas, consisting mainly of methane [123]. The AD is an optimal process for treating a biodegradable fraction of MSW, agriculture waste (animal manures, energy crops, algal biomass, harvest remains), food industry waste (food/beverage processing, dairy, starch) or sewage sludge [135]. The four-step process can be carried out into single-stage or multi-stage AD systems, even though the bottom one requires additional research. The overall process is determined by complex relations between various operating parameters, growth factors, system design, and the type of reactor [123]. Type of the feedstock is essential for the selection of system design and type of the reactor, as well as it affects growth factors and operational parameters [107]. During the process, pH is stringently controlled since it influences the bacteria efficiency, consequently the success rate of the process as well. Nowadays, most of the AD systems are operated in continuous single-stage mode, processing various biodegradable waste [136]. Even though anaerobic digestion is a complex process with higher investment and operational costs, installed capacities increased from 2 to 11 million tonnes, over the last two decades [123]. Installed capacities are expected to increase even more since the generation of biodegradable waste is inevitable, while AD looks like a promising waste management method [137]. Nevertheless, further research focus should be given to multi-stage AD, where high-quality biogas can be produced, and cost reduction to achieve economically viable production.

4.1.5. Carbon capture and utilisation

Carbon capture and utilisation technologies are an important part of the supply chain for the production of alternative fuels using recycled CO_2 emissions. The title indicates that carbon capture technologies are focused on extracting CO_2 emissions from the point source or directly from the air and then utilising it where needed [4]. Lately, these technologies have been marked to play a complementary role in future energy systems since they can be operated in flexible mode. This allows grid stabilization through Power-to-X (PtX) processes once when higher penetration of VRES is achieved [64]. PtX implies the utilisation of captured CO_2 into some form of electrofuels, reducing the need for battery storages, simultaneously producing a valuable liquid or gaseous fuels [138]. Major technologies for carbon capture, include pre-combustion capture, oxyfuel combustion, chemical looping combustion (CLC), post-combustion capture, capture from fermentation processes, and direct air capture (DAC). An extensive review of the presented processes is given by Mikulčić et al. [4]. Even though CCU technologies might have remarkable efficiency (up to 98% for amine scrubbing) in terms of CO_2 emissions, they inevitably affect overall system efficiency due to the high energy penalty for its operation. The techno-economic analysis which was carried out by Bhave et al. [139], estimates the cost at 145–185 €/t for 50 MW plant, with CLC being the least expensive, and pre-combustion being the most expensive. It should be mentioned that CCU technologies are mostly in the R&D phase, except post-combustion amine scrubbing and pre-combustion natural gas processing [140]. Since the introduction of electrofuels, the CCU

technologies are assessed through their role in PtX production pathways, which might become an essential market for scaling up technology on a commercial level. Finally, even though carbon capture has an important role in the future energy system due to operational flexibility, meeting the cost-competitive price of operation is a crucial step for broader deployment [141]. The bottom one is especially important since the installation of a carbon capture system results with significant energy penalty and reduced overall system efficiency.

4.2. Fuel blends pyrolysis for enhanced characteristics of biofuels

Pyrolysis is a thermochemical conversion method where thermal decomposition takes place in the absence of oxygen. Derived products are carbonized residue, liquids, and gases. Lately, pyrolysis has been introduced as a promising technique for the conversion of waste materials into valuable fuels and chemicals [30]. Depending on the desired product distribution, pyrolysis is operated at different temperature ranges. In case the liquid yield is preferred, temperatures go up to 600 °C for most of the feedstock, while gasification is carried out on temperatures above 700 °C [55].

Biomass pyrolysis is most often carried out on temperatures between 200 and 450 °C, where feedstock is converted to high-quality liquids, pyrolytic gases, and carbon-rich char residue [79]. Product yield depends on operating conditions and the feedstock type, while obtained products usually need to undergo refinery processes prior to utilisation. In an example, bio-oils generally contain lower heating values and are unstable at a higher temperature, while pyrolysis gases may contain a high share of CO_2 [142]. Recently, significant research efforts are given to convert biomass feedstock into valuable fuels and chemicals. Especially interesting is the pyrolysis of waste materials like sawdust, agricultural waste, various straws, energy crops and similar [126]. Even though pyrolysis can significantly enhance biomass properties, further upgrade in terms of heating value, lower viscosity, high acidity, and thermal stability requires additional efforts. Interesting might be the synergistic effect that occurs during the co-pyrolysis of biomass with waste plastics [143]. Plastic has a high share of carbon and hydrogen, and the heating value similar to those of fossil fuels [144]. Besides, low share or complete absence of oxygen in the elemental composition reduces the yield of oxygenated compounds, marked as the main drawback of biofuels. Several research showed that co-pyrolysis significantly enhance the bio-oil properties in terms of heating value, thermal stability and viscosity. Since the chemical and mechanical recycling of plastics is expensive, while for some types not even feasible, co-pyrolysis seems like a promising method for waste management as well [145]. Besides, the different type of non-recyclable waste can be co-pyrolyzed with biomass, like sewage sludge (SS) [95], food waste [108], MSW [82], rubbers [86], etc. Even though conducted investigations showed that product properties are greatly enhanced in the co-pyrolysis process, more needs to be done to reduce the yield of various pollutants that constrain immediate utilisation. In Table 3, Ultimate and Proximate analysis of various waste materials, investigated as a potential co-pyrolysis feedstock is given. Characteristics given in Table 3 are essential for the feedstock selection and adjustments in co-pyrolysis or co-gasification process.

The most valuable pyrolysis product is bio-oil, which yield is favored when a high concentration of Volatile matter (VM) in the feedstock is present. This is found for waste plastic, marking them as an ideal feedstock for co-pyrolysis to enhance bio-oil properties. Moreover, the ash content and fixed carbon, which constrains liquid yield, is pronouncedly low for plastics. Finally, the pyrolysis of plastic yields a significant number of different hydrocarbons which is preferred in terms of heating value [144]. Nevertheless, using plastics in energy recovery raises several serious issues as well. Since the plastic materials are produced from fossil fuels and synthesized with different additives, toxic and hazardous compounds might be found in the obtained pyrolysis product [152]. Mainly, this is related to the formation of different PAHs, dioxins, furans, toxic hydrocarbons, and similar [125]. Moreover, a significant amount of chlorine-containing compounds might be found in both liquid and gaseous phases, which are not just toxic, but corrosive and therefore, unfavorable for further exploitation [153].

Conducted experimental investigations showed that the liquid yield of co-pyrolysis is of better quality than those of plastics and biomass pyrolysis alone [154]. Zhang et al. [155] investigated the catalytic co-pyrolysis of pine sawdust and plastics (polyethylene PE, polypropylene PP, and polystyrene PS) in order to maximise the production of aromatics and olefins. The best-case scenario showed that the overall yield of aromatics and olefins could be enhanced by 36%, and 35% respectively for PE/pine sawdust ratio 4:1 at 600 °C. Lu et al. [156], confirmed the thesis that the interaction of plastic and biomass leads to the reduction of oxygen and water content in the liquid fraction, and as a consequence, obtained oil has higher heating values and stability. Zhang et al. [56] investigated the potential for bio-jet fuel upgrade through the synergistic effect of biomass and plastic co-pyrolysis. Results showed that catalytic microwave pyrolysis could yield a sufficient number of hydrocarbons (42.66%) to meet jet-fuel specifications. There are numerous other examples of biomass/plastic co-pyrolysis under different conditions and with different goals. Conducted research showed that the synergistic effect significantly enhances individual characteristics, even though a cautious approach should be maintained due to the evolution of toxic and hazardous compounds. Besides plastics,

Table 3
Ultimate and Proximate Analysis of different biomass and plastic materials.

	Ultimate Analysis				Proximate Analysis			
	Volatiles	Moisture	Ash	Fixed carbon	C	H	N	O
	wt.% (different basis)				*wt.% dry basis*			
Miscanthus [146]	69	4.7	3.0	22.67	49.6	5.9	1.06	42.84
Grasses[a]	69.0	12.6	4.3	16.8	49.2	6.1	0.9	43.7
Straws[a] [147]	66.7	10.2	7.8	15.3	49.4	6.1	1.2	43.2
Shells and husks[a] [147]	64.6	12.4	18.6	4.4	50.2	6.3	1.4	41.9
Sawdust[b] [147]	84.6	–	1.1	14.3	49.08	6.0	0.5	43.7
Furniture waste [148]	72.9	12.1	3.2	11.8	51.8	6.1	0.3	41.8
Sugarcane bagasse [147]	76.6	10.4	1.9	11.1	49.8	6.7	0.2	43.9
Macroalgae [147]	45.1	10.7	21.1.	23.1	43.2	6.2	2.2	45.8
HDPE [149]	97.15	–	0.8	–	86.5	15.1	–	–
PP [149]	96.9	–	1.0	–	84.7	15.3	–	–
PET [149]	84.1	–	–	13.9	64.1	3.7	–	34.2
Rigid polyurethane foam [150]	83.2	–	6.2	10.6	62.7	6.3	6.4	24.0
Sewage sludge [151]	57.22	5.42	31.27	6.09	36.11	5.25	6.50	–

[a] Mean Value obtained after analysis of different samples from the respective group.
[b] Measured at the dry basis.

sewage sludge (SS) could be used in fuel blends with biomass in order to deal with its disposal problems. Pyrolysis of sewage sludge solely at 800 °C, yields around 55% of the gaseous phase with the methane, hydrogen, and CO as the main constituents, and the heating value of 19.27 MJ/Nm^3 [157]. The SS is not a potential candidate for a bio-oil upgrade, but it can be used to obtain high-quality syngas and char residue. While syngas could be further utilized in gas turbines, quality biochar (free of pathogens due to high temperature), could be used as a fertilizer. Furthermore, biomass and SS can be pelletized together and used for power generation. The benefits of this method are the following; reduction of energy demand for the production of pellets, while the breaking force and Meyer's hardness are significantly higher. In addition, moisture absorption of biomass-SS pellets was lower, ignition temperature was reduced, and combustion temperature and performance were enhanced [151].

4.3. Current challenges and future trends

Currently, there are numerous constraints for greater deployment of alternative fuels. First of all, the availability of fossil fuels makes it hard for alternative fuels to meet cost-competitive production costs. In the case of biofuels and waste fuels, a quality criterion is the main concern; lower heating value, higher acidity, thermal stability and similar limits wider deployment of current commercially available biofuels. Nevertheless, research in this field is ongoing for some time with the constant enhancement of produced fuels, implying that the role of such fuel is not questionable in the future. On the other hand, considered chemicals (H_2, NH_3 and alcohol derived fuels) have well-known production procedure, but they are predominately synthesized for industrial needs. This implies that higher production costs are not a concern for such an application, but the further reduction is expected if the intention is to use them as a fuel. Furthermore, deployment of new fuels requires modification on existing utilisation technologies. While biofuels and alcohol derived fuels could be effectively utilized in existing IC engines with slight modifications, development of new technologies or significant modifications are required in case of hydrogen and ammonia. Fuel cells, developed for hydrogen utilisation, shows excellent perspective to be deployed for both stationary and portable applications, even though additional work is required to optimise operating parameters and increase efficiency. The last obstacle for the broader deployment of alternative fuels is the production, which needs to shift toward clean and sustainable solutions. In the case of biofuels, this predominately implies utilisation of waste agricultural and industrial biomass residues to produce high-quality clean fuels. Simultaneously, to achieve carbon neutrality, production of synthetic fuels should shift toward new solutions which do not include processing of fossil fuels as a feedstock. Additionally, synthesis of alternative fuels should be coupled with VRES, allowing them higher penetration into the energy system, simultaneously reducing the carbon footprint of produced fuels. Coupling the synthesis with VRES could also reduce the production costs once when a higher share of intermittent renewable sources is achieved. A notable trend in research is the direct utilisation of solar energy for fuel synthesis. The main advantage of solar production is in fact that there is no need for an external energy source. Nevertheless, the low conversion efficiency of solar energy is greatly influencing the overall process efficiency, making solar production economically uncompetitive. In addition, significant research efforts are given to bring technologies that can be operated in flexible mode on a commercial scale. This is especially important for electrolysis and carbon capture technologies which are used to produce essential feedstock (H_2 and CO_2) for alternative fuels synthesis. Coupling these technologies with VRES would have multiple benefits like reducing the production costs, decreasing the curtailments in power production, and improving grid stability. While talking about thermochemical conversion methods for alternative fuel production, significant research efforts are given to bring such processes on a larger scale and commercial level. Pyrolysis and gasification are especially interesting since they can process various waste materials and convert them into valuable fuels or chemicals. Recently, the research focus is shifted to enhance biofuels properties through co-pyrolysis or co-gasification with high calorific waste materials (i.e. end-of-life plastics). This is not only important for fuel synthesis but as a waste management method as well.

5. Conclusion

Alternative fuels are inevitable in the future decarbonized energy system. Even more, alternative fuels are especially essential to decarbonize transport and industry sector, where electricity will have a much lower impact, or it is not suitable as a replacement. In this review, the main goal of the authors was to present current potential alternative fuels within their applications, and present prospective alternative routes for their production. The bottom one is significantly important since it can be seen that current production pathways mainly rely on fossil fuels in both terms, the feedstock and fuels. Following conclusion are derived from this review:

- Biofuels, especially biodiesel and solid biomass, are the only alternatives available on a commercial level and already utilized for transport and industrial needs. Since their consumption is expected to increase even more in the future, new solutions should be found to achieve sustainability. Thermochemical conversion of raw feedstock through pyrolysis or gasification, as well as the anaerobic digestion of biodegradable waste, looks like promising solutions where future research efforts should be given. Additionally, waste management can effectively be incorporated within the production of enhanced biofuels, simultaneously tackling environmental concerns and improving biofuels properties.
- Chemicals like hydrogen and ammonia were tested as an alternative fuel for various utilisation technologies. Hydrogen has high energy density which marks it as a potential solution for high-temperature industrial processes or transport sector that requires such fuels. Nevertheless, hydrogen is widely used for other purposes as well, which implies that only a limited amount would be available for fuel application. Moreover, a new distribution network is required for greater deployment of hydrogen, which presents serious drawback. Ammonia, on the other hand, has a lower heating value, several safety concerns, and poor combustion properties. This suggests that role of ammonia as an alternative fuel will be very limited. Nevertheless, ammonia has a great hydrogen gravimetric density and could be used as an energy carrier or storage since the distribution is not a concern.
- Alcohol derived fuels are known alternative for some time. Nevertheless, commercial application on a greater scale is doubtful. Besides, lower heating values, which imply higher fuel intake, additional modifications or the development of dedicated IC engines, is necessary to achieve higher efficiencies. Nevertheless, such fuels show interesting characteristics when used in fuel blends, especially in terms of reducing pollutant emissions. In addition, methanol, as the simplest alcohol was successfully tested for marine application, with encouraging results regarding the engine performance and reduction of exhaust emissions.
- Greater deployment of alternative fuels can be expected once when the cost-competitive production is met. Strategic pushback can have a significant effect on this; nevertheless, the final price of produced fuels should be similar to conventional fuels. Higher penetration of VRES would allow this cost reduction since there will be more periods with an excess of electricity production, which can be effectively utilized for alternative fuel synthesis. Simultaneously, this would allow even greater penetration of intermittent renewable sources, since the produced alternative fuels can act as energy storage.

- Finally, production pathways should shift toward sustainable solutions and coupling with VRES. Predominantly this implies direct utilisation of solar energy to drive the production process or integration of various technologies like electrolysis and carbon capture with the VRES to achieve clean production of feedstock used for fuel synthesis.

Declaration of competing interest

The authors declare the following financial interests/personal relationships which may be considered as potential competing interests: Prof Neven Duic, which is co-author of this work, was blinded from the review process.

CRediT authorship contribution statement

H. Stančin: Writing - original draft, Writing - review & editing, Visualization, Conceptualization, Methodology. **H. Mikulčić:** Writing - original draft, Writing - review & editing, Methodology. **X. Wang:** Supervision, Writing - review & editing, Formal analysis. **N. Duić:** Supervision.

References

[1] Lund H, Østergaard PA, Connolly D, Mathiesen BV. Smart energy and smart energy systems. Energy 2017;137:556–65. https://doi.org/10.1016/j.energy.2017.05.123.

[2] Ž Tomšić, Rajšl I, Filipović M. Techno-economic analysis of common work of wind and combined cycle gas turbine power plant by offering continuous level of power to electricity market. J Sustain Dev Energy, Water Environ Syst 2018;6:276–90. https://doi.org/10.13044/j.sdewes.d5.0186.

[3] Aktaş A, Kırçiçek Y. A novel optimal energy management strategy for offshore wind/marine current/battery/ultracapacitor hybrid renewable energy system. Energy 2020;199. https://doi.org/10.1016/j.energy.2020.117425.

[4] Mikulčić H, Ridjan Skov I, Dominković DF, Wan Alwi SR, Manan ZA, Tan R, et al. Flexible Carbon Capture and Utilization technologies in future energy systems and the utilization pathways of captured CO2. Renew Sustain Energy Rev 2019;114. https://doi.org/10.1016/j.rser.2019.109338.

[5] Acar C. A comprehensive evaluation of energy storage options for better sustainability. Int J Energy Res 2018;42:3732–46. https://doi.org/10.1002/er.4102.

[6] Ridjan I, Mathiesen BV, Connolly D. Terminology used for renewable liquid and gaseous fuels based on the conversion of electricity: a review. J Clean Prod 2016;112:3709–20. https://doi.org/10.1016/j.jclepro.2015.05.117.

[7] Brynolf S, Taljegard M, Grahn M, Hansson J. Electrofuels for the transport sector: a review of production costs. Renew Sustain Energy Rev 2018;81:1887–905. https://doi.org/10.1016/j.rser.2017.05.288.

[8] Lester MS, Bramstoft R, Münster M. Analysis on electrofuels in future energy systems: a 2050 case study. Energy 2020;199. https://doi.org/10.1016/j.energy.2020.117408.

[9] Schmidt O, Gambhir A, Staffell I, Hawkes A, Nelson J, Few S. Future cost and performance of water electrolysis: an expert elicitation study. Int J Hydrogen Energy 2017;42:30470–92. https://doi.org/10.1016/j.ijhydene.2017.10.045.

[10] Cruz MRM, Fitiwi DZ, Santos SF, Catalão JPS. A comprehensive survey of flexibility options for supporting the low-carbon energy future. Renew Sustain Energy Rev 2018;97:338–53. https://doi.org/10.1016/j.rser.2018.08.028.

[11] Wang A, Austin D, Song H. Investigations of thermochemical upgrading of biomass and its model compounds: opportunities for methane utilization. Fuel 2019;246:443–53. https://doi.org/10.1016/j.fuel.2019.03.015.

[12] Wang M, Dewil R, Maniatis K, Wheeldon J, Tan T, Baeyens J, et al. Biomass-derived aviation fuels : challenges and perspective. Prog Energy Combust Sci 2019;74:31–49. https://doi.org/10.1016/j.pecs.2019.04.004.

[13] Sharma A, Strezov V. Life cycle environmental and economic impact assessment of alternative transport fuels and power-train technologies. Energy 2017;133:1132–41. https://doi.org/10.1016/j.energy.2017.04.160.

[14] Bajwa DS, Peterson T, Sharma N, Shojaeiarani J, Bajwa SG. A review of densified solid biomass for energy production. Renew Sustain Energy Rev 2018;96:296–305. https://doi.org/10.1016/j.rser.2018.07.040.

[15] Bloess A, Schill WP, Zerrahn A. Power-to-heat for renewable energy integration: a review of technologies, modeling approaches, and flexibility potentials. Appl Energy 2018;212:1611–26. https://doi.org/10.1016/j.apenergy.2017.12.073.

[16] Dorotić H, Doračić B, Dobravec V, Pukšec T, Krajačić G, Duić N. Integration of transport and energy sectors in island communities with 100% intermittent renewable energy sources. Renew Sustain Energy Rev 2019;99:109–24. https://doi.org/10.1016/j.rser.2018.09.033.

[17] Global IRENA. Energy transformation: a roadmap to 2050. Abu dhabi. 2018.

[18] McDonagh S, Deane P, Rajendran K, Murphy JD. Are electrofuels a sustainable transport fuel? Analysis of the effect of controls on carbon, curtailment, and cost of hydrogen. Appl Energy 2019;247:716–30. https://doi.org/10.1016/j.apenergy.2019.04.060.

[19] Lehtveer M, Brynolf S, Grahn M. What future for electrofuels in transport? Analysis of cost competitiveness in global climate mitigation. Environ Sci Technol 2019;53:1690–7. https://doi.org/10.1021/acs.est.8b05243.

[20] Abdalla AM, Hossain S, Nisfindy OB, Azad AT, Dawood M, Azad AK. Hydrogen production, storage, transportation and key challenges with applications: a review. Energy Convers Manag 2018;165:602–27. https://doi.org/10.1016/j.enconman.2018.03.088.

[21] Parra D, Valverde L, Pino FJ, Patel MK. A review on the role, cost and value of hydrogen energy systems for deep decarbonisation. Renew Sustain Energy Rev 2019;101:279–94. https://doi.org/10.1016/j.rser.2018.11.010.

[22] Valera-Medina A, Xiao H, Owen-Jones M, David WIF, Bowen PJ. Ammonia for power. Prog Energy Combust Sci 2018;69:63–102. https://doi.org/10.1016/j.pecs.2018.07.001.

[23] Giddey S, Badwal SPS, Munnings C, Dolan M. Ammonia as a renewable energy transportation media. ACS Sustainable Chem Eng 2017;5:10231–9. https://doi.org/10.1021/acssuschemeng.7b02219.

[24] Milani M, Montorsi L. Energy recovery of the biomass from livestock farms in Italy: the case of Modena province. J Sustain Dev Energy, Water Environ Syst 2018;6:464–80. https://doi.org/10.13044/j.sdewes.d6.0199.

[25] Perkins G, Bhaskar T, Konarova M. Process development status of fast pyrolysis technologies for the manufacture of renewable transport fuels from biomass. Renew Sustain Energy Rev 2018;90:292–315. https://doi.org/10.1016/j.rser.2018.03.048.

[26] Widjaya ER, Chen G, Bowtell L, Hills C. Gasification of non-woody biomass: a literature review. Renew Sustain Energy Rev 2018;89:184–93. https://doi.org/10.1016/j.rser.2018.03.023.

[27] Çelebi Y, Aydın H. An overview on the light alcohol fuels in diesel engines. Fuel 2019;236:890–911. https://doi.org/10.1016/j.fuel.2018.08.138.

[28] Svanberg M, Ellis J, Lundgren J, Landälv I. Renewable methanol as a fuel for the shipping industry. Renew Sustain Energy Rev 2018;94:1217–28. https://doi.org/10.1016/j.rser.2018.06.058.

[29] Makarichi L, Jutidamrongphan W, Techato K anan. The evolution of waste-to-energy incineration: a review. Renew Sustain Energy Rev 2018;91:812–21. https://doi.org/10.1016/j.rser.2018.04.088.

[30] Al-Salem SM. Feedstock and optimal operation for plastics to fuel conversion in pyrolysis. Elsevier Inc.; 2018. https://doi.org/10.1016/B978-0-12-813140-4.00005-4.

[31] Hassan H, Lim JK, Hameed BH. Recent progress on biomass co-pyrolysis conversion into high-quality bio-oil. Bioresour Technol 2016;221:645–55. https://doi.org/10.1016/j.biortech.2016.09.026.

[32] Shukla V, Kumar N, Resources E. Environmental concerns and sustainable development, vol. 1; 2020. https://doi.org/10.1007/978-981-13-6358-0.

[33] Sher F, Iqbal SZ, Liu H, Imran M, Snape CE. Thermal and kinetic analysis of diverse biomass fuels under different reaction environment: a way forward to renewable energy sources. Energy Convers Manag 2020;203:112266. https://doi.org/10.1016/j.enconman.2019.112266.

[34] Verhelst S, Turner JW, Sileghem L, Vancoillie J. Methanol as a fuel for internal combustion engines. Prog Energy Combust Sci 2019;70:43–88. https://doi.org/10.1016/j.pecs.2018.10.001.

[35] Awad OI, Mamat R, Ali OM, Sidik NAC, Yusaf T, Kadirgama K, et al. Alcohol and ether as alternative fuels in spark ignition engine: a review. Renew Sustain Energy Rev 2018;82:2586–605. https://doi.org/10.1016/j.rser.2017.09.074.

[36] Scopus Database n.d.

[37] Demirci A, Koten H, Gumus M. The effects of small amount of hydrogen addition on performance and emissions of a direct injection compression ignition engine. Therm Sci 2018;22:1395–404. https://doi.org/10.2298/TSCI170802004D.

[38] El-Emam RS, Özcan H. Comprehensive review on the techno-economics of sustainable large-scale clean hydrogen production. J Clean Prod 2019;220:593–609. https://doi.org/10.1016/j.jclepro.2019.01.309.

[39] Acar C, Dincer I. Review and evaluation of hydrogen production options for better environment. J Clean Prod 2019;218:835–49. https://doi.org/10.1016/j.jclepro.2019.02.046.

[40] Cano ZP, Banham D, Ye S, Hintennach A, Lu J, Fowler M, et al. Batteries and fuel cells for emerging electric vehicle markets. Nat Energy 2018;3:279–89. https://doi.org/10.1038/s41560-018-0108-1.

[41] Brooks KP, Sprik SJ, Tamburello DA, Thornton MJ. Design tool for estimating chemical hydrogen storage system characteristics for light-duty fuel cell vehicles. Int J Hydrogen Energy 2018;43:8846–58. https://doi.org/10.1016/j.ijhydene.2018.03.090.

[42] Afif A, Radenahmad N, Cheok Q, Shams S, Kim JH, Azad AK. Ammonia-fed fuel cells: a comprehensive review. Renew Sustain Energy Rev 2016;60:822–35. https://doi.org/10.1016/j.rser.2016.01.120.

[43] Kojima Y. A green ammonia economy economy. 10th Annu NH3 Fuel Conf; 2013.

[44] QAFCO. Ammonia storage tanks - MDR n.d. https://www.mcdermott.com/What-We-Do/Project-Profiles/QAFCO-Ammonia-Storage-Tanks. [Accessed 23 December 2019].

[45] Yapicioglu A, Dincer I. A review on clean ammonia as a potential fuel for power generators. Renew Sustain Energy Rev 2019;103:96–108. https://doi.org/10.1016/j.rser.2018.12.023.

[46] Oumer AN, Hasan MM, Baheta AT, Mamat R, Abdullah AA. Bio-based liquid fuels as a source of renewable energy: a review. Renew Sustain Energy Rev 2018;88:82–98. https://doi.org/10.1016/j.rser.2018.02.022.

[47] Salian K, Strezov V. Biofuels from microalgae, vol. 3. Elsevier; 2017. https://doi.org/10.1016/B978-0-12-409548-9.10114-9.

[48] Biodiesel standards/specification n.d. https://www.biofuelsystems.com/biodiesel/specification.htm. [Accessed 6 May 2020].
[49] Karmakar B, Halder G. Progress and future of biodiesel synthesis: advancements in oil extraction and conversion technologies. Energy Convers Manag 2019;182:307–39. https://doi.org/10.1016/j.enconman.2018.12.066.
[50] Othman MF, Adam A, Najafi G, Mamat R. Green fuel as alternative fuel for diesel engine: a review. Renew Sustain Energy Rev 2017;80:694–709. https://doi.org/10.1016/j.rser.2017.05.140.
[51] Petranović Z, Bešenić T, Vujanović M, Duić N. Modelling pollutant emissions in diesel engines, influence of biofuel on pollutant formation. J Environ Manag 2017;203:1038–46. https://doi.org/10.1016/j.jenvman.2017.03.033.
[52] Nabi MN, Rasul MG, Anwar M, Mullins BJ. Energy, exergy, performance, emission and combustion characteristics of diesel engine using new series of non-edible biodiesels. Renew Energy 2019. https://doi.org/10.1016/j.renene.2019.03.066.
[53] Tamilselvan P, Nallusamy N, Rajkumar S. A comprehensive review on performance, combustion and emission characteristics of biodiesel fuelled diesel engines. Renew Sustain Energy Rev 2017;79:1134–59. https://doi.org/10.1016/j.rser.2017.05.176.
[54] Mohd Noor CW, Noor MM, Mamat R. Biodiesel as alternative fuel for marine diesel engine applications: a review. Renew Sustain Energy Rev 2018;94:127–42. https://doi.org/10.1016/j.rser.2018.05.031.
[55] Gvero PM, Papuga S, Mujanić I, Vasković S. Pyrolysis as a key process in biomass combustion and thermochemical conversion. Therm Sci 2016;20:1209–22. https://doi.org/10.2298/TSCI151129154G.
[56] Zhang X, Lei H, Zhu L, Qian M, Zhu X, Wu J, et al. Enhancement of jet fuel range alkanes from co-feeding of lignocellulosic biomass with plastics via tandem catalytic conversions. Appl Energy 2016;173:418–30. https://doi.org/10.1016/j.apenergy.2016.04.071.
[57] Leonzio G. State of art and perspectives about the production of methanol, dimethyl ether and syngas by carbon dioxide hydrogenation. J CO2 Util 2018;27:326–54. https://doi.org/10.1016/j.jcou.2018.08.005.
[58] Andika R, Nandiyanto ABD, Putra ZA, Bilad MR, Kim Y, Yun CM, et al. Co-electrolysis for power-to-methanol applications. Renew Sustain Energy Rev 2018;95:227–41. https://doi.org/10.1016/j.rser.2018.07.030.
[59] Iaquaniello G, Centi G, Salladini A, Palo E, Perathoner S, Spadaccini L. Waste-to-methanol: process and economics assessment. Bioresour Technol 2017;243:611–9. https://doi.org/10.1016/j.biortech.2017.06.172.
[60] Tountas AA, Peng X, Tavasoli AV, Duchesne PN, Dingle TL, Dong Y, et al. Towards solar methanol: past, present, and future. Adv Sci 2019. https://doi.org/10.1002/advs.201801903.
[61] Zhen X. Methanol as an internal combustion on engine fuel. Elsevier B.V.; 2017. https://doi.org/10.1016/B978-0-444-63903-5.00011-X.
[62] Gupta A, Mishra PC. Emission and friction analysis of IC engine running in methanol blend. Tribol Ind 2018;40:10–8. https://doi.org/10.24874/ti.2018.40.01.02.
[63] Kamaruddin MZF, Kamarudin SK, Daud WRW, Masdar MS. An overview of fuel management in direct methanol fuel cells. Renew Sustain Energy Rev 2013;24:557–65. https://doi.org/10.1016/j.rser.2013.03.013.
[64] Hoppe W, Bringezu S, Wachter N. Economic assessment of CO2-based methane, methanol and polyoxymethylene production. J CO2 Util 2018;27:170–8. https://doi.org/10.1016/j.jcou.2018.06.019.
[65] Sivakumar G, Vail DR, Xu J, Burner DM, Lay JO, Ge X, et al. Bioethanol and biodiesel: alternative liquid fuels for future generations. Eng Life Sci 2010;10:8–18. https://doi.org/10.1002/elsc.200900061.
[66] Odziemkowska M, Matuszewska A, Czarnocka J. Diesel oil with bioethanol as a fuel for compression-ignition engines. Appl Energy 2016;184:1264–72. https://doi.org/10.1016/j.apenergy.2016.07.069.
[67] Ashtineh H, Pishvaee MS. Alternative fuel vehicle-routing problem: a life cycle analysis of transportation fuels. J Clean Prod 2019;219:166–82. https://doi.org/10.1016/j.jclepro.2019.01.343.
[68] Wu Y, Zhang X, Zhang Z, Wang X, Geng Z, Jin C, et al. Effects of diesel-ethanol-THF blend fuel on the performance and exhaust emissions on a heavy-duty diesel engine. Fuel 2020;271. https://doi.org/10.1016/j.fuel.2020.117633.
[69] Kan X, Wei L, Li X, Li H, Zhou D, Yang W, et al. Effects of the three dual-fuel strategies on performance and emissions of a biodiesel engine. Appl Energy 2020;262. https://doi.org/10.1016/j.apenergy.2020.114542.
[70] Dinali MN, Dincer I. Renewable energy based dimethyl-ether production system linked with industrial waste heat. J Energy Resour Technol Trans ASME 2019;141. https://doi.org/10.1115/1.4044056.
[71] Tomatis M, Mahmud Parvez A, Afzal MT, Mareta S, Wu T, He J, et al. Utilization of CO2 in renewable DME fuel production: a life cycle analysis (LCA)-based case study in China. Fuel 2019;254. https://doi.org/10.1016/j.fuel.2019.115627.
[72] Raza M, Chen L, Ruiz R, Chu H. Influence of pentanol and dimethyl ether blending with diesel on the combustion performance and emission characteristics in a compression ignition engine under low temperature combustion mode. J Energy Inst 2019;92:1658–69. https://doi.org/10.1016/j.joei.2019.01.008.
[73] Taghavifar H, Nemati A, Walther JH. Combustion and exergy analysis of multi-component diesel-DME-methanol blends in HCCI engine. Energy 2019;187. https://doi.org/10.1016/j.energy.2019.115951.
[74] Semelsberger TA, Borup RL, Greene HL. Dimethyl ether (DME) as an alternative. Fuel 2006;156:497–511. https://doi.org/10.1016/j.jpowsour.2005.05.082.
[75] IRENA. Five-yearglobal supply and demand projections. 2014. p. 65.
[76] Beuchelt TD, Nassl M. Applying a sustainable development lens to global biomass potentials. 2019. 10–2.
[77] Mostafa ME, Hu S, Wang Y, Su S, Hu X, Elsayed SA, et al. The significance of pelletization operating conditions: an analysis of physical and mechanical characteristics as well as energy consumption of biomass pellets. Renew Sustain Energy Rev 2019;105:332–48. https://doi.org/10.1016/j.rser.2019.01.053.
[78] Gillespie GD, Everard CD, Fagan CC, McDonnell KP. Prediction of quality parameters of biomass pellets from proximate and ultimate analysis. Fuel 2013;111:771–7. https://doi.org/10.1016/j.fuel.2013.05.002.
[79] Kumar R, Strezov V, Lovell E, Kan T, Weldekidan H, He J, et al. Bio-oil upgrading with catalytic pyrolysis of biomass using Copper/zeolite-Nickel/zeolite and Copper-Nickel/zeolite catalysts. Bioresour Technol 2019;279:404–9. https://doi.org/10.1016/j.biortech.2019.01.067.
[80] Sawant SS, Gajbhiye BD, Mathpati CS, Pandit R, Lali AM. Microalgae as sustainable energy and its cultivation. IOP Conf Ser Mater Sci Eng 2018;360. https://doi.org/10.1088/1757-899X/360/1/012025.
[81] Zhang X, Lei H, Chen S, Wu J. Catalytic co-pyrolysis of lignocellulosic biomass with polymers: a critical review. Green Chem 2016;18:4145–69. https://doi.org/10.1039/c6gc00911e.
[82] Lombardi L, Carnevale E, Corti A. A review of technologies and performances of thermal treatment systems for energy recovery from waste. Waste Manag 2015;37:26–44. https://doi.org/10.1016/j.wasman.2014.11.010.
[83] Bešenić T, Mikulčić H, Vujanović M, Duić N. Numerical modelling of emissions of nitrogen oxides in solid fuel combustion. J Environ Manag 2018;215:177–84. https://doi.org/10.1016/j.jenvman.2018.03.014.
[84] Suriapparao DV, Boruah B, Raja D, Vinu R. Microwave assisted co-pyrolysis of biomasses with polypropylene and polystyrene for high quality bio-oil production. Fuel Process Technol 2018;175:64–75. https://doi.org/10.1016/j.fuproc.2018.02.019.
[85] Jin Q, Wang X, Li S, Mikulčić H, Bešenić T, Deng S, et al. Synergistic effects during co-pyrolysis of biomass and plastic: gas, tar, soot, char products and thermogravimetric study. J Energy Inst 2019;92:108–17. https://doi.org/10.1016/j.joei.2017.11.001.
[86] Kan T, Strezov V, Evans T. Fuel production from pyrolysis of natural and synthetic rubbers. Fuel 2017;191:403–10. https://doi.org/10.1016/j.fuel.2016.11.100.
[87] Tavares G, Zsigraiova Z, Semiao V, Carvalho MDG. A case study of fuel savings through optimisation of MSW transportation routes. Manag Environ Qual Int J 2008;19:444–54. https://doi.org/10.1108/14777830810878632.
[88] Bora AP, Gupta DP, Durbha KS. Sewage sludge to bio-fuel: a review on the sustainable approach of transforming sewage waste to alternative fuel. Fuel 2020;259. https://doi.org/10.1016/j.fuel.2019.116262.
[89] Hu X, Gholizadeh M. PT. Elsevier B.V. And science press. 2019. https://doi.org/10.1016/j.jechem.2019.01.024.
[90] Al-Salem SM, Antelava A, Constantinou A, Manos G, Dutta A. A review on thermal and catalytic pyrolysis of plastic solid waste (PSW). J Environ Manag 2017;197:177–98. https://doi.org/10.1016/j.jenvman.2017.03.084.
[91] Zhou H, Wu C, Onwudili JA, Meng A, Zhang Y, Williams PT. Polycyclic aromatic hydrocarbons (PAH) formation from the pyrolysis of different municipal solid waste fractions. Waste Manag 2015;36:136–46. https://doi.org/10.1016/j.wasman.2014.09.014.
[92] Brown TW, Bischof-niemz T, Blok K, Breyer C, Lund H, Mathiesen BV. Response to ' Burden of proof : a comprehensive review of the feasibility of 100 % renewable-electricity systems. Renew Sustain Energy Rev 2018;92:834–47. https://doi.org/10.1016/j.rser.2018.04.113.
[93] Georgiopoulou M, Lyberatos G. Life cycle assessment of the use of alternative fuels in cement kilns: a case study. J Environ Manag 2018;216:224–34. https://doi.org/10.1016/j.jenvman.2017.07.017.
[94] Mikulčić H, von Berg E, Vujanović M, Wang X, Tan H, Duić N. Numerical evaluation of different pulverized coal and solid recovered fuel co-firing modes inside a large-scale cement calciner. Appl Energy 2016;184:1292–305. https://doi.org/10.1016/j.apenergy.2016.05.012.
[95] Jiang L, Yuan X, Xiao Z, Liang J, Li H, Cao L, et al. A comparative study of biomass pellet and biomass-sludge mixed pellet: energy input and pellet properties. Energy Convers Manag 2016;126:509–15. https://doi.org/10.1016/j.enconman.2016.08.035.
[96] Naqi A, Jang JG. Recent progress in green cement technology utilizing low-carbon emission fuels and raw materials: a review. Sustain Times 2019;11. https://doi.org/10.3390/su11020537.
[97] Wu Y, Tao Y, Deng Z, Zhou J, Xu C, Zhang B. A fuzzy analysis framework for waste incineration power plant comprehensive benefit evaluation from refuse classification perspective. J Clean Prod 2020;258. https://doi.org/10.1016/j.jclepro.2020.120734.
[98] Brunner PH, Rechberger H. Waste to energy - key element for sustainable waste management. Waste Manag 2015;37:3–12. https://doi.org/10.1016/j.wasman.2014.02.003.
[99] Horvath S, Fasihi M, Breyer C. Techno-economic analysis of a decarbonized shipping sector : technology suggestions for a fleet in 2030 and 2040, vol. 164; 2018. p. 230–41. https://doi.org/10.1016/j.enconman.2018.02.098.
[100] Varga B, Sagoian A, Mariasiu F. Prediction of electric vehicle range: a comprehensive review of current issues and challenges. Energies 2019;12:946. https://doi.org/10.3390/en12050946.
[101] Pan ZF, An L, Wen CY. Recent advances in fuel cells based propulsion systems for unmanned aerial vehicles. Appl Energy 2019;240:473–85. https://doi.org/10.1016/j.apenergy.2019.02.079.
[102] Jabari F, Mohammadi-ivatloo B, Ghaebi H, Bannae-sharifian MB. Biogas fueled combined cooling, desalinated water and power generation systems. J Clean Prod 2019;219:906–24. https://doi.org/10.1016/j.jclepro.2019.01.272.

[103] Chacartegui R, Sánchez D, Muñoz de Escalona JM, Muñoz A, Sánchez T. Gas and steam combined cycles for low calorific syngas fuels utilisation. Appl Energy 2013;101:81–92. https://doi.org/10.1016/j.apenergy.2012.02.041.

[104] Ghenai C. Combustion of syngas fuel in gas turbine can combustor. 2010. https://doi.org/10.1155/2010/342357. 2010.

[105] Ul Hai I, Sher F, Yaqoob A, Liu H. Assessment of biomass energy potential for SRC willow woodchips in a pilot scale bubbling fluidized bed gasifier. Fuel 2019;258:116143. https://doi.org/10.1016/j.fuel.2019.116143.

[106] Kan T, Strezov V, Evans T. Effect of the heating rate on the thermochemical behavior and biofuel properties of sewage sludge pyrolysis. Energy Fuels 2016;30:1564–70. https://doi.org/10.1021/acs.energyfuels.5b02232.

[107] Bedoić R, Čuček L, Ćosić B, Krajnc D, Smoljanić G, Kravanja Z, et al. Green biomass to biogas – a study on anaerobic digestion of residue grass. J Clean Prod 2019;213:700–9. https://doi.org/10.1016/j.jclepro.2018.12.224.

[108] Opatokun SA, Lopez-Sabiron AM, Ferreira G, Strezov V. Life cycle analysis of energy production from food waste through anaerobic digestion, pyrolysis and integrated energy system. Sustain Times 2017;9. https://doi.org/10.3390/su9101804.

[109] Hlavsová A, Corsaro A, Raclavská H, Juchelková D, Škrobánková H, Frydrych J. Syngas production from pyrolysis of nine composts obtained from nonhybrid and hybrid perennial grasses. 2014. 2014.

[110] Bongartz D, Doré L, Eichler K, Grube T, Heuser B, Hombach LE, et al. Comparison of light-duty transportation fuels produced from renewable hydrogen and green carbon dioxide. Appl Energy 2018;231:757–67. https://doi.org/10.1016/j.apenergy.2018.09.106.

[111] Stern AG. A new sustainable hydrogen clean energy paradigm. Int J Hydrogen Energy 2018;43:4244–55. https://doi.org/10.1016/j.ijhydene.2017.12.180.

[112] Thompson ST, James BD, Huya-Kouadio JM, Houchins C, DeSantis DA, Ahluwalia R, et al. Direct hydrogen fuel cell electric vehicle cost analysis: system and high-volume manufacturing description, validation, and outlook. J Power Sources 2018;399:304–13. https://doi.org/10.1016/j.jpowsour.2018.07.100.

[113] Balamurugan T, Arun A, Sathishkumar GB. Biodiesel derived from corn oil – a fuel substitute for diesel. Renew Sustain Energy Rev 2018;94:772–8. https://doi.org/10.1016/j.rser.2018.06.048.

[114] Chiong MC, Chong CT, Ng JH, Lam SS, Tran MV, Chong WWF, et al. Liquid biofuels production and emissions performance in gas turbines: a review. Energy Convers Manag 2018;173:640–58. https://doi.org/10.1016/j.enconman.2018.07.082.

[115] Zhang X, Lei H, Zhu L, Qian M, Zhu X, Wu J, et al. Enhancement of jet fuel range alkanes from co-feeding of lignocellulosic biomass with plastics via tandem catalytic conversions. Appl Energy 2016;173:418–30. https://doi.org/10.1016/j.apenergy.2016.04.071.

[116] Sileghem L, Van De Ginste M, Ginste M, Van De. Methanol as a fuel for modern spark-ignition engines: efficiency study. Ghent Univ; 2011.

[117] Jurić F, Petranović Z, Vujanović M, Katrašnik T, Vihar R, Wang X, et al. Experimental and numerical investigation of injection timing and rail pressure impact on combustion characteristics of a diesel engine. Energy Convers Manag 2019;185:730–9. https://doi.org/10.1016/j.enconman.2019.02.039.

[118] Berndes G, Hoogwijk M, van den Broek R. Potential contribution of bioenergy to the world's future energy demand. Contrib Biomass Futur Glob Energy Supply a Rev 17 Stud, 25; 2007. p. 335–67.

[119] Kang K, Qiu L, Sun G, Zhu M, Yang X, Yao Y. Codensification technology as a critical strategy for energy recovery from biomass and other resources - a review. Renew Sustain Energy Rev 2019;116:109414. https://doi.org/10.1016/j.rser.2019.109414.

[120] Kijo-Kleczkowska A, Środa K, Kosowska-Golachowska M, Musiał T, Wolski K. Experimental research of sewage sludge with coal and biomass co-combustion, in pellet form. Waste Manag 2016;53:165–81. https://doi.org/10.1016/j.wasman.2016.04.021.

[121] Wang Z, Shen D, Wu C, Gu S. Thermal behavior and kinetics of co-pyrolysis of cellulose and polyethylene with the addition of transition metals. Energy Convers Manag 2018;172:32–8. https://doi.org/10.1016/j.enconman.2018.07.010.

[122] Li Y, Lin Y, Zhao J, Liu B, Wang T, Wang P, et al. Control of NO x emissions by air staging in small- and medium-scale biomass pellet boilers. Environ Sci Pollut Res 2019. https://doi.org/10.1007/s11356-019-04396-8.

[123] Van DP. A review of anaerobic digestion systems for biodegradable waste: configurations , operating parameters , and current trends, 25; 2020. p. 1–17.

[124] Alvarez J, Kumagai S, Wu C, Yoshioka T, Bilbao J, Olazar M, et al. Hydrogen production from biomass and plastic mixtures by pyrolysis-gasification. Int J Hydrogen Energy 2014;39:10883–91. https://doi.org/10.1016/j.ijhydene.2014.04.189.

[125] Kwon EE, Oh JI, Kim KH. Polycyclic aromatic hydrocarbons (PAHs) and volatile organic compounds (VOCs) mitigation in the pyrolysis process of waste tires using CO_2 as a reaction medium. J Environ Manag 2015;160:306–11. https://doi.org/10.1016/j.jenvman.2015.06.033.

[126] González-García S, Bacenetti J. Exploring the production of bio-energy from wood biomass. Italian case study. Sci Total Environ 2019;647:158–68. https://doi.org/10.1016/j.scitotenv.2018.07.295.

[127] Lombardi L, Carnevale E, Corti A. A review of technologies and performances of thermal treatment systems for energy recovery from waste. 2014. https://doi.org/10.1016/j.wasman.2014.11.010.

[128] Chapman A, Itaoka K, Hirose K, Davidson FT, Nagasawa K, Lloyd AC, et al. A review of four case studies assessing the potential for hydrogen penetration of the future energy system. Int J Hydrogen Energy 2019;44:6371–82. https://doi.org/10.1016/j.ijhydene.2019.01.168.

[129] Ogawa T, Takeuchi M, Kajikawa Y. Analysis of trends and emerging technologies in water electrolysis research based on a computational method: a comparison with fuel cell research. Sustain Times, vol. 10; 2018. https://doi.org/10.3390/su10020478.

[130] Mazza A, Bompard E, Chicco G. Applications of power to gas technologies in emerging electrical systems. Renew Sustain Energy Rev 2018;92:794–806. https://doi.org/10.1016/j.rser.2018.04.072.

[131] Kim JS, Boardman RD, Bragg-Sitton SM. Dynamic performance analysis of a high-temperature steam electrolysis plant integrated within nuclear-renewable hybrid energy systems. Appl Energy 2018;228:2090–110. https://doi.org/10.1016/j.apenergy.2018.07.060.

[132] Boulamanti A, Moya JA. Production costs of the chemical industry in the EU and other countries: ammonia, methanol and light olefins. Renew Sustain Energy Rev 2017;68:1205–12. https://doi.org/10.1016/j.rser.2016.02.021.

[133] Wang Q, Guo J, Chen P. Recent progress towards mild-condition ammonia synthesis, vol. 36. Elsevier B.V. and Science Press; 2019. https://doi.org/10.1016/j.jechem.2019.01.027.

[134] Toyne D, Schmuecker J. Our demonstration farm renewable hydrogen and ammonia generation system. 2017. p. 1–17.

[135] Farfan J, Lohrmann A, Breyer C. Integration of greenhouse agriculture to the energy infrastructure as an alimentary solution. Renew Sustain Energy Rev 2019;110:368–77. https://doi.org/10.1016/j.rser.2019.04.084.

[136] Bedoić R, Bulatović VO, Čuček L, Ćosić B, Špehar A, Pukšec T, et al. A kinetic study of roadside grass pyrolysis and digestate from anaerobic mono-digestion. Bioresour Technol 2019;292. https://doi.org/10.1016/j.biortech.2019.121935.

[137] Guo M, Song W, Buhain J. Bioenergy and biofuels: history, status, and perspective. Renew Sustain Energy Rev 2015;42:712–25. https://doi.org/10.1016/j.rser.2014.10.013.

[138] Eveloy V, Gebreegziabher T. A review of projected power-to-gas deployment scenarios. Energies 2018;11:1824. https://doi.org/10.3390/en11071824.

[139] Bhave A, Taylor RHS, Fennell P, Livingston WR, Shah N, Dowell N Mac, et al. Screening and techno-economic assessment of biomass-based power generation with CCS technologies to meet 2050 CO2 targets. Appl Energy 2017;190:481–9. https://doi.org/10.1016/j.apenergy.2016.12.120.

[140] Hetland J, Yowargana P, Leduc S, Kraxner F. Carbon-negative emissions: systemic impacts of biomass conversion. A case study on CO2 capture and storage options. Int J Greenh Gas Control 2016;49:330–42. https://doi.org/10.1016/j.ijggc.2016.03.017.

[141] Luh S, Budinis S, Schmidt TJ, Hawkes A. Decarbonisation of the industrial sector by means of fuel switching. In: Electrification and CCS. Comput. Aided chem. Eng., vol. 43. Elsevier B.V.; 2018. p. 1311–6. https://doi.org/10.1016/B978-0-444-64235-6.50230-8.

[142] Carapellucci R, Giordano L. Upgrading existing gas-steam combined cycle power plants through steam injection and methane steam reforming. Energy 2019;173:229–43. https://doi.org/10.1016/j.energy.2019.02.046.

[143] Ephraim A, Pham Minh D, Lebonnois D, Peregrina C, Sharrock P, Nzihou A. Co-pyrolysis of wood and plastics: influence of plastic type and content on product yield, gas composition and quality. Fuel 2018;231:110–7. https://doi.org/10.1016/j.fuel.2018.04.140.

[144] Anuar Sharuddin SD, Abnisa F, Wan Daud WMA, Aroua MK. A review on pyrolysis of plastic wastes. Energy Convers Manag 2016;115:308–26. https://doi.org/10.1016/j.enconman.2016.02.037.

[145] Al-Salem SM, Lettieri P, Baeyens J. Recycling and recovery routes of plastic solid waste (PSW): a review. Waste Manag 2009;29:2625–43. https://doi.org/10.1016/j.wasman.2009.06.004.

[146] Strezov V, Evans TJ, Hayman C. Thermal conversion of elephant grass (Pennisetum Purpureum Schum) to bio-gas, bio-oil and charcoal. Bioresour Technol 2008;99:8394–9. https://doi.org/10.1016/j.biortech.2008.02.039.

[147] Vassilev SV, Baxter D, Andersen LK, Vassileva CG. An overview of the chemical composition of biomass. Fuel 2010;89:913–33. https://doi.org/10.1016/j.fuel.2009.10.022.

[148] Uzoejinwa BB, He X, Wang S, El-Fatah Abomohra A, Hu Y, Wang Q. Co-pyrolysis of biomass and waste plastics as a thermochemical conversion technology for high-grade biofuel production: recent progress and future directions elsewhere worldwide. Energy Convers Manag 2018;163:468–92. https://doi.org/10.1016/j.enconman.2018.02.004.

[149] Chattopadhyay J, Pathak TS, Srivastava R, Singh AC. Catalytic co-pyrolysis of paper biomass and plastic mixtures (HDPE (high density polyethylene), PP (polypropylene) and PET (polyethylene terephthalate)) and product analysis. Energy 2016;103:513–21. https://doi.org/10.1016/j.energy.2016.03.015.

[150] Stančin H, Růžičková J, Mikulčić H, Raclavská H, Kucbel M, Wang X, et al. Experimental analysis of waste polyurethane from household appliances and its utilization possibilities. J Environ Manag 2019;243:105–15. https://doi.org/10.1016/j.jenvman.2019.04.112.

[151] Li H, Jiang LB, Li CZ, Liang J, Yuan XZ, Xiao ZH, et al. Co-pelletization of sewage sludge and biomass: the energy input and properties of pellets. Fuel Process Technol 2015;132:55–61. https://doi.org/10.1016/j.fuproc.2014.12.020.

[152] Bernardo M, Lapa N, Gonçalves M, Barbosa R, Mendes B, Pinto F, et al. Toxicity of char residues produced in the co-pyrolysis of different wastes. Waste Manag 2010;30:628–35. https://doi.org/10.1016/j.wasman.2009.10.015.

[153] Lu P, Huang Q, Bourtsalas AC, Thanos, Themelis NJ, Chi Y, Yan J. Review on fate of chlorine during thermal processing of solid wastes. J Environ Sci (China) 2019;78:13–28. https://doi.org/10.1016/j.jes.2018.09.003.

[154] Olajire A, Gebreegziabher T, Ng DKS, Wai C. Mixed-waste pyrolysis of biomass and plastics waste e A modelling approach to reduce energy usage. Energy 2014;1–9. https://doi.org/10.1016/j.energy.2014.05.063.

[155] Zhang H, Nie J, Xiao R, Jin B, Dong C, Xiao G. Catalytic Co-pyrolysis of biomass and different plastics (polyethylene , polypropylene, and polystyrene) to improve hydrocarbon yield in a fluidized-bed reactor. 2014.

[156] Lu P, Huang Q, Thanos, Bourtsalas AC, Chi Y, Yan J. Synergistic effects on char and oil produced by the co-pyrolysis of pine wood, polyethylene and polyvinyl chloride. Fuel 2018;230:359–67. https://doi.org/10.1016/j.fuel.2018.05.072.

[157] Ledakowicz S, Stolarek P, Malinowski A, Lepez O. Thermochemical treatment of sewage sludge by integration of drying and pyrolysis/autogasification. Renew Sustain Energy Rev 2019;104:319–27. https://doi.org/10.1016/j.rser.2019.01.018.

PAPER 2

Process Safety and Environmental Protection 145 (2021) 1–11

Contents lists available at ScienceDirect

Process Safety and Environmental Protection

journal homepage: www.elsevier.com/locate/psep

Co-pyrolysis and synergistic effect analysis of biomass sawdust and polystyrene mixtures for production of high-quality bio-oils

H. Stančin[a,*], M. Šafář[b], J. Růžičková[b], H. Mikulčić[a,c], H. Raclavská[b,d], X. Wang[c], N. Duić[a]

[a] University of Zagreb, Faculty of Mechanical Engineering and Naval Architecture, Ivana Lučića 5, 10 000, Zagreb, Croatia
[b] ENET CENTRE VSB-Technical University Ostrava, 17. listopadu 2172/15, 708 00, Ostrava, Czech Republic
[c] Department of Thermal Engineering, Xi'an Jiaotong University, Xi'an, Shaanxi, Xianning West Road, Xi'an, China
[d] VŠB – Technical University of Ostrava, Czech Republic, Faculty of Mining and Geology, 17. listopadu 2172/15, 708 00 Ostrava, Czech Republic

ARTICLE INFO

Article history:
Received 27 April 2020
Received in revised form 14 July 2020
Accepted 15 July 2020
Available online 17 July 2020

Keywords:
Co-pyrolysis
Polystyrene
Sawdust
Synergistic effect
Oil composition

ABSTRACT

Usage of traditional biomass raises serious concerns regarding its sustainability due to the inefficient combustion in household stoves and potential over-usage if the intention is to replace fossil fuels in power plants. Co-pyrolysis of biomass feedstock with different waste materials, especially plastics, might be a promising alternative for sustainable usage of enhanced biofuels. Even more, co-pyrolysis can help to integrate waste management schemes into the power production sector. Plastics materials have properties similar to those of fossil fuels in terms of heating value and the absence of oxygenated compounds; therefore, they could significantly improve the properties of biomass products, especially bio-oils. Especially interesting for this method is polystyrene (PS) since it yields a high share of liquid fraction, which is the most valuable pyrolytic product. In this work, co-pyrolysis was performed for a mixture of waste biomass sawdust (oak, poplar and fir wood) and waste polystyrene from dairy product packaging. Pyrolysis was carried out for sawdust and polystyrene alone, and their respective fuel blends (PS/SD 25–75%, PS/SD 50–50%, PS/SD 75–25%) from room temperature to 600 °C with a retention time of half an hour. The highest yield of liquid fraction was noticed for mixtures with 75 % of PS, while the lowest one was for blends with 25 % of PS, with a yield of 83.86 % and 62.33 %, respectively. Additionally, the mass spectrometric analysis was carried out to determine the chemical composition of the obtained oil.

1. Introduction

Besides electrification, additional high-energy-density alternative fuels are inevitable for successful energy transition (Foley and Olabi, 2017). This is due to the fact that electrification of high-temperature processes (Mikulčić et al., 2016) or long-range voyages might not be efficient and practical (Ridjan et al., 2016). Biomass and biofuels are already used as an alternative energy source, even though the sustainability of such practice is questionable, due to their usage in poorly efficient stoves with low efficiency (Aberilla et al., 2019). Liquid biofuels, which are already deployed on a commercial scale, have severe drawbacks like low heating value, a high share of oxygenated compounds (35–60 %), poor thermal stability, higher viscosity and acidity (H. Hassan et al., 2016a). To enhance biofuels properties, different thermochemical methods like pyrolysis (Gvero et al., 2016), gasification (Widjaya et al., 2018), and anaerobic digestion (Bedoić et al., 2019) are lately promoted as a potential solution. Pyrolysis is interesting since it can simultaneously enhance the properties of obtained pyrolysis fractions (liquid, gas, solid), especially bio-oil, which has the greatest commercial potential for utilisation (Chiong et al., 2018). Since the pyrolysis itself can partially prevail the drawbacks mentioned above, co-pyrolysis with waste materials, especially plastics, was introduced (Zhang et al., 2014). About 27 million tons of plastic waste is generated in EU in 2018 of which only 31.1 % is recycled, while the rest is landfilled or used in energy recovery processes (PlasticsEurope, 2018). The oil obtained from plastic pyrolysis have some excellent characteristics similar to conventional gasoline, like high heating value and hydrocarbon content (Miskolczi and Nagy, 2012). Nevertheless, in such oils higher share of harmful compounds like polycyclic aromatic hydrocarbons (PAHs), furans, dioxins, benzenes and similar is present, which constrains wider application or requires complicated and expensive after-treatment (Kwon et al., 2015). Co-pyrolysis looks

* Corresponding author.
E-mail addresses: hrvoj.stancin@fsb.hr (H. Stančin), michal.safar@vsb.cz (M. Šafář), jana.ruzickova@vsb.cz (J. Růžičková), hrvoje.mikulcic@fsb.hr (H. Mikulčić), helena.raclavska@vsb.cz (H. Raclavská), wxb005@mail.xjtu.edu.cn (X. Wang), neven.duic@fsb.hr (N. Duić).

https://doi.org/10.1016/j.psep.2020.07.023
0957-5820/

like a promising solution since it can process waste materials and convert them into highly valuable fuels or chemicals (Abnisa and Wan Daud, 2014). Therefore, utilisation of waste biomass (sawdust, wood chips, branches) and end-of-life plastics might be a great solution to tackle multiple challenges (Chattopadhyay et al., 2016). Produced alternative fuels can be utilised where appropriate; waste management could be efficiently integrated with the energy sector, while biomass consumption can be maintained at sustainable levels since the need for feedstock is partially satisfied with waste plastics.

Up to know, significant research efforts are given to find the optimal conditions and bring the process on a larger scale. Abnisa and Wan Daud (2014) provide a review on the co-pyrolysis process regarding the feedstock selection, process parameters, decomposition mechanisms and product yield. Additionally, the study gives a comprehensive review of the characteristics of common waste plastic materials with their Ultimate and Proximate analysis, and potential utilisation as a pyrolysis feedstock. Uzoejinwa et al. (2018) gave an in-depth review with achieved accomplishments in field and prospects for future work. In this work, main products of thermal decomposition of various biomass and plastic materials are given, alongside their main degradation mechanism. Even more, the author's present a very detailed review regarding the synergistic effect that occurs between investigated feedstock, as well as their possible reaction mechanisms. As a prospect for future work and directions, the authors suggest the usage of an acidic catalyst to enhance the selectivity of products, but also the usage of microalgae and seaweed biomass as a feedstock. Yang et al. (2016) investigated the fast co-pyrolysis of low-density polyethene (LDPE) with three different biomass feedstock. In this study, the detailed analysis is given regarding the oil characterisation, and it is concluded that co-pyrolysis enhances the yield of hydrocarbons through the synergistic effect. H. Hassan et al. (2016a) (2016b) provide a good insight on recent progress on biomass co-pyrolysis for bio-oil production, including both catalytic and non-catalytic. E. B. Hassan et al. (2016a) (2016b) analysed the aromatic hydrocarbon yield from fast co-pyrolysis of torrefied biomass and polystyrene (PS). This study shows that co-pyrolysis can significantly enhance the yield of aromatics while decreasing the content of oxygenated compounds. Moreover, in this study, a potential mechanism for the formation of major aromatic hydrocarbons is given. Özsin and Pütün (2018) present a comparative study on the co-pyrolysis of biomass with different plastics. The study concludes that the synergistic effect and product yield, besides process parameters, depends on biomass-plastic feedstock ratio in the fuel blend. Nevertheless, all mixtures express the reduction of oxygenated compounds and increment in heating value. Ephraim et al. (2018) analysed the synergistic effect and product yield for various plastic materials. Even though all investigated samples expressed synergy, opposite trends are noticed, which implies that product yield depends on feedstock selection. Finally, various kinetic analyses are performed to investigate the influence of different atmospheric conditions (Mikulčić et al., 2019), and the catalytic effect on product yield (Miskolczi et al., 2019). Especially interesting is the co-pyrolysis of biomass with waste PS, which yields a high share of liquids with aromatic hydrocarbons required to meet fuel specifications (Sanahuja-Parejo et al., 2019). Since some form of waste PS materials are inappropriate for conventional recycling methods or are not even included in plastic recycling schemes, this marks them as an ideal feedstock for co-pyrolysis.

In this study, biomass sawdust is co-pyrolysed with waste PS, with an aim to investigate the influence of plastic content on bio-oil properties. Up to know, process parameters and their influence on product yield were widely investigated, while more needs to be done regarding the feedstock selection. The main objective of this study is to analyse the influence of plastic content on bio-oil quality by evaluating the level of synergy between feedstock and observing the composition of bio-oils derived from mixture co-pyrolysis. Even though the introduction of plastic content enhances the bio-oil properties, it was noticed that after some point, a further increment of plastic share in the mixture has more negative impact promoting the formation of unwanted compounds. Therefore, determination of the optimal mixing ratio is essential to produce high-quality biofuels, but even more, to reduce the need for expensive after-treatment methods.

2. Materials and methods

2.1. Material characterisation

Samples investigated in this study were waste plastic and biomass sawdust materials. The plastic feedstock was waste polystyrene (PS) previously used as a packaging material for dairy products, while biomass was obtained from a local sawmill in the form of sawdust (SD) mixture of beech, oak and fir with the unknown shares. Prior to experimental investigations, sample preparation was carried out by shredding, grinding and sieving into finer particles (0.125–0.25 mm) to obtain homogenous fractions. Materials were obtained with unknown chemical and elemental composition. The elemental characterisation (Ultimate analysis) was carried out by the FlashSmart Analyzer on about 2 mg of a sample, and the results are given in Table 1. Proximate analysis was performed on a Mettler-Toledo TGA-DSC-2 using 70 mL Al_2O_3 crucibles. Around 10 mg of each sample was heated to 110 °C at 10 °C/min under a high purity nitrogen gas streamflow of 50 mL/min (with a supplemental N_2 balance protective gas flow of 20 mL/min). Samples were held at 110 °C for 30 min to drive off residual moisture and then heated up to 900 °C, which was maintained for 30 min. The mass loss in this step is attributed to volatile matter. Subsequently, the sample was heated to 950 °C at 10 °C/min under air atmosphere, and this mass loss is considered to be fixed carbon (Xue et al., 2018).

2.2. Thermal decomposition investigation

To determine optimal co-pyrolysis conditions, thermogravimetric analysis (TGA) was carried using TGA/DSC 2 Thermoanalyzer Mettler Toledo. Samples were investigated individually and in mixtures with different shares: PS/SD 25–75%, PS/SD 50–50%, PS/SD 75–25%. Samples of about 10 mg were heated in Al_2O_3 crucibles of 70 μL, from room temperature to 600 °C, at a heating rate of 10 °C/min. Since the aim of the work is to investigate the influence of slow pyrolysis on the product yield and distribution, the heating rate was selected at 10 °C/min which is the most often used heating rate for slow pyrolysis. The selection of final temperature was based on the sawdust and PS properties, and the results from previous investigations. The 600 °C was chosen to achieve maximum decomposition of the biomass sample and to reduce solid residue at the end of a process. Nitrogen was selected as a carrier gas since it is inert and widely available and used for such application. The gas flow of 20 mL/min was used as sufficient for maintaining the inert atmosphere, and the retention time was 30 min. The retention time of 30 min was used to maximise the conversion rate of sawdust sample since its decomposition is not finished when the final temperature is reached.

2.3. Pyrolysis conditions and product analysis

The pyrolysis experiments were performed in a stainless-steel fixed bed reactor. The temperature of the reactor was controlled

Table 1
Ultimate and Proximate analysis of polystyrene and sawdust samples (dry matter).

	C (%)	H (%)	N (%)	O (%)	Ash (%)	Volatile matter (%)	Fixed carbon (%)	Moisture(%)
PS	89.58	8.22	–	0.92	1.28	98.36	0.22	0.04
Sawdust	46.49	6.03	2.47	44.51	0.50	78.78	20.66	5.85

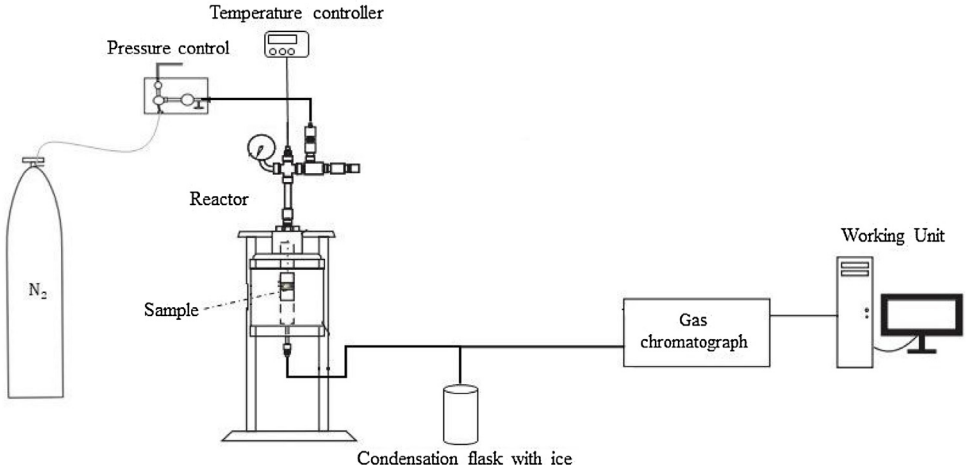

Fig. 1. Experimental setup used for the pyrolysis and co-pyrolysis of investigated samples.

by a PID temperature controller (Model 4836, Parr), whereas a K-type thermocouple sensed the temperature of the reaction. A more detailed description of the reaction set-up has been described by Hlavsová et al. (2014). The experiments were carried out under a nitrogen atmosphere with a flow rate of 80 mL/min. Approximately 2 g of the sample was placed in the reactor and heated at 10 °C/min to a final temperature of 600 °C. The final temperature was maintained for about 30 min or until the complete release of pyrolysis gases. Samples were pyrolysed individually and in respective mixtures. The yield of the solid fraction was calculated by weighing the sample mass before and the residual mass after the pyrolysis. The yield of pyrolysis gas was calculated at N_2 free-vol.%, and it is based on the volume fractions obtained from gas chromatography (GC) and densities of individual gas components. Condensable gases were cooled down using an ice bath and collected in liquid form at the end of a reactor. Share of liquid fraction was calculated by the difference. The experiments were duplicated to validate the results.

The pyrolysis liquids were diluted 1:10 by dichloromethane. An internal standard of 1,3,5-tri-tert. butylbenzene (100 ng/μL, Merck) was added. Composition analysis was done by GC/MS (Agilent 7890, 5975 C). About 1 μL aliquot of sample was injected in split ratio 1:10 by MultiPurpose Sampler (MPS, Gerstel, Muelheim an der Ruhr) into Agilent 7890 A equipped with a HP 5 ms column (60 m x 025 mm x 025 μm, Agilent J&W). The injector temperature was set at 250 °C. Helium was used as carrier gas at a constant flow rate 1 mL/min. The organic compounds were separated (on column) by the following programme: 48 °C (retention time 2.5 min.) to 280 °C (hold time 0.5 min.) with a rate 5 °C/min. The transfer line temperature was set at 280 °C, quadrupole and ion-source temperature 150 and 230 °C. The mass spectrometric analysis was performed in the range of $m/z = 35–650$. The identification and quantification of the individual organic compounds were carried out by standards and programs Agilent Qualitative and Unknown analysis. Fig. 1 presents the experimental setup used in this study for the co-pyrolysis, while it can also be used for gasification. The similar setup, with only a few modifications, was also used by Hlavsová et al. (2014), where syngas production was studied from the pyrolysis of various Perennial grasses.

3. Results

3.1. Thermogravimetric analysis (TGA)

Thermogravimetric analysis (TGA) is an important technique used to determine the thermal decomposition mechanism of investigated feedstock (Rostek and Biernat, 2013). The TGA is especially important to determine optimal operating co-pyrolysis conditions, especially when samples have a different origin, composition and thermal stability. Fig. 2 presents the thermogravimetric (TG) curves for individual samples (a) and corresponding mixtures (b). As it can be seen (Fig. 2a) thermal decomposition of PS consists of one step between 367 °C and 482 °C, with a peak at 425 °C. When the temperature reaches 600 °C, solid residue is about 5.67 %, additionally lowered to ~5 % after 30 min of retention time. Similar results are already reported in the literature (Singh et al., 2019a;, 2019b). Thermal decomposition of biomass sawdust consists of three stages, starting at around 50 °C with the dehydration up to 200 °C, where approximately 5 % of mass loss is noticed. The second stage, between 200 and 370 °C, presents the most intensive decomposition with a peak at around 350 °C, where mostly cellulose and hemicellulose, is decomposed (Zhang et al., 2016). In this stage, the mass of the sample is more than halved to approximately 37 %. The last stage follows a linear trend, and when the temperature reaches 600 °C biochar mass is about 21 %. After a retention time of 30 min, the final mass is slightly below 10 % of initial weight, indicating higher lignin and mineral content in the investigated sample (Reshad et al., 2019).

Obtained TG curves for polystyrene and sawdust mixtures (Fig. 2b) shows an obvious synergy compared to the individual analysis. All blends express three stages of decomposition, starting with the evaporation at around 65 °C up to 100 °C. For the mixture with a low share of PS, the evaporation stage is not notably affected. With the gradual increase of the PS content, the onset temperature for moisture evaporation for SD is decreased from 65 °C to 58 °C for the mixture with 50 % of PS, and to 53 °C for the mixture with 75 % of PS. This implies that plastic content affects the moisture evaporation of the biomass component by lowering the onset temperature. In addition, PS reduced the intensity of evaporation, and as it can be

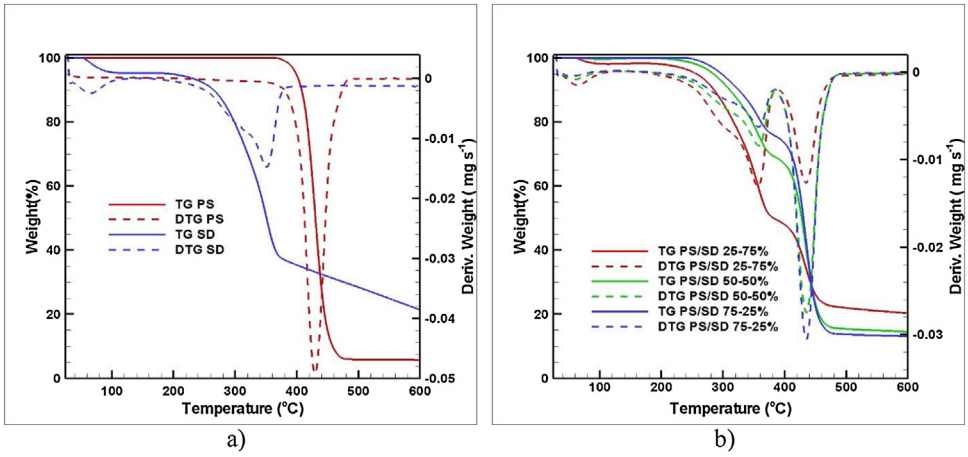

Fig. 2. TG curves for individual sawdust and PS samples (a) and their respective mixtures (b).

Table 2
Initial and final mass of investigated samples.

Sample	Initial mass [mg]	Final mass[mg]	Conversion rate [%]
Sawdust	10.602	1.048	90.12
PS	10.935	0.616	94.37
PS/SD 25–75%	11.667	2.193	81.20
PS/SD 50–50%	12.139	1.654	86.37
PS/SD 75–25%	11.161	1.367	87.75

seen from Fig. 2b, only the mixture where SD is a dominant component has a visible mass loss. Similar to individual TGA of SD, second stage decomposition starts slightly below 200 °C, and goes up to 380 °C, with a peak at 360 °C. In this stage, the introduction of PS broadens the temperature range in which conversion is happening by lowering the initial temperature, simultaneously increasing the final stage temperature. The highest mass loss is noticed for the mixture with 75 % of SD, which suggests that the biomass components (cellulose and hemicellulose) play an important role in this temperature range. The last stage of decomposition starts at around 400 °C, and it goes up to 480 °C, after which the mass loss is almost negligible. In the last stage, the synergy effect is the most evident since the decomposition process is significantly accelerated, and conversion is finished before reaching the final temperature. It is interesting to notice that the mixture with 75 % of SD has the lowest conversion in this stage, which implies that biomass decomposition is dominant for mild temperatures (Parihar et al., 2007). Blend with the 75 % of PS, expressed the most intense degradation in the third stage, which is expected since that individual TGA showed that in this temperature range PS decompose rapidly. Mixture with an equal share of both feedstocks shows similar behaviour to those where PS is dominant. Therefore, it can be stated that the addition of PS promotes the conversion of hardly degradable lignin component, reducing the need for retention time. Table 2 presents the initial and final mass for investigated samples. Additionally, the conversion rate in percentages is given to see in which portion is used feedstock converted to liquid and gaseous products. As it can be seen the conversion rate for investigated mixtures is slightly lower, indicating that the interaction between them during the process hinders theoretically possible conversion rate obtained from individual pyrolysis.

3.2. Pyrolysis product analysis

3.2.1. Product yield

Before being introduced to co-pyrolysis, PS and SD were pyrolysed individually to obtain referent values and calculate the theoretical yield of pyrolytic products. Theoretical yield is then compared with experimentally obtained values to determine the level of synergy between investigated feedstock. Fig. 3 presents the experimentally obtained values for all investigated samples. As expected, the dominant fraction from the pyrolysis of PS is liquid with a yield of 96.02 %, while the share of a gas fraction is almost negligible (<1 %). Previous investigations show the yield of liquid fraction between 80–90 % [21, 24, 25], while Ephraim et al. (2018) reported the yield higher than 99 %. On the other hand, the main products from the SD pyrolysis are gases (48.10 %), followed by liquid and char with a yield of 31.39 % and 20.51 %, respectively. Van Nguyen et al. (2019) pyrolysed the pine sawdust, where product distribution was following; 48.83 % of bio-oil, 31.29 % of char, and 19.88 % of gases. It can be seen that even though the product shares are similar, the distribution is entirely different. This is due to the fact that product distribution from biomass pyrolysis is strongly influenced by the content of cellulose, hemicellulose and lignin (Vassilev et al., 2010). Higher lignin share indicates higher char yield, while the cellulose component promotes the yield of liquids and gases. Biomass is also characterised by a higher share of fixed carbon and ash content which favours char yields (Milani and Montorsi, 2018), while plastics have a high share of volatiles (>90 %) which promotes liquid yield. Therefore, if there is a synergy in the co-pyrolysis process, it is expected that obtained values from investigated mixtures will be between these obtained from individual pyrolysis.

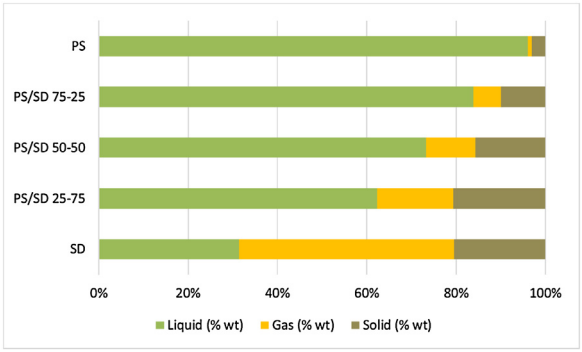

Fig. 3. Product yield from individual pyrolysis and PS/SD blends co-pyrolysis.

From the co-pyrolysis, the highest liquid (oil) yield (83.86 %) is noticed for the mixture where PS is dominant in the blend, while the lowest yield (62.32 %) is obtained for the blend where SD is a major component. The yield of gas and solid fractions shows the opposite behaviour, and the highest yield is noticed for the mix-

ture with 75 % of SD where the yields are 17.01 % and 20.66 %, respectively. Mixture with an equal share of PS and sawdust, yield the values which are in between of these obtained from the co-pyrolysis of blends where a dominant component is either PS or SD. In Fig. 3 it is interesting to notice how the increment of PS content promotes the yield of liquids, simultaneously decreasing the share of gas and solid products, which suggest that synergistic effect is achieved in the process (Anuar Sharuddin et al., 2016). Even more, it should be emphasised that the addition of only 25 % of PS to the mixture, completely changed the product distribution compared to the individual sawdust pyrolysis. Even though the gases are the main products of sawdust pyrolysis, 25 % of PS in fuel mixture doubled the liquid yield entirely on the expense of gas generation. The share of char is not significantly affected, which is expected since the PS decomposition yields an almost negligible amount of solid residue due to high volatile content. This suggests that PS could be effectively used with different types of biomass to improve the oil yield which is especially important for the pyrolysis of sawdust mixtures, where often precise composition and content of major biomass components is not known. More on this will be discussed in the following subsection.

3.2.2. Synergistic effect

To determine the level of synergy, experimental results are compared to the theoretical values. Theoretical values (Y_{cal}) are calculated using the following Eq. (1):

$$Ycal = WSDYSD + WPSYPS \quad (1)$$

Where $W_{SD/PS}$ stands for proportions of each component in investigated mixtures, and $Y_{SD/PS}$ presents the values obtained from the individual pyrolysis (Ephraim et al., 2018). Existence and level of synergy are determined by the difference between experimentally obtained values and calculated ones using Eq. (2). According to H. Hassan et al. (2016a) (2016b), it can be stated that synergy exists when the difference between the experimental and calculated values are positive.

$$\Delta Y = Yexp\text{-}Ycal \quad (2)$$

Fig. 4 presents the charts with the calculated theoretical and experimentally obtained values for liquid (a), gas (b) and char (c) products. As can be seen, the most significant synergy is achieved for a liquid fraction (Fig. 4a), especially for the mixture with 25 % of PS. As the content of PS increase, synergy is still evident but with lower intensity, which is expected since the experimental values are approaching theoretical (Sanahuja-Parejo et al., 2019). The same is noticed for the char yield (Fig. 4b), where the mixture with the 25 % of PS shows the highest synergy effect, which decreases as the PS content increase. Nevertheless, strong negative synergy is observed for gas yield (Fig. 4c). This indicates that interaction between PS and SD promotes the yield of oil and char, on the expense of gas generation. It is interesting to notice that in literature, positive values for char are almost always reported (Abnisa and Wan Daud, 2014), while the synergy for oil and gas yield strongly depends on feedstock selection and process conditions. High heating rates, temperatures and longer residence time will promote the formation of gaseous compounds (Ephraim et al., 2018) as the products of secondary oil cracking (Akancha et al., 2019; Reshad et al., 2019).

Detailed values regarding each fraction yield from investigated blends are presented in Table 3 alongside the calculated level of synergy. For the pyrolysis of pure PS and SD theoretical values are equal to experimental (Exp.), since they represent the maximum yield of products for investigated samples. Therefore, the level of synergy ΔY is equal to zero.

Comparing to the investigation carried out by Ephraim et al. (2018), where poplar wood was co-pyrolysed with PS at 750 °C, a higher level of synergy is achieved for all investigated mixtures. In addition, Ephraim et al. (2018) noticed negative synergy for oil yield and positive synergy for gas yield, probably due to the higher reactor temperature. Even though strong negative synergy is visible for gas yield in this study, the total yield is still higher compared to the mentioned study. Since the different type of biomass feedstock is used in these two studies, this indicates that biomass feedstock plays a dominant role for product distribution, while PS is responsible for maximizing the oil yield on the expense of gaseous and solid fraction (Al-Salem, 2018). The investigation carried out by Reshad et al. (2019), where rubber seed cake was investigated with waste PS at 500 °C presents results that confirm the above-stated statement.

3.2.3. Liquid products characterisation

The liquid fraction obtained from co-pyrolysis is the most abundant, and the most valuable in terms of potential commercial utilisation (Paradela et al., 2009). Firstly, pyrolysis was performed solely for SD to obtain a liquid fraction that represents a referent case of bio-oil. Altogether, obtained bio-oil is composed of 90 different organic compounds, while only 43 of them are present with a notable share of at least 1 %, which was chosen as a threshold for further analysis. Approximately 20 % of the identified compounds are disregarded from further analysis. Selected compounds represent about 80 % of the bio-oil composition, and most of them can be considered oxygenated with at least one oxygen atom. Only non-oxygenated compounds found are styrene, toluene and polycyclic aromatic hydrocarbons (PAHs) which combined accounts for about 13 % of oil composition. Compounds with the highest yield are listed in Table 4. In general, bio-oil has a heterogeneous structure with a wide variety of identified compounds where most of them are present in traces or with meagre share (Guo et al., 2015).

On the other hand, oil derived from the PS pyrolysis is composed mostly of aromatic and polycyclic aromatic hydrocarbons. Even though altogether 89 various organic compounds are identified, only 20 of them are represented in notable share (>0.50 %), and they account for ~90 % of all identified compounds. Moreover, the nine selected compounds which are given in Table 5. account for about 82 % of all identified compounds which implies that liquid fraction derived from the pyrolysis of PS have more homogenous composition then bio-oil, even though the total number of identified compounds is similar. Most probably, this is due to simple PS composition which primarily decomposes on monomer styrene, compared to complex biomass decomposition which undergoes through various dehydration, decarbonylating, and decarboxylation reactions (Codignole Luz et al., 2018). Results obtained for PS oil are similar to those found in the literature regarding the yield of major compounds (Budsaereechai et al., 2019). Nevertheless, the lower yield is noticed for ethylbenzene, while there is a complete absence of toluene. Moreover, Cyclohexane, 1,3,5-triphenyl-, which is classified as PS impurity, is identified with a significant share, which was not previously reported in the literature. In general, a relatively lower share of monomer styrene, and a pronouncedly higher share of styrene derivatives, suggests that longer retention time and lower heating rates promote the secondary cracking reactions and formation of various aromatic hydrocarbons (Miandad et al., 2017).

Chemical characterisation of derived oil from the co-pyrolysis of PS/SD blends is one of the main objectives of this study. For all investigated blends, it was noticed the increase of the total number of derived compounds from 90, for individual pyrolysis, to more than 120 from co-pyrolysis. Detailed analysis showed that the dominant compound found in derived oils are those which are also found in PS oil, indicating that plastic material is dominant for the yield of liquid products (Al-Salem, 2019). Table 6 presents the yield of selected compounds and their respective share. It is interesting to observe

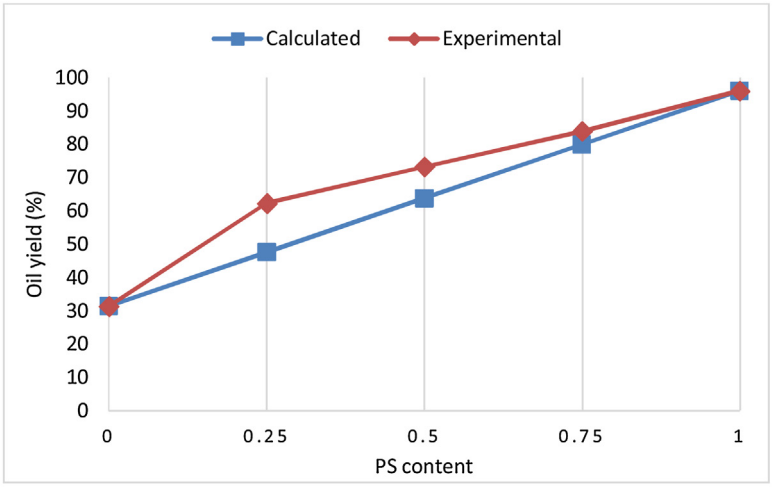

a) oil yield

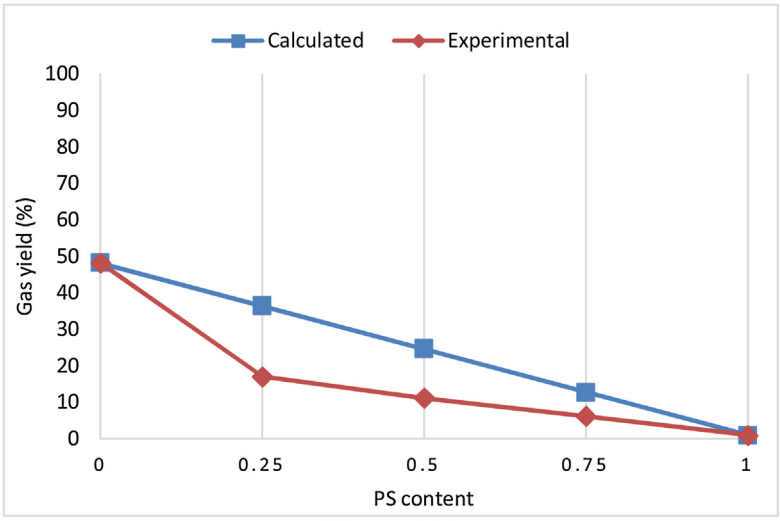

b) gas yield

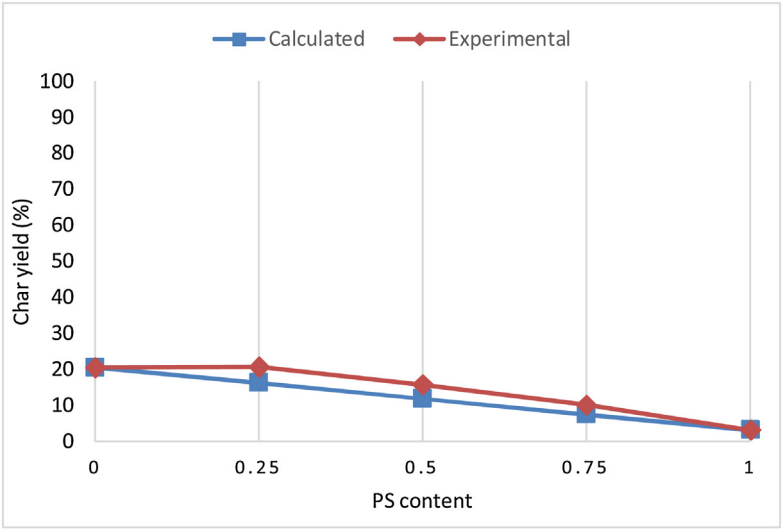

c) char yield

Fig. 4. Evaluation of synergistic effect for each fraction yield.

that the increment of PS in the mixture decrease the yield of styrene and promote the yield of toluene, suggesting that SD influences the secondary cracking of monomer styrene. This is also confirmed by the high yield of monomer styrene (27.38 %) for mixture with 25 % of PS. Moreover, it is interesting to compare the yield of Naphthalene, 1,2,3,4-tetrahydro-2-phenyl- identified in bio-oil, as well as the PS

Table 3
Theoretical and experimental values for product yield and calculated level of synergy.

Sample	Liquid fraction			Gas fraction			Solid fraction		
	Theoretical	Exp.	ΔY	Theoretical	Exp.	ΔY	Theoretical	Exp.	ΔY
PS	96.02	96.02	0	0.92	0.92	0	3.06	3.06	0
Sawdust	31.39	31.39	0	48.10	48.10	0	20.51	20.51	0
PS/SD 25–75%	47.55	62.32	14.77	36.31	17.01	−19.29	16.15	20.66	4.52
PS/SD 50–50%	63.71	73.22	9.52	24.51	11.08	−13.43	11.78	15.70	3.91
PS/SD 75–25%	79.86	83.86	4.00	12.71	6.10	−6.61	7.42	10.03	2.61

Table 4
Most significant compounds identified in bio-oil.

Compound	Share [%]
1,6-Anhydro-b-D-glucopyranose (levoglucosan)	2.09
2,6-Dimethoxytoluene	2.14
2-Methoxyphenol	2.74
2-Pentanone	2.59
4-Methoxyphenol	2.39
Acetophenone	5.86
Dodecanoic acid	2.19
Furfural	5.81
Naphthalene	1.85
Naphthalene, 1,2,3,4-tetrahydro-2-phenyl-	6.82
Propanone	2.05
Styrene	1.90
Toluene	2.93
Vanillin	2.92
Sum of selected compounds	**42.39**
Compounds with a share below 1.0 %	**37.43**

Table 5
Most significant compounds identified in PS oil.

Compound	Share [%]
α-Methylstilbene	7.11
α-Methylstyrene	10.95
1-(4-Methylphenyl)-4-phenylbuta-1,3-diene	1.66
1,2-Diphenylcyclopropane	3.52
1,3,5,7-Cyclooctatetraene	4.57
Benzene, 1,1′-(1,3-propanediyl) bis-	6.24
Cyclohexane, 1,3,5-triphenyl-	17.71
Ethylbenzene	4.84
Naphthalene, 1,2,3,4-tetrahydro-2-phenyl-	10.77
Styrene	16.47
Sum of selected compounds	**82.19**
Compounds with a share below 0.5 %	**17.81**

oil. Mixture with 25 % of PS expressed a considerable reduction in yield of this PAH compared to individual pyrolysis. Further increment of PS content promotes the higher yield of this compound, with the maximum share of 8.73 % for a mixture where PS is dominant, which is still lower compared to the individual pyrolysis of PS. Since there is no obvious increase in the yield of other PAHs, it can be stated that SD hinders the formation of these harmful compounds, as a positive outcome of feedstock interaction. In addition, the increase of PS in the mixture decreases the yield of Cyclohexane, 1,3,5-triphenyl-. This phenomenon is interesting since the Cyclohexane, 1,3,5-triphenyl- is PS derivative product; thus, it is expected that its yield would increase with the increment of PS content. It is also interesting to observe the yield of toluene which increases with the increment of plastic content, even though this compound was not found in PS oil. Toluene is a product of secondary cracking of styrene monomer, which is obviously encouraged by the feedstock interaction in the co-pyrolysis (Miandad et al., 2016). Finally, it should be noted that increment of PS in fuel mixtures promotes the formation of benzene-based compounds, which could constrain further utilisation of obtained oils since such compounds are classified as carcinogenic.

Table 6
The yield of selected compounds in investigated mixtures.

Compound	PS/SD 25–75% Share [%]	PS/SD 50–50% Share [%]	PS/SD 75–25% Share [%]
α-Methylstyrene	4.82	7.69	8.33
1,2-Diphenylcyclopropane	2.24	3.23	4.04
Benzene, 1,1′-(1,3-propanediyl) bis-	3.65	6.46	7.98
benzene, 1,1′,1″-[5-methyl-1-pentene-1,3,5-triyl] tris-	5.10	0.90	0.61
Cyclohexane, 1,3,5-triphenyl-	19.97	8.99	11.70
Cyclopentane, methyl-	3.44	1.18	0.73
Ethylbenzene	7.25	11.28	8.76
Naphthalene, 1,2,3,4-tetrahydro-2-phenyl-	5.95	7.32	8.73
Styrene	27.38	23.40	15.21
Toluene	1.12	5.70	8.15
Sum of selected compounds	**80.91**	**76.15**	**74.25**
Compounds with share below 0.5 %	**19.09**	**23.85**	**25.75**

One of the most significant drawbacks for the bio-oil utilisation is the high share of oxygenated compounds, which results with reduced heating value and poor thermal stability (Forbes et al.,

Table 7
Yield of oxygenated and potentially harmful compounds.

Investigated sampleOrganic group	Bio-oil[%]	PS oil [%]	PS/SD 25–75% [%]	PS/SD 50–50% [%]	PS/SD 75–25% [%]
Phenols	12.25		3.72	1.73	1.13
Ketones	16.16		<1.0 %	<1.0 %	<1.0 %
PAHs/Furans	11.86	12.14	6.86	9.43	10.26
Alcohols	4.21				
Ethers/Acids	9.27				
Aldehydes	9.62				
Sugars	3.21				
Benzene-based	<1	12.67	13.48	16.24	16.62
C-content					
C_4-C_{12}	69.10	37.98	45.53	51.57	42.52
C_8-C_{16}	43.00	66.07	54.25	64.38	57.31
C_{24}		17.71	25.07	9.89	12.31

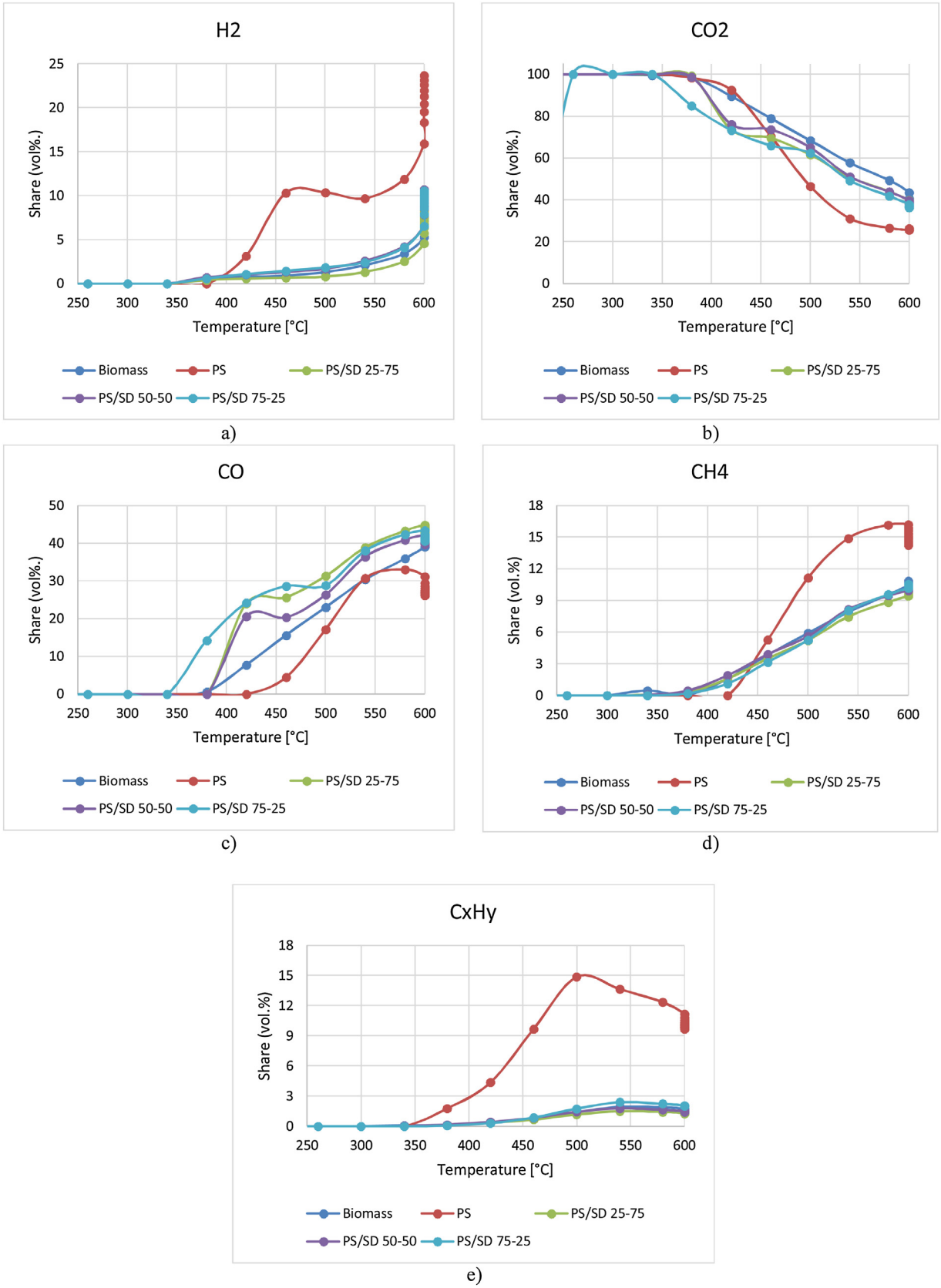

Fig. 5. Distribution of gaseous products for all investigated samples.

2014). Introduction of PS is expected to reduce the yield of such compounds and instead, promote the formation of hydrocarbons. Table 7 summarised selected organic groups and compounds which are found in investigated oils. An additional comparison is carried out regarding the C-content range of identified organic compounds. The division is made between gasoline-like (C_4-C_{12}) and jet-fuel (C_8-C_{16}) compounds (Akancha et al., 2019).

Obtained bio-oil has a significant number of oxygenated compounds like phenols, ketones, aldehydes, ethers, acids, and a notable amount of sugars and alcohols. Besides, a pronouncedly high share of PAHs and furans is identified, slightly below 12 %. In general, bio-oil is composed of gasoline range compounds C_{4-12} (69.10 %), while major compounds found in PS oil are high aromatic hydrocarbons (79.33 %), which would fit jet fuel requirements regarding the C-content. Even though aromatics have great calorific value, their combustion releases a large amount of smoke and harmful species, raising severe environmental and health concerns. For this reason, their share in fuel composition is restricted to 40 % for gasoline fuels, 25 % in the case of JP-4, and only 5 % for JP-7 fuels (Peng et al., 2017). Surprisingly, almost the same share of PAHs (12.14 %) is identified in PS oil and bio-oil. Analysis of oil obtained from co-pyrolysis express expected behaviour in terms of decreasing the oxygen-containing compounds and increment of hydrocarbon content (Sanahuja-Parejo et al., 2019). Nevertheless, only 25 % of PS in the blend, almost completely reduce the content of oxygenated compounds, simultaneously increasing the share of higher hydrocarbons. Of all identified organic groups in bio-oil, only Phenols remained with a notable yield of 3.72 %, while the rest are present in traces. In addition, blend with 25 % of PS showed the most significant reduction in terms of PAHs content, from almost 12 % for individual pyrolysis to 6.86 %. The yield of PAHs is especially interesting. While the individual pyrolysis yields a high share of such compounds, investigated mixtures expressed notable reduction, especially for these with lower plastic content. Increment of PS content in investigated blend leads to further decrease of oxygenated species; nevertheless, higher generation of PAHs is noticed. This indicates that the optimal mixture ratio might promote the interaction between feedstock, which hinders the cumulative yield of PAHs found in oil from individual pyrolysis (Zhou et al., 2014).

Majority of identified compounds in bio-oil are in the range of gasoline-like compounds regarding the C-content, while PS oil is mostly composed of higher aromatics. Influence of the plastic content on the selectivity of produced compounds from investigated mixtures is evident. An only small portion of plastic in fuel mixture promotes the formation of compounds with higher carbon content reaching the maximum value for mixture with an equal share of both fractions. As the content of plastic increase in the mixture, homogeneity of oil is slightly reduced. Most probably, this is due to thermal decomposition of monomer styrene on toluene, various benzene-based compounds and PAHs (E. B. Hassan et al., 2016a;, 2016b). This statement is in agreement with Table 6, where a notable reduction of styrene share is identified as the plastic content increase. For this reason, in Table 7, there can be seen the reduction of the share of identified compounds for mixture with 75 % of PS regarding the C-content. It should be emphasised that there is no actual decrease of such compounds in obtained oil, but the oil has a more heterogeneous structure with a significant number of species presented in traces or with a yield below 0.5 %.

3.2.4. Gas product characterisation

The gaseous product can be considered as the by-products of pyrolysis, especially when the process is carried out on mild temperatures below 700 °C, after which gasification takes place (Widjaya et al., 2018). Therefore, characterisation of a gaseous fraction is interesting in terms to evaluate the potential of obtained syngas which could be utilised as an energy source for pyrolysis.

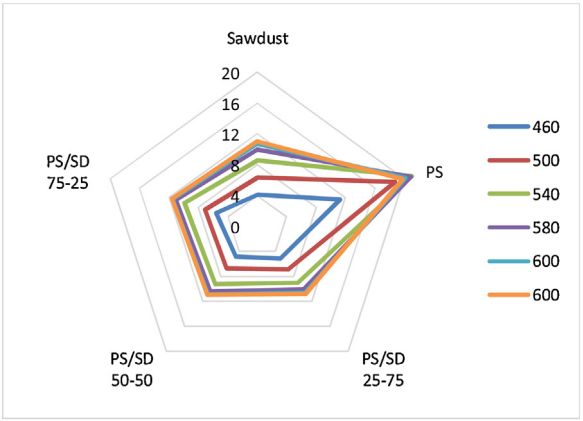

Fig. 6. Calculated High heating value [MJ/m3] for obtained syngas compositions.

From Fig. 4b, it is visible that for gas fraction synergistic effect is negative, and gas yield is significantly lower compared to the theoretical yield. Dominant compounds for all investigated samples are carbon dioxide (CO_2) and carbon monoxide (CO). Valuable compounds preferred in syngas (Janković et al., 2020), like methane (CH_4) and hydrogen (H_2), are present with significantly lower share, while the share of higher hydrocarbons (C_xH_y) is almost negligible. The yield of H_2O is avoided since the sawdust was dried at 40 °C before being introduced to experiments. Fig. 5 presents the distribution of obtained syngas components within the temperature dependence. Highest generation of valuable gases like H_2, CH_4, and C_xH_y is observed for pyrolysis of pure PS, which also express the lowest yield of CO_2 and CO. In general, syngas obtained from the co-pyrolysis of various blends have a similar composition as the gas fraction obtained from individual SD pyrolysis, which is expected since the PS, has a meagre gas yield. The CO_2 and CO are the predominant components of syngas obtained from SD and mixtures pyrolysis, and they account for about 80 % of volume share (Arregi et al., 2017). Remaining is equally divided between H_2 and CH_4, while the yield of higher hydrocarbons is below 2 %. As expected, temperature increment favours the yield of syngas components as a result of secondary oil cracking (Waheed et al., 2013). Even though the PS has small influence regarding the gas product yield and distribution, its influence is still visible from figure Fig. 5b) and c). Addition of PS to fuel mixture lowered the temperature where the release of CO and CO_2 is noticed, suggesting that the introduction of plastic and interaction with sawdust feedstock lowers the temperature where the decomposition mechanism starts. This is a piece of valuable information for process optimisation, indicating that retention time and final temperature should be carefully selected to favour oil yield. It is interesting to notice that for all samples retaining the temperature at 600 °C, promotes the formation of H_2 on the expense of CH_4 and higher hydrocarbons. This implies that longer retention time supports the secondary cracking of hydrocarbons to favour the yield of hydrogen, already reported by (Singh et al., 2019a;, 2019b).

$$\mathrm{HHV} = \sum \frac{\mathrm{HHVi} * \varphi \mathrm{i}}{100} [\mathrm{MJ/m3}] \tag{3}$$

For obtained syngas composition, high heating values are calculated using Eq. 3, where HHV_i presents the higher heating value of each gas component in MJ/m^3, and φ_i stands for volume share (vol.%) of respective component (Ephraim et al., 2018).

Higher heating values (HHV) are calculated for all investigated temperatures, and the results are given in Fig. 6. Highest heating value is ~11.5 MJ/m^3, calculated for the blend with PS/SD 75–25%. In general, HHVs at 600 °C are between 10–11 MJ/m^3, while only

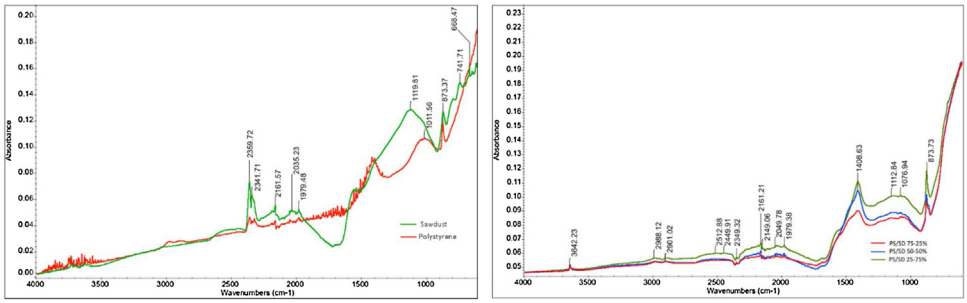

Fig. 7. FTIR spectra of char from a) individual pyrolysis, and b) respective blends.

PS exhibits values above 20 MJ/m^3; nevertheless, its yield is almost negligible (<1 %).

3.2.5. Char characterisation

Char characterisation was done by FTIR analysis. Fig. 7 shows the FTIR spectra for individual samples a), and respective fuel blends b). Intensive stretching in the range above 3500 cm^{-1} for PS is due to the high aromatics content. At 2341 and 2359 cm^{-1} it is observed intense stretch of the carbonyl group (C═O) for sawdust, while the stretching in the range between 2035-2161 cm^{-1} corresponds to C—O group. Intensive peaks are noticed for PS between 1400−1700 cm^{-1}, which should correspond to the skeletal aromatic vibrations (C–H). Below 1000 cm^{-1}, C–H stretching of aromatics is notified for both samples (Sogancioglu et al., 2017).

FTIR spectra obtained from co-pyrolysis of fuel blends express excellent matching. Stretching at 3643 cm^{-1} corresponds to the stretching of both alcohols and aromatics groups. Small peaks below 3000 cm^{-1} probably come from stretching in phenols and alcohols which are biomass products. The intensive peak is observed at 2348 cm^{-1}, which represents the stretching of carbonyl group from sawdust and evolution of CO_2. At around 2161 cm^{-1} stretching of C—O is noticed which corresponds to the evolution of CO. The most intensive peak is observed at 1408 cm^{-1} for all blends, especially those with higher SD content which implies cellulose deformation. Once again, a sharp peak is noticed for 873 cm^{-1} which presents the styrene compound. Below 800 cm^{-1} stretching of higher hydrocarbons and C–H group is observed for all blends.

4. Conclusion

Co-pyrolysis of biomass sawdust and PS was carried out in a fixed-bed reactor with an aim to produce oil fraction and investigate the influence of plastic content on product quality. Results showed that PS significantly improve the yield of liquid fraction in both terms, quantity and quality. Only 25 % of PS in mixture doubled the yield of bio-oil from 31 to 62 %, simultaneously reducing the yield of oxygenated compounds characteristics for conventional bio-oils and promoting the formation of valuable aromatic hydrocarbons. Additionally, co-pyrolysis reduced the yield of harmful PAHs, especially visible for mixture with 25 % of PS. Further increment of PS in the fuel mixture, reduced the yield of oxygenated compounds, nevertheless higher generation of unwanted benzene-based compounds and toxic PAHs is noticed as well. This is most probably result of a secondary cracking of monomer styrene which was obviously promoted by the interaction with biomass feedstock. Moreover, this resulted with the reduced homogeneity of obtained oil, since it was noted a significant increase in yield of various compounds presented in traces or with share below 0.5 %. This information calls for cautious approach and more in-depth analysis regarding the optimal plastic content in fuel mixture.

Even though aromatic hydrocarbons have great calorific value, their share in commercial fuel is restricted to a maximum 40 % since their combustion release smoke and toxic species. This indicates that PS might be a great solution to improve the oil yield and prevail the need for aromatic selective catalyst, but its share in mixtures should be limited. Since 25 % of PS in fuel mixtures greatly improved the bio-oils properties, and further increment leads to several unwanted side-effects, this share could be considered optimal. For further work, it might be interesting to introduce the polypropylene (PP) in fuel mixtures with sawdust and PS. This is due to the fact that PP degrades in similar temperature range as PS, while mainly decompose on aliphatic hydrocarbons which are more appropriate in fuel mixtures then aromatics. Therefore, co-pyrolysis of sawdust, PS and PP could yield an optimal share of hydrocarbons that could meet fuel standards and specifications. Besides, fast pyrolysis with lower final temperature, shorter retention time and usage of appropriate catalyst could additionally improve the yield and properties of derived bio-oils, reducing the need for after-treatment methods and broadening application possibilities.

Declaration of Competing Interest

The authors declare that they have no known competing financial interests or personal relationships that could have appeared to influence the work reported in this paper.

Acknowledgement

This work was supported by the research projects of the Ministry of Education, Youth and Sport of the Czech Republic: “OP RDE grant number CZ.02.1.01/0.0/0.0/16_019/0000753 Research centre for low-carbon energy technologies”.

The co-authors Dr. Hrvoje Mikulčić and Prof. Xuebin Wang greatly acknowledge the financial support of the National Natural Science Foundation of China (Nos. 51676157 and 51761125012), and the Post-doctoral international exchange program by the China Postdoctoral Foundation.

References

Aberilla, J.M., Gallego-Schmid, A., Azapagic, A., 2019. Environmental sustainability of small-scale biomass power technologies for agricultural communities in developing countries. Renew. Energy 141, 493–506, http://dx.doi.org/10.1016/j.renene.2019.04.036.

Abnisa, F., Wan Daud, W.M.A., 2014. A review on co-pyrolysis of biomass: an optional technique to obtain a high-grade pyrolysis oil. Energy Convers. Manage. 87, 71–85, http://dx.doi.org/10.1016/j.enconman.2014.07.007.

Akancha, Kumari, Singh, N., R.K, 2019. Co-pyrolysis of waste polypropylene and rice bran wax– production of biofuel and its characterization. J. Energy Inst. 92, 933–946, http://dx.doi.org/10.1016/j.joei.2018.07.011.

Al-Salem, S.M., 2018. Feedstock and optimal operation for plastics to fuel conversion in pyrolysis. In: Plastics to Energy: fuel, Chemicals, and Sustainability Implications. Elsevier Inc., http://dx.doi.org/10.1016/B978-0-12-813140-4.00005-4.

Al-Salem, S.M., 2019. Thermal pyrolysis of high density polyethylene (HDPE) in a novel fixed bed reactor system for the production of high value gasoline range hydrocarbons (HC). Process Saf. Environ. Prot. 127, 171–179, http://dx.doi.org/10.1016/j.psep.2019.05.008.

Anuar Sharuddin, S.D., Abnisa, F., Wan Daud, W.M.A., Aroua, M.K., 2016. A review on pyrolysis of plastic wastes. Energy Convers. Manage. 115, 308–326, http://dx.doi.org/10.1016/j.enconman.2016.02.037.

Arregi, A., Amutio, M., Lopez, G., Artetxe, M., Alvarez, J., Bilbao, J., Olazar, M., 2017. Hydrogen-rich gas production by continuous pyrolysis and in-line catalytic reforming of pine wood waste and HDPE mixtures. Energy Convers. Manage. 136, 192–201, http://dx.doi.org/10.1016/j.enconman.2017.01.008.

Bedoić, R., Čuček, L., Ćosić, B., Krajnc, D., Smoljanić, G., Kravanja, Z., Ljubas, D., Pukšec, T., Duić, N., 2019. Green biomass to biogas – a study on anaerobic digestion of residue grass. J. Clean. Prod. 213, 700–709, http://dx.doi.org/10.1016/j.jclepro.2018.12.224.

Budsaereechai, S., Hunt, A.J., Ngernyen, Y., 2019. Catalytic pyrolysis of plastic waste for the production of liquid fuels for engines. RSC Adv. 9, 5844–5857, http://dx.doi.org/10.1039/c8ra10058f.

Chattopadhyay, J., Pathak, T.S., Srivastava, R., Singh, A.C., 2016. Catalytic co-pyrolysis of paper biomass and plastic mixtures (HDPE (high density polyethylene), PP (polypropylene) and PET (polyethylene terephthalate)) and product analysis. Energy 103, 513–521, http://dx.doi.org/10.1016/j.energy.2016.03.015.

Chiong, M.C., Chong, C.T., Ng, J.H., Lam, S.S., Tran, M.V., Chong, W.W.F., Mohd Jaafar, M.N., Valera-Medina, A., 2018. Liquid biofuels production and emissions performance in gas turbines: a review. Energy Convers. Manage. 173, 640–658, http://dx.doi.org/10.1016/j.enconman.2018.07.082.

Codignole Luz, F., Cordiner, S., Manni, A., Mulone, V., Rocco, V., 2018. Biomass fast pyrolysis in screw reactors: prediction of spent coffee grounds bio-oil production through a monodimensional model. Energy Convers. Manage. 168, 98–106, http://dx.doi.org/10.1016/j.enconman.2018.04.104.

Ephraim, A., Pham Minh, D., Lebonnois, D., Peregrina, C., Sharrock, P., Nzihou, A., 2018. Co-pyrolysis of wood and plastics: Influence of plastic type and content on product yield, gas composition and quality. Fuel 231, 110–117, http://dx.doi.org/10.1016/j.fuel.2018.04.140.

Foley, A., Olabi, A.G., 2017. Renewable energy technology developments, trends and policy implications that can underpin the drive for global climate change. Renew. Sustain. Energy Rev. 68, 1112–1114, http://dx.doi.org/10.1016/j.rser.2016.12.065.

Forbes, E.G.A., Easson, D.L., Lyons, G.A., McRoberts, W.C., 2014. Physico-chemical characteristics of eight different biomass fuels and comparison of combustion and emission results in a small scale multi-fuel boiler. Energy Convers. Manage. 87, 1162–1169, http://dx.doi.org/10.1016/j.enconman.2014.06.063.

Guo, M., Song, W., Buhain, J., 2015. Bioenergy and biofuels: History, status, and perspective. Renewable Sustainable Energy Rev. 42, 712–725, http://dx.doi.org/10.1016/j.rser.2014.10.013.

Gvero, P.M., Papuga, S., Mujanić, I., Vasković, S., 2016. Pyrolysis as a key process in biomass combustion and thermochemical conversion. Therm. Sci. 20, 1209–1222, http://dx.doi.org/10.2298/TSCI151129154G.

Hassan, E.B., Elsayed, I., Eseyin, A., 2016a. Production high yields of aromatic hydrocarbons through catalytic fast pyrolysis of torrefied wood and polystyrene. Fuel 174, 317–324, http://dx.doi.org/10.1016/j.fuel.2016.02.031.

Hassan, H., Lim, J.K., Hameed, B.H., 2016b. Recent progress on biomass co-pyrolysis conversion into high-quality bio-oil. Bioresour. Technol. 221, 645–655, http://dx.doi.org/10.1016/j.biortech.2016.09.026.

Hlavsová, Adéla, Corsaro, Agnieszka, Raclavská, Helena, Juchelková, Dagmar, Hana Škrobánková, J.F., 2014. Syngas Production from Pyrolysis of Nine Composts Obtained from Nonhybrid and Hybrid Perennial Grasses. Bioenergy its Environ. Impacts 2014, 11, http://dx.doi.org/10.1155/2014/723092.

Janković, B., Manić, N., Stojiljković, D., 2020. The gaseous products characterization of the pyrolysis process of various agricultural residues using TGA–DSC–MS techniques. J. Therm. Anal. Calorim. 139, 3091–3106, http://dx.doi.org/10.1007/s10973-019-08733-4.

Kwon, E.E., Oh, J.I., Kim, K.H., 2015. Polycyclic aromatic hydrocarbons (PAHs) and volatile organic compounds (VOCs) mitigation in the pyrolysis process of waste tires using CO<inf>2</inf> as a reaction medium. J. Environ. Manage. 160, 306–311, http://dx.doi.org/10.1016/j.jenvman.2015.06.033.

Miandad, R., Barakat, M.A., Aburiazaiza, A.S., Rehan, M., Nizami, A.S., 2016. Catalytic pyrolysis of plastic waste: a review. Process Saf. Environ. Prot. 102, 822–838, http://dx.doi.org/10.1016/j.psep.2016.06.022.

Miandad, R., Barakat, M.A., Aburiazaiza, A.S., Rehan, M., Ismail, I.M.I., Nizami, A.S., 2017. Effect of plastic waste types on pyrolysis liquid oil. Int. Biodeterior. Biodegrad. 119, 239–252, http://dx.doi.org/10.1016/j.ibiod.2016.09.017.

Mikulčić, H., Klemeš, J.J., Vujanović, M., Urbaniec, K., Duić, N., 2016. Reducing greenhouse gasses emissions by fostering the deployment of alternative raw materials and energy sources in the cleaner cement manufacturing process. J. Clean. Prod. 136, 119–132, http://dx.doi.org/10.1016/j.jclepro.2016.04.145.

Mikulčić, H., Jin, Q., Stančin, H., Wang, X., Li, S., Tan, H., Duić, N., 2019. Thermogravimetric analysis investigation of polyurethane plastic thermal properties under different atmospheric conditions. J. Sustain. Dev. Energy, Water Environ. Syst. 7, 355–367, http://dx.doi.org/10.13044/j.sdewes.d6.0254.

Milani, M., Montorsi, L., 2018. Energy recovery of the biomass from livestock farms in italy: the case of Modena province. J. Sustain. Dev. Energy, Water Environ. Syst. 6, 464–480, http://dx.doi.org/10.13044/j.sdewes.d6.0199.

Miskolczi, N., Nagy, R., 2012. Hydrocarbons obtained by waste plastic pyrolysis: comparative analysis of decomposition described by different kinetic models. Fuel Process. Technol. 104, 96–104, http://dx.doi.org/10.1016/j.fuproc.2012.04.031.

Miskolczi, N., Juzsakova, T., Sója, J., 2019. Preparation and application of metal loaded ZSM-5 and y-zeolite catalysts for thermo-catalytic pyrolysis of real end of life vehicle plastics waste. J. Energy Inst. 92, 118–127, http://dx.doi.org/10.1016/j.joei.2017.10.017.

Özsin, G., Pütün, A.E., 2018. A comparative study on co-pyrolysis of lignocellulosic biomass with polyethylene terephthalate, polystyrene, and polyvinyl chloride: synergistic effects and product characteristics. J. Clean. Prod. 205, 1127–1138, http://dx.doi.org/10.1016/j.jclepro.2018.09.134.

Paradela, F., Pinto, F., Gulyurtlu, I., Cabrita, I., Lapa, N., 2009. Study of the co-pyrolysis of biomass and plastic wastes. Clean Technol. Environ. Policy 11, 115–122, http://dx.doi.org/10.1007/s10098-008-0176-1.

Parihar, M.F., Kamil, M., Goyal, H.B., Gupta, A.K., Bhatnagar, A.K., 2007. An experimental study on pyrolysis of biomass. Process Saf. Environ. Prot. 85, 458–465, http://dx.doi.org/10.1205/psep07035.

Peng, J., Hu, M., Du, Z., Wang, Y., Zheng, J., Zhang, W., Yang, Y., Qin, Y., Zheng, R., Xiao, Y., Wu, Y., Lu, S., Wu, Z., Guo, S., Mao, H., Shuai, S., 2017. Gasoline aromatic: a critical determinant of urban secondary organic aerosol formation. Atmos. Chem. Phys. Discuss., 1–20, http://dx.doi.org/10.5194/acp-2017-254.

PlasticsEurope; EPRO, 2018 2018. Plastics – the Facts. Plast. – Facts., pp. 38.

Reshad, A.S., Tiwari, P., Goud, V.V., 2019. Thermal and co-pyrolysis of rubber seed cake with waste polystyrene for bio-oil production. J. Anal. Appl. Pyrolysis 139, 333–343, http://dx.doi.org/10.1016/j.jaap.2019.03.010.

Ridjan, I., Mathiesen, B.V., Connolly, D., 2016. Terminology used for renewable liquid and gaseous fuels based on the conversion of electricity: a review. J. Clean. Prod. 112, 3709–3720, http://dx.doi.org/10.1016/j.jclepro.2015.05.117.

Rostek, E., Biernat, K., 2013. Thermogravimetry as a research method in the transformationprocesses of waste rubber and plastic products for energy carriers (WtE and WtL processes). J. Sustain. Dev. Energy, Water Environ. Syst. 1, 163–171, http://dx.doi.org/10.13044/j.sdewes.2013.01.0012.

Sanahuja-Parejo, O., Veses, A., Navarro, M.V., López, J.M., Murillo, R., Callén, M.S., García, T., 2019. Drop-in biofuels from the co-pyrolysis of grape seeds and polystyrene. Chem. Eng. J. 377, http://dx.doi.org/10.1016/j.cej.2018.10.183.

Singh, R.K., Ruj, B., Sadhukhan, A.K., Gupta, P., 2019a. Thermal degradation of waste plastics under non-sweeping atmosphere: part 1: effect of temperature, product optimization, and degradation mechanism. J. Environ. Manage. 239, 395–406, http://dx.doi.org/10.1016/j.jenvman.2019.03.067.

Singh, R.K., Ruj, B., Sadhukhan, A.K., Gupta, P., 2019b. Impact of fast and slow pyrolysis on the degradation of mixed plastic waste: product yield analysis and their characterization. J. Energy Inst. 92, 1647–1657, http://dx.doi.org/10.1016/j.joei.2019.01.009.

Sogancioglu, M., Yel, E., Ahmetli, G., 2017. Investigation of the effect of polystyrene (PS) waste washing process and pyrolysis temperature on (PS) pyrolysis product quality. In: Energy Procedia. Elsevier Ltd, pp. 189–194, http://dx.doi.org/10.1016/j.egypro.2017.07.029.

Uzoejinwa, B.B., He, X., Wang, S., El-Fatah Abomohra, A., Hu, Y., Wang, Q., 2018. Co-pyrolysis of biomass and waste plastics as a thermochemical conversion technology for high-grade biofuel production: recent progress and future directions elsewhere worldwide. Energy Convers. Manage. 163, 468–492, http://dx.doi.org/10.1016/j.enconman.2018.02.004.

Van Nguyen, Q., Choi, Y.S., Choi, S.K., Jeong, Y.W., Kwon, Y.S., 2019. Improvement of bio-crude oil properties via co-pyrolysis of pine sawdust and waste polystyrene foam. J. Environ. Manage. 237, 24–29, http://dx.doi.org/10.1016/j.jenvman.2019.02.039.

Vassilev, S.V., Baxter, D., Andersen, L.K., Vassileva, C.G., 2010. An overview of the chemical composition of biomass. Fuel 89, 913–933, http://dx.doi.org/10.1016/j.fuel.2009.10.022.

Waheed, Q.M.K., Nahil, M.A., Williams, P.T., 2013. Pyrolysis of waste biomass: investigation of fast pyrolysis and slow pyrolysis process conditions on product yield and gas composition. J. Energy Inst. 86, 233–241, http://dx.doi.org/10.1179/1743967113Z.00000000067.

Widjaya, E.R., Chen, G., Bowtell, L., Hills, C., 2018. Gasification of non-woody biomass: a literature review. Renew. Sustain. Energy Rev. 89, 184–193, http://dx.doi.org/10.1016/j.rser.2018.03.023.

Xue, J., Chellappa, T., Ceylan, S., Goldfarb, J.L., 2018. Enhancing biomass + coal Co-firing scenarios via biomass torrefaction and carbonization: case study of avocado pit biomass and Illinois No. 6 coal. Renew. Energy 122, 152–162, http://dx.doi.org/10.1016/j.renene.2018.01.066.

Yang, J., Rizkiana, J., Widayatno, W.B., Karnjanakom, S., Kaewpanha, M., Hao, X., Abudula, A., Guan, G., 2016. Fast co-pyrolysis of low density polyethylene and biomass residue for oil production. Energy Convers. Manage. 120, 422–429, http://dx.doi.org/10.1016/j.enconman.2016.05.008.

Zhang, H., Nie, J., Xiao, R., Jin, B., Dong, C., Xiao, G., 2014. Catalytic Co-pyrolysis of Biomass and Di Ff Erent Plastics (Polyethylene, Polypropylene, and Polystyrene) to Improve Hydrocarbon Yield in a Fluidized-bed Reactor.

Zhang, X., Lei, H., Chen, S., Wu, J., 2016. Catalytic co-pyrolysis of lignocellulosic biomass with polymers: a critical review. Green Chem. 18, 4145–4169, http://dx.doi.org/10.1039/c6gc00911e.

Zhou, H., Wu, C., Meng, A., Zhang, Y., Williams, P.T., 2014. Effect of interactions of biomass constituents on polycyclic aromatic hydrocarbons (PAH) formation during fast pyrolysis. J. Anal. Appl. Pyrolysis 110, 264–269, http://dx.doi.org/10.1016/j.jaap.2014.09.007.

PAPER 3

Renewable Energy 196 (2022) 1218–1228

Contents lists available at ScienceDirect

Renewable Energy

journal homepage: www.elsevier.com/locate/renene

Influence of plastic content on synergistic effect and bio-oil quality from the co-pyrolysis of waste rigid polyurethane foam and sawdust mixture

H. Stančin [a, b, *], M. Šafář [c], J. Růžičková [c], H. Mikulčić [e, a], H. Raclavská [c, d], X. Wang [e], N. Duić [a]

[a] University of Zagreb, Faculty of Mechanical Engineering and Naval Architecture, Croatia
[b] Department of Earth and Environmental Sciences, Faculty of Science and Engineering, Macquarie University, Sydney, NSW, 2109, Australia
[c] VŠB – Technical University of Ostrava, Czech Republic
[d] ENET CENTRE VSB-Technical University Ostrava, Czech Republic
[e] Department of Thermal Engineering, Xi'an Jiaotong University, Xi'an, Shaanxi, China

ARTICLE INFO

Article history:
Received 3 December 2021
Received in revised form
23 June 2022
Accepted 9 July 2022
Available online 14 July 2022

This work was presented at the 16th Conference on *Sustainable Development of Energy, Water and Environment Systems – SDEWES*, in Dubrovnik, Croatia, from 10th to 15th October 2021.

Keywords:
Co-pyrolysis
Polyurethane
Sawdust
Product analysis
Chemical composition
Utilization possibility

ABSTRACT

Current disposal of end-of-life plastics by landfilling or incineration raises serious environmental concerns, simultaneously representing an irretrievable loss of valuable resources. Especially this is evident for materials that have a complex structure, like polyurethane foams. In this work, co-pyrolysis with sawdust was carried out to analyze and evaluate the product quality for further utilization as alternative fuels. The introduction of polyurethane increased the oil yield but in a limited range since no significant difference was observed between the mixture with 25 and 75% of polyurethane content. In addition, the chemical analysis showed that small addition of polyurethane is sufficient to eliminate most of the oxygenated compounds derived from sawdust. Nevertheless, the obtained liquid products are mostly benzenamines that do not meet the criteria for fuel composition. Analysis of the synergistic effect shows that the strongest impact is visible for a small branch of plastic content where liquid yield was promoted at the expense of gas. With a further increment of plastic content, this effect fades away, except for the solid residue where remains constant. Finally, a brief analysis of the gaseous fraction showed that obtained products are preferred in syngas composition, with notable hydrogen yield as the most valuable constituent.

1. Introduction

Polyurethane foams (PU) are widely used polymers, with about 18 million tons produced in 2016, utilized for various applications in the automotive industry and as insulation or structural material for different appliances [1]. They are made in rigid, flexible, and viscoelastic forms [2]; therefore, their properties might vary significantly, greatly influencing their end-of-life treatment. Landfilling and incineration are the most used methods to deal with this problem, resulting in the inevitable loss of valuable resources and raising environmental issues. Simon et al. [3] brought a detailed review of potential methods for chemical recycling of waste polyurethane foams, emphasizing that recycled materials have limited application possibilities. Pyrolysis or gasification might be a promising alternative since it can convert waste materials into valuable fuels and chemicals, as mentioned in a review by Kemona and Piotrowska [4]. Nevertheless, while the rest of the polymers, such as polystyrene (PS) [5,6], polypropylene (PP) [7], or polyethylene (PE) [8,9], were widely investigated for alternative fuel production, the studies which are dealing with PU treatment by thermochemical conversion methods are seldom.

Most of the studies in the literature deal with the investigation of kinetics or thermal degradation mechanism rather than the

* Corresponding author. University of Zagreb, Croatia.
E-mail addresses: hrvoje.stancin@fsb.hr (H. Stančin), michal.safar@vsb.cz (M. Šafář), jana.ruzickova@vsb.cz (J. Růžičková), hrvoje.mikulcic@fsb.hr (H. Mikulčić), helena.raclavska@vsb.cz (H. Raclavská), neven.duic@fsb.hr (N. Duić).

https://doi.org/10.1016/j.renene.2022.07.047
0960-1481/

Abbreviations

GC	Gas chromatography
HHV	High heating value
MDA	3,4-Methylenedioxyamphetamine
PAHs	Polycyclic Aromatic Hydrocarbons
PE	Polyethylene
PP	Polypropylene
PS	Polystyrene
PU	Polyurethane
PUR	Rigid polyurethane foam
SD	Sawdust
TGA	Thermogravimetric analysis
$W_{SD/PUR}$	Share of component
Y_{cal}	Calculated value
Y_{exp}	Experimental value
ΔY	Synergy level

product compounds analysis. Garrido et al. [10] investigated the pollutant emissions from the pyrolysis of flexible polyurethane foam, focusing on the formation and yield of PAHs, furans, and chlorine-containing compounds. At 850 °C, the formation of such compounds was highest, implying potential constraints for the gasification as the recycling method. Garrido and Font [11] investigated the thermal decomposition of flexible PU in nitrogen and air atmosphere, finding that this parameter influences the number of steps in the decomposition mechanism. In the case of the inert atmosphere, the process consists of two steps, while three steps are observed for the oxidative environment. This observation is even more valuable when put in the context that the rest of the polymers have a single-step decomposition mechanism. Yao et al. [12] performed pyrolysis on rigid PU from waste refrigerators in an inert atmosphere using nitrogen. They found that decomposition consists of three stages: the initial stage from 38 to 400 °C, the second stage between 400 and 550 °C, and the last stage between 550 and 1000 °C. This shows that the thermal decomposition mechanism of PU strongly depends on its type (rigid or flexible), which is a direct consequence of its chemical structure, usage of additives, and production process. Furthermore, the fact that PUs have a three-step decomposition mechanism is important for co-pyrolysis since biomass and PU could directly interact when decomposed.

Nishiyama et al. [13] analyzed the derived products from the pyrolysis and concluded that they are primarily linear hydrocarbons or oxygenated, benzene-containing species. The nitrogen-containing products (4-amino-4′-isocyanate diphenyl methane - MAI, 4,4′-Methylenedianiline -MDA) expressed the highest intensity, which is expected since they are used during the synthesis. The yield of linear hydrocarbons is favored for fuel purposes, but the yield of nitrogen-containing species should be minimized. One of the possible solutions might be co-pyrolysis with biomass, where feedstock interaction coupled with process parameters could reduce the yield of potentially harmful compounds [14]. Another benefit of such practice is resolving problems related to biomass-derived fuels like poor thermal stability, lower heating value, high viscosity or acidity, and similar [15]. Moreover, due to the limited biomass availability and geographical distribution, it is necessary to find alternative exploitation routes to maximize its potential in future energy systems while simultaneously maintaining consumption within sustainable boundaries [16].

Hassan et al. [17] provided a comprehensive review of progress in biomass pyrolysis. The study emphasized the importance of co-pyrolysis with hydrogen-rich feedstock such as waste plastics to improve product properties. Biomass feedstock was widely investigated and, even more, used to produce high-quality bio-oils that are currently blended with conventional gasoline. Even though the drawbacks mentioned above constrain wider biofuel deployment or its usage in the aviation sector. Arregi et al. [18] performed pyrolysis of pine sawdust and high-density polyethylene for hydrogen-rich gas production. The results from the ultimate and proximate analysis of pine sawdust are similar to the sawdust mixture used in this study, even though the type of wood is entirely different. Yet, the product distribution is completely different, suggesting the importance of the structural composition of the biomass sample. Ahmed et al. [19] pyrolyzed *Acacia* sawdust for bio-oil production at temperatures between 400 and 600 °C. The highest oil yield was noticed for 500 °C, which dramatically decreased with the temperature increment to 600 °C, mostly to yield a higher share of non-condensable gases. This observation suggests that at least 500 °C is required to enhance bio-oil yield. Further temperature increment is beneficial to reduce solid residue, but secondary cracking will occur and increase gaseous yield at the expense of liquid fraction. Liu et al. [20] performed catalytic pyrolysis over the pine sawdust with almost the same composition as the one used in this study. They found that the addition of catalyst has a limited impact on product distribution, while it might promote the secondary reactions at higher temperatures to increase the gas yield. Kai et al. [21] performed the co-pyrolysis of corn stalk and high-density polyethylene. They concluded that the strongest synergy between biomass-plastic samples is achieved for small plastic content (<20%), and the blending ratio has a low impact on the evolution of gaseous products. The strongest synergistic effect for small plastic content is also detected in a study by Ephraim et al. [22], where polystyrene and polyvinyl chloride were used.

Thermogravimetric, kinetic and thermodynamic analysis of PU and sawdust (SD) mixture was carried out in our previous work as the first step to evaluating the potential of selected feedstock for the co-pyrolysis [23]. The three-step decomposition mechanism is observed for PU, which also overlaps with the SD decomposition area, suggesting that the feedstock might interact significantly when decomposed. Since the chemical properties and thermal decomposition of PUs are pronouncedly different from the rest of typical polymers and more similar to biomass feedstock, it is interesting to investigate how this interaction reflects on final product distribution. Up to now, there have been no attempts to utilize waste rigid polyurethane foam and biomass in the co-pyrolysis to produce alternative fuels. Therefore, this works aims to provide an in-depth analysis of the chemical composition of obtained pyrolytic oil, which is not found in the literature. Besides, a brief analysis of obtained syngas fraction will be given, even though the research focuses on maximizing liquid yield. Furthermore, the influence of plastic content on product quantity and quality is evaluated by observing the synergistic effect between investigated feedstocks. Finally, the appropriate conclusions regarding the PU potential for alternative fuel production are drawn.

2. Materials and methods

Under this section, the used materials are presented with their origin, sample preparation procedure, and the preliminary results obtained from the ultimate and proximate analysis. This is followed up by a detailed explanation of used experimental methods to ensure the reproducibility of results. The experiments and liquid fraction sampling for chemical characterization have been duplicated to ensure the accuracy of the results.

2.1. Material characterization

Samples investigated in this study were waste rigid polyurethane foam (PUR) obtained from the discharged refrigerator and used as an insulation material. Biomass feedstock was a sawdust mixture of beech, oak, and fir wood with the unknown shares obtained from a local sawmill. Samples were prepared by shredding, grinding, and sieving into finer particles (0.125–0.25 mm) to ensure the mixture's homogeneity. Besides, in the previous work where utilization properties of PUR were investigated, it was found that this particle size is the most promising for thermochemical processes since the lowest amounts of harmful compounds are detected in that range [24].

PUR was obtained with the known ultimate and proximate analysis values. The sawdust properties are investigated according to ISO 17225-1:2021 [25]. The heating values are measured using the bomb calorimeter and following the procedure determined in the standard ISO 18125:2017 [26]. As can be seen, the heating value for PUR is pronouncedly higher than that of SD but still dramatically lower compared to the heating values of the majority of other plastics like PS, PP, or PE, which are above 40 MJ/kg [27]. Moreover, a high share of nitrogen (~7%) is detected in the PUR sample, which is not the case for other conventional polymers. Finally, from the proximate analysis of the PUR sample, a high share of volatile matter can be noticed, which is beneficial for the yield of liquid and gaseous fractions. Nevertheless, almost 6% of ash in the composition suggests that a high yield of solid residue can be expected at the end of the process. The results are summarised in Table 1.

2.2. Thermal decomposition investigation

Thermogravimetric analysis (TGA) was carried out using TGA/DSC 2 Thermoanalyzer Mettler Toledo. The TGA is an inevitable step in the experimental investigation of the thermal decomposition mechanism, and it is often used to determine optimal process conditions for pyrolysis [28]. Samples were investigated individually and in mixtures with different shares: PUR/SD 25–75%, PUR/SD 50-50%, PUR/SD 75-25%. Samples of about 10 mg were heated in Al2O3 crucibles of 70 μ1, from room temperature to 600 °C, at a heating rate of 10 °C/min. As a carrier, gas nitrogen was used with a flow rate of 20 ml/min. The final temperature is selected based on previous research presented in the Introduction section. While Ahmed et al. [19] pointed out that the highest liquid yield is obtained at 500 °C, the process was further extended to 600 °C to minimize the final solid residue. This is because previous studies on PU samples show that the significant mass loss is still evident after 500 °C.

2.3. Pyrolysis conditions and product analysis

The pyrolysis experiments were performed in a stainless-steel fixed bed reactor. A detailed description of the experimental setup and reactor components used in this work has been described by Hlavsova et al. [29] in their original research. The experiments were conducted under a nitrogen atmosphere with an 80 ml/min flow rate. Approximately 2 g of the sample was placed in the reactor and heated at 10 °C/min to a final temperature of 600 °C. The final temperature was maintained for about 30 min or until the complete release of pyrolysis gases. The moderate heating rate of 10 °C/min was selected based on our previous kinetic analysis, which showed no significant differences in the decomposition mechanism for the applied heating rates [23]. Samples were examined individually and in mixtures with the shares as mentioned above. The yield of the solid fraction was calculated by weighing the sample mass before and the residual mass after the pyrolysis. The output of pyrolysis gas was calculated at N_2 free-vol.%, based on the volume fractions obtained from gas chromatography (GC) and densities of individual gas components. Condensable gases were cooled down using an ice bath and collected in liquid form at the end of a reactor. The share of the liquid fraction was calculated by the difference. A detailed description of the gas chromatography and mass spectrometry properties and conditions can be found in our previous work, where co-pyrolysis of polystyrene and biomass sawdust was investigated [6].

2.4. Measurements uncertainties

Measurements for the chemical characterization of the obtained oils were repeated twice. The standard deviation for compounds detected in the PUR-derived oil ranges from 0.25% (1,3-benzene dicarboxylic acid bis (2-ethylhexyl) ester) to 5.59% (MDA). The standard deviation for oils from PUR/SD mixture analysis is between 0.54% (2-hydroxy-3-methyl-2-cyclopenten-1-one) and 5.79% for MDA.

At the same time, the reproducibility was determined for the oil obtained from individual PUR pyrolysis in the range of 1.25% for the MDA to 9.40% for the 3-methylbenzeneamine and the reproducibility for bio-oil from PUR/SD analysis was in the range of 2.15% (MDA) to 8.2% (3-methylbenzeneamine).

3. Results

In this section in-depth analysis of liquid fraction was carried out to determine feedstock potential for alternative fuel production. Besides, a preliminary examination is performed for gaseous fraction, and the main observation from TGA are summarised at the beginning of the interpretation of the results. Finally, the synergistic effect that occurs during the feedstock interaction is evaluated at the end of this section.

3.1. Thermogravimetric and derivative thermogravimetric analysis

Another study presents a detailed thermogravimetric analysis of individual samples and respective mixtures [23]. Nevertheless, prepared samples were subjected to TGA before the pyrolysis to compare the accuracy between investigations (Fig. 1). As expected, for the SD sample, moisture evaporation goes up to 110 °C, accounting for 5% of mass loss. The primary decomposition step starts at ~240 °C, peaks at 350 °C, and ends immediately at 380 °C. The last stage, where mostly lignin is decomposed, takes a linear pathway until 600 °C, and the final residue is approximately 20%. Most polymers like PS, PE, or PP have a single-stage decomposition mechanism [30], while in the case of PUR, three stages can be observed. In the first drying stage, the mass loss is negligible. At

Table 1
Ultimate and proximate analysis of PUR and sawdust samples.

	C (%)	H (%)	N (%)	O (%)	Ash (%)	Volatile matter (%)	Moisture (%)	Fixed carbon (%)	HHV (MJ/kg)
PUR	63.9	6.5	6.8	22.8	5.8	82.0	2.7	9.5	26.7
Sawdust	47.3	6.0	0.3	46.4	1.4	73.0	7.4	18.2	17.3

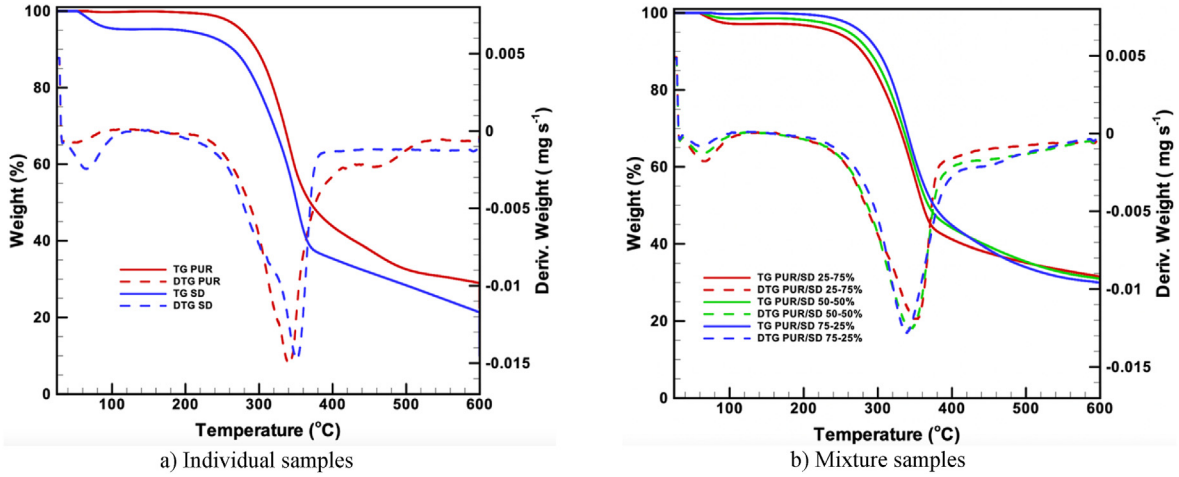

Fig. 1. TG and DTG curves for individual samples a) and mixtures b) thermal decomposition.

~280 °C, the primary decomposition stage begins, with the main peak at 340 °C, similar to SD. At this temperature, almost half of the sample is decomposed. The second slight peak can be observed at 450 °C, indicating that PUR has a broader temperature range in which decomposition occurs than SD. The last stage of decomposition starts at 480 °C, and until 600 °C, about 10% of the sample is decomposed, and the final mass is slightly below 30%. As can be observed, the decomposition mechanism has three stages, also found in the study by Jao et al. [12], even though the temperature ranges slightly differ.

The thermal decomposition of investigated mixtures shows similar behavior to the analysis of the individual samples. The mixture, where the sawdust is a dominant compound, has a visible mass loss due to evaporation and expresses a more intensified curve breakdown at 360 °C, observed for the biomass decomposition as well. The second decomposition stage for all mixtures happens in a broader temperature range, except for the sample where SD is the main constituent. In that case, the second stage ends slightly above 400 °C, while for the rest of the mixtures goes up to 500 °C. Similar behavior is also observed for PUR decomposition, probably due to the decomposition of halogenic compounds. The final mass is around 30%, similar to the PUR sample and other mixtures. These final masses are still considerably high, even though the process was extended to 600 °C. Nevertheless, a further increment in temperature would initiate secondary crackings and promote the yield of the gaseous fraction, which is not an objective of this study.

3.2. Pyrolysis product analysis

Individual pyrolysis of investigated samples shows a similar share of solid residue in the range of 20–22%. Nevertheless, the distribution of volatiles, gas and liquid fractions express completely different trends (Fig. 2). In the case of the SD sample, the dominant fraction is syngas with a share of 48%, followed by bio-oil yield with ~31%. From PUR pyrolysis, the predominant product is an oil with a yield of 61%, even though a notable amount of gaseous fraction (17%) is also detected. The oil yield from PUR is pronouncedly lower than conventional polymers like PS, where the yield of a liquid fraction can go up to 96% [6]. A high share of syngas from SD pyrolysis may be attributed to cellulose decomposition, which is the main driver for yielding non-condensable volatiles with low carbon numbers (<C_4). Such results might indicate that cellulose is the principal constituent of the used biomass sample. Nevertheless, to

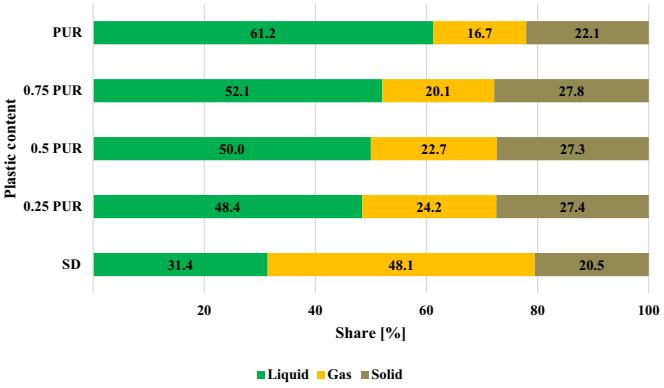

Fig. 2. Product yield from individual pyrolysis and PUR/SD blends co-pyrolysis.

confirm this hypothesis, deconvolution of the TGA curve should be carried out to determine the structural composition of the sawdust sample [31].

For the mixtures pyrolysis, the yield of a solid fraction is slightly higher than individual samples (~27%) but more-less constant for all investigated mixtures. In general, the solid residue is a consequence of fixed carbon and ash content, and obtained values for individual samples are expected. Nevertheless, in the case of mixtures, the share of solid residue is increased, probably due to the feedstock interaction during the process and their mutual influence that hinders complete decomposition and release of volatiles. The yield of liquid fraction is extensively promoted by introducing PUR to the fuel mixture, from 31% for the SD sample to around 50% for all investigated mixtures. This was achieved at the expense of the gaseous fraction, which decreased to only 20% for the mixture with 75% PUR content. The introduction of only 25% of PUR halved the yield of gases compared to results from sawdust pyrolysis. Once again, this confirms the hypothesis that waste plastics can significantly enhance the liquid yield from co-pyrolysis [32]. Nevertheless, it is interesting to observe the potential for improving the oil yield by introducing PUR into the mixture. Even in the case of 75% of PUR content, the oil yield barely surpasses 50%. In addition, the difference in oil yield between the mixture with 25% and 75% of PUR content is below 4%. Such observation indicates that the polyurethane potential for incrementing oil yield is greatly limited. This can be confirmed by comparing previous work where PS was investigated [6], since only 25% of PS in the mixture doubled the

yield of liquid fraction, and further increment of PS content had a visible impact on final product distribution, promoting the oil yield. Even more, the share of the solid fraction was reduced with the increment of PS content. At the same time, this study found that mixtures have an even higher share of a solid residue than individual samples, and the mixing ratio does not play an important role. Similar was also found for the co-pyrolysis of corn stover with PP [33]. The addition of PP has a visible effect on promoting the yield of the liquid fraction at the expense of others. Nevertheless, in that case, the yield of a gaseous fraction remains relatively high (42–48%) since individual polypropylene pyrolysis yields about 40% of gases. Finally, the selection of biomass feedstock also has an important role in product distribution. Zhang et al. [34] summarised the results of microwave-assisted co-pyrolysis of various biomass and plastics, where it was found that oil yield is mostly under 50%, even in the case of PS, PP, or PE. Such low oil yield from co-pyrolysis occasionally occurs when the biomass sample has a high share of ash content in the structure, typical for straws or some other types of biomass residues [35].

A detailed analysis of liquid and gaseous products is given in the following sections. Furthermore, the influence of PU content on final product distribution will be discussed through the analysis of the synergistic effect. The solid fraction is not further investigated since the utilization possibilities are relatively low. A promising solution for its utilization might be as an additive to enhance wood pellets' quality [36].

3.3. Chemical characterization of the liquid fraction

Analysis of liquid fraction composition showed that bio-oil from SD pyrolysis consists of 90 compounds, while 94 are detected in the liquid from PUR pyrolysis. In the case of mixtures, the number of identified compounds with visible shares is 94. It should be emphasized that some other compounds may be present in traces, but their significance can be neglected in this case. Identified compounds belong to organic groups like aromatic amines (benzenamines), aromatic hydrocarbons, phenols, alcohols, PAHs, ketones, acids, and aldehydes. The share of organic groups in the obtained oils is given in Fig. 3. For better visibility in the given figure, the term *Rest* encompasses toluene, indole, sugars, and furans, which are present with a minor share.

As can be seen, in the case of bio-oil from SD pyrolysis, the dominant are oxygen-containing compounds like phenols (24%), ketones (22%), and aldehydes (12%), which is expected and already reported in the literature [28,29]. Besides, a significant amount of acids and PAHs are detected (~9% and ~10%, respectively), which is not beneficial for fuel purposes. The formation of PAHs from biomass pyrolysis occasionally occurs through the acetylene addition mechanism, where acetylene reacts with naphthalenes to promote the yield of PAHs [37]. Since the share of acetylene and naphthalene is relatively low in bio-oil, it can be presumed that the acetylene addition mechanism has occurred here. Liu et al. [38] suggest torrefaction of biomass sample before the pyrolysis to reduce the yield of unwanted compounds like furans, aldehydes, and acids. This technique improves the bio-oil quality, even though it reduces its quantity.

On the other hand, the benzenamines (~72%) are the dominant compounds from PUR pyrolysis, followed by aromatic hydrocarbons (~8%). The high yield of benzenamines and low yield of hydrocarbons is comparably different from the pyrolysis product of biomass, or plastic materials, where mostly aliphatic or aromatic hydrocarbons are obtained [39]. In addition, a significant amount (~6% each) of phenols and alcohols is detected as well, most probably as a consequence of PUR synthesis [2].

When it comes to mixtures, it can be seen that the share of PUR has a significant influence on liquid product distribution. Only a small introduction of PUR almost wholly removed the aldehydes and sugars, while it significantly reduced the yield of ketones, acids, and most importantly, PAHs below 3%. It is especially interesting to observe the creation of PAHs, which are only present in traces for individual PUR pyrolysis. This is probably because the significant generation of PAHs from polyurethane starts at 700 °C [24], with the highest yield above 1000 °C, where soot and char are formed [40]. Therefore, at 600 °C, the generation of such compounds is hindered for a liquid fraction, while various benzeneamines (42%) and aromatic hydrocarbons (13%) are promoted. In the case of phenols, the reduction was almost negligible for this mixture with 25% of PUR, which can be attributed to the fact that PUR oil also yields these compounds; therefore, a complete removal is impossible.

Further increment of PUR content almost completely removed the ketones and acids, significantly influencing the yield of phenols.

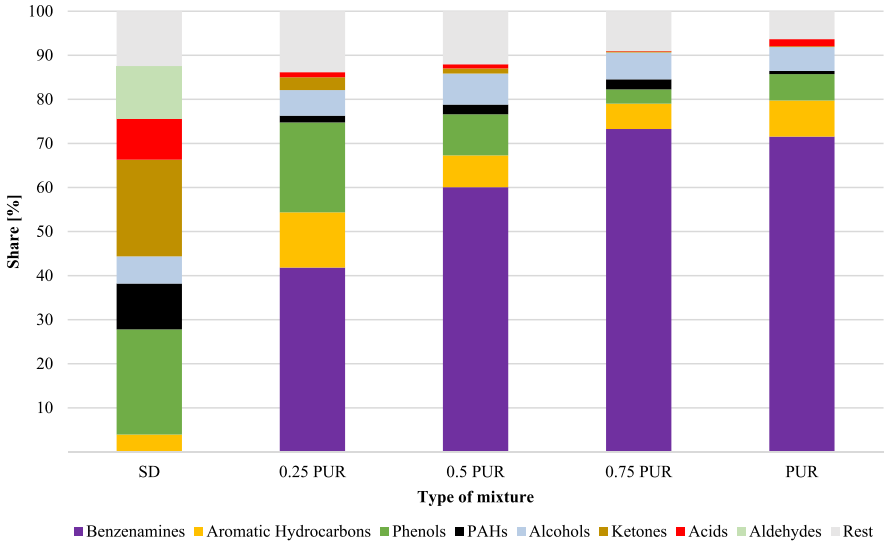

Fig. 3. Identified organic groups in the obtained bio-oils.

For the mixture with 50% PUR, the yield of phenols is halved, while further increment of PUR content to 75% reduced the yield to only 3%. Removing phenols is strongly preferred since they can cause jet-fuel surface deposits and corrosion [41].

Simultaneously, with the reduction of oxygen-containing organic groups, the formation of benzenamines was promoted, and they are the dominant constituents of the mixture's oils. Nevertheless, benzenamines are not preferred in the fuel composition, and even more, by observing the organic groups of derived oils, it can be stated that their potential for further refinement to fuel is minimal. They could be better utilized elsewhere in the chemical industry.

Detailed compound analysis was conducted by setting the threshold, which excluded those with a yield lower than 1.5% from further investigation. As shown in Fig. 4, most identified compounds are found with the yield below this threshold, indicating that the obtained oils have a strongly heterogeneous composition. For the bio-oil from SD, 69 such compounds account for 43.8% of the oil composition, and their number increases with the increment of PUR content. For the PUR-derived oil, 86 compounds are present in traces with a share below 1.5%, representing only 25.2% of all identified compounds, and suggesting a more homogenous structure than bio-oil. Liu et al. [38] suggests higher final temperatures to achieve a higher level of homogeneity in bio-oil composition.

Most compounds with a yield between 1.5 and 5% are found in bio-oil (18), following the decreasing trend with the increment of PUR content, and only 4 of them are detected in the oil from individual PUR pyrolysis. The same trends are noted for their share in the obtained oils. Compounds in that range represent more than 37% of the bio-oil composition, but their yield is decreased to only 11% for individual PUR pyrolysis. In the case of bio-oil, phenols and ketones are the most prominent groups detected in that range, but there is also the presence of PAHs and acids, which should be carefully monitored.

Finally, the threshold for a significant share was set at 5%, and almost all obtained oils have three compounds detected above this threshold, while only PUR-derived oil has four. Even though their total number is pronouncedly lower, their shares in derived oils are significant. For the bio-oil, they represent more than 18% of the composition, rapidly increasing with PUR content increment to the final value of almost 64% for individual PUR pyrolysis. As expected, all such compounds from PUR oil belong to benzenamines, while in bio-oil, they are furans, ketones, and PAHs.

Identified compounds in bio-oil are similar to those found in work by Yuan et al. [42]. Furfural, acetophenone, and 1,2,3,4-tetrahydro-2-phenyl-naphthalene have the highest share (~6%), while the yield of the other selected compounds (18 of them) is between 1.5 and 3%. For the PUR-derived oil, 4,4′-methylene bis-benzenamine, also known as 4,4′-Methylenedianiline (MDA), has the highest yield, accounting for almost 39% of oil composition. The high share of MDA is also reported in the study by Nishiyama et al. [13]. The MDA is a colorless or white solid with a low melting point, used as a precursor for polyurethane synthesis; therefore, its higher share is not unexpected [43]. Besides, it is classified as a potentially carcinogenic compound, and its presence in the fuel is not allowed. Another compound with a significant share is 3-methyl-benzenamine (m-toluidine), with a yield of 11.5%. It is a viscous liquid classified as the aromatic amine used to produce dyes [44]. The 2,3-dimethyl-benzenamine and aniline also have a significant share of almost 7%, and the rest of the selected compounds are in the range between 1.6 and 4.5%. A comparison between Table 2 and Table 3

Table 2
Selected compounds from individual pyrolysis of SD.

Selected compounds detected in bio-oil	Share [%]
1,2-cyclopentadiene	1.6
1,6-Anhydro-b-D-glucopyranose (levoglucosan)	2.1
2,6-Dimethoxytoluene	2.1
2-Methoxy-4-vinylphenol	1.9
2-Methoxyphenol	2.7
2-Pentanone	2.6
4-Methoxyphenol	2.4
Acetic acid	1.9
Acetophenone	5.9
Dodecanoic acid	2.2
Furfural	5.8
Naphthalene	1.9
1,2,3,4-tetrahydro-2-phenyl- naphthalene	6.8
2,6-dimethoxy-phenol	1.6
2,6-dimethoxy-4-(2-propenyl)- phenol	1.5
Propanone	2.1
Pyrocatechol	1.5
Styrene	1.9
Tetradecanoic acid	1.9
Toluene	2.9
Vanillin	2.9
Share of selected compounds	56.2

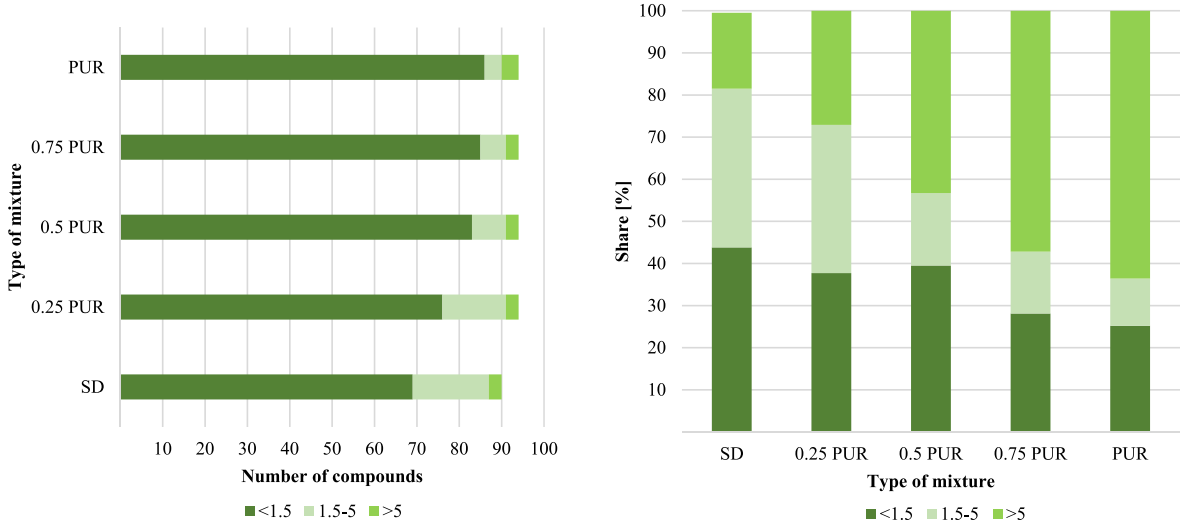

Fig. 4. Number of identified compounds (left) and their share in the derived oil (right).

Table 3
Selected compounds from individual pyrolysis of PUR.

Selected compounds detected in PUR derived oil	Share [%]
1,1′-Biphenyl]-4,4′-diamine, 3,3′-dimethyl-	2.5
1,1':3′,1''-Terphenyl, 5′-phenyl-	4.5
1,3-Benzenedicarboxylic acid, bis(2-ethylhexyl) ester	1.6
1-propoxy-2-Propanol	2.7
Aniline	6.8
2,3-dimethyl-benzenamine	6.7
3-methyl-benzenamine	11.5
4,4′-methylene bis-benzenamine (MDA)	38.7
Share of selected compounds	**74.9**

reveals that PUR yields more homogenous oil since eight selected compounds are responsible for almost 75% of oil composition. In contrast, in the case of bio-oil, 21 selected compounds account for only 56% of the composition.

When it comes to mixture analysis, it can be seen from Table 4 that most of the identified and selected compounds are these also found from individual PUR pyrolysis (Table 3). This indicates that the plastic fraction is the main driver for the liquid yield, but also it directly influences the selectivity of the compounds inside the derived oil. The 4,4′-Methylenedianiline (MDA) is once again the compound with the highest yield, and its share increases with the increment of PUR content. Like in PUR-derived oil, 3-methyl-benzenamine and aniline are compounds with a significant share among all investigated mixtures. The difference in their yield for investigated mixtures is less pronounced than MDA. Like bio-oil composition, the mix with 25% PUR content has a higher heterogeneity level than others. The 18 selected compounds with a share above 1.5% account for 62.3% of oil composition. At the same time, nine selected compounds are responsible for almost 72% of oil composition in a PUR-dominant mixture. In general, it can be stated that compounds identified in the derived oil from the individual pyrolysis and mixture co-pyrolysis are predominantly valuable chemicals rather than compounds preferred in the composition of alternative liquid fuels [45]. This is because they have attached oxygen or nitrogen atoms to their structure, limiting utilization possibilities. While the former often causes thermal instability, the bottom one may promote the formation of nitrogen oxides (NO_X) [46], and both dramatically lower the heating values [47]. Besides, several acidic chemicals suggest that such bio-oil has higher acidity, which could also cause corrosion.

Table 4
List of selected compounds from mixture analysis.

Selected compounds from mixture analysis	0.25 PUR	0.5 PUR	0.75 PUR
		[%]	
Aniline	9.9	10.6	11.9
2,3-dimethyl-benzenamine	3.9	3.1	5.0
3-methyl-benzenamine	9.6	12.0	15.8
4,4-methylenebis-benzenamine (MDA)	7.5	20.7	29.5
1,1':3′,1''-Terphenyl, 5′-phenyl-	3.6	1.7	1.7
2-(2-hydroxypropoxy)-1-propanol	1.6	1.5	1.8
2-(phenylmethyl)-benzenamine	3.0	4.1	2.7
1H-Indole, 2,6-dimethyl-	1.8		1.5
3,4-dimethyl- benzenamine	2.2		2.0
4-ethyl-2-methoxy-phenol	2.7	1.9	
Diphenylmethane		1.9	
Catechol		1.6	
2,3-Dimethyl-4-biphenylamine		1.5	
1,1′-Biphenyl, 2-methyl-	2.4		
1-(4-methylphenyl)-1H-Pyrrole	2.6		
2-hydroxy-3-methyl-2-Cyclopenten-1-one	1.6		
methyl-cyclopentane	1.8		
2-methoxy-phenol	2.6		
trans-Isoeugenol	1.8		
2,6-dimethoxy-4-(2-propenyl)-phenol	2.0		
2,6-dimethoxy-phenol	1.7		
Share of selected compounds	**62.3**	**60.5**	**71.9**

3.4. Syngas composition

In the following subsection, the evolution of gaseous compounds: carbon monoxide (CO), carbon dioxide (CO_2), hydrogen (H_2), methane (CH_4), and higher hydrocarbons (C_xH_y) from the co-pyrolysis of sawdust and waste rigid polyurethane foam is analyzed (Fig. 5). The evolution of gases starts at 360 °C, where primarily CO_2 is identified, which remains the dominant product during the whole process for all investigated samples. The volumetric share of CO_2 varies between 39% (mixture with 0.25 of PUR) to 46% for pure PUR pyrolysis (Fig. 5d). Removal of CO_2 can be achieved by amine scrubbing, a standard biogas upgrading method [48]. Interestingly, the residence time did not significantly impact the evolution of syngas species because the composition didn't change significantly after reaching the final temperature. The same trend is noticed for the rest of the investigated non-condensable gases. The residence time is represented in Fig. 5 by three repeating values of 600 °C, the final temperature at which samples were held for 30 min.

The syngas composition obtained from the pyrolysis of individual sawdust shows that around 61% vol. of identified gases are preferred in the syngas composition (H_2, CH_4, CO). The highest yield (~40%) is noticed for CO, while the share of hydrogen and methane is around 8.4 and 11%, respectively. The share of higher hydrocarbons is almost negligible, with a yield below 2% vol. for all investigated samples; therefore, it won't be discussed further. It can only be stated that a low output of such gases can be expected since they are cracked at higher temperatures to methane and hydrogen [49]. This is supported by Fig. 5 a) and b), where it can be seen that the yield of these two compounds is increasing with the temperature increment. Besides, the secondary cracking of liquid fraction also occurs, resulting in the share increment of methane, but even more pronounced hydrogen. As the most valuable compound, the share of hydrogen (Fig. 5a) is the lowest for the sawdust sample, but it goes up to almost 25% for the pyrolysis of PUR. A high share of H_2 (>50%) is also found in the study [40] for the temperatures 1000–1300 °C, where gasification was performed on the same sample to investigate the effect of temperature and residence time on gas yield. The H_2 yield from the investigated mixtures is between values obtained from the individual samples and increases with the increment of polyurethane content (Table 5). The methane yield is similar for all investigated mixtures, between 8.8 and 10.6%, and decreases with the increment of PUR content (Fig. 5b). The lowest CH_4 yield is noticed for the individual pyrolysis of PUR, with a value of 6.9% vol. The most significant difference is observed in carbon monoxide yield, as shown in Fig. 5c. For the fraction where the dominant compound is sawdust, the outcome is almost the same as for the individual pyrolysis of the sawdust sample. This is expected since the cellulose and hemicellulose are responsible for the evolution of CO. With the further increment of polyurethane content, the share of CO is dramatically falling, and it is slightly above 20% for the pyrolysis of individual PUR.

The yield of syngas compounds is summarised in Table 5. The presented volumetric share of observed gases is obtained at a final temperature of 600 °C and after a residence time of 12 min. Since no significant change is noticed, this was selected as a representative share of obtained syngas. The only interesting observation after 30 min of residence time is seen for the hydrogen yield, which share was increased by approximately 2% vol. in all investigated mixtures, while the share of other compounds did not change significantly. The effect of residence time for PUR gasification is

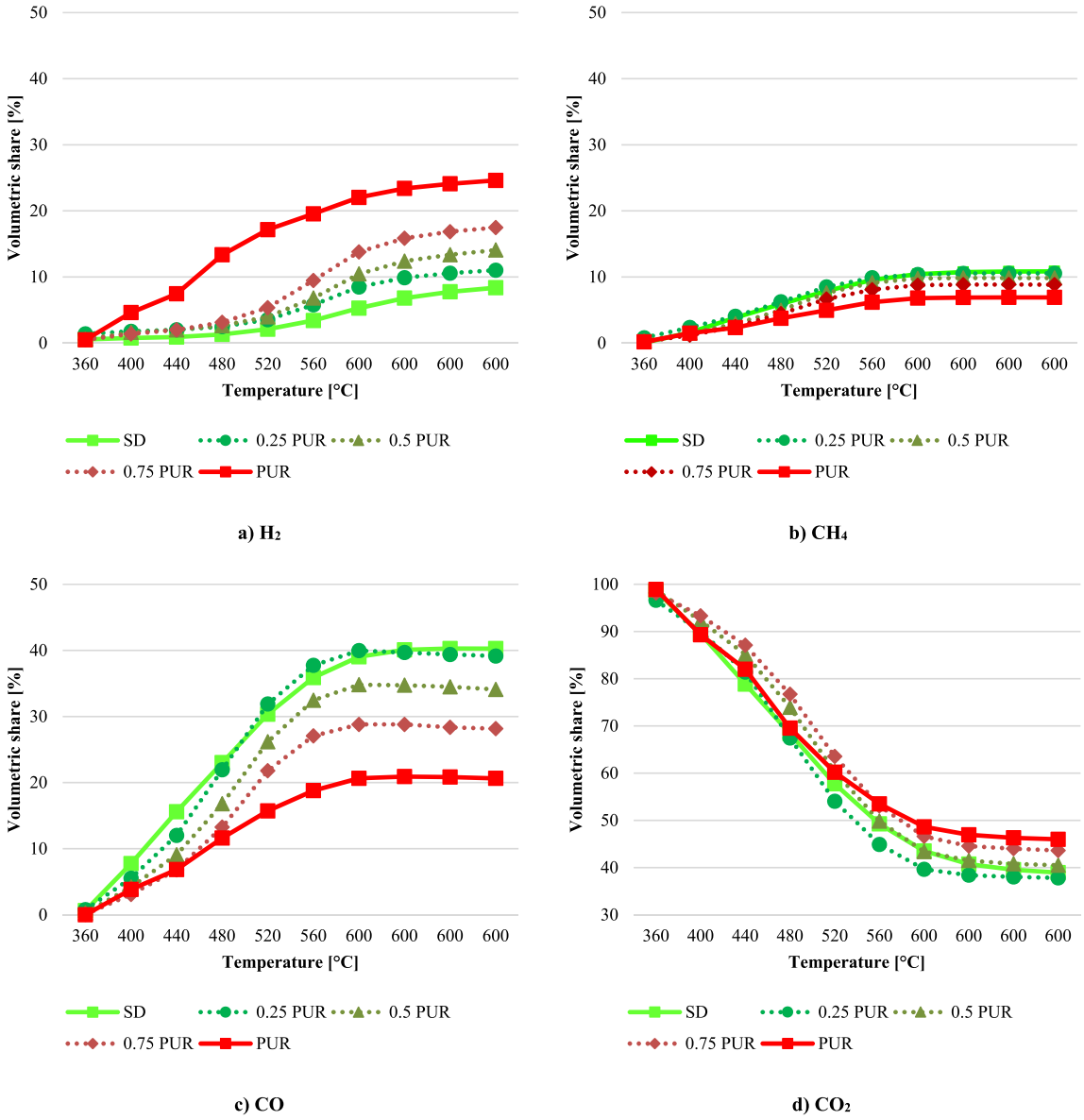

Fig. 5. Distribution of gaseous products for all investigated samples.

Table 5
The syngas composition of investigated samples.

	H_2	CH_4	CO	CO_2	C_xH_y
			[% vol.]		
Sawdust	8.4	10.9	40.3	38.9	1.6
0.25 PUR	11.0	10.6	39.2	37.8	1.5
0.5 PUR	14.1	9.8	34.1	40.5	1.5
0.75 PUR	17.5	8.8	28.2	43.6	1.9
PUR	24.6	6.9	20.6	46.0	1.8

more pronounced at higher temperatures; since then, the secondary cracking of heavy hydrocarbons from the volatiles is promoted over formed soot and char particles [40]. This study found that the content of H_2 increased with time due to breaking the bonds between higher hydrocarbons to promote the formation of lighter compounds or pure H_2. Furthermore, the increase of CO content and the decrease of CO_2 is mainly because the bottom one reacts with char particles as an oxidant and promotes the formation of other compounds [49].

3.5. Synergistic effect

The synergistic effect is the main driver for product distribution from the co-pyrolysis of biomass and waste plastics. To determine the level of synergy, experimental results are compared to the theoretical values. Theoretical values (Y_{cal}) are calculated using the following Equation (1):

$$Y_{cal} = W_{SD}Y_{SD} + W_{PUR}Y_{PUR} \quad (1)$$

Where $W_{SD/PUR}$ stands for proportions of each component in investigated mixtures, and $Y_{SD/PUR}$ presents the values obtained from the individual pyrolysis [22]. The existence and level of synergy are determined by the difference between experimentally obtained values and calculated ones using Equation (2). According

to [17], it can be stated that synergy exists when the difference between the experimental and calculated values is positive.

$$\Delta Y = Y_{exp}\text{-}Y_{cal} \quad (2)$$

Table 6 summarizes the calculated synergy levels for the three fractions considering the plastic content inside the mixture. The obtained values show that the main trade-off occurs between the volatiles fractions, liquid, and gas, while the synergy level is almost constant in the case of solid fractions.

The trendlines illustrate this phenomenon even better, and they are plotted in Fig. 6. As can be seen, the highest synergies are achieved for the fraction with 25% of PUR content, and the level of synergy decreases with the increment of plastic content. A decrease in the synergistic effect is evident in Fig. 6 since the values are approaching the horizontal axis. Kai et al. have already reported this phenomenon [21], where a mixture with 20% of high-density PE expressed the highest synergy, and Ephraim et al. [22], where the highest synergy effect is observed for a mix where plastic content does not exceed 40%. These observations, confirmed on several cases and feedstocks, imply that the share of plastic fraction inside the mixture should be limited to some extent if the goal is to promote a high-quality liquid yield.

Interestingly, the co-pyrolysis shows a constant level of synergy for the yield of solid residue, which is approximately 6% in all investigated mixtures. The yield of a solid fraction is around 27% from all investigated mixtures, slightly higher than individual analysis (20–22%). Since the yield of solid fraction from individual pyrolysis is relatively similar, and theoretical yield presumes the same behavior (Table 6), the constant values obtained for synergy level are not unexpected. In addition, since the solid yield mainly depends on the share of ash content and fixed carbon of initial feedstock, the final mass is usually similar to the sum of these two indicators from the proximate analysis. Consequently, the same relations are valid for their mixtures when considering their respective shares. Therefore, the solid fraction is less dependent on chemical reactions that are taking place inside the reactor due to volatile fraction degradation, and it is more predictable.

Nevertheless, the trade-off between volatile fractions is the most interesting to analyze since these two fractions have the best utilization possibilities. The introduction of PUR increased the oil yield at the expense of the gaseous fraction. This can easily be confirmed by summing up the synergy values from each fraction for a particular mixture and considering that solid residue is almost constant for investigated mixtures. Only a minor introduction of PUR reduced the gas yield by more than 16% and increased the liquid output by nearly 10%, compared to theoretically expected. As the plastic content increases, the synergy level decreases, as observed in previous work for polystyrene and the sawdust co-pyrolysis [6], but also in the studies mentioned above. For the mixture where PUR is a dominant constituent, negative synergy is noticed for the yield of volatile fractions, even though it should be emphasized that the obtained experimental values are close to theoretically expected (Table 6).

Table 6
Theoretical and experimental values for product yield and calculated level of synergy.

	Liquid yield			Gas yield			Solid yield		
	Cal.	Exp.	ΔY	Cal.	Exp.	ΔY	Cal.	Exp.	ΔY
0.25 PUR	38.85	48.41	9.56	40.26	24.17	−16.09	20.89	27.43	6.53
0.5 PUR	46.30	49.98	3.68	32.41	22.67	−9.74	21.28	27.35	6.07
0.75 PUR	53.76	52.06	−1.71	24.57	20.12	−4.45	21.67	27.82	6.15

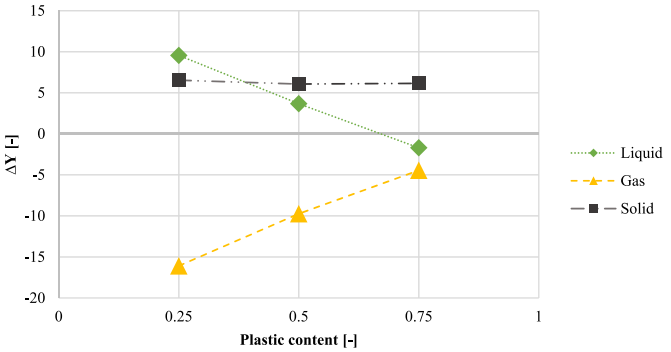

Fig. 6. Synergistic effect for investigated mixtures within the dependence of plastic content.

The mixture with higher plastic content expresses better agreement with theoretically calculated yield, implying that product yield prediction from the co-pyrolysis might be more straightforward when the plastic material is the dominant compound since its decomposition mechanism is much simpler than biomass. This assumption is in accordance with the results from mixture analysis, where biomass was the predominant compound and where the highest synergy and discrepancies in calculated and experimentally obtained results are noticed.

4. Conclusion

The co-pyrolysis of biomass sawdust and PUR showed that their thermal decomposition could yield valuable chemical products. Nevertheless, their utilization as alternative fuels in the future energy system does not look feasible due to the high share of nitrogen-containing compounds. Moreover, obtained products are rather valuable chemicals than fuel constituents that could be used to synthesize new materials and chemicals. The main findings of the work are summarised as follows:

- The addition of PUR to the mixture can enhance the oil yield from the co-pyrolysis process. Nevertheless, its impact is limited since only a slight increment (<4%) in the yield is noticed between the mixture with 25 and 75% of PUR content. Even though only small addition of PUR reduces the yield of a gaseous fraction by 24% compared to individual SD pyrolysis. Simultaneously, for all investigated mixtures, the increment of solid residue was noted compared to individual pyrolysis, accounting for ~27% of the initial mass.
- The composition of bio-oil from sawdust pyrolysis expresses a strong heterogeneous structure with the highest share of oxygenated compounds like phenols, ketones, aldehydes, and acids. A significant share of PAHs is detected as well. Conversely, the PUR-derived oil has a more homogenous structure since more than 70% of identified compounds belong to the benzenamines group.
- With the increment of PUR content in the mixtures, the oil composition becomes more homogenous with the highest yield of benzenamines, especially MDA, 3-methyl-benzenamine, and aniline, which account for more than 55% of oil structure. Furthermore, even the mixtures with an equal share of both feedstock yield chemical compounds found in PUR-derived oil rather than bio-oil. Finally, the small addition of plastic content to mixture composition could significantly enhance the liquid yield and remove most unwanted oxygenated compounds derived from sawdust pyrolysis.

- Syngas evaluation shows that introducing PUR can significantly enhance hydrogen yield and reduce the output of carbon monoxide and methane. In general, the evolution of gases starts at 360 °C due to cellulose and hemicellulose degradation. At 600 °C, the composition of the gaseous fraction becomes permanent, implying that residence time doesn't have a significant impact.
- The greatest synergy level is observed for the mixture with 25% of PUR, and the synergistic effect fades away with a further increment of plastic content. The most significant trade-off is noted for volatile fractions, where the liquid formation is promoted at the expense of a gaseous one. This is especially evident in the case of a mixture with 25% of PUR, where the synergistic effect for liquid yield accounts for 9.5%. The yield of solid fractions expresses a constant synergy level of 6%.

Declaration of competing interest

The authors declare that they have no known competing financial interests or personal relationships that could have appeared to influence the work reported in this paper.

Acknowledgement

The study was funded by the research project of the Ministry of Education, Youth and Sports of the Czech Republic: The OP RDE grant number CZ.02.1.01/0.0/0.0/16_019/0000753 "Research Centre for Low-Carbon Energy Technologies"

References

[1] Y. Deng, R. Dewil, L. Appels, R. Ansart, J. Baeyens, Q. Kang, Reviewing the thermo-chemical recycling of waste polyurethane foam, J. Environ. Manag. 278 (Jan. 2021), https://doi.org/10.1016/j.jenvman.2020.111527.
[2] W. Yang, Q. Dong, S. Liu, H. Xie, L. Liu, J. Li, Recycling and disposal methods for polyurethane foam wastes, Procedia Environmental Sciences 16 (Jan. 2012) 167–175, https://doi.org/10.1016/j.proenv.2012.10.023.
[3] D. Simón, A.M. Borreguero, A. de Lucas, J.F. Rodríguez, Recycling of polyurethanes from laboratory to industry, a journey towards the sustainability, Waste Manag. 76 (2018) 147–171, https://doi.org/10.1016/j.wasman.2018.03.041.
[4] A. Kemona, M. Piotrowska, Polyurethane recycling and disposal: methods and prospects, Polymers 12 (8) (2020), https://doi.org/10.3390/POLYM12081752.
[5] J. Nisar, G. Ali, A. Shah, M. Iqbal, R.A. Khan, Sirajuddin, F. Anwar, R. Ullah, M.S. Akhter, Fuel production from waste polystyrene via pyrolysis: kinetics and products distribution, Waste Manag. 88 (Apr. 2019) 236–247, https://doi.org/10.1016/j.wasman.2019.03.035.
[6] H. Stančin, M. Šafář, J. Růžičková, H. Mikulčić, H. Raclavská, X. Wang, N. Duić, Co-pyrolysis and synergistic effect analysis of biomass sawdust and polystyrene mixtures for production of high-quality bio-oils, Process Saf. Environ. Protect. 145 (Jan. 2021) 1–11, https://doi.org/10.1016/j.psep.2020.07.023.
[7] D.v. Suriapparao, B. Boruah, D. Raja, R. Vinu, Microwave assisted co-pyrolysis of biomasses with polypropylene and polystyrene for high quality bio-oil production, Fuel Process. Technol. 175 (Jun. 2018) 64–75, https://doi.org/10.1016/j.fuproc.2018.02.019.
[8] S.M. Al-Salem, Thermal pyrolysis of high density polyethylene (HDPE) in a novel fixed bed reactor system for the production of high value gasoline range hydrocarbons (HC), Process Saf. Environ. Protect. 127 (Jul. 2019) 171–179, https://doi.org/10.1016/j.psep.2019.05.008.
[9] J. Chattopadhyay, T.S. Pathak, R. Srivastava, A.C. Singh, Catalytic co-pyrolysis of paper biomass and plastic mixtures (HDPE (high density polyethylene), PP (polypropylene) and PET (polyethylene terephthalate)) and product analysis, Energy 103 (May 2016) 513–521, https://doi.org/10.1016/j.energy.2016.03.015.
[10] M.A. Garrido, R. Font, J.A. Conesa, Pollutant emissions during the pyrolysis and combustion of flexible polyurethane foam, Waste Manag. 52 (2016) 138–146, https://doi.org/10.1016/j.wasman.2016.04.007.
[11] M.A. Garrido, R. Font, Pyrolysis and combustion study of flexible polyurethane foam, J. Anal. Appl. Pyrol. 113 (2015) 202–215, https://doi.org/10.1016/j.jaap.2014.12.017.
[12] Z. Yao, S. Yu, W. Su, W. Wu, J. Tang, W. Qi, Comparative study on the pyrolysis kinetics of polyurethane foam from waste refrigerators, Waste Manag. Res. 38 (3) (2020) 271–278, https://doi.org/10.1177/0734242X19877682.
[13] Y. Nishiyama, S. Kumagai, S. Motokucho, T. Kameda, Y. Saito, A. Watanabe, H. Nakatani, T. Yoshioka, Temperature-dependent pyrolysis behavior of polyurethane elastomers with different hard- and soft-segment compositions, J. Anal. Appl. Pyrol. 145 (2020), 104754, https://doi.org/10.1016/j.jaap.2019.104754. October 2019.
[14] H. Stančin, H. Mikulčić, X. Wang, N. Duić, A review on alternative fuels in future energy system, Renew. Sustain. Energy Rev. 128 (2020), https://doi.org/10.1016/j.rser.2020.109927.
[15] Q. Van Nguyen, Y.S. Choi, S.K. Choi, Y.W. Jeong, Y.S. Kwon, Improvement of bio-crude oil properties via co-pyrolysis of pine sawdust and waste polystyrene foam, J. Environ. Manag. 237 (May 2019) 24–29, https://doi.org/10.1016/j.jenvman.2019.02.039.
[16] P.A. Østergaard, N. Duic, Y. Noorollahi, S.A. Kalogirou, Recent advances in renewable energy technology for the energy transition, Renew. Energy vol. 179 (Dec. 01, 2021) 877–884, https://doi.org/10.1016/j.renene.2021.07.111. Elsevier Ltd.
[17] H. Hassan, J.K. Lim, B.H. Hameed, Recent progress on biomass co-pyrolysis conversion into high-quality bio-oil, Bioresour. Technol. vol. 221 (Dec. 01, 2016) 645–655, https://doi.org/10.1016/j.biortech.2016.09.026. Elsevier Ltd.
[18] A. Arregi, M. Amutio, G. Lopez, M. Artetxe, J. Alvarez, J. Bilbao, M. Olazar, Hydrogen-rich gas production by continuous pyrolysis and in-line catalytic reforming of pine wood waste and HDPE mixtures, Energy Convers. Manag. 136 (2017) 192–201, https://doi.org/10.1016/j.enconman.2017.01.008.
[19] A. Ahmed, M.S. Abu Bakar, R.S. Sukri, M. Hussain, A. Farooq, S. Moogi, Y.K. Park, Sawdust pyrolysis from the furniture industry in an auger pyrolysis reactor system for biochar and bio-oil production, Energy Convers. Manag. 226 (August) (2020), 113502, https://doi.org/10.1016/j.enconman.2020.113502.
[20] P. Liu, Y. Wang, Z. Zhou, H. Yuan, T. Zheng, Gas fuel production derived from pine sawdust pyrolysis catalyzed on alumina, Asia Pac. J. Chem. Eng. 15 (4) (2020) 1–11, https://doi.org/10.1002/apj.2456.
[21] X. Kai, T. Yang, S. Shen, R. Li, TG-FTIR-MS study of synergistic effects during co-pyrolysis of corn stalk and high-density polyethylene (HDPE), Energy Convers. Manag. 181 (2) (2019) 202–213, https://doi.org/10.1016/j.enconman.2018.11.065.
[22] A. Ephraim, D. Pham Minh, D. Lebonnois, C. Peregrina, P. Sharrock, A. Nzihou, Co-pyrolysis of wood and plastics: influence of plastic type and content on product yield, gas composition and quality, Fuel 231 (April) (2018) 110–117, https://doi.org/10.1016/j.fuel.2018.04.140.
[23] H. Stančin, H. Mikulčić, N. Manić, D. Stojiljković, M. Vujanović, X. Wang, N. Duić, Thermogravimetric and kinetic analysis of biomass and polyurethane foam mixtures Co-Pyrolysis, Energy 237 (Dec. 2021), https://doi.org/10.1016/j.energy.2021.121592.
[24] H. Stančin, J. Růžičková, H. Mikulčić, H. Raclavská, M. Kucbel, X. Wang, N. Duić, Experimental analysis of waste polyurethane from household appliances and its utilization possibilities, J. Environ. Manag. 243 (2019), https://doi.org/10.1016/j.jenvman.2019.04.112.
[25] ISO 17225-1:2021(en), Solid biofuels — fuel specifications and classes — Part 1: general requirements. https://www.iso.org/obp/ui/#iso:std:iso:17225:-1:ed-2:v1:en:sec:C. (Accessed 1 December 2021).
[26] ISO - ISO 18125, Solid biofuels — determination of calorific value. https://www.iso.org/standard/61517.html, 2017. (Accessed 1 December 2021).
[27] S.M. Al-Salem, A. Antelava, A. Constantinou, G. Manos, A. Dutta, A review on thermal and catalytic pyrolysis of plastic solid waste (PSW), J. Environ. Manag. vol. 197 (Jul. 15, 2017) 177–198, https://doi.org/10.1016/j.jenvman.2017.03.084. Academic Press.
[28] E. Rostek, K. Biernat, Thermogravimetry as a research method in the transformation processes of waste rubber and plastic products for energy carriers (WtE and WtL processes), J. Sustain. Dev. Energy Water Environ. Syst. 1 (2) (Jun. 2013) 163–171, https://doi.org/10.13044/j.sdewes.2013.01.0012.
[29] A. Hlavsová, A. Corsaro, H. Raclavská, D. Juchelková, H. Škrobánková, J. Frydrych, Syngas production from pyrolysis of nine composts obtained from nonhybrid and hybrid perennial grasses, Sci. World J. (2014), https://doi.org/10.1155/2014/723092.
[30] D. Li, S. Lei, P. Wang, L. Zhong, W. Ma, G. Chen, Study on the pyrolysis behaviors of mixed waste plastics, Renew. Energy 173 (2021) 662–674, https://doi.org/10.1016/j.renene.2021.04.035.
[31] N.G. Manić, B.B. Janković, V.M. Dodevski, D.D. Stojiljković, V.V. Jovanović, Multicomponent modelling kinetics and simultaneous thermal analysis of Apricot Kernel Shell pyrolysis, J. Sustain. Dev. Energy Water Environ. Syst. N/A (N/A) (2020), https://doi.org/10.13044/j.sdewes.d7.0307, 0–0.
[32] M.V. Rocha, A.J. Vinuesa, L.B. Pierella, M.S. Renzini, Enhancement of bio-oil obtained from co-pyrolysis of lignocellulose biomass and LDPE by using a natural zeolite, Therm. Sci. Eng. Prog. 19 (Oct. 2020), https://doi.org/10.1016/j.tsep.2020.100654.
[33] F. Wu, H. Ben, Y. Yang, H. Jia, J. Wang, G. Han, Effects of different conditions on Co-pyrolysis behavior of corn stover and polypropylene, Polymers 12 (2020), https://doi.org/10.3390/polym12040973.
[34] Y. Zhang, S. Fan, T. Liu, M.M. Omar, B. Li, Perspectives into intensification for aviation oil production from microwave pyrolysis of organic wastes, Chem. Eng. Process.-Process Intensif. 176 (Jun. 2022), https://doi.org/10.1016/j.cep.2022.108939.
[35] M. Concepcion Maguyon-Detras, M.P. Victoria Migo, N. van Hung, M. Gummert, M.C. Maguyon-Detras, M. v P. Migo, N. v Hung, M. Gummert, Thermochemical conversion of rice straw, Sustain. Rice Straw Manag. (2020) 43–64, https://doi.org/10.1007/978-3-030-32373-8_4.
[36] R. García, M.V. Gil, A. Fanjul, A. González, J. Majada, F. Rubiera, C. Pevida,

Residual pyrolysis biochar as additive to enhance wood pellets quality, Renew. Energy 180 (Dec. 2021) 850–859, https://doi.org/10.1016/J.RENENE.2021.08.113.
[37] T. Sitek, J. Pospíšil, J. Poláčik, M. Špiláček, P. Varbanov, Fine combustion particles released during combustion of unit mass of beechwood, Renew. Energy 140 (Sep. 2019) 390–396, https://doi.org/10.1016/J.RENENE.2019.03.089.
[38] S. Liu, G. Wu, Y. Gao, B. Li, Y. Feng, J. Zhou, X. Hu, Y. Huang, S. Zhang, H. Zhang, Understanding the catalytic upgrading of bio-oil from pine pyrolysis over CO2-activated biochar, Renew. Energy 174 (2021) 538–546, https://doi.org/10.1016/j.renene.2021.04.085.
[39] Y. Zhang, S. Fan, T. Liu, Q. Xiong, A review of aviation oil production from organic wastes through thermochemical technologies, Appl. Energy Combust. Sci. 9 (Mar. 2022), 100058, https://doi.org/10.1016/j.jaecs.2022.100058.
[40] X. Wang, Q. Jin, J. Zhang, Y. Li, S. Li, H. Mikulčić, M. Vujanović, H. Tan, N. Duić, Soot formation during polyurethane (PU) plastic pyrolysis: the effects of temperature and volatile residence time, Energy Convers. Manag. 164 (2018) 353–362, https://doi.org/10.1016/j.enconman.2018.02.082.
[41] H. Zhu, E. Janusson, J. Luo, J. Piers, F. Islam, G.B. McGarvey, A.G. Oliver, O. Granot, J. Scott McIndoe, Phenol-selective mass spectrometric analysis of jet fuel, Analyst 142 (17) (Aug. 2017) 3278–3284, https://doi.org/10.1039/C7AN00908A.
[42] H. Yuan, H. Fan, R. Shan, M. He, J. Gu, Y. Chen, Study of synergistic effects during co-pyrolysis of cellulose and high-density polyethylene at various ratios, Energy Convers. Manag. 157 (2018) 517–526, https://doi.org/10.1016/j.enconman.2017.12.038. December 2017.
[43] 4,4'-Methylenedianiline | C13H14N2 - PubChem.".
[44] m-Toluidine | C6H4CH3NH2 - PubChem.".
[45] H. Li, S. Feng, Z. Yuan, Q. Wei, C.C. Xu, Highly efficient liquefaction of wheat straw for the production of bio-polyols and bio-based polyurethane foams, Ind. Crop. Prod. 109 (August) (2017) 426–433, https://doi.org/10.1016/j.indcrop.2017.08.060.
[46] F. Jurić, M. Stipić, N. Samec, M. Hriberšek, S. Honus, M. Vujanović, Numerical investigation of multiphase reactive processes using flamelet generated manifold approach and extended coherent flame combustion model, Energy Convers. Manag. 240 (Jul. 2021), 114261, https://doi.org/10.1016/j.enconman.2021.114261.
[47] X. Guo, L. Wang, L. Zhang, S. Li, J. Hao, Nitrogenous emissions from the catalytic pyrolysis of waste rigid polyurethane foam, J. Anal. Appl. Pyrol. 108 (2014) 143–150, https://doi.org/10.1016/j.jaap.2014.05.006.
[48] R.S. Cavaignac, N.L. Ferreira, R. Guardani, Techno-economic and environmental process evaluation of biogas upgrading via amine scrubbing, Renew. Energy 171 (2021) 868–880, https://doi.org/10.1016/j.renene.2021.02.097.
[49] H. Weldekidan, V. Strezov, R. Li, T. Kan, G. Town, R. Kumar, J. He, G. Flamant, Distribution of solar pyrolysis products and product gas composition produced from agricultural residues and animal wastes at different operating parameters, Renew. Energy 151 (2020) 1102–1109, https://doi.org/10.1016/j.renene.2019.11.107.

PAPER 4

Energy 237 (2021) 121592

Contents lists available at ScienceDirect

Energy

journal homepage: www.elsevier.com/locate/energy

Thermogravimetric and kinetic analysis of biomass and polyurethane foam mixtures Co-Pyrolysis

H. Stančin [a, *], H. Mikulčić [a, c], N. Manić [b], D. Stojiljković [b], M. Vujanović [a], X. Wang [c], N. Duić [a]

[a] University of Zagreb, Faculty of Mechanical Engineering and Naval Architecture, Ivana Lučića 5, 10000, Zagreb, Croatia
[b] University of Belgrade, Faculty of Mechanical Engineering, Kraljice Marije 16, Belgrade, Serbia
[c] Department of Thermal Engineering, Xi'an Jiaotong University, Xianning West Road, Xi'an, Shaanxi, China

ARTICLE INFO

Article history:
Received 29 January 2021
Received in revised form
17 July 2021
Accepted 23 July 2021
Available online 28 July 2021

Keywords:
Thermogravimetric analysis
Kinetic analysis
Sawdust
Polyurethane
Co-pyrolysis

ABSTRACT

Alternative fuels are crucial for the decarbonisation of high-energy demanding processes. The utilisation of waste materials to produce alternative fuels is especially interesting since, the co-pyrolysis of waste plastics and biomass was lately introduced as promising method since the synergistic effect might enhance the product properties compared to those from individual pyrolysis. Furthermore, the utilisation of waste biomass, like sawdust, is interesting since it does not influence the sustainability of biomass consumption, and even more, it avoids the usage of raw feedstock. Thermogravimetric analysis is performed to determine the thermal degradation behaviour and kinetic parameters of investigated mixtures to find the most appropriate utilisation method. Co-pyrolysis was conducted for three mixtures with the following biomass/polyurethane ratios: 75-25%, 50-50%, 25–75%, over a temperature range of 30 −800 °C, at three heating rates 5, 10 and 20 °C/min, under an inert atmosphere. Obtained results were subjected to comprehensive kinetic analysis to determine effective activation energy using the iso-conversional model-free methods and provide a detailed analysis of the samples' thermal degradation process. This work aimed to identify the main thermal decomposition stages during co-pyrolysis of biomass and polyurethane mixtures and provide the mixture composition's influence on the considered thermochemical conversion process.

1. Introduction

Recycling waste and end-of-life plastic materials represent serious issues nowadays, with the potential to arise even more in the future due to increased consumption. About 27 million tons of plastic waste is generated in the EU in 2018. Of which 31.1% is recycled, 41.6% is used for energy recovery while the rest is land-filled, implying the irrevocable loss of valuable resources [1]. This problem is especially evident in complex plastics waste, which is not built by polymerisation but synthesised from different compounds, like polyurethane foam [2]. Polyurethane foams (PUF) are among the most used polymers worldwide, utilised in a flexible or rigid form for automotive purposes or as insulation and structural material. By selecting different polyols and isocyanates, the primary building block of PUF, the manufacturer can produce more than 150 different foam types. Moreover, the PUF is often treated with various flame retardants due to application requirements, which complicates their recycling procedure [3]. Lately, thermochemical conversion into useful chemicals or fuels is proposed as a potential method to deal with its disposal problem. The pyrolysis is especially interesting since valuable liquids, gases, and biochar are obtained, which can be further utilised where appropriate [4]. Stančin et al. studied thermal degradation of waste rigid polyurethane foam (PUR) by thermogravimetric analysis (TGA), intending to investigate particle size's influence on solid residue chemical composition. They found a significant amount of harmful and hazardous compounds that constrain the direct application of obtained products. Major unwanted compounds found are various benzene-based species, chlorine-containing compounds, polycyclic aromatic hydrocarbons (PAHs), furans, and similar [5]. Guo et al. conducted catalytic gasification of PUR to maximise the hydrogen yield. Calcium carbonate had the best catalytic effect and promoted a significant amount of hydrogen (~80 vol%), offering an alternative

* Corresponding author.
E-mail address: hrvoje.stancin@fsb.hr (H. Stančin).

https://doi.org/10.1016/j.energy.2021.121592
0360-5442/

thermochemical route for PUR recycling [6]. Numerous researchers widely investigated the kinetics of polyurethane foams over the years by conducting TGA. The kinetic and thermodynamic analysis is useful for getting a good insight about the changes of a kinetic model during the process, but also to investigate the favorable process conditions to achieve predetermined goals of the considered thermochemical conversion process. Finally, kinetic and thermodynamic analysis results can serve as a basis for potential numerical modeling and simulations [7]. Garrido and Font [8] investigated a flexible PUF decomposition mechanism, at different heating rates, with the final temperature of 900 °C. They concluded that in the first degradation stage, urethane bonds are broken to produce isocyanates, while in the second stage, ether polyols are decomposed forming, mostly a solid residue. Yao et al. [9] recently performed a kinetic analysis of PUR from the discharged refrigerator, confirming the three-stage decomposition mechanism and the Flynn–Wall–Ozawa method as the most reliable for obtaining activation energies of PUF decomposition. Mikulčić et al. [10] investigated the thermal decomposition of PUR under different atmospheres. They concluded that the decomposition mechanism under the oxygen-enriched atmosphere could be roughly divided into two stages, starting with the devolatilisation and followed up by the oxidation of residues.

Various waste biomass was widely investigated as the prominent feedstock for sustainable alternative fuel production through pyrolysis or co-pyrolysis [11]. Nevertheless, due to complex biomass composition, their thermal degradation behaviour dramatically varies [12]. Luo et al. [13] conducted the pyrolysis on beech sawdust and used model-free analysis to assess activation energies. The thermal decomposition was divided into three stages by observing the extent of conversion. Additionally, activation energies are calculated with the conclusion that Friedman's method corresponds to the real values. Zhang et al. [14] investigated the thermal decomposition of wood sawdust. Once again, it was confirmed that the sawdust decomposition consists of three steps, being the most intensive in the second one, where mostly cellulose and hemicellulose are decomposed. In addition, it was concluded that sawdust pyrolytic kinetic consists of multi-step reactions due to the presence of pseudo components, which decomposes independently. Manić et al. [15] carried out multi-component modeling kinetics and thermal analysis of apricot kernel shell using four pseudo-components. The analysis showed that the cellulose component dominant the process, and the influence is slightly increased when higher heating rates are applied. Most of the studies deals with co-pyrolysis of biomass or sawdust from one type of wood. Alam et al. [16] investigated the co-pyrolysis of bamboo sawdust and low-density polyethylene, concluding that the higher heating rates shift the peak temperature toward higher values and broaden the temperature range in which decomposition takes place. Other works deal with co-pyrolysis of torrefied poplar wood with polyethylene [17], oak wood with different types of waste plastics [18], eucalyptus biomass residue with polystyrene [19], pine woodchips with the six most common plastics waste [20]. As can be seen, most of the studies deal with the individual analysis of polyurethane kinetics. The extended results which would cover the thermodynamic perspective are widely missing. On the other hand, various biomass feedstock was widely investigated in numerous research. Nevertheless, the work where sawdust mixture composed of different types of biomass is co-pyrolyzed with PUR is not found in the literature. The introduction of polyurethane to the co-pyrolysis process extends the state-of-the-art of polyurethane decomposition analysis. The inclusion of the thermodynamic part complements the knowledge gap of thermal decomposition investigation by broadening the knowledge on the influence of mixture composition on process dynamics.

This work reveals the thermogravimetric analysis (TGA) and kinetic analysis of waste biomass sawdust (SD) composed from different types of wood and PUR. As already mentioned above, PUR recycling requires complicated procedures; therefore, thermochemical recycling routes might be a promising alternative. Thermogravimetric analysis is used in this study to obtain necessary kinetic parameters such as activation energy, pre-exponential factor, and similar. In addition, we have provided an analysis of thermodynamic parameters, which are seldom in the literature. Since the decomposition mechanism of PUR is more similar to biomass than plastics, it is of great interest to investigate their interaction during the process and mutual influence on kinetic and thermodynamic parameters. The results from this study can be used to evaluate the feedstock suitability for co-pyrolysis and even more to provide a comprehensive insight for determining optimal process conditions such as mixing ratio, heating rate, and final temperature. Therefore, the main novelty of this work lies in the fact that for the first time, sawdust and polyurethane were investigated in fuel blend with an aim to derive appropriate conclusions regarding the feedstock suitability for the process and backed up by analysis of favorable process conditions.

2. Materials and methods

2.1. Materials and experimental procedure

The samples used in this study were waste sawdust mixture composed of fir, oak, and beech wood obtained from a local sawmill, while the PUR was previously used as an insulation material for refrigerators. Investigations were carried out for individual and mixture samples with the following shares: 25 % PUR, 50 % PUR, and 75 % PUR. The sample preparation was done according to the standard procedure [21]. In addition, the samples were tested to obtain data of ultimate and proximate analyses following the relevant standard [22]. Results are given in Table 1. Selected particle sizes of the samples were between 0.125 and 0.25 mm, to ensure homogeneity of the mixture. In addition, in the previous research [5], it was determined that this is the optimal particle size of selected PUR regarding the yield of organic compounds, especially those that might represent a threat to human health such as PAHs, furans, benzene containing compounds, and similar. Sample masses were about 10 mg, which is widely used for TGA. Samples were heated from room temperature up to 800 °C, since higher temperatures are applied for gasification. Different heating rates were used to investigate the influence of this parameter on process kinetics. As an inert carrier gas, Argon was used to avoid reactions with released volatiles. Furthermore, the prepared sample was also conducted to the Simultaneous Thermal Analysis (STA), which provides data for TGA and DTA simultaneously on the same sample. The NETZSCH STA 445 F5 Jupiter system was used for STA measurements under the following conditions:

- particle size 0.125–0.25 mm
- sample mass: 10 ± 0.5 mg.
- temperature range: from room temperature to 800 °C.
- heating rates: $\beta = 5$, 10 and 20 °C/min.
- the carrier gas: pure Argon with the total gas flow rate of 70 mL/min.

2.2. Methods for calculation of energy activation and thermodynamic parameters

In this work, model-free methods were used to avoid potential errors in the calculation of energy activation that might arise from

Table 1
Results of Ultimate and Proximate analysis of investigated samples.

	Ultimate Analysis[a] (wt.%)					Proximate analysis (wt.%)				HHV (MJ/kg)
Sample	C	H	O[b]	N	S	Moisture	Volatiles	Fixed carbon	Ash	
PUR	63.90	6.45	16.96	6.74	–	2.71	82.01	9.51	5.78	26.73
SD	47.33	6.04	44.77	0.31	0.02	7.35	72.95	18.28	1.42	17.30

[a] On a dry basis.
[b] By the difference.

the misidentification of an appropriate kinetic model. Since the biomass decomposition is extremely complex, and the sawdust mixture is composed of different types of biomass, the probability of selecting the wrong model was too high. In addition, model-free analysis opens an opportunity to investigate the change of activation energy in dependence with the extent of conversion, suggesting the changes in reaction mechanisms and kinetics. If model-fitting methods are applied, one can only extract the average value for the whole process, which is not beneficial for the analysis of the reaction model and kinetics of the process.

Activation energies are calculated using the four model-free isoconversional methods, Friedman (Eq. (1)), Kissinger-Akahira-Sonuse (KAS) (Eq. (2)), Ozawa-Flynn-Wall (OFW) (Eq. (3)), and Starink (Eq. (4)):

$$\ln\left(\beta\frac{d\alpha}{dT}\right) = \ln[Af(\alpha)] - \frac{E}{RT} \quad \text{Eq. 1}$$

$$\ln\left(\frac{\beta}{T^2}\right) = \ln\left[\frac{AR}{EG(\alpha)}\right] - \frac{E}{RT} \quad \text{Eq. 2}$$

$$\ln\beta = \left[\frac{0.0048*AE}{RG(\alpha)}\right] - 1.052\left(\frac{E}{RT}\right) \quad \text{Eq. 3}$$

$$\ln\left(\frac{\beta}{T^{1.92}}\right) = C_s - 1.0008\frac{E}{RT} \quad \text{Eq. 4}$$

In the equations mentioned above, α represents the degree of conversion, β is the heating rate, T is the temperature A, E, and R are the pre-exponential coefficient, the activation energy, and the universal gas constant, respectively. Activation energies in the Eqs. (1)–(4) are calculated as a function of the extent of conversion (α). In Eq. (1), Friedman's method for a different α value, a set of ln ($\beta(d\alpha/dT)$) and $1/T$ pairs corresponding to each heating rate were collected and plotted to a straight line. The slope of each straight line, ($-E/R$), was used to obtain the activation energy. In Eq. (2), for the KAS method, at each degree of conversion, the pairs of ln (β/T^2) and $1/T$ data points were obtained and plotted once again to a straight line. The slope ($-E/R$) is then used to calculate the activation energy. In the case of the OFW method (Eq. (3)), data points are collected for pairs of lnβ and $1/T$ which were fitted to a straight line. From the slope ($-1.052\,(E/R)$), activation energy is calculated. In the Starink method (Eq. (4)) at a given extent of conversion α, the data points of ln ($\beta/T^{1.92}$) versus $1/T$ are plotted to a straight line at different temperature heating rates, and the slope of the line corresponds to -1.0008E/R. Therefore, the apparent activation energy E is calculated from the slope of the straight line.

Thermodynamic parameters, including the pre-exponential factor, are calculated using the following equations (5)–(8):

- Pre-exponential factor (A)

$$A = \frac{\beta*E*\exp\left(\frac{E}{R*T_m}\right)}{R*T_m^2} \quad \text{Eq. 5}$$

- Changes of enthalpy (ΔH)

$$\Delta H = E - RT_\alpha \quad \text{Eq. 6}$$

- Changes in entropy (ΔS)

$$\Delta S = \frac{\Delta H - \Delta G}{T_m} \quad \text{Eq. 7}$$

- Changes of free Gibbs energy (ΔG)

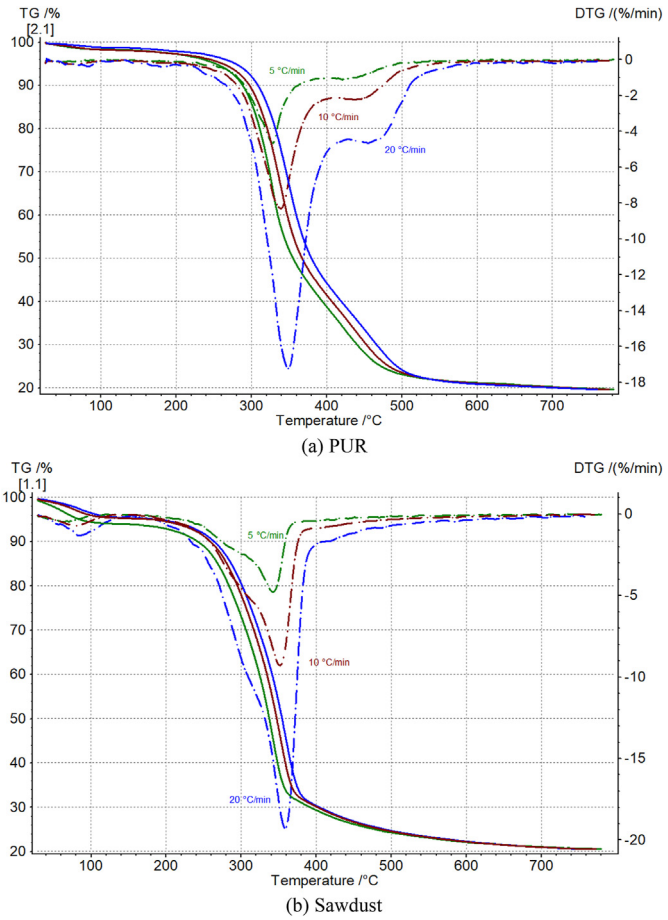

Fig. 1. TG (solid lines) and DTG (dotted lines) curves from PUR (a) and Sawdust (b) pyrolysis.

$$\Delta G = E + R*T_m*\ln\left(\frac{K_B*T_m}{h*A}\right) \quad \text{Eq. 8}$$

where K_B represents Boltzmann constant (1.381×10^{23} J/K), h Plank constant (6.626×10^{34} J), T_m the DTG peak temperature, and T_α the temperature at the degree of conversion α [23]. To calculate the pre-exponential factor from Eq. (5), it was assumed the first-order kinetic reaction with the kinetic model $f(\alpha) = (1-\alpha)$. As can be seen from equations (6)–(8), the pre-exponential factor A, and activation energy E are mandatory to calculate enthalpy changes, entropy, and free Gibbs energy.

2.3. Error analysis of experimental work

Regarding the error analysis of the experimental work, the proximate and ultimate analysis was performed according to standard test methods, which already include the defined procedures for measurement accuracy and measurement error handling. These procedures were applied to the data of proximate and ultimate analysis presented in this paper, and the obtained experimental values are presented according to the standard test requirements and common practice of presenting this type of data on a defined basis in order to be comparable with the literature data.

With regard to TG-DTG experimental work, the error analysis considers a comprehensive calibration and measurement procedure that precedes the sample measurement. The calibration procedure defined by the equipment manufacturer provides the accuracy of the measurement and is performed once every six months. The calibration procedure considers the used protective gas for the balance and selected heating rate. Furthermore, before each measurement to correction of the signals is performed by measurements with empty crucibles to correct the measured signals and handle the mass balance deviations. After that, the measurement with the crucible with the sample and reference crucible is performed and obtained correction signal is applied on measurement data through the manufacturer software used for the analysis. Those are common procedures for this type of experimental equipment which guarantee the accuracy of the measurements declared by the equipment manufacturer.

3. Results

3.1. Thermogravimetric analysis of sawdust and polyurethane foam samples

Fig. 1 presents the thermogravimetric (TG) and derivative thermogravimetric curves (DTG) for individual sample pyrolysis, obtained at three different heating rates. The PUR decomposition can be roughly divided into three stages, already reported by Yao et al. [9]. Up to 200 °C, the sample's decomposition is barely visible, and the mass loss is below 3.5 % for all investigated heating rates. The onset temperature for the second stage is at approximately 300 °C, and 303 °C for the heating rates of 5 and 10 °C/min, while the onset temperature for the heating rate of 20 °C/min is slightly higher ~311 °C. The decomposition peak is identified at 328 °C (5 °C/min), and it is further shifted to higher temperatures with the increment of heating rates to 338 and 348 °C, respectively. Similar values and trends for peak position are also reported by Xu et al. [24]. The first peak in DTG curves ends in the temperature range between 380 and 406 °C, and the endpoint is shifted toward a higher temperature with the heating rate increment. The remaining masses at this point are ~47 % for 5 and 10 °C/min, while higher mass loss is noticed for the heating rate of 20 °C/min (42.5 %), which is expected since the temperature range is shifted toward higher values for more than 20 °C. This first peak represents the main degradation stage, where mostly urethane bonds are broken, and isocyanates and polyols are decomposed [25,26]. The second flat peak immediately follows the end of the first peak. The second peak of the DTG curve can be explained as a secondary cracking of 1,1-Dichloro-1-fluoroethane and similar halogenated compounds in an inert atmosphere and degradation of the soft segment [4]. Jiao et al. [27] studied the degradation characteristics of PUR under inert and oxidative atmosphere, and they found that this second peak is even more expressed in an oxidative environment. Besides, the

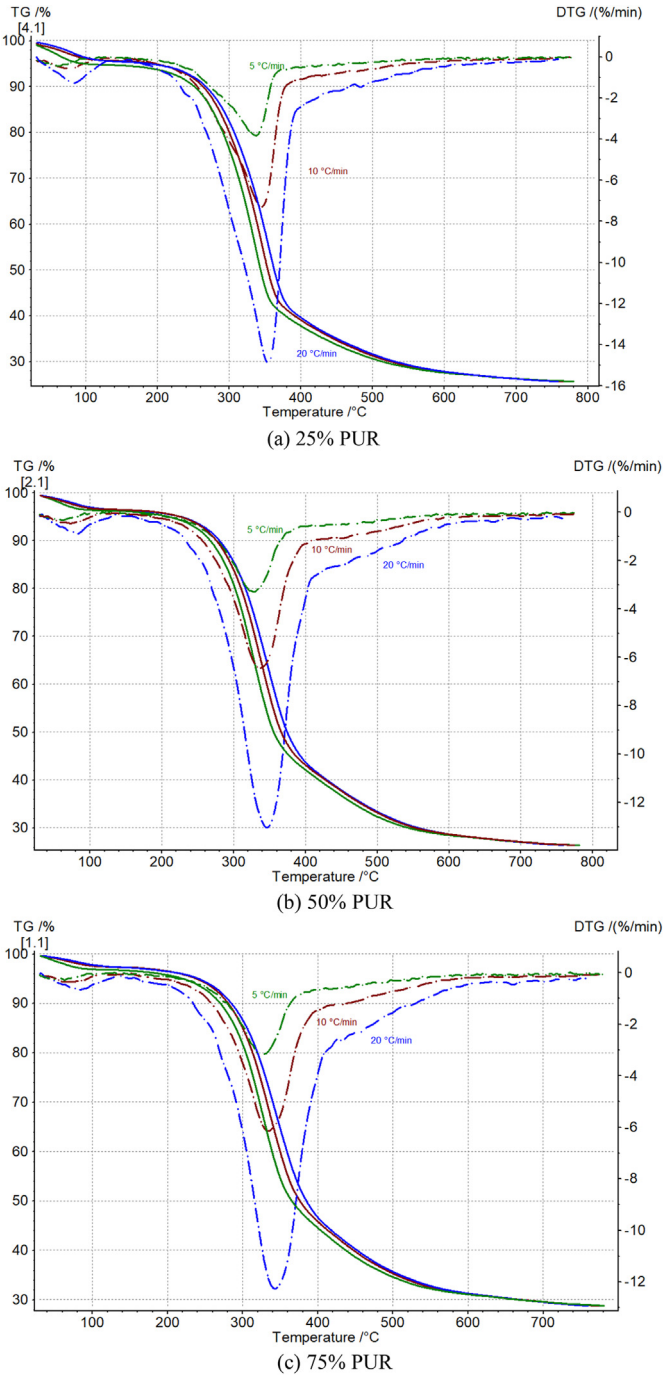

Fig. 2. TG (solid lines) and DTG (dotted lines) curves from sawdust and PUR mixture pyrolysis a) 25 % PUR b) 50 % PUR c) 75 % PUR.

increment of heating rate had a visible impact on this stage of degradation, being more pronounced for higher heating rates and broadening the temperature range in which decomposition happens. At approximately 480 °C, this second stage ends, and all samples have an almost identical mass loss, between 60 and 70 % of the initial mass. Nevertheless, in the last stage, the mass loss is more intensive for higher heating rates, even though, in general, thermal decomposition in this stage is almost negligible. The final mass differs for investigated samples, being the lowest for 20 °C/min (19.7 %), and highest for 5 °C/min (23.3 %). By observing the TG and DTG curves, the increment of heating rate broadens the temperature range in which thermal degradation is happening and promotes the sample decomposition.

The sawdust decomposition also consists of three steps, starting with the moisture evaporation (~5 % of mass loss), being followed by the most intensive second stage where mostly hemicellulose and cellulose content is decomposed (>60 % of mass loss), and finally slow decomposition of the lignin content until the end of the process (~10% of mass loss). For the heating rate of 5 °C/min, the first stage ends at 110 °C, after which the curve remains flat until 220 °C, where degradation slowly starts to progress once again. The first stage for higher rates goes up to ~140 °C, where most of the moisture is evaporated. The second stage begins at approximately 290 °C for 5 °C/min, and with the further increment of heating rate is shifted toward higher values to 296 and 302 °C, respectively. As can be seen, the increment of heating rate broadens the temperature range in which decomposition is happening, similar to PUR, and also shifted the peak in DTG curves from 342 to 352 and 358 °C, respectively. This phenomenon where the increment of heating rate shifts the temperature range toward higher values is already reported in several studies [28,29]. Mainly this is due to the heat transfer limitations and existence of temperature gradient between the surface and inner part of the particles, which influences the release of volatiles [16]. The main peak corresponds to the decomposition of the cellulose content [14]. The small shoulder in the peak can be noticed at 5 °C/min, corresponding to hemicellulose degradation. As the heating rate increase, this shoulder becomes less visible, already reported for sawdust decomposition [30]. The second stage ends at 370 °C for the 5 °C/min, and at 376 °C and 383 °C for the heating rates of 10 and 20 °C/min, respectively. At the end of this stage remaining mass is approximately 26 % for all samples. In the last stage, mass loss follows the linear pathway until the end of the process, even though there is no visible mass loss after 600 °C. This last stage accounts for the degradation of the lignin content. The final mass is slightly lower for 5 °C/min (19.6 %) compared to the other two samples, where the final mass is about 20.6 %.

3.2. Thermogravimetric analysis of sawdust and polyurethane foam mixtures

Regarding the thermal decomposition of the investigated mixtures, it is observed from TG curves (Fig. 2) that the sample where sawdust is a dominant compound express similar behaviour to the decomposition of the individual SD. In contrast, for the mixtures with 50 and 75 % of PUR content, the decomposition is similar to the individual PUR sample. The first stage is slightly influenced by the introduction of PUR content to the mixture. As the content of PUR increases, the mass loss decrease, as expected since this is mostly due to moisture evaporation. Regarding the heating rate, the first stage seems to be poorly influenced by this parameter, and mixture composition plays a more important role [29]. The only visible difference is at a heating rate of 5 °C/min, where slightly greater mass loss is noticed, similar to the SD sample.

The second stage onset temperature is poorly influenced by the mixture composition since the temperatures are in a similar range, while the more pronounced difference is for various heating rates. For the mixture with 25 % of PUR, onset temperature increase with the increment of heating rate and are 280, 290, and 298 °C, respectively. The peak temperatures are also shifted toward higher values with the heating rate increment from 338 to 354 °C, noticed for other mixtures. The difference between peak temperature is negligible for the mixture with 50 and 75 % of PUR content but still increase from 328 °C to 334 and 344 °C, as the heating rate increase. The end of the first peak is at 360 °C for 5 °C/min for all mixtures, which slightly increases with the increment of heating rate and PUR content in the mixture. For the heating rate of 20 °C/min, the end temperature of the first peak increase with the increment of PUR content to approximately 376, 380, and 400 °C, respectively. The first peak's end is immediately followed by the second one, similar to individual PUR pyrolysis. Precise determination of the second peak-end temperature is difficult, but it can be arbitrarily taken at about 500 °C since, at these points, DTG curves are very close to zero. Even though it should be emphasized that the second peak is more influence by the heating rate and mixture composition. With both parameters increment, the end temperature tends to shift toward values higher than 500 °C. In this second stage, the sample with 25 % of PUR expresses similar behavior compared to the SD, while mixtures with 50 and 75 % of PUR are closer to the individual PUR decomposition. The final temperature of the second stage is greatly influenced by both factors, mixture composition and heating rates. For the former one, it can be seen that the introduction of PUR broadened the temperature range in which decomposition takes place. Simultaneously, the second peak from the PUR degradation is smoothened and less pronounced in the DTG curve. This implies that biomass hinders secondary cracking of 1,1-Dichloro-1-fluoroethane, and with a higher share of biomass fraction in an investigated mixture, this peak is significantly reduced. For the mixture where SD is the dominant compound, the influence of both parameters is more visible compared to the rest of the samples.

The influence of the heating rate on the last stage of degradation is almost negligible. The mass of the residues at 600 °C is almost the same for all investigated heating rates and mixtures, except at 5 °C/min for the mixture with 25 % of PUR, where the final mass is slightly lower. Lower final mass at a lower heating rate is expected since, in this case, sufficient time is provided for the complete release of volatiles. Besides, with the increment of PUR content in the mixture, the final mass of the residue is increased. Interestingly, with the increment of heating rate, the final mass decrease for the mixture with 50 and 75 % of PUR, also noticed for the individual PUR decomposition. On the other hand, for the mixture with 25 % of PUR, the final mass increase with the increment of heating rate, also observed for pure SD degradation.

In general, from the TG and DTG curves, it can be seen that the decomposition areas of individual samples overlap and taking place in a similar temperature range, which is very beneficial for the occurrence of the synergistic effect between them. The existence of synergy can be confirmed by the final mass of investigated mixtures, which are higher than those from individual pyrolysis or

Table 2
Final masses from individual and mixture pyrolysis at various heating rates.

Final mass [%]	5 °C/min	10 °C/min	20 °C/min
Sawdust	19.6	20.6	20.7
25 % PUR	22.9	24.9	25.7
50 % PUR	27.2	26.4	26.6
75 % PUR	28.8	28.6	28.1
PUR	23.3	21.8	19.7

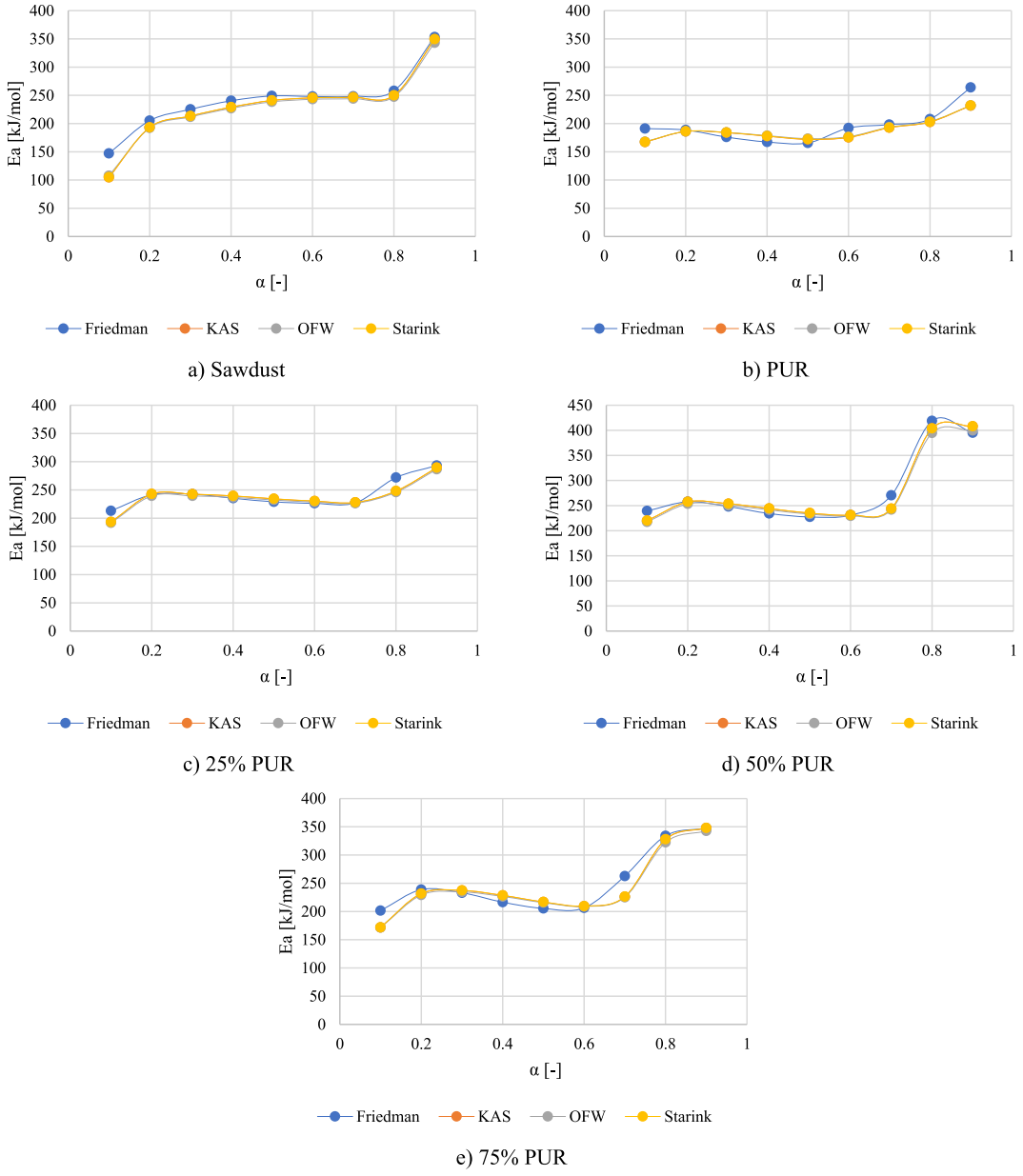

Fig. 3. Calculated activation energies for individual samples and respective mixtures.

theoretically expected. The existence of synergy can also be seen from the second peak of the second stage since the biomass influenced its intensity. The DTG curves are considerably smoothened compared to individual PUR pyrolysis, indicating that the sawdust has an important role in this temperature range for the decomposition intensity. Simultaneously, the PUR influence on the first stage of decomposition and the onset temperature for the second stage seems to be limited. In contrast, a more significant influence is noticed for the end temperature of this stage and the overall process. An increase of PUR content increased the final mass of the residue for all investigated mixtures. Regarding the heating rate, for the mixture with 25 % of PUR, increment in the heating rate increased the final mass of the residue, observed for individual SD decomposition, while the opposite trend is noticed for the mixture with 50 and 75 % of PUR content. Results are summarised in Table 2.

3.3. The activation energy of individual samples and their respective mixtures

The activation energy (E_a) was calculated using the model-free isoconversional Friedman, Kissinger-Akahira-Sonuse, Ozawa-Flynn-Wall, and Starink methods. Obtained values show excellent statistical correspondence by observing the statistical R^2 factor (>0.94947) for the range of conversion between $\alpha = 0.1–0.9$. Below and above these points, obtained activation energies show bigger discrepancies and lower statistical agreement, already reported in the literature [14]. In general (Fig. 3a–e), it can be seen that there are only slight differences between the used methods. Moreover, the only visible differences are spotted between Friedmann and other methods, while the results from the KAS, OFW, and Starink greatly correlate.

The E_a of polyurethane is lower than the rest of the plastics, and

it depends on the isocyanate index, which represents the hard segment of the PUFs. With the increment of this parameter, the E_a tends to increase, representing the existence of the stronger bonds in such a composition. Reported mean values in the literature differ but are in general below 200 kJ/mol [31], which is significantly lower compared to the polyethylene (PE), polystyrene (PS), or polypropylene (PP), where mean values are ~250 kJ/mol [32]. The mean activation energy of PUR used in this work is about 192 kJ/mol for KAS, OFW, and Starink method with an excellent statistical agreement ($R^2 > 0.9970$), while a slightly higher value (~202 kJ/mol) is obtained using the Friedman method, once again with a remarkable statistical agreement ($R^2 = 0.9985$).

Firstly, activation energy sharply increases up to $\alpha = 0.1$ (E_a~200 kJ/mol), suggesting that a higher amount of energy is required to initiate PUR decomposition. In the range of $\alpha = 0.1–0.5$, E_a gradually decreases to approximately 165 kJ/mol. In this stage, urethane bonds are broken, allowing the thermal decomposition of isocyanates and polyols. In the range between $\alpha = 0.5–0.6$, it is noticed a bounce to 190 kJ/mol, which clearly shows the two-degradation mechanism that occurs during the PUR decomposition [26]. This is followed up by a constant increase until $\alpha = 0.8$. At this point, most of the sample is already decomposed, resulting in the steep increment of E_a. As can be seen, calculated values using different methods show great similarity. The difference between Starink and KAS methods is for all investigated samples, and at almost all conversion rates below 1 kJ/kmol, therefore the lines are almost entirely overlapping. In the case of the Starink and OFW method, the differences are between 2 and 3 kJ/kmol, therefore the OFW curve is seen only for higher conversion rates or as a shadow for $\alpha < 0.8$. The activation energy of the initial and final stage seems to be a little underestimated by KAS, OFW, and Starink method, but the trends and values are in good agreement.

Values obtained from the decomposition of the sawdust are significantly higher compared to results reported in previous investigations. For the Friedman method, the mean activation energy is 241 kJ/mol, while for the other methods is slightly lower and about 229 kJ/mol. A similar underestimation of mean activation energy is also observed for the PUR sample. Zhang et al. [14] reported E_a for wood sawdust ~190 kJ/mol, Mishra and Mohanty [28] reported ~170 kJ/mol for pine wood, and 148–181 kJ/mol for sawdust depending on the used method. Alam et al. [16] reported even higher values (265–353 kJ/mol) for the bamboo sawdust for the conversion range ($\alpha = 0.1–0.8$). The activation energy of wheat straw is between 154 and 379 kJ/kmol, while beech sawdust individually has an activation energy in the range between 155 and 316 kJ/kmol [13]. Besides, Luo et al. [13] emphasized the importance of observing activation energy in the separate conversion ranges. Therefore, the division was made for the conversion ranges in the following way: first stage $\alpha = 0.05–0.45$, second stage $\alpha = 0.45–0.7$, and final stage $\alpha = 0.7–0.85$, after which the obtained values show strong divergence. A similar division can be applied for the sample used here as well. In the beginning, up to $\alpha = 0.1$, activation energy sharply increases due to moisture evaporation.

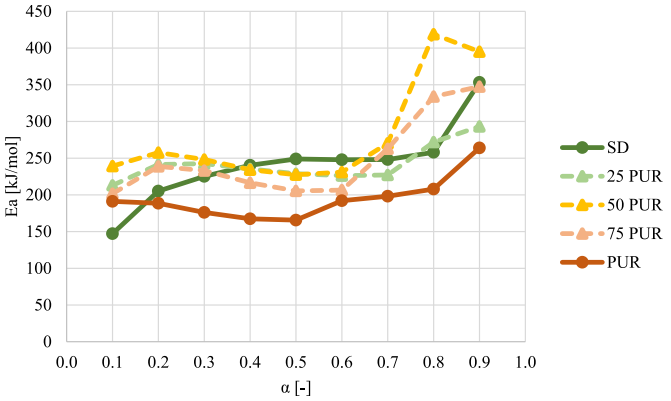

Fig. 4. Friedman's activation energies for investigated samples.

After this point, the curve takes a gradual increase until the $\alpha = 0.5$. Most of the cellulose and hemicellulose content is decomposed in this stage, known as the active pyrolysis area. In the range $\alpha = 0.5–0.8$, the values remain constant, and lignin is mostly decomposed. In the final stage, the E_a sharply increases since most of the material is already decomposed. Once again, similar to the PUR sample, KAS, OFW, and Starink method seems to underestimate E_a values for the first stage of conversion since slightly visible differences are spotted. These differences are becoming less visible as the α continues to increase, and after $\alpha = 0.6$ are almost negligible.

The obtained values of the E_a with respect to the conversion rate (α) for investigated mixtures are more similar to SD than the PUR sample being in the range between 200 and 250 kJ/mol for most of the process. The mean E_a obtained for investigated mixtures is summarised in Table 3. As can be seen, the mixture with a small PUR content expresses the lowest values of E_a (~239 kJ/mol). This is an interesting observation since the individual SD expresses the highest values; therefore, it would be expected the same for the mixture where SD is a dominant compound. Nevertheless, the highest values are noted for the mixture with equal content of both compounds (~277 kJ/mol), which decreases with the further increment of PUR share to ~247 kJ/mol for the mixture with 75 % of PUR. The sawdust influence is visible from the conversion range up to $\alpha = 0.2$, where E_a gradually increases, similar to the SD sample. For the mixture where SD is a dominant compound, the second conversion stage is between $\alpha = 0.2–0.7$, where E_a continuously decrease. This is a completely reverse trend compared to the SD sample, which indicates the apparent influence of PUR content. After the conversion rate of $\alpha = 0.7$, values for E_a start to increase, suggesting that the conversion process has reached the final stage. In the mixture where polyurethane is a dominant compound, the second stage is between conversion rate $\alpha = 0.2–0.6$, once again with decreasing trend. Between $\alpha = 0.6–0.7$, a slight bounce of E_a is reported, followed by a steep increase until the end of the process. This slight bounce is also reported for individual PUR pyrolysis,

Table 3
Activation energy and statistical agreement from investigated samples.

Activation energy [kJ/mol]	Friedman		KAS		OFW		Starink	
	E_a	R^2	E_a	R^2	E_a	R^2	E_a	R^2
Sawdust	241.80	0.9629	229.33	0.9494	227.45	0.9591	229.54	0.9499
25 % PUR	239.42	0.9793	235.95	0.9699	233.91	0.9743	236.17	0.9701
50 % PUR	277.35	0.9485	272.85	0.9520	269.22	0.9572	273.05	0.9523
75 % PUR	247.47	0.9785	240.80	0.9600	237.79	0.9664	241.02	0.9603
PUR	202.27	0.9985	192.00	0.9970	192.57	0.9973	192.28	0.9970

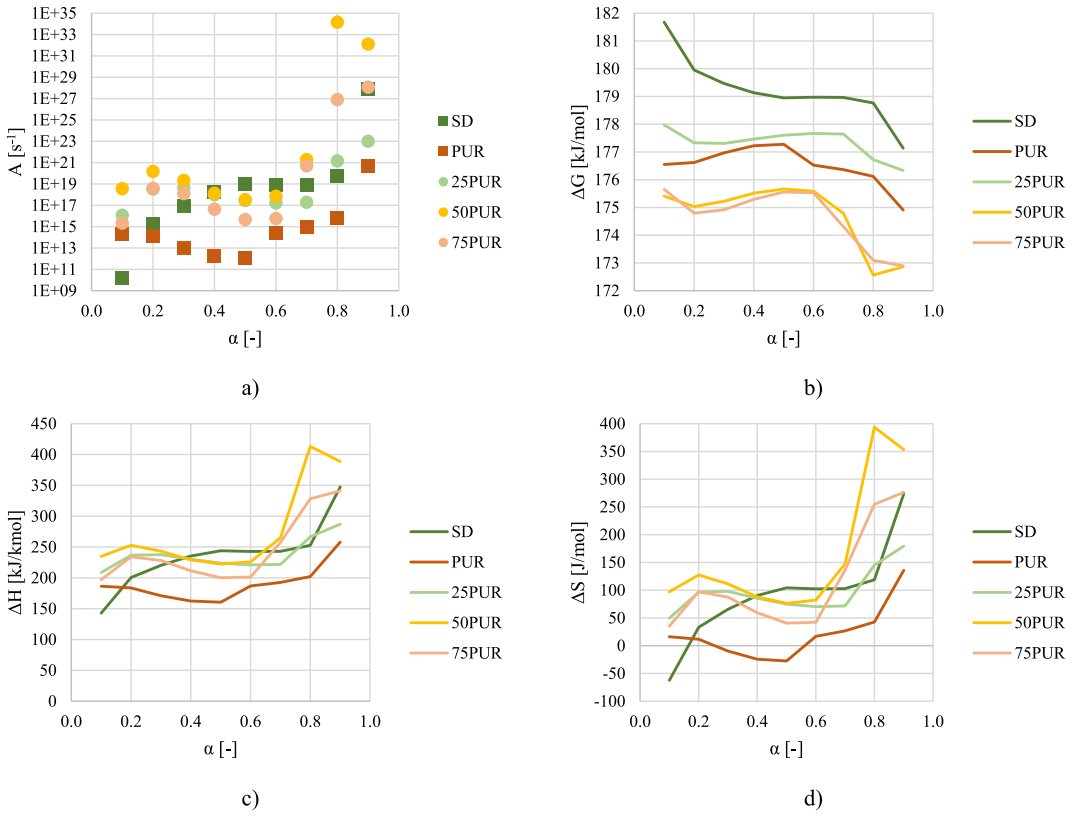

Fig. 5. Thermodynamic parameters calculated at a heating rate of 10 °C/min.

even though it can be seen here that the values are shifted toward higher values of conversion rate. Mixtures with an equal share of each fraction express similar behaviour as the other two mixtures regarding the curve trend. Nevertheless, reported values of E_a are higher compared to other mixtures, especially after $\alpha = 0.7$. This implies that its heterogeneity limits the thermal degradation of mixtures, and therefore, the final mass and end of decomposition are achieved at lower conversion rates.

Comparison of E_a between investigated mixtures suggests that biomass plays a dominant role in the first part of the process ($\alpha < 0.2$), but in the second stage, PUR seems to have a more critical role. Even though the reported values of activation energy are more similar to SD, the decreasing trend noticed for all mixtures suggests that PUR has an important role in process dynamics. The last stage seems to be influenced the most by the mixture composition. In the case of the sample with 25 % of PUR, the increase in the last stage is gradual and starts after the conversion rate of 0.7, while for the other two mixtures increase is steep and starts at $\alpha = 0.6$. Since the mixture where sawdust is the dominant compound also has the lowest final mass, this might suggest that the higher content of the PUR in the mixture hinders the thermal degradation of the sample. Nevertheless, since it is evident that the introduction of the PUR decreased the E_a in the main stage, it is more likely that the heterogeneity of the mixture is more influential for this part.

3.4. Analysis of thermodynamic parameters

In this section, apparent Friedman's activation energies are used to calculate the thermodynamic parameters such as pre-exponential factor and changes of free Gibbs energy, enthalpy, and entropy. In Fig. 4, obtained E_a from Friedman method at 10 °C/min are plotted. This heating rate is used to reduce the impact of constituent interaction that increases at higher heating rates. Once again, the PUR content's influence on the activation energies in the conversion range between 0.2 and 0.6 is evident, even though the obtained values are closer to SD values. Besides, it can be seen that at $\alpha = 0.7$, the activation energy of the mixtures has a steep increment, which is in line with the results from the TG analysis and the final mass of their residues.

The values of pre-exponential factors vary over the range of conversion Fig. 5a. The pre-exponential factor was calculated based on Friedman's method and with the general assumption that a conversion function considers reaction order equals 1 [9]. In general, for all investigated samples, they are above 10^9 s^{-1} immediately after $\alpha = 0.1$. For the sawdust sample, these values are remarkably high ($10^{13}<A<10^{27}$) in the conversion range of $0.1 < \alpha < 0.9$. In the case of the PUR sample, these values are pronouncedly lower and, in the range, $10^{13}<A<10^{20}$. A decrease in the activation energy is followed up by a reduction of a pre-exponential factor in this range, which is then again followed up by the huge jump at higher conversion rates. Pre-exponential factors of investigated mixtures vary in a similar range as these from individual sample analysis. The steep increment is noticed after $\alpha = 0.7$, which is in line with the previously reported results. For all mixtures, the pre-exponential factors are closer to the SD sample. Based on the adopted assumption, the obtained pre-exponential factor represents the theoretical approach, and further research will consider the determination of specific conversion functions for all analysed samples, which will enable a more detailed analysis of pre-exponential factors. The Gibbs free energy (ΔG) changes are almost negligible for the conversion range $0.1 < \alpha < 0.9$, and only a slight decrease is noticed in all samples for approximately $\Delta 5$ kJ/mol. The highest values are calculated for the sawdust sample, which reduces with the increment of PUR content, and finally, the

lowest values are reported for individual polyurethane decomposition (Fig. 5b).

The enthalpy change (ΔH) indicates the difference in energy between the reagent and activated complex (Fig. 5c). For the SD sample, ΔH increases with the conversion range, suggesting that lignin in biomass structure requires more energy for decomposition than hemicellulose and cellulose, which are decomposed in earlier stages. Nevertheless, reported values are high during the whole process, similar to lignin (~239 kJ/mol), indicating high lignin content or complex structure due to heterogenous sawdust composition. In comparison, the enthalpy change for maple leaf residue is only between 68 and 85 kJ/kmol [33]. On the other hand, the calculated values for the PUR are significantly lower (186–257 kJ/mol) and are following the trend of E_a and *A*. This means that the values firstly decrease until $\alpha = 0.5$, and then increase until the end of the process, implying that the PUR sample has clear two stages of degradation, already described above. Firstly, the urethane bond and isocyanates are decomposed, followed by the decomposition of volatiles in the second stage between $\alpha = 0.5–0.8$. The same trend is noticed for the investigated mixtures, even though obtained values are pronouncedly higher and closer to the SD sample. Since the values of ΔH in range $\alpha = 0.3–0.7$ are lower for investigated mixtures than that of individual sawdust, it can be stated that the synergistic effect in that range has a beneficial impact of reducing required heat needed to form activated complex [34].

Entropy represents the disorder degree of the system. Lower entropy values imply that the system underwent some changes and has reached a new state of its own thermodynamic equilibrium. For the SD sample, entropy varies between −62.40 and 273.45 J/mol. This implies that the SD sample achieves a more ordered state at the beginning of the process since the moisture is evaporated and only solid-state remains. As the process proceeds, the solid sample starts to decompose, producing a high amount of gases, and therefore a change of entropy significantly increases with the increment of conversion rate. The evolution of gases from this sawdust mixture is confirmed in the investigation carried out by Stančin et al. [35]. For PUR, entropy starts to increase until $\alpha = 0.12$ (20.53 J/mol) and then starts to decrease immediately to −28.51 J/mol for $\alpha = 0.48$. After this point, an increment is observed once again until the end of conversion. The entropy of the mixture behaves in the same way as the PUR sample regarding the increasing-decreasing trend. Nevertheless, for the mixture, negative values are not reported at any stage of the process. The visible difference between the mixtures is the turning point at which conversion rate takes an increasing or decreasing trend. For the mixture where SD is the major compound, this is at $\alpha = 0.14$ and $\alpha = 0.66$, while for the PUR dominant mixture, this is at $\alpha = 0.22$ and $\alpha = 0.56$. In the case of a mixture with an equal share of both compounds, this is at $\alpha = 0.16$ and $\alpha = 0.54$. Results are given in Fig. 5d.

4. Conclusion

Thermogravimetric analysis of sawdust and polyurethane samples used in this study shows that their decomposition mechanism regarding the shape of the TG curve broadly correlates. This is due to the nature of PUR building units, which are more similar to biomass samples than conventional plastics. The main decomposition stages overlap in a temperature range between 300 and 400 °C, even though the chemical nature and reaction mechanism are entirely different. Thermogravimetric curves of the investigated mixtures are showing different behaviour, depending on the dominant constituent. Nevertheless, for the mixture with an equal share of SD and PUR, reported values of mass loss and thermal decomposition stages are closer to individual PUR analyses. The influence of the heating rate on thermal decomposition is evident since the increment in heating rate shifted peak temperatures and broaden the range in which degradation takes place for all investigated samples. For the individual PUR analysis and mixtures with 50 and 75 % of PUR, an increment of heating rate promotes the degradation, and lower final masses are reported. At the same time, a reverse trend is observed for SD and SD-dominant mixtures.

Calculated activation energies show that there is only a slight difference between the used methods. The KAS, OFW, and Starink methods underestimate E_a in the initial and final stages, while the values are similar for the main conversion range. The highest values are reported for individual SD pyrolysis, while the lowest ones are noted for polyurethane degradation. Besides, a constant increment of E_a is recorded for SD, while for the PUR, values first increase, then decrease, and finally jump to high values at the end of the process. This suggests a clear distinction between the two stages in PUR decomposition, which is also observed for analysed mixtures, even though reported values are closer to SD.

From the presented results, it is obvious that both heating rate and mixture composition have an important influence on process dynamics. As the heating rate increase, thermal degradation is broadened and shifted to higher temperatures. For the mixture composition, it can be stated that at some critical share of plastic content in the range between 25 and 50 %, PUR starts to dominate the decomposition mechanism since the investigated parameters are following the trend similar to that of individual PUR, even though the values are closer to SD sample. For future work, the focus should be shifted to the SD-PUR mixture analysis with a lower share of plastic content (25–50 %) since, in this range, unpredicted behaviour is observed. Even more, a critical point after which the plastic material starts to dictate the degradation mechanism might be located in this area.

Credit author statement

H. Stančin: Conceptualization, experimental investigation, results interpretation, Writing – original draft H.Mikulčić; - numerical investigation, reviewing and editing, Visualization, N.Manić; - Methodology, experimental and numerical investigation, draft preparation, result extraction, D.Stojiljković; - experimental and numerical investigation, result extraction, M.Vujanović; - Supervision, reviewing and editing. X.Wang - Supervision. N.Duić; - Supervision.

Declaration of competing interest

The authors declare that they have no known competing financial interests or personal relationships that could have appeared to influence the work reported in this paper.

References

[1] PlasticsEurope, EPRO. Plastics – the facts. Plast – Facts 2018;2018:38.
[2] Simón D, Borreguero AM, de Lucas A, Rodríguez JF. Recycling of polyurethanes from laboratory to industry, a journey towards the sustainability. Waste Manag 2018;76:147–71. https://doi.org/10.1016/j.wasman.2018.03.041.
[3] Crescentini TM, May JC, McLean JA, Hercules DM. Mass spectrometry of polyurethanes. Polymer (Guildf) 2019;121624:181. https://doi.org/10.1016/j.polymer.2019.121624.
[4] Yao Z, Yu S, Su W, Wu D, Liu J, Wu W, et al. Probing the combustion and pyrolysis behaviors of polyurethane foam from waste refrigerators. J Therm Anal Calorim 2020;141:1137–48. https://doi.org/10.1007/s10973-019-09086-8.
[5] Stančin H, Růžičková J, Mikulčić H, Raclavská H, Kucbel M, Wang X, et al. Experimental analysis of waste polyurethane from household appliances and its utilization possibilities. J Environ Manag 2019;243:105–15. https://doi.org/10.1016/j.jenvman.2019.04.112.
[6] Guo X, Song Z, Zhang W. Production of hydrogen-rich gas from waste rigid polyurethane foam via catalytic steam gasification. Waste Manag Res 2020.

https://doi.org/10.1177/0734242X19899710.
[7] Jurić F, Stipić M, Samec N, Hriberšek M, Honus S, Vujanović M. Numerical investigation of multiphase reactive processes using flamelet generated manifold approach and extended coherent flame combustion model. Energy Convers Manag 2021;114261:240. https://doi.org/10.1016/j.enconman.2021.114261.
[8] Garrido MA, Font R. Pyrolysis and combustion study of flexible polyurethane foam. J Anal Appl Pyrolysis 2015;113:202–15. https://doi.org/10.1016/j.jaap.2014.12.017.
[9] Yao Z, Yu S, Su W, Wu W, Tang J, Qi W. Comparative study on the pyrolysis kinetics of polyurethane foam from waste refrigerators. Waste Manag Res 2020;38:271–8. https://doi.org/10.1177/0734242X19877682.
[10] Mikulčić H, Jin Q, Stančin H, Wang X, Li S, Tan H, et al. Thermogravimetric analysis investigation of polyurethane plastic thermal properties under different atmospheric conditions. J Sustain Dev Energy. Water Environ Syst 2019;7:355–67. https://doi.org/10.13044/j.sdewes.d6.0254.
[11] Stančin H, Mikulčić H, Wang X, Duić N. A review on alternative fuels in future energy system. Renew Sustain Energy Rev 2020;128. https://doi.org/10.1016/j.rser.2020.109927.
[12] Ferreiro AI, Rabaçal M, Costa M. A combined genetic algorithm and least squares fitting procedure for the estimation of the kinetic parameters of the pyrolysis of agricultural residues. Energy Convers Manag 2016;125:290–300. https://doi.org/10.1016/j.enconman.2016.04.104.
[13] Luo L, Guo X, Zhang Z, Chai M, Rahman MM, Zhang X, et al. Insight into pyrolysis kinetics of lignocellulosic biomass: isoconversional kinetic analysis by the modified Friedman method. Energy Fuel 2020;34:4874–81. https://doi.org/10.1021/acs.energyfuels.0c00275.
[14] Zhang X, Deng H, Hou X, Qiu R, Chen Z. Pyrolytic behavior and kinetic of wood sawdust at isothermal and non-isothermal conditions. Renew Energy 2019;142:284–94. https://doi.org/10.1016/j.renene.2019.04.115.
[15] Manić NG, Janković BB, Dodevski VM, Stojiljković DD, Multicomponent Modelling Kinetics Jovanović VV, Thermal Simultaneous. Analysis of apricot kernel shell pyrolysis. J Sustain Dev Energy Water Environ Syst 2020. https://doi.org/10.13044/j.sdewes.d7.0307.
[16] Alam M, Bhavanam A, Jana A, Viroja J kumar S, Peela NR. Co-pyrolysis of bamboo sawdust and plastic: synergistic effects and kinetics. Renew Energy 2020;149:1133–45. https://doi.org/10.1016/j.renene.2019.10.103.
[17] Kim YM, Jae J, Kim BS, Hong Y, Jung SC, Park YK. Catalytic co-pyrolysis of torrefied yellow poplar and high-density polyethylene using microporous HZSM-5 and mesoporous Al-MCM-41 catalysts. Energy Convers Manag 2017;149:966–73. https://doi.org/10.1016/j.enconman.2017.04.033.
[18] Abbas-Abadi MS, Van Geem KM, Fathi M, Bazgir H, Ghadiri M. The pyrolysis of oak with polyethylene, polypropylene and polystyrene using fixed bed and stirred reactors and TGA instrument. Energy 2021;121085:232. https://doi.org/10.1016/j.energy.2021.121085.
[19] Samal B, Vanapalli KR, Dubey BK, Bhattacharya J, Chandra S, Medha I. Influence of process parameters on thermal characteristics of char from co-pyrolysis of eucalyptus biomass and polystyrene: its prospects as a solid fuel. Energy 2021;121050:232. https://doi.org/10.1016/j.energy.2021.121050.
[20] Navarro MV, López JM, Veses A, Callén MS, García T. Kinetic study for the co-pyrolysis of lignocellulosic biomass and plastics using the distributed activation energy model. Energy 2018;165:731–42. https://doi.org/10.1016/j.energy.2018.09.133.
[21] ISO - ISO 14780. Solid biofuels — sample preparation n.d. 2017.
[22] ISO 17225–1. Solid biofuels — fuel specifications and classes — Part 1: general requirements n.d. 2014.
[23] Yuan X, He T, Cao H, Yuan Q. Cattle manure pyrolysis process: kinetic and thermodynamic analysis with isoconversional methods. Renew Energy 2017;107:489–96. https://doi.org/10.1016/j.renene.2017.02.026.
[24] Xu M, Guan J, Wang J. Pyrolysis behavior and kinetics of polyurethane insulation materials from waste refrigerators. Adv Mater Res 2012;356–360:1752–8. https://doi.org/10.4028/www.scientific.net/AMR.356-360.1752.
[25] Nishiyama Y, Kumagai S, Motokucho S, Kameda T, Saito Y, Watanabe A, et al. Temperature-dependent pyrolysis behavior of polyurethane elastomers with different hard- and soft-segment compositions. J Anal Appl Pyrolysis 2020;104754:145. https://doi.org/10.1016/j.jaap.2019.104754.
[26] Jiao L, Xu G, Wang Q, Xu Q, Sun J. Kinetics and volatile products of thermal degradation of building insulation materials. Thermochim Acta 2012;547:120–5. https://doi.org/10.1016/j.tca.2012.07.020.
[27] Jiao L, Xiao H, Wang Q, Sun J. Thermal degradation characteristics of rigid polyurethane foam and the volatile products analysis with TG-FTIR-MS. Polym Degrad Stabil 2013;98:2687–96. https://doi.org/10.1016/j.polymdegradstab.2013.09.032.
[28] Mishra RK, Mohanty K. Pyrolysis kinetics and thermal behavior of waste sawdust biomass using thermogravimetric analysis. Bioresour Technol 2018;251:63–74. https://doi.org/10.1016/j.biortech.2017.12.029.
[29] Slopiecka K, Bartocci P, Fantozzi F. Thermogravimetric analysis and kinetic study of poplar wood pyrolysis. Appl Energy 2012;97:491–7. https://doi.org/10.1016/j.apenergy.2011.12.056.
[30] Oyedun AO, Tee CZ, Hanson S, Hui CW. Thermogravimetric analysis of the pyrolysis characteristics and kinetics of plastics and biomass blends. Fuel Process Technol 2014;128:471–81. https://doi.org/10.1016/j.fuproc.2014.08.010.
[31] Wang H, Wang QS, He JJ, Mao ZL, Sun JH. Study on the pyrolytic behaviors and kinetics of rigid polyurethane foams. Procedia Eng 2013;52:377–85. https://doi.org/10.1016/j.proeng.2013.02.156.
[32] Han B, Chen Y, Wu Y, Hua D, Chen Z, Feng W, et al. Co-pyrolysis behaviors and kinetics of plastics-biomass blends through thermogravimetric analysis. J Therm Anal Calorim 2014;115:227–35. https://doi.org/10.1007/s10973-013-3228-7.
[33] Ahmad MS, Klemeš JJ, Alhumade H, Elkamel A, Mahmood A, Shen B, et al. Thermo-kinetic study to elucidate the bioenergy potential of Maple Leaf Waste (MLW) by pyrolysis, TGA and kinetic modelling. Fuel 2021;293. https://doi.org/10.1016/j.fuel.2021.120349.
[34] Wen Y, Zaini IN, Wang S, Mu W, Jönsson PG, Yang W. Synergistic effect of the co-pyrolysis of cardboard and polyethylene: a kinetic and thermodynamic study. Energy 2021;120693:229. https://doi.org/10.1016/j.energy.2021.120693.
[35] Stančin H, Šafář M, Růžičková J, Mikulčić H, Raclavská H, Wang X, et al. Co-pyrolysis and synergistic effect analysis of biomass sawdust and polystyrene mixtures for production of high-quality bio-oils. Process Saf Environ Protect 2021;145:1–11. https://doi.org/10.1016/j.psep.2020.07.023.

PAPER 5

Thermogravimetric and Kinetic Analysis of Waste Biomass and Plastic Mixtures

H. Stančin[a,*], H.Mikulčić[a,c], N.Manić[b], D.Stojiljković[b], M.Vujanović[a], N.Duić[a]

[a]University of Zagreb, Faculty of Mechanical Engineering and Naval Architecture, Ivana Lučića 5, 10000 Zagreb, Croatia
[b]University of Belgrade, Faculty of Mechanical Engineering, Kraljice Marije 16, Belgrade, Serbia
[c]Department of Thermal Engineering, Xi'an Jiaotong University, Xi'an, Shaanxi, Xianning West Road, Xi'an, China
[*]hrvoje.stancin@fsb.hr

Keywords: thermogravimetric analysis, kinetic analysis, sawdust, polystyrene, polypropylene, co-pyrolysis

Abstract

Thermogravimetric and kinetic analysis of biomass and plastic co-pyrolysis can provide valuable inputs for a better understanding of decomposition mechanisms. Such inputs are important for selecting the appropriate process conditions but can also be helpful for process modelling. This work investigates the properties of heterogenous sawdust in a mixture with polypropylene and polystyrene. Thermogravimetric analysis is conducted to determine the decomposition mechanism and kinetic parameters of investigated mixtures and to derive appropriate conclusions regarding their further utilization potential. Co-pyrolysis was performed on mixtures with the following biomass/plastic ratios: 75-25%, 50-50%, 25-75%, over a temperature range of 30-550 °C, at four heating rates 5, 10, 20, and 30 °C/min, with pure argon as a carrier gas. Obtained results were then subjected to comprehensive kinetic and thermodynamic analysis. The primary goal was to determine effective activation energies using model-free methods, pre-exponential factors, and elementary thermodynamic parameters such as changes in enthalpy, entropy, and free Gibbs energy. Finally, the influence of the heating rate and mixture composition was extensively investigated by analyzing calculated parameters.

5.1. Introduction

Recycling waste and end-of-life plastics emerged as one of the most severe issues nowadays with limited potential to be resolved by conventional recycling techniques. About 27 million tons of plastic waste was generated in the EU in 2018, of which only 31% is recycled, 42% is utilized in the energy recovery process, and almost 30% is landfilled,

resulting in the irrevocable loss of valuable resources [1]. Energy recovery is especially interesting for such materials since it offers a sustainable method to deal with generated waste, but even more, it opens the possibility of producing alternative fuels that can be used elsewhere [2].

Biomass has been widely investigated since it is a feedstock that has been utilized in numerous energy applications for a long time. Nevertheless, some issues constrain the broader deployment of such fuels, like lower heating value, high acidity and viscosity, thermal instability, and similar [3]. For this reason, lately, co-pyrolysis with hydrogen-rich feedstock such as plastics arise as a potential solution to overcome these drawbacks [4]. Complex biomass structural composition depends on its origin, so the decomposition mechanism can vary considerably [5]. The decomposition is even more complicated when it comes to waste biomass such as sawdust (SD), which often consists of different types of wood with a higher share of extractives like minerals. Alam et al. co-pyrolyzed the homogenous bamboo sawdust with low-density polyethylene (LDPE) [6]. The main conclusion is that the increment of heating rates shifts the position of the peak temperatures and broadens the range of degradation mechanism. Luo et al. conducted pyrolysis on beech sawdust intending to determine the decomposition mechanism and activation energies [7]. The three stages of the degradation mechanism have been identified by analysing the conversion rate. Zhang et al. studied wood sawdust in the pyrolysis process [8]. Observations confirmed the three stages of the decomposition mechanism, with the active pyrolysis stage as the most intensified due to the cellulose and hemicellulose degradation.

Like biomass, waste plastics were extensively investigated for fuel production individually and in blends with biomass. Han et al. analysed the kinetic behaviour of polypropylene (PP), two types of polyethylene (LDPE/HDPE), and polyvinyl chloride (PVC) with pine sawdust [9]. The most important observation from this work is that plastics soften at a lower temperature, but it doesn't decompose. In addition, this softening hinders heat and mass transfer, reflecting lower conversion rates for biomass fraction. Suriapparao et al. conducted microwave-assisted co-pyrolysis of PP and PS with a different type of biomass to investigate the plastic influence on bio-oil quality [10]. The results show that PP and PS can enhance the bio-oil quality; nevertheless, more should be done to examine interactions of volatiles during the process. Burra and Gupta investigated the kinetics of pinewood and plastic wastes in co-pyrolysis [11]. Among the used plastics was the PP, for

which it was concluded that two pseudo components are required for the modelling process, and the highest synergy was observed for a mixture with a low share of PP. Stančin et al. investigated kinetics and thermodynamics parameters from the sawdust and polyurethane foam (PUR) mixtures co-pyrolysis at different heating rates [12]. The results show that Friedman's method gives the most accurate data regarding the activation energy (E_a). In addition, due to the nature of PUR, the main decomposition steps overlap even though the chemical mechanisms are entirely different. Finally, interesting observations were noticed regarding the behaviour of mixtures, which was more similar in values and trendline to individual PUR pyrolysis rather than SD. Wang et al. reviewed the possibilities to co-pyrolyze biomass and different types of waste plastics [13]. Even though the results regarding the obtained product are extensively presented, the data regarding the kinetic and thermodynamic parameters are either missing or briefly given. A similar is noted in the work by Zhang et al., where the focus is more on the obtained products than the process's kinetics [14].

This study presents the thermogravimetric analysis (TGA) on waste biomass sawdust (SD) composed of fir, oak, and beech wood with PP and PS. Even though these plastic materials have been widely investigated, the kinetic and thermodynamic analysis results are limited. This is especially evident in the case of co-pyrolysis with biomass, where most of the research focus was on the analysis of obtained pyrolysis products. Therefore, in this research, the complete focus was given to investigating the decomposition mechanism and related parameters of individual and respective sample mixtures. This is important to evaluate the feedstock interaction during the decomposition process, which is crucial in the process modelling.

5.2. Materials and methods

5.2.1. Materials and experimental procedure

The sawdust sample is a mixture composed of fir, oak, and beech wood obtained from a local sawmill, while polypropylene and polystyrene were previously used as packaging materials for dairy products and cutlery. Investigations were carried out for individual and mixture samples where plastic content varied between 25 and 75%. The sample preparation was done according to the standard procedure [15]. The following standard was used [16] to determine investigated samples' ultimate and proximate parameters. Results are presented in Table 5.1. Previously prepared samples were conducted

to Simultaneous Thermal Analysis (STA), providing the data for TGA and DTA analysis on the same sample. The NETZSCH STA 445 F5 Jupiter system was used for STA measurements. The mass of the sample was 10 mg with a deviation of ± 0.5 mg. Samples were heated from room temperature to 550 °C under the four heating rates of 5, 10, 20, and 30 °C/min. Argon was used as a carrier gas with a 70 mL/min flow.

Table 5.1 - Results of Ultimate and Proximate analysis of investigated samples

	Ultimate Analysis[a] (wt.%)					Proximate analysis (wt.%)				HHV (MJ/kg)
Sample	C	H	O[b]	N	S	Moisture	Volatiles	FC	Ash	
PP	85.5	12.4	1.9	0.1	0.1	0.3	98.7	-	1.0	45.9
PS	90.3	8.5	1.0	0.1	0.1	0.2	99.3	-	0.5	39.2
SD	47.3	6.0	46.4	0.3	-	7.4	72.9	18.3	1.4	17.3

[a]On a dry basis
[b]By the difference

5.2.2. Methods for calculation of energy activation and thermodynamic parameters

For the analysis of activation energies (Ea), the four model-free isoconversional methods were used as follows: Friedman (Eq. 5.1), Kissinger-Akahira-Sonuse (Eq. 5.2), and Ozawa-Flynn-Wall (Eq. 5.3):

$$\ln(\beta \frac{d\alpha}{dT}) = \ln[Af(\alpha)] - \frac{E}{RT} \quad \text{Eq. 5.1}$$

$$\ln(\frac{\beta}{T^2}) = \ln\left[\frac{AR}{EG(\alpha)}\right] - \frac{E}{RT} \quad \text{Eq. 5.2}$$

$$\ln \beta = \left[\frac{0.0048 * AE}{RG(\alpha)}\right] - 1.052(\frac{E}{RT}) \quad \text{Eq. 5.3}$$

Where α stands for the degree of conversion, β represents the heating rate, and T is the temperature. The pre-exponential coefficient is A, E is the activation energy, and R represents the universal gas constant. The thermodynamic parameters and the pre-exponential factors are calculated with the following equations 5.4-5.7:

- Pre-exponential factor (A) $$A = \frac{\beta * E * \exp(\frac{E}{R * T_m})}{R * T_m^2} \quad \text{Eq. 5.4}$$
- Changes of enthalpy (ΔH) $$\Delta H = E - RT_\alpha \quad \text{Eq. 5.5}$$

- Changes in entropy (ΔS) $$\Delta S = \frac{\Delta H - \Delta G}{T_m}$$ Eq. 5.6

- Changes of free Gibbs energy (ΔG) $$\Delta G = E + R * T_m * \ln(\frac{K_B * T_m}{h * A})$$ Eq. 5.7

Where K_B is Boltzmann constant (1.381×10^{23} J/K), h stands for the Plank constant (6.626×10^{34} Js), T_m is determined as the DTG peak temperature, and T_α is the temperature at the degree of conversion α [17].

5.3.Results

5.3.1. Thermogravimetric analysis of individual samples

Figure 5.1 presents the thermogravimetric (TG) curves for individual polypropylene and polystyrene decomposition obtained at four different heating rates. The sawdust decomposition was detailly investigated in previous work [12]; therefore, it won't be discussed extensively here. Briefly, decomposition starts with moisture evaporation below 100 °C and ends at 110 °C for a slow heating rate (5 °C/min) and 140 °C for higher heating rates (10 and 20 °C/min). The mass loss in this stage is around 5%. The main stage, where mostly cellulose and hemicellulose are decomposed, starts at about 290 °C for a slow heating rate, while increment of heating rates shifted this to slightly higher temperatures of 300 °C. From DTG curves, decomposition peaks are noted at 342, 352, and 358 °C, respectively. This shift in the temperature range due to the heating rate increment was already pointed out in a couple of other studies [18-19]. The main reason for this phenomenon is heat transfer limitation derived from a temperature gradient between the inner part and particle surface which block the complete release of volatiles [6]. The second stage ends between 370 °C (5 °C/min) and 383 °C (20 °C/min). Mass loss is more than 60% of the initial sample at this stage. In the last step, lignin is decomposed, and the final mass is about 20% of the initial sample.

As expected, the single-step mechanism is observed in the case of individual polypropylene and polystyrene decomposition (Figure 5.1). This single-step mechanism is already reported in the literature for plastic materials [20]. The degradation of polypropylene starts at approximately 400 °C for all heating rates. The main peak is observed at 445 °C for a slow heating rate, gradually shifting to 455, 470, and 475 °C with the increment of heating rates, respectively. The visible degradation ends at approximately 470 for 5 and 10°C/min,

while for the high heating rate of 20 and 30 °C/min end temperature is slightly below 500 °C. Polystyrene degradation starts a bit earlier compared to PP, at 375 °C. Consequently, the peaks occur at a lower temperature as well, between 405 °C for 5 °C/min and 435 °C in case of 30 °C/min. The degradation is completed at 450 °C for 5 and 10 °C/min heating rates, while a slightly broader range is noted for high heating rates with an end temperature of approximately 475 °C. Regarding the final mass, in the case of PP, about 5% of solid residue is left, while almost 18% is observed in the case of PS. The value for PP is expected since it is already reported in the literature [10]. Nevertheless, the value for PS is relatively high and unexpected since the values found in the literature are pronouncedly lower [21]. This might be the consequence of some contamination or impurities related to the synthesis procedure's usage or nature. The bottom one in the first place refers to the desired density (extruded, expanded, foam, etc.), which can significantly influence the properties of the plastic.

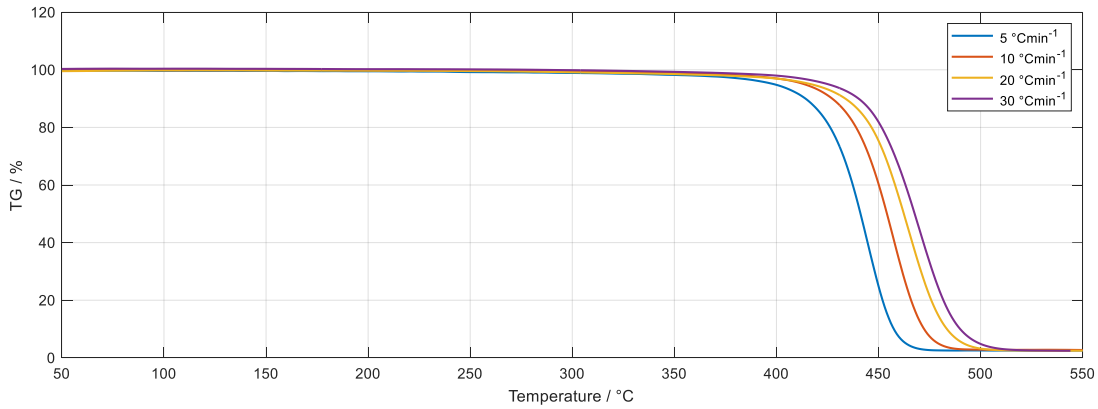

a) Polypropylene

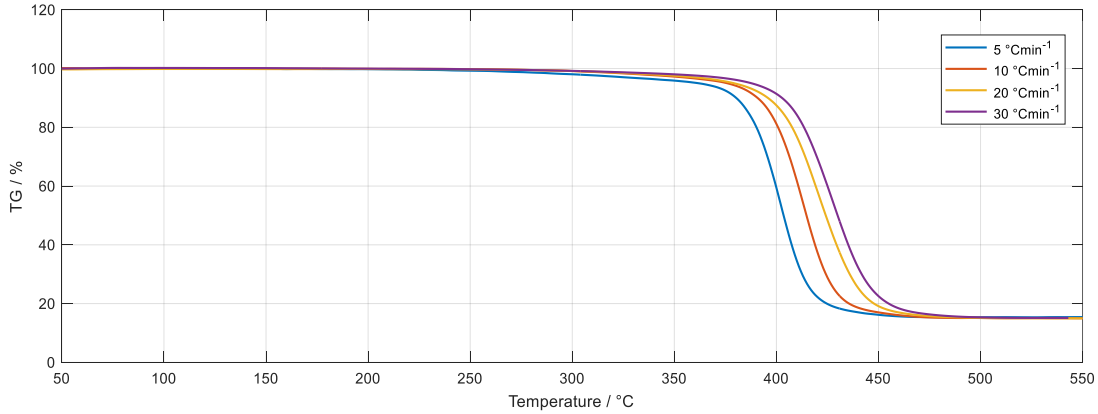

b) Polystyrene

Figure 5.1 - TG curves of Polypropylene (a) and Polystyrene (b) decomposition

5.3.2. Thermogravimetric analysis of sawdust and polypropylene and polystyrene mixtures

The thermal degradation of mixtures is presented in Figure 5.2 and Figure 5.3. It is observed from TG curves that the samples with 25 and 50% plastic content express two stages of degradation. The first stage, up to 400 °C, is primarily due to the decomposition of the biomass component, while the second stage represents plastic decomposition. Besides, for the mixtures with 25% of plastics, it can be noted a small evaporation step below 100 °C accounted for less than 5% mass loss. The influence of the heating rate on this first stage is just slightly visible for investigated mixtures of both plastic materials. In the case of PP (Figure 5.3), increment of heating rates shifted the temperatures of the first peaks for approximately 5 °C with each increment of the rate, from 345 °C for 5 °C/min to 355 °C for 20 and 30 °C/min. Similar behaviour is also noted for PS (Figure 5.2), with exactly the same positions as the first peaks. This implies that at this temperature range, only sawdust is decomposed. It should be noted that the increment of plastic content greatly reduces the intensity of the first peak. Even though this is expected, the reduction is quite pronounced for the mixtures with an equal share of both feedstocks, suggesting that plastics may hinder the complete sawdust decomposition in the first stage. This phenomenon was already reported by Han et al. and here confirmed for both investigated plastics [9]. This might directly affect the final product yield and distribution in the pyrolysis process but should be examined more. The end of the first stage is at about 375 °C for the case of 5 and 10 °C/min, while for higher heating rates of 20 and 30 °C/min, the end temperature is increased to 390 °C. As expected, the mixtures where sawdust is the main compound have a higher mass loss in this first stage due to the decomposition of cellulose and hemicellulose. Almost half of the mass sample is decomposed in the first stage. As the share of the plastic fraction increases, the mass loss decreases. Therefore, for the mixtures with an equal share of both feedstocks, the remaining masses at the end of the first stages are between 70-75%. Further increment of plastic content to 75% of the mixture composition reduces mass loss even more, and the remaining mass is up to 80%. It should be emphasised that the heating rate has a limited influence on mass loss in the first stage. A slow heating rate of 5°C/min ensures better heat transfer and release of volatiles. Therefore, the mass losses are more pronounced in this case. Nevertheless, the differences between the slowest and fastest heating rates are less than 10% in sample mass. Finally, it can be stated that the decomposition mechanism of

the first stage is more influenced by the mixture composition rather than the heating rate [19]. The TG and DTG curves clearly show that fast-heating rates of 20 and 30 °C/min express almost identical behaviour. The only visible stand-out is noted for 5 °C/min, even though this influence also disappears as the share of plastics increases.

The second stage follows up immediately after the completion of the first one. In the case of PP-derived mixtures, the lag between the two stages of degradation is slightly more pronounced, especially for the mixture with 25% of PP (plateau in Figure 5.3a). The second stage almost overlaps with the first one for PS-containing mixtures, which can be expected since the onset temperature for individual PS degradation is 375 °C. Consequently, the second peak corresponding to plastic decomposition appears earlier in the case of PS than PP. The main degradation step of the second stage for PS-containing mixtures occurs between 420 and 430 °C and increases with the increment of the heating rate. The sawdust has a limited influence on the position of the second peak since it is just slightly shifted to higher temperatures compared to individual PS analysis. The end of the second stage is slightly above 450 °C, similar to individual PS decomposition, which confirms that the influence of SD on the second stage is limited. Nevertheless, the influence of the mixture composition is a crucial parameter for the final mass. A mixture with 25% of PS has a quite high final mass of residue, which accounts for the 25% of the initial mass. This is even higher than the results from individual SD analysis, where approximately 20% of the final mass was observed. Further increment of the PS reduces the final mass below 20%, with only minor differences observed between applied heating rates. Generally, the heating rate has a moderate influence on the second stage of degradation. While the impact on final mass is almost negligible, the intensity and the position of the second peak are highly dependent on this parameter. An increment of the heating rate shifts the peak positions and end temperatures to higher values, broadening the range in which decomposition occurs. Besides, the degradation intensity is considerably higher with high heating rates, suggesting that most volatiles are released in the narrow temperature range shortly before the process completes. Due to that fact, the residence time of volatiles released in the second stage is reduced, which might benefit the yield of condensable products obtained as bio-oil [22].

For the PP-containing mixtures, the second peak's position corresponds to the peak from individual PP decomposition. There are no visible differences among the investigated mixtures, which means that PP decomposition dominates in this stage. This is also supported

by the fact that the mixtures with a higher portion of PP have a broader range in which decomposition occurs, similar to individual analysis. Nevertheless, there are pronounced differences in terms of applied heating rates. An increment of heating rate firstly shifts the temperature of the second peak to higher values but also broadens the range in which decomposition takes place. This difference between the slowest and fastest applied heating rate can be up to 40 °C in terms of ending temperature. Since both investigated parameters, heating rate and mixture composition, have a notable impact on the second stage, the differences between final masses are more pronounced. The mixture with 25% sawdust has a final residue of 20%, similar to individual SD. This is further reduced by incrementing plastic content to 15 and 10%, respectively. It is interesting to notice that in the case of a mixture with 75% of PP, the lowest final mass (5%) is noted for the heating rates of 10 and 20 °C/min, while almost 10% is observed for 5 °C/min.

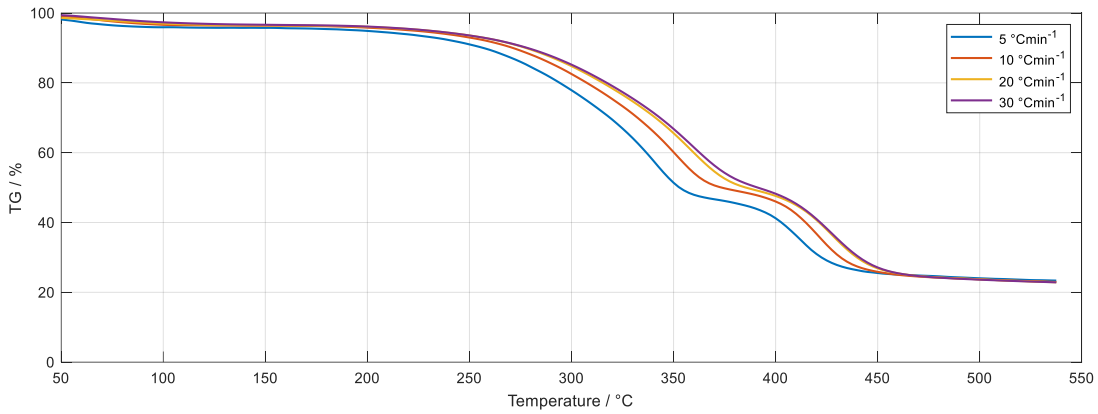

a) 25% PS

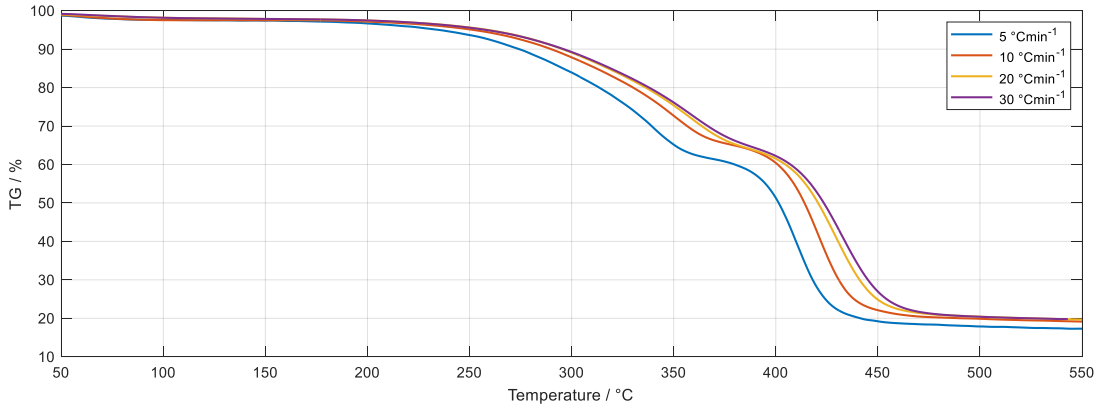

b) 50% PS

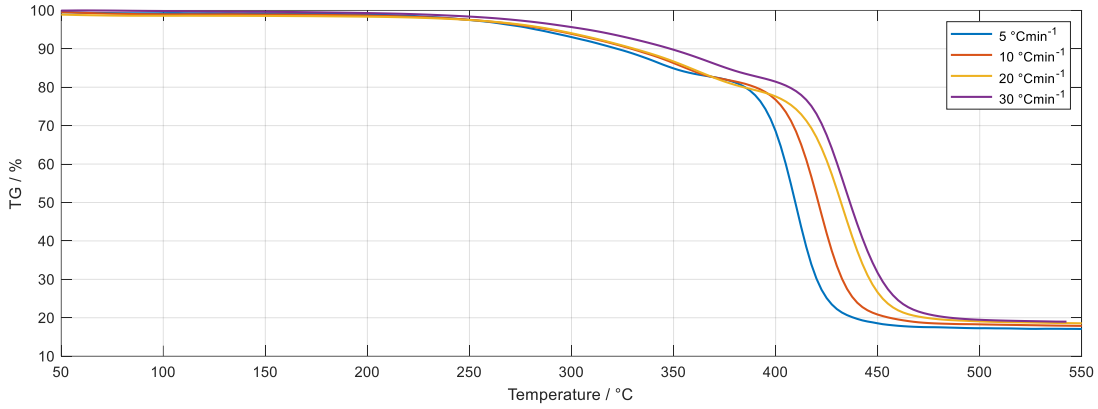

c) 75% PS

Figure 5.2 - TG curves from sawdust and PS mixture pyrolysis a) 25% PS b) 50% PS c) 75% PS

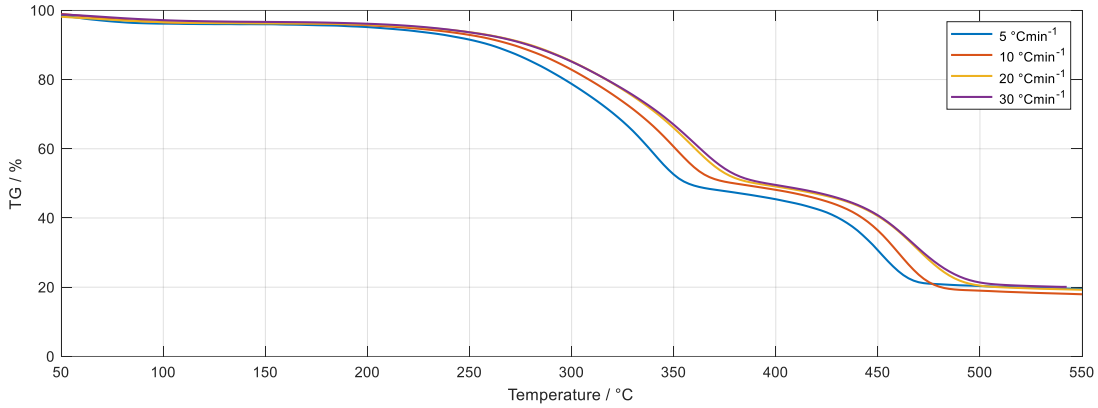

a) 25% PP

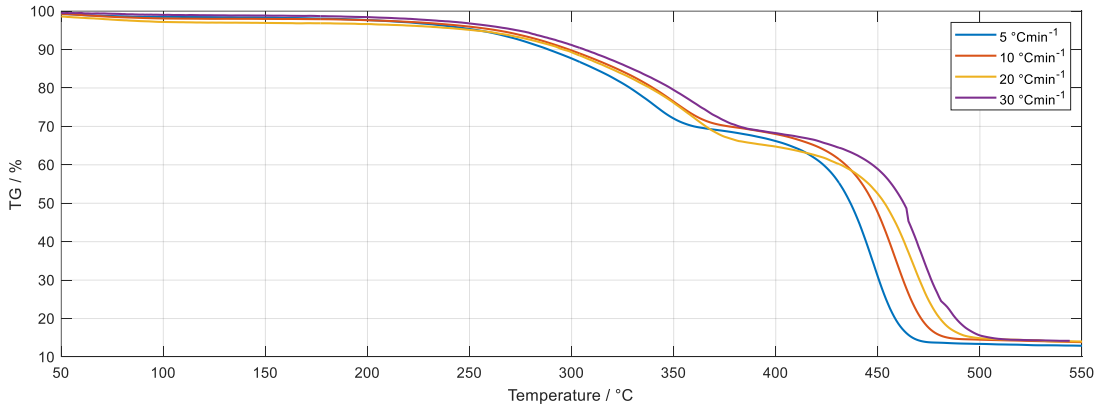

b) 50% PP

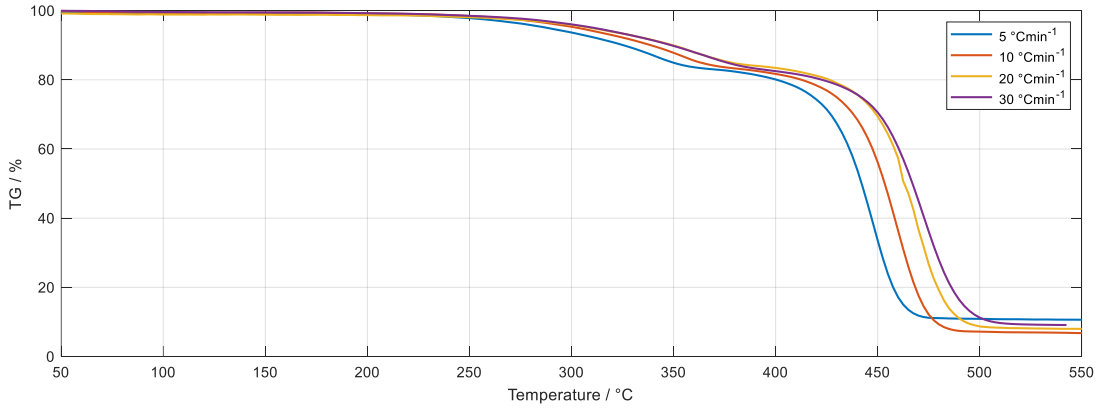

c) 75% PP

Figure 5.3 - TG curves from sawdust and PP mixture pyrolysis a) 25% PP b) 50% PP c) 75% PP

Table 5.2 summarises the final mass values for all investigated samples and applied heating rates. Interestingly, only the mixture with 25% of PS yields a higher final mass of residue than individual sample analysis. This implies that the synergistic effect could be very strong for this mixture and that feedstock interaction hinders the complete release of volatiles. As can be seen, the influence of heating rates on final mass residue is less pronounced than the mixture composition is.

Table 5.2 - Final mass of solid residues from individual and mixture pyrolysis at investigated heating rates

Final mass [%]	5 °C/min	10 °C/min	20 °C/min	30 °C/min
Sawdust	*19.6*	*20.6*	*20.7*	-
25% PP	19.5	18.0	19.2	20.1
50% PP	12.9	13.9	14.0	14.2
75% PP	10.6	6.8	8.0	9.1
PP	*2.6*	*2.7*	*2.5*	*2.5*
25% PS	23.4	22.9	22.9	22.9
50% PS	17.3	19.1	19.7	19.8
75% PS	17.1	17.9	18.6	19.0
PS	*15.4*	*15.0*	*14.9*	*15.1*

5.3.3. The activation energy of individual samples and their respective mixtures

The activation energy (E_a) was calculated using the model-free isoconversional Friedman, Kissinger-Akahira-Sonuse, and Ozawa-Flynn-Wall methods. Obtained values show excellent statistical correspondence by observing the statistical R^2 factor (>0.877) for the range of conversion between α=0.1-0.9. Below and above these points, obtained activation energies show bigger discrepancies and lower statistical agreement, as already reported in the literature [8]. In general, only minor differences are observed between the used methods (Figure 5.4). The results are plotted in separate figures for each method.

For individual samples, the activation energies follow the same pathway for the whole range of conversion (α=0.1.-0.9). In the case of PS, the activation energies are around 290 kJ/mol at α=0.1 for all used methods. As the decomposition proceeds, the values of activation energies decrease, following the linear pathway until the end of the process. Friedman's method gives the activation energy of 220 kJ/mol at α=0.9, while 229 kJ/mol is obtained for the other methods. It should be noted that the reported values and trends are entirely different and reversed here compared to a study by Ozsin et al. [23]. In this work, we have found significantly higher values, which might explain why the final mass was notably higher here. Activation energies of PP show slightly lower values at α=0.1, being 283, 280, 277 for Friedman, KAS, and OFW methods. As the decomposition continues, a minor increase of 10 kJ/mol is noted for KAS and OFW at α=0.3, starting with a linear

decrease until the end of the process. Final activation energy values at α=0.9 show more significant discrepancies between the methods used. For Friedman's method, 198 kJ/mol is calculated, while KAS and OFW give pronouncedly higher values of 248 kJ/mol. Once again, values reported in this work are greatly higher than those found by Han et al., 2014a, and the trend is also reversed. Here, the Ea is high at the beginning of the process and decreases as the conversion proceeds, while in the case of Han et al., the values are constantly increasing throughout the process. Sawdust was analysed in previous work, but it should be briefly mentioned that activation energies can be divided into three stages. The first one is between conversion rates 0.1 and 0.2, with a steep increment from 150 to 200 kJ/mol. The second stage expresses a linear increase from 200 to 250 kJ/mol for α=0.2-0.8. This stage is known as the active pyrolysis area, where mostly cellulose and hemicellulose are decomposed. The steep increase is again noted in the last stage, with a final value of 350 kJ/mol at α=0.9. This steep increase in the last stage for the SD can be expected since most of the sample is already decomposed here. In the case of plastics, this phenomenon is not observed since the final residue of plastic is occasionally below 5% of initial mass, which means that decomposition is happening in a broader conversion range, and it is usually done at this last stage. Literature reported that mean values for sawdust Ea differ, but the most often are below 200 kJ/mol [24]. This is pronouncedly lower in comparison with polyethylene (PE), polystyrene (PS), or polypropylene (PP), where mean values are about 250 kJ/mol [25]. From Table 5.3 it is visible that mean activation energies for PS, and PP used in this work are close to values reported in the literature with a remarkable coefficient of determination (R2).

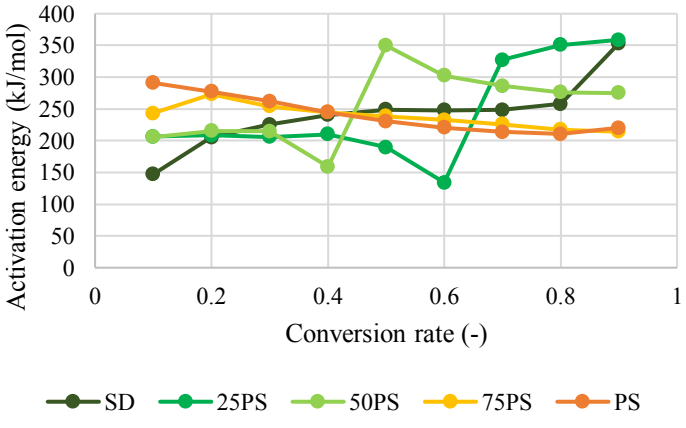

a) Friedman

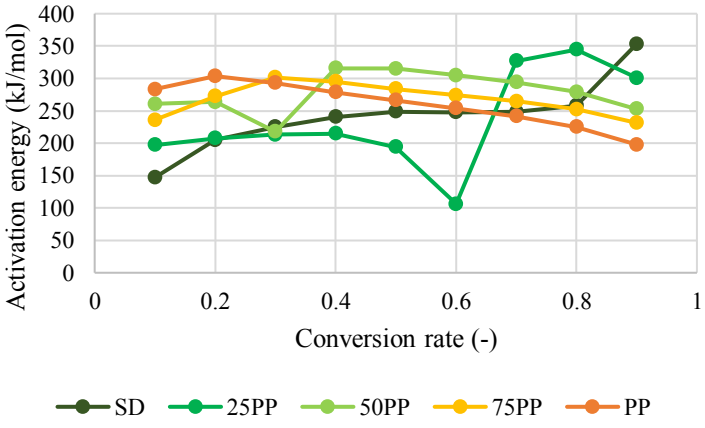

b) Friedman

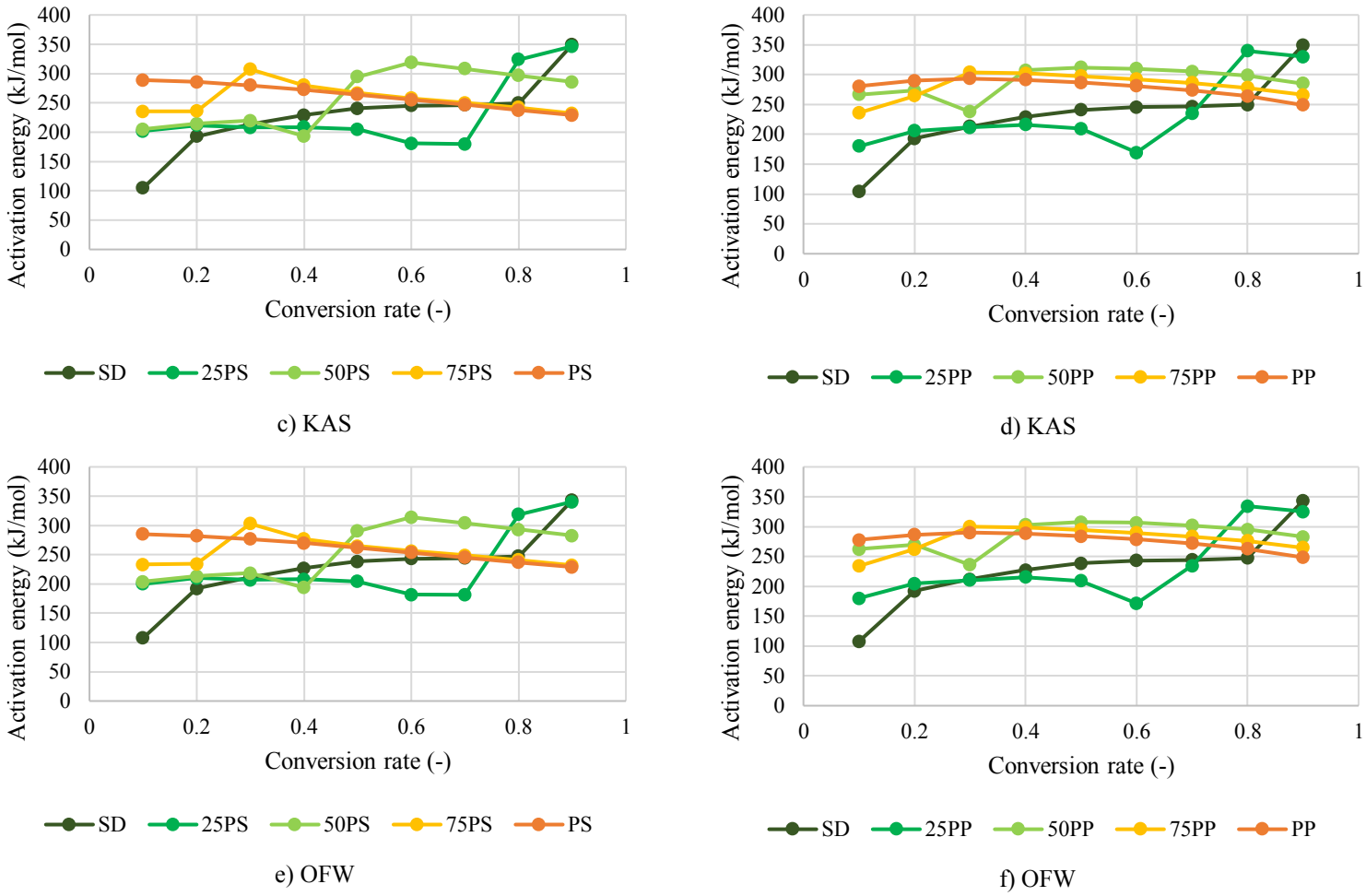

Figure 5.4 - Calculated activation energies for individual samples and respective mixtures for investigated samples - PS (left), PP (right)

Analysis of activation energies of investigated mixtures is important to identify their decomposition mechanism, which can later be used in the modelling procedure. As can be seen, the activation energies are strongly dependent on mixture composition. In addition, similar to individual sample analysis, the activation energies of all investigated mixtures show slight differences between Friedman's and the other two methods, where values are almost identical. For the mixtures where SD is the dominant compound, a slight increase of activation energies in the first stage (α=0.4) can be observed, like individual SD. In the case of a 25% PS mixture, the activation energy at α=0.1 is 200 kJ/mol, which is only slightly increased to 210 kJ/mol at α=0.4. The values are similar for the methods used. On the other hand, for the mixture with 25% PP at α=0.1, Friedman's method gives 200 kJ/mol, while KAS and OFW values are around 180 kJ/mol. Since the sawdust decomposition is happening at the beginning of the process, and the values from Friedman's method correspond to those obtained for PS mixtures, it is evident that KAS and OFW underestimate activation energies

for the mixture with 25% PP. The second stage for this mixture can be observed between the conversion range of 0.4 and 0.6. In this range, activation energies continuously decrease, but the values between the methods used are more pronounced. Friedman's method shows greatly lower values at α=0.6, which is for the mixture with 25% PS 134 kJ/mol, while 106 kJ/mol is noted for 25% PP. The KAS and OFW values are 180 and 170 kJ/mol for mixtures with 25% PS and PP, respectively. After this, a sharp increase is noted until α=0.8, indicating the changes in the decomposition mechanism. At this stage, activation energies are higher compared to individual samples, which might imply that sawdust and plastic decomposition interfere. Friedman's method slightly overestimates the E_a for the mixture with 25% PS. For all other mixtures, between 320 and 340 kJ/mol is obtained. The activation energy slightly increases for the mixture with 25% PS until the end of the process, while for the mixture with 25% PP, a minor reduction occurs.

The equal share of sawdust and plastic compounds reflects an equal division between the conversion ranges. For the PS/SD mixtures, the first stage is between conversion rates 0.1 and 0.4, where a more-less constant value of activation energies (~215 kJ/mol) is observed, with a smooth decrease to 193 kJ/mol at the end. This reduction is more pronounced in the case of Friedman's method. Between conversion rates 0.4 and 0.5, a steep increment can be seen, indicating the decomposition mechanism shift from sawdust to PS component. This change in mechanism shows more uncertainties for the Friedman method compared to KAS and OFW. The second stage of decomposition occurs in the range $0.5<\alpha<0.9$, where activation energy slowly decreases to final values of 275 and 285 kJ/mol for Friedman and the other two methods, respectively.

A mixture with an equal share of polypropylene and sawdust shows interesting results in terms of decomposition stages. The first stage, related to sawdust decomposition, goes until α=0.3, which is quite a short range compared to one attributed to PP decomposition. Here, the activation energy decreases from starting value of about 260 kJ/mol to 236 kJ/mol for KAS and OFW methods and slightly lower 218 kJ/mol for Friedman's. This follows a sharp jump to almost 310 kJ/mol at α=0.4. The second stage, which accounts for PP decomposition, shows a decreasing trend of activation energies. Friedman's method gives 253 kJ/mol as the final value, while slightly higher values (~285 kJ/mol) are noted for KAS and OFW methods. It should be emphasised that obtained values for the second stage's activation energies are pronouncedly higher than individual PS and PP decomposition. This

suggests that sawdust decomposition that is proceeding has a significant influence on the degradation of plastic components afterwards. This is an important observation related to pyrolysis since it shows that there are notable volatile interactions inside the reactor.

Finally, a mixture with dominant plastic compounds expresses almost the same behaviour as the individual plastic samples. Only discontinuity is seen at the beginning of the degradation until α=0.3, where values sharply rise from 234 to 307 kJ/mol for both types of plastic feedstock. After this, the activation energies are almost overlapping until the α=0.9. For both plastic fractions, PS and PP, the final value of activation energy is around 230 kJ/mol. For both plastics, Friedman's method underestimates the final activation energy for 20 and 30 kJ/mol for PS and PP, respectively.

Table 5.3 - Activation energy and respective statistical agreement for investigated samples

Activation energy [kJ/mol]	Friedman		KAS		OFW	
	E_a	R^2	E_a	R^2	E_a	R^2
Sawdust	241.8	*0.963*	229.3	*0.949*	227.5	*0.959*
25% PP	230.6	*0.887*	228.0	*0.973*	226.8	*0.887*
50% PP	274.4	*0.947*	285.1	*0.943*	281.7	*0.946*
75% PP	264.1	*0.965*	278.4	*0.958*	275.7	*0.995*
PP	259.2	*0.988*	276.8	*0.985*	274.5	*0.986*
25% PS	238.1	*0.914*	228.7	*0.899*	227.2	*0.906*
50% PS	253.2	*0.917*	254.9	*0.907*	252.5	*0.914*
75% PS	235.8	*0.938*	254.9	*0.944*	253.0	*0.946*
PS	239.9	*0.995*	254.5	*0.993*	252.7	*0.994*

Results given in Table 5.3 represents the mean activation energy for all investigated samples and used methods. Since the mixtures have two decomposition mechanisms, they can only be used as orientational values. From the results, it is interesting that mixtures with an equal share of both feedstocks express the highest values. This could mean that mixture heterogeneity, most visible here, greatly impacts the required energy to decompose samples.

5.3.4. Analysis of thermodynamic parameters

Apparent Friedman's activation energies are used to calculate the pre-exponential factors and thermodynamic parameters. A similar analysis was not found in the literature; therefore, the results cannot be compared. In Figure 5.5 a) and b), are plotted calculated values of E_a from the Friedman method at 10 °C/min. Usage of this heating rate for

thermodynamic calculations reduces the impact of constituent interaction that increases with the increment of the heating rate. Since the extensive analysis of activation energies is given in the previous chapter, it won't be discussed further here.

The pre-exponential factor was calculated based on Friedman's method and with the general assumption that a conversion function considers reaction order equals 1 [9]. In general, for all investigated samples, they are above 10^{10} s^{-1} immediately after α=0.1. For the sawdust sample, these values are remarkably high ($10^{13}<A<10^{27}$) in the conversion range of $0.1<\alpha<0.9$ and are increasing as the conversion proceeds. A complete reversal trend is observed for plastic materials. For both plastic samples, the pre-exponential factor is high at the beginning of conversion ($1.8x10^{20}$, and $7.6x10^{17}$ s^{-1} for PS and PP, respectively) and then gradually decreases (Figure 5.5c) and d)). This implies that samples are highly reactive at the beginning of the decomposition, but this characteristic fades away as the conversion intensifies. The values of pre-exponential factors greatly vary for PS-containing mixtures, especially for the mixtures with 25 and 50% of PS. Steep increments are observed at conversion ranges 0.6 and 0.4 for mixtures with 25, and 50% of PS, respectively, suggesting the change of decomposition mechanism already reported above. This observation also applies to the changes in enthalpy and entropy, which will be discussed later. In the second stage of decomposition, values of pre-exponential factors are further increased. This implies frequent collision occurs between volatiles released from SD decomposition in the previous step and PS in this stage. In the case of a mixture with 25% of PP, the first stage and mechanism change are quite similar to the counterpart with PS, with slightly lower values. Lower values of pre-exponential factors mean that PP notably hinders sawdust decomposition, probably due to plastics softening. This is even more evident from the mixture with 50% of PP, where pre-exponential values follow the trend of the individual PP sample. Observed values of the pre-exponential factor for the second stage are lower in the case of PP-containing mixtures compared to PS ones, suggesting the lower reactivity of PP.

The changes in Gibbs energy are almost negligible thorough-out the process (Figure 5.5 e), f)). It is only interesting to see that the values for the mixture with 25% of PS are similar to individual SD decomposition. On the other hand, the values for the mixture with 25% PP are more like individual PP decomposition. This again confirms the hypothesis that PP significantly impacts sawdust decomposition since even a small presence greatly influences the process.

The changes in enthalpy and entropy are firmly following the activation energy trendline. This is expected since activation energy and enthalpy changes actually have the same meaning, and they represent the amount of energy that needs to be brought to the system to initiate chemical reactions. Therefore, from a thermodynamic perspective, it can be stated that introducing a small plastic fraction (up to 25%) reduced the required energy to support the sawdust decomposition. Nevertheless, it causes a tremendous increase in energy needed for the second stage of decomposition, visible in Figure 5.5 g) and h). A mixture with an equal share of SD and PS follows a similar trendline as a mixture with 25% of PS until the changes in the decomposition mechanism. In this case, an even greater amount of energy is required to initiate plastic fraction decomposition. Even though once initiated, the reactions require less energy, and enthalpy changes are decreased, like individual PS. The opposite is noticed for the mixture with an equal share of SD and PP. Here, the presence of PP immediately raises the required energy to initiate the mixture decomposition. Nevertheless, in the case of PP-containing mixtures, its presence didn't affect the second stage of the process that much. Obtained changes in enthalpy are higher than individual PP, but their differences are visibly lower compared to PS-containing mixtures.

Changes in entropy give information about the level of order inside the system. Higher entropy also implies higher reactivity of the system. As expected, the highest level of disorder for analysed mixtures occurs after the change of decomposition mechanism (Figure 5.5 i) and j)). Therefore, it can be stated that interaction between biomass and plastic-derived compounds can only happen in the second stage of decomposition. In this stage, temperatures are sufficient to initiate plastic decomposition and support the complete decomposition of the solid and volatile products obtained in the previous step.

Finally, the results for mixtures with 75% of PS or PP were not discussed solely because values strongly correlate with the values from the individual sample analysis. The only valuable observation is related to reduced values of all investigated parameters at the beginning of the process. This means that a small portion of biomass can slightly lower the energy consumption at the beginning of the process. Still, the process will be governed by a plastic decomposition mechanism.

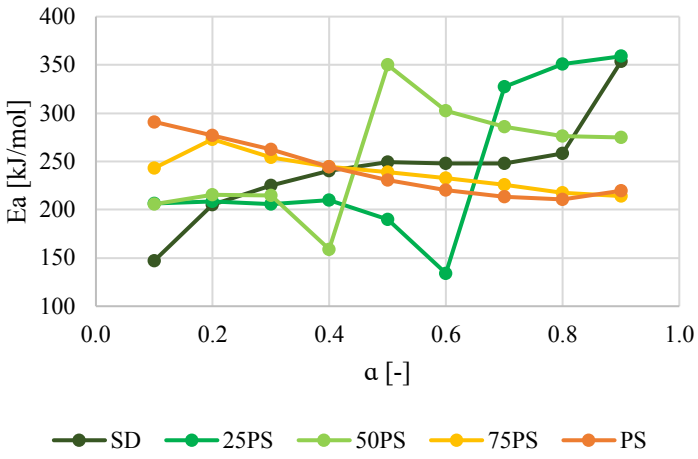
Ea [kJ/mol]
400
350
300
250
200
150
100
0.0
0.2
0.4
0.6
0.8
1.0
α [-]
SD
25PS
50PS
75PS
PS

a)

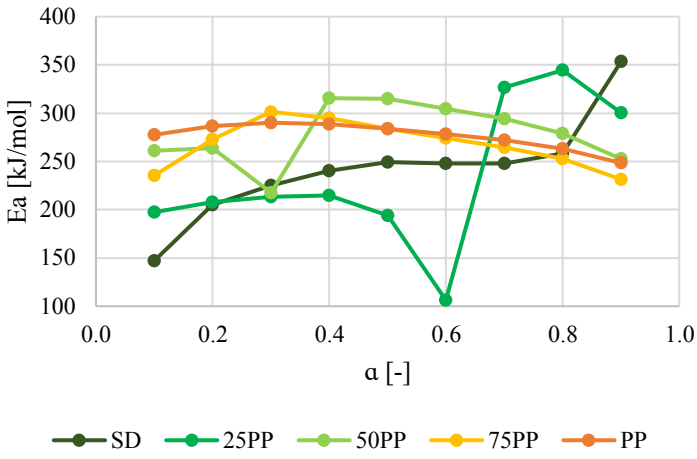
Ea [kJ/mol]
400
350
300
250
200
150
100
0.0
0.2
0.4
0.6
0.8
1.0
α [-]
SD
25PP
50PP
75PP
PP

b)

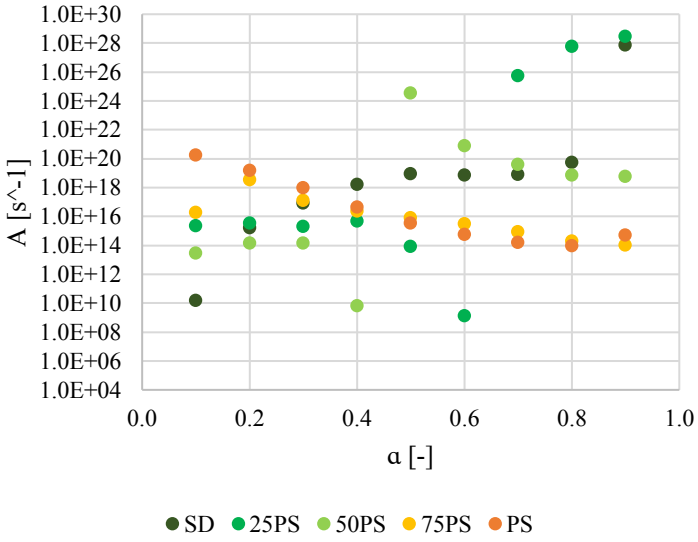
A [s^-1]
1.0E+30
1.0E+28
1.0E+26
1.0E+24
1.0E+22
1.0E+20
1.0E+18
1.0E+16
1.0E+14
1.0E+12
1.0E+10
1.0E+08
1.0E+06
1.0E+04
0.0
0.2
0.4
0.6
0.8
1.0
α [-]
SD
25PS
50PS
75PS
PS

c)

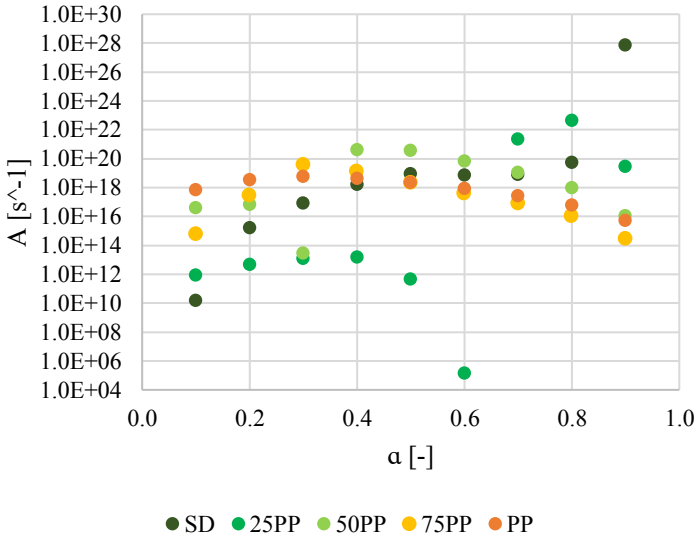
A [s^-1]
1.0E+30
1.0E+28
1.0E+26
1.0E+24
1.0E+22
1.0E+20
1.0E+18
1.0E+16
1.0E+14
1.0E+12
1.0E+10
1.0E+08
1.0E+06
1.0E+04
0.0
0.2
0.4
0.6
0.8
1.0
α [-]
SD
25PP
50PP
75PP
PP

d)

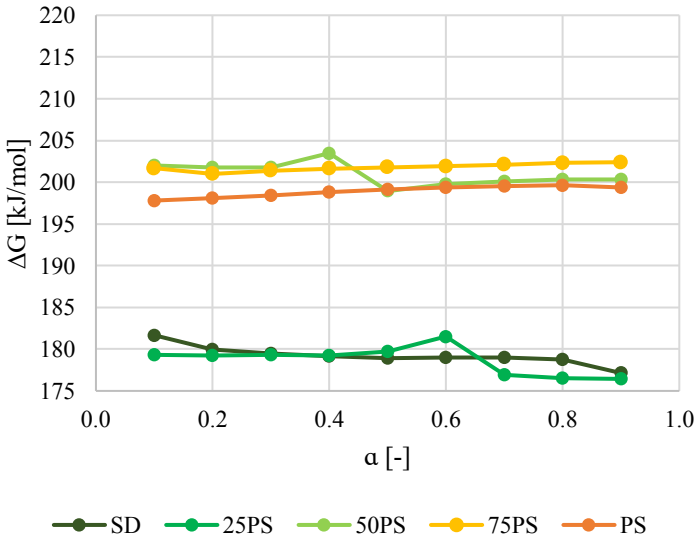
ΔG [kJ/mol]
220
215
210
205
200
195
190
185
180
175
0.0
0.2
0.4
0.6
0.8
1.0
α [-]
SD
25PS
50PS
75PS
PS

e)

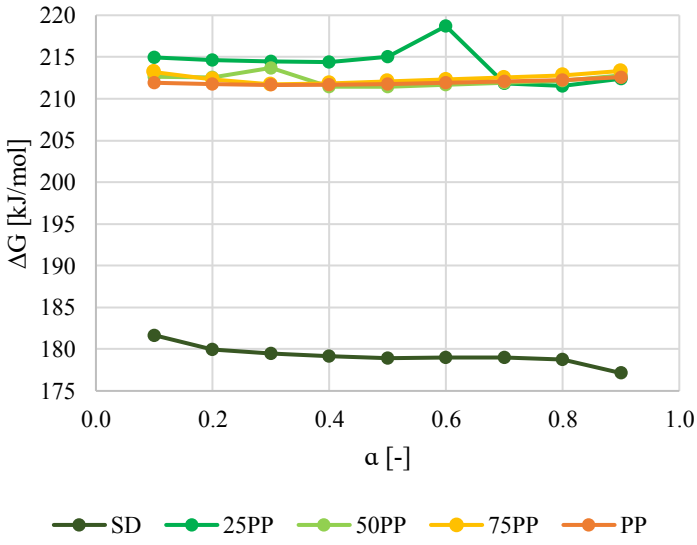
ΔG [kJ/mol]
220
215
210
205
200
195
190
185
180
175
0.0
0.2
0.4
0.6
0.8
1.0
α [-]
SD
25PP
50PP
75PP
PP

f)

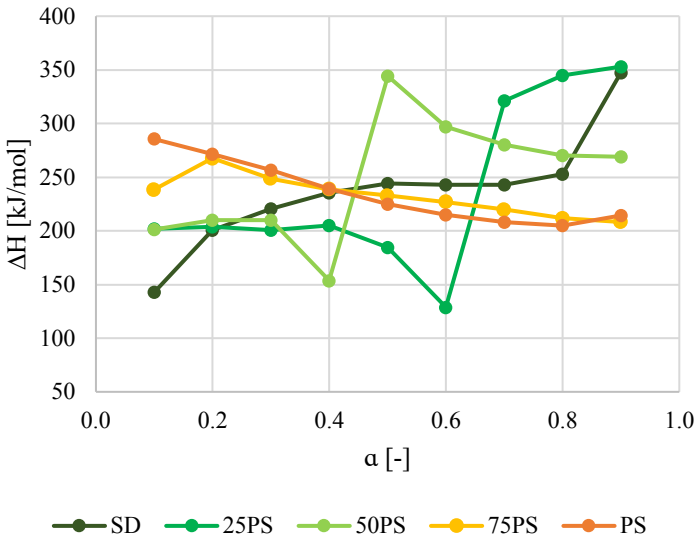

g)

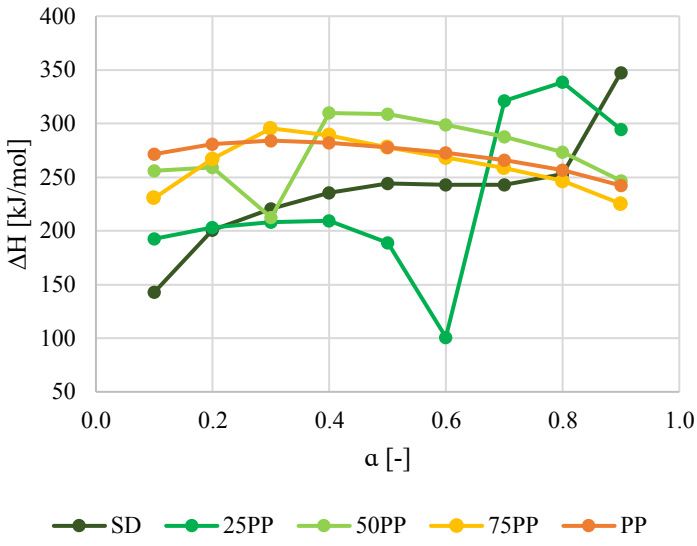

h)

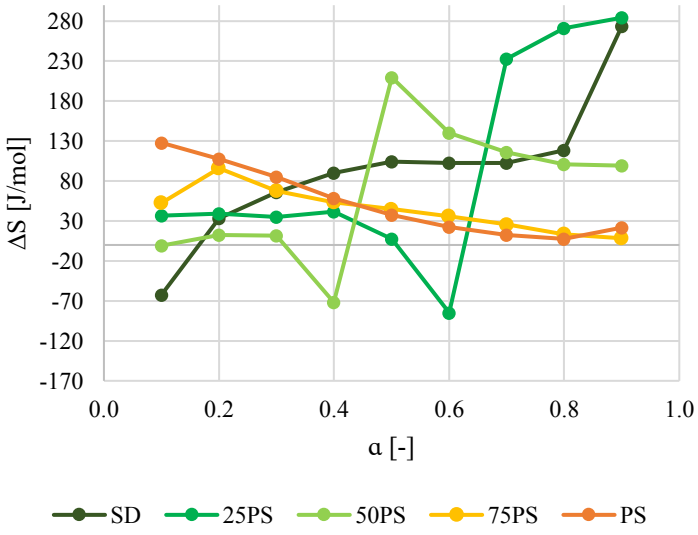

i)

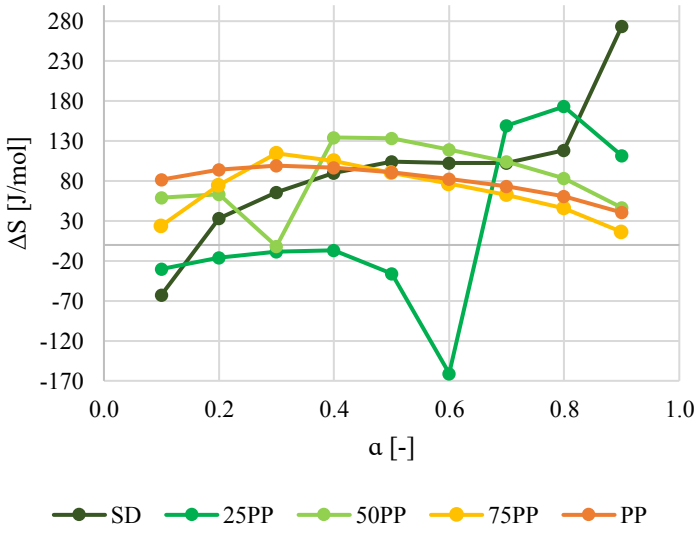

j)

Figure 5.5 - Thermodynamic parameters for analysed samples; a-b) activation energy, c-d) pre-exponential factors, e-f) Gibbs free energy, g-h) changes in enthalpy, i-j) changes in entropy

5.4. Conclusion

Carried out work that consisted of thermogravimetric, kinetic, and thermodynamic analysis, shows some interesting results and valuable inputs for experimental and computational modelling of the co-pyrolysis process:

- The heating rate has a limited impact on process kinetics in a way that the increment of the heating rate slightly shifts the observed temperatures to higher values. The impact on the final mass of residue is almost negligible since the differences are less than 3%.

- The mixture's composition greatly influences the final mass residue, which decreases with the increment of plastic content. Furthermore, the mixture composition plays a crucial role in the decomposition mechanism and, consequently, the kinetic and thermodynamic parameters. First of all, the share of each component determines the conversion range at which changes in the decomposition mechanism occur. Secondly, a low portion of sawdust decreases the mean activation energies of the process, while a high share of plastic fraction closes the values to individual plastic samples. Finally, the highest values of activation energies are noted for the mixture with an equal share of both feedstocks, indicating that the mixture's heterogeneity is an important issue.
- For the mixtures with equal shares of both components, polypropylene leads the decomposition mechanism almost through the entire conversion range, while polystyrene follows the sawdust mechanism. This implies that PP can soften and hinder the SD decomposition in the first stage, consequently interfering with heat and mass transfer.

References

[1] PlasticsEurope; EPRO, 'Plastics – the Facts', *Plastics – the Facts 2018*, p. 38, 2018.

[2] H. Stančin, H. Mikulčić, X. Wang, and N. Duić, 'A review on alternative fuels in future energy system', *Renewable and Sustainable Energy Reviews*, vol. 128, 2020, doi: 10.1016/j.rser.2020.109927.

[3] H. Hassan, J. K. Lim, and B. H. Hameed, 'Recent progress on biomass co-pyrolysis conversion into high-quality bio-oil', *Bioresource Technology*, vol. 221. Elsevier Ltd, pp. 645–655, Dec. 01, 2016. doi: 10.1016/j.biortech.2016.09.026.

[4] X. Zhang, H. Lei, S. Chen, and J. Wu, 'Catalytic co-pyrolysis of lignocellulosic biomass with polymers: A critical review', *Green Chemistry*, vol. 18, no. 15. Royal Society of Chemistry, pp. 4145–4169, 2016. doi: 10.1039/c6gc00911e.

[5] X. Hu and M. Gholizadeh, *Biomass pyrolysis: A review of the process development and challenges from initial researches up to the commercialisation stage*, vol. 39. Elsevier B.V. and Science Press, 2019. doi: 10.1016/j.jechem.2019.01.024.

[6] M. Alam, A. Bhavanam, A. Jana, J. kumar S. Viroja, and N. R. Peela, 'Co-pyrolysis of bamboo sawdust and plastic: Synergistic effects and kinetics', *Renew Energy*, vol. 149, pp. 1133–1145, 2020, doi: 10.1016/j.renene.2019.10.103.

[7] L. Luo *et al.*, 'Insight into Pyrolysis Kinetics of Lignocellulosic Biomass: Isoconversional Kinetic Analysis by the Modified Friedman Method', *Energy and Fuels*, vol. 34, no. 4, pp. 4874–4881, 2020, doi: 10.1021/acs.energyfuels.0c00275.

[8] X. Zhang, H. Deng, X. Hou, R. Qiu, and Z. Chen, 'Pyrolytic behavior and kinetic of wood sawdust at isothermal and non-isothermal conditions', *Renew Energy*, vol. 142, pp. 284–294, 2019, doi: 10.1016/j.renene.2019.04.115.

[9] B. Han *et al.*, 'Co-pyrolysis behaviors and kinetics of plastics-biomass blends through thermogravimetric analysis', *J Therm Anal Calorim*, vol. 115, no. 1, pp. 227–235, Jan. 2014, doi: 10.1007/s10973-013-3228-7.

[10] D. v. Suriapparao, B. Boruah, D. Raja, and R. Vinu, 'Microwave assisted co-pyrolysis of biomasses with polypropylene and polystyrene for high quality bio-oil production', *Fuel Processing Technology*, vol. 175, pp. 64–75, Jun. 2018, doi: 10.1016/j.fuproc.2018.02.019.

[11] K. G. Burra and A. K. Gupta, 'Kinetics of synergistic effects in co-pyrolysis of biomass with plastic wastes', *Appl Energy*, vol. 220, pp. 408–418, Jun. 2018, doi: 10.1016/j.apenergy.2018.03.117.

[12] H. Stančin *et al.*, 'Thermogravimetric and kinetic analysis of biomass and polyurethane foam mixtures Co-Pyrolysis', *Energy*, vol. 237, Dec. 2021, doi: 10.1016/j.energy.2021.121592.

[13] Z. Wang, K. G. Burra, T. Lei, and A. K. Gupta, 'Co-pyrolysis of waste plastic and solid biomass for synergistic production of biofuels and chemicals-A review', *Progress in Energy and Combustion Science*, vol. 84. Elsevier Ltd, May 01, 2021. doi: 10.1016/j.pecs.2020.100899.

[14] X. Zhang, H. Lei, S. Chen, and J. Wu, 'Catalytic co-pyrolysis of lignocellulosic biomass with polymers: A critical review', *Green Chemistry*, vol. 18, no. 15. Royal Society of Chemistry, pp. 4145–4169, 2016. doi: 10.1039/c6gc00911e.

[15] 'ISO - ISO 14780:2017 - Solid biofuels — Sample preparation'.

[16] 'ISO 17225-1:2014(en), Solid biofuels — Fuel specifications and classes — Part 1: General requirements'.

[17] X. Yuan, T. He, H. Cao, and Q. Yuan, 'Cattle manure pyrolysis process: Kinetic and thermodynamic analysis with isoconversional methods', *Renew Energy*, vol. 107, pp. 489–496, 2017, doi: 10.1016/j.renene.2017.02.026.

[18] R. K. Mishra and K. Mohanty, 'Pyrolysis kinetics and thermal behavior of waste sawdust biomass using thermogravimetric analysis', *Bioresour Technol*, vol. 251, pp. 63–74, 2018, doi: 10.1016/j.biortech.2017.12.029.

[19] K. Slopiecka, P. Bartocci, and F. Fantozzi, 'Thermogravimetric analysis and kinetic study of poplar wood pyrolysis', *Appl Energy*, vol. 97, pp. 491–497, 2012, doi: 10.1016/j.apenergy.2011.12.056.

[20] R. Miandad, M. A. Barakat, A. S. Aburiazaiza, M. Rehan, and A. S. Nizami, 'Catalytic pyrolysis of plastic waste: A review', *Process Safety and Environmental Protection*, vol. 102, pp. 822–838, 2016, doi: 10.1016/j.psep.2016.06.022.

[21] H. Stančin *et al.*, 'Co-pyrolysis and synergistic effect analysis of biomass sawdust and polystyrene mixtures for production of high-quality bio-oils', *Process Safety and Environmental Protection*, vol. 145, pp. 1–11, Jan. 2021, doi: 10.1016/j.psep.2020.07.023.

[22] F. Abnisa and W. M. A. Wan Daud, 'A review on co-pyrolysis of biomass: An optional technique to obtain a high-grade pyrolysis oil', *Energy Convers Manag*, vol. 87, pp. 71–85, Nov. 2014, doi: 10.1016/j.enconman.2014.07.007.

[23] G. Özsin, A. E. Pütün, and E. Pütün, 'Investigating the interactions between lignocellulosic biomass and synthetic polymers during co-pyrolysis by simultaneous thermal and spectroscopic methods', *Biomass Convers Biorefin*, vol. 9, no. 3, pp. 593–608, Sep. 2019, doi: 10.1007/s13399-019-00390-9.

[24] H. Wang, Q. S. Wang, J. J. He, Z. L. Mao, and J. H. Sun, 'Study on the pyrolytic behaviors and kinetics of rigid polyurethane foams', *Procedia Eng*, vol. 52, pp. 377–385, 2013, doi: 10.1016/j.proeng.2013.02.156.

[25] B. Han *et al.*, 'Co-pyrolysis behaviors and kinetics of plastics-biomass blends through thermogravimetric analysis', *J Therm Anal Calorim*, vol. 115, no. 1, pp. 227–235, Jan. 2014, doi: 10.1007/s10973-013-3228-7.

PAPER 6

Co-pyrolysis of three-component biomass-plastic mixture for alternative fuel production

Stančin, H[1]; Strezov, V[1]

[1] *School of Natural Sciences, Faculty of Science and Engineering, Macquarie University, Sydney, 2109, NSW, Australia*

Abstract

Thermochemical conversion of waste materials recently gained significant attention since it opens the opportunity for the simultaneous production of alternative fuels while tackling issues related to waste management. Co-pyrolysis of waste biomass and plastics is very promising since the demand for feedstock can be satisfied from different streams, while obtained products have higher value properties. In this work, detailed experimental analysis and product characterisation is performed for three individual samples (pine sawdust, polypropylene, polystyrene) and their respective mixtures with 50% of sawdust, and 50% of plastics equally divided between polypropylene and polystyrene. Results showed that feedstock interaction during co-pyrolysis generally enhances the product properties compared to individual pyrolysis. In the case of pyrolysis oil, a high yield of almost 80% is obtained, with hydrocarbons as the most prominent constituents. Higher than theoretically expected liquid yield is achieved at the expense of gaseous fraction. Since sawdust is the primary source of gases, the mixture's gas composition was weakly affected by the introduction of plastics. Finally, the synergistic effect that occurs between biomass and plastics moderately impacts solid residue, which is slightly increased compared to theoretical values. It can be stated that introducing plastics greatly improves the properties of pyrolytic products, especially when aiming to maximise high-quality liquid yield.

8.1. Introduction

Energy transition requires utilisation of novel, sustainable and alternative fuels, which should fill the gap where electrification is not sufficient or feasible. Chemicals, like hydrogen, ammonia and methanol, are widely promoted due to their properties related to carbon neutrality when produced from renewable sources. Moreover, the thermochemical conversion of various feedstock into valuable products is rapidly gaining more attention [1]. Pyrolysis or biomass gasification is a known process that converts raw feedstock into liquid (oils), gases and charred products [2]. Nevertheless, there are several significant constraints when it comes to biomass-derived products. Since biomass is mainly built of oxygen containing atoms, a high share of

oxygenated compounds is also identified in derived products [3]. In the case of gaseous products, this reflects on the high share of carbon dioxide (CO_2) and monoxide (CO), with bio-oils also containing oxygenated compounds [4], mainly belonging to the organic groups like alcohols ketones, acids, and esters. The presence of such compounds is not wanted if the intention is to produce alternative fuels since they reduce the heating value, cause thermal instability and inhibit corrosion [5]. While biomass is considered the most promising alternative due to its abundance and carbon neutrality, sustainability questions are lately raised due to potential over-use of biomass [6-7]. Therefore, the primary focus should be shifted to maximum utilisation of waste biomass potential, like sawdust, and forestry residues, etc.

Similarly, pyrolysis is also a promising solution to end-of-life plastics [8]. Various plastics have been subjected to experimental investigations with the aim to produce alternative fuels. Nevertheless, not all types of plastics are suitable for the process. Polyvinyl chloride (PVC) has high chlorine content [9], polyethylene terephthalate (PET) and high-density polyethylene (HDPE) have good mechanical recycling potential that should be promoted [10-11], while polyurethane foams (PUR) yield high share of nitrogen-containing compounds like amines [12], which is not suitable for fuel production. That leaves low-density polyethylene (LDPE), polypropylene (PP) and polystyrene (PS) as a potential feedstock for the process. In addition, LDPE is hard to separate from mixed waste plastics, raising severe issues in input feedstock control. PP and PS are abundant waste materials used in different applications with minimal conventional recycling potential. Therefore, their utilisation in pyrolysis offers excellent potential to deal with waste management while simultaneously producing high-quality fuels. Production of high-quality fuels seems to be especially interesting since pyrolysis oil built of hydrocarbons is the main product of plastic decomposition [13]. Even more, PP primarily yields linear and cyclic hydrocarbons compatible with fuel requirements [14], while aromatics are the main compounds from PS pyrolysis [15]. Aromatics are preferred in fuel composition, especially in aviation, due to high heating values and octane number, but to a limited extent since they release dense smoke, which can cause engine choking [16].

Co-pyrolysis was introduced to resolve issues related to individual pyrolysis of either biomass or plastics [17]. In co-pyrolysis, plastic serves as a hydrogen donor to biomass, enhancing the properties of derived products by increasing hydrocarbon content at the expense of oxygenated organic groups [18-19]. Additionally, co-pyrolysis relieves the pressure on a supply chain for raw feedstock since the demand is divided among different waste streams. Up to now, co-pyrolysis has been conducted for a wide range of feedstock [20-25], but most of the studies offer limited information regarding the product characterisation due to dispersed

research focus. A comprehensive assessment and characterisation of all obtained products, particularly those found in pyrolysis oil, are important to give better insight into product selectivity based on feedstock interaction. Better understating of process dynamics is inevitable in designing optimal mixture composition and scaling up the process on a commercial level.
For the purposes of this work, theoretical background analysis supported by individual experiments is carried out before determining co-pyrolysis mixture composition and process parameters. Based on these results, the three-component mixture was selected with the precise role and share for each component. The mixture's composition is set to maximise oil yield with predominantly hydrocarbon content. Pine sawdust is the main constituent ensuring low carbon impact, while the role of plastics is to enhance hydrocarbon content and maximise liquid yield. The selected mixture is subjected to a series of experiments, from thermogravimetric and thermal analysis through pyrolysis and detailed characterisation of pyrolytic products to determine their potential applications.

8.2. Materials and methods

8.2.1. Sample preparation

Samples used in this study were waste plastics (PS and PP) and radiata pine sawdust (SD). The plastic samples were previously used as packaging materials for food products (PP) and disc cases (PS). Before subjecting to experimental investigations, samples were shredded, sieved, and dried. Particle sizes were <0.125 mm for SD and <0.45 mm for plastics obtained through sieving to ensure a satisfactory level of mixture homogeneity. Drying was carried out in a vacuum oven at 70 ºC for three hours to remove moisture content. All experiments were performed for individual samples and their mixture with 50% SD and 50% plastics equally divided between PS and PP.

To determine the elemental composition of the samples, analysis was performed according to the standard procedure [26]. The ultimate analysis was carried out for raw samples and the charred residue collected from 600 ºC. Proximate analysis was carried out on 1±0.010 g of samples to determine the share of volatile matter (VM) [27], moisture [28], and ash content [29]. Additionally, fixed carbon (FC) was calculated by the difference.

8.2.2. Thermal analysis

Thermal analysis was carried out in an infrared furnace by heating the samples from room temperature to 1000 ºC at a constant heating rate of 10 ºC/min. Samples masses were 1 g ±

0.15 g. Nitrogen was used to ensure an inert atmosphere with a 5 ml/min flow rate. The experimental setup and calculation methods are described in detail by Strezov et al. [30]. Besides determining the nature of reactions, results were also used to determine the final temperature for pyrolysis, considering the temperature lag between the samples' surface and centre.

8.2.3. Thermogravimetric analysis

Thermogravimetric analysis (TGA) was carried out on Mettler Toledo TGA/DSC 1 STARe system instrument. Samples with an initial mass of about 11 mg were heated from room temperature to 1000 ºC at a heating rate of 10 ºC/min under an inert atmosphere. Nitrogen was used as carrier gas with a 20 ml/min flow. Results were used to determine the sample decomposition mechanism and final masses of solid residue.

8.2.4. Pyrolysis and oil characterisation

The pyrolysis of individual samples and their mixture was performed in an infrared furnace for pyrolysis temperatures of 500 and 600 ºC. The heating rate was 10 ºC/min, with nitrogen as carrier gas at a 10 ml/min flow rate. Initial sample masses varied due to their densities being 825, 950, 1250 and 1400 mg for SD, mixture, PP and PS, respectively. The liquid fraction was collected at the end of the tube, diluted with dichloromethane and stored in the freezer before being subjected to gas chromatography-mass spectrometry (GC/MS) to determine chemical composition. The liquid yield was calculated by the difference between initial mass and solid and gas yields. Before GC/MS analysis, pyrolysis oils were dehydrated with sodium sulfite (anhydrous) to remove moisture content and filtrated using washed silica gel to remove impurities. To remove organic compounds, silica gel was previously baked at 450 ºC between 24-48h.

Spectral analysis was carried out by Agilent Technologies 5977A MSD with an integrated 7890B GC system equipped with an HP 5 ms column (30 m x 250 μm x 0.25 μm). The samples were injected at 300 ºC in splitless mode with helium as carrier gas at a constant 1 ml/min flow rate. The organic compounds were separated by the oven programme starting at 40 ºC with a retention time of 2 min, heating at 4 ºC/min to 300 ºC and hold up time of 45 min. The transfer line temperature was set at 300 ºC, with quadrupole and ion-source temperatures of 150 and 250 ºC, respectively. The organic compounds were identified and quantified by internal standards of the Agilent Qualitative software database and through comparison with literature.

8.2.5. Gas chromatography

The gas characterisation was conducted using Agilent Technologies 490 micro GC. Column 1 consisted of 5 m PBQ + 10m MS5A, while column 2 was 10 m PPU. Samples with 100 mg mass were pyrolysed from room temperature to 1000 ºC at a heating rate of 10 ºC/min. Helium was used as a carrier gas with a 50 ml/min flow. Before entering the chromatograph, gases were cooled in an ice bath to ensure that only non-condensable gases passed through. The gas yield was calculated on a He-free basis.

8.2.6. Fourier Transform Infrared Spectroscopy

Fourier Transform Infrared Spectroscopy (FTIR) was performed for the raw samples and charred residue collected at 600 and 1000 ºC. Nicolet 6700 FT-IR was used to determine the spectral compositions from 4000 to 500 cm^{-1} wavenumber. The results were compared with the internal software spectra database (OMNIC Spectra) and related literature.

8.3. Results

8.3.1. Ultimate and proximate analysis

Results from the ultimate (elemental) and proximate analysis are summarised in Table 8.1. They are in agreement with the results found in the literature [1, 4, 31], with high carbon and hydrogen content observed in PS and PP, with a low oxygen share. This confirms the hypothesis that plastic samples can act as hydrogen donors. On the other hand, sawdust comes with a relatively high share of oxygen, which also translates to a higher contribution of oxygen in the mixture. The proximate analysis showed a high share of volatile matter (>87%) in all samples, which can be beneficial for achieving higher liquid yields. Furthermore, the share of ash and FC is very low for individual samples, consequentially in the mixture (1.3%), indicating low solid residue at the end of the process. Moisture share in SD is slightly higher (9.3%) but still in the acceptable range for pyrolysis [32].

Table 8.1 - Results from ultimate and proximate analysis

	Ultimate analysis					Proximate analysis			
	C	**H**	**N**	**S**	**O***	**VM**	**Ash**	**Moisture**	**FC***
SD	46.2	6.4	-	-	47.4	87.9	0.6	9.3	2.2
PP	81.9	14.6	-	-	3.5	96.3	2.5	0.6	0.7
PS	90.9	7.8	-	-	1.3	99.6	0.1	0.3	-
Mixture	62.9	8.6	-	-	28.5	93.9	1.1	4.8	0.2

*calculated by the difference

8.3.2. Thermogravimetric and thermal analysis

Thermogravimetric analysis is typically applied as a preliminary experimental method to determine the decomposition mechanism of the sample. Plastic samples, such as PS and PP, have been widely investigated [33-35], and results from their analysis are mostly very similar among the studies. This is because polymer materials are built from monomer units which decompose simultaneously in a very narrow temperature range [34]. Discrepancies can occur if plastic is heavily treated with additives in the production stage or due to some external impurities collected during the exploitation stage. Plastic samples used in this study have degradation mechanisms already reported in the literature and corresponding to the results from their proximate analysis (Table 8.1). Since the share of ash and FC is initially low, the remaining solid residue at the end of the process is also expected to be low. Results for all samples are presented in Figure 8.1.

PS starts to decompose at around 350 ºC with a very steep mass loss in a single step. At 450 ºC, decomposition is finished, with a final mass residue of only 1.1%. Similarly, PP decomposition starts at a slightly higher temperature of 400 ºC and continues until 490 ºC, where most of the sample is already decomposed, resulting in a final mass of 3.7%.

Biomass decomposition exhibits a more complicated degradation mechanism than plastic samples. It consists of three structural constituents: cellulose, hemicellulose and lignin with variable proportions among the different types of biomasses. In addition, even the same kind of biomass could express different degradation mechanisms because of ash or moisture contents. This is especially evident when it comes to ash content, which is a consequence of the mineral presence and related to the type of soil where biomass was grown [36]. The SD used in this study starts with moisture evaporation until ~200 ºC with a mass loss of about 7%. This step is immediately followed by the most intensive stage of degradation, where mostly cellulose and hemicellulose are decomposed. Between 200 and 400 ºC, most of the initial sample mass has deteriorated, and the residue is only 23% of the initial mass. Further heating

results in additional mass loss, even though degradation intensity slows down. At 500 ºC remaining mass is around 18.5%, which is further reduced to 15.5% at 600 ºC. At the end of the process, the mass residue is only 12% of the initial mass. Between 600 and 1000 ºC, only 3% of the sample mass is decomposed, suggesting that selected SD could be a promising feedstock for pyrolysis since most of the sample is decomposed when reaching 600 ºC.

For the degradation of the biomass and plastic mixture, similar to the individual SD, moisture evaporation starts immediately at the beginning of the process and goes up to 130 ºC with a total mass loss of approximately 4%. Mass loss is slightly less pronounced than individual SD but corresponds to moisture content from the proximate analysis. The primary decomposition step starts at around 250 ºC with cellulose and hemicellulose degradation and continues up to approximately 400 ºC. Even though this area correlates with individual SD degradation mechanism, the introduction of plastics reduces the intensity of decomposition and shifts toward slightly higher temperatures. At approximately 400 ºC, where 60% of the mass is left, the degradation mechanism shifts due to initiated plastic degradation. From individual samples, it was visible that plastic degradation is very intense and in a narrow temperature range. The same is noticed for the mixture, even though the degradation intensity is lower than for individual plastics, probably due to charred residue from the previous stage, which interferes with heat transfer. By reaching 500 ºC, most of the sample is already decomposed, and the remaining mass is only 13.2%. Further temperature increments have almost negligible effects on final mass. At 600 ºC, solid residue accounts for 12% of initial mass, which can be only reduced to 10% if the sample is heated up to 1000 ºC.

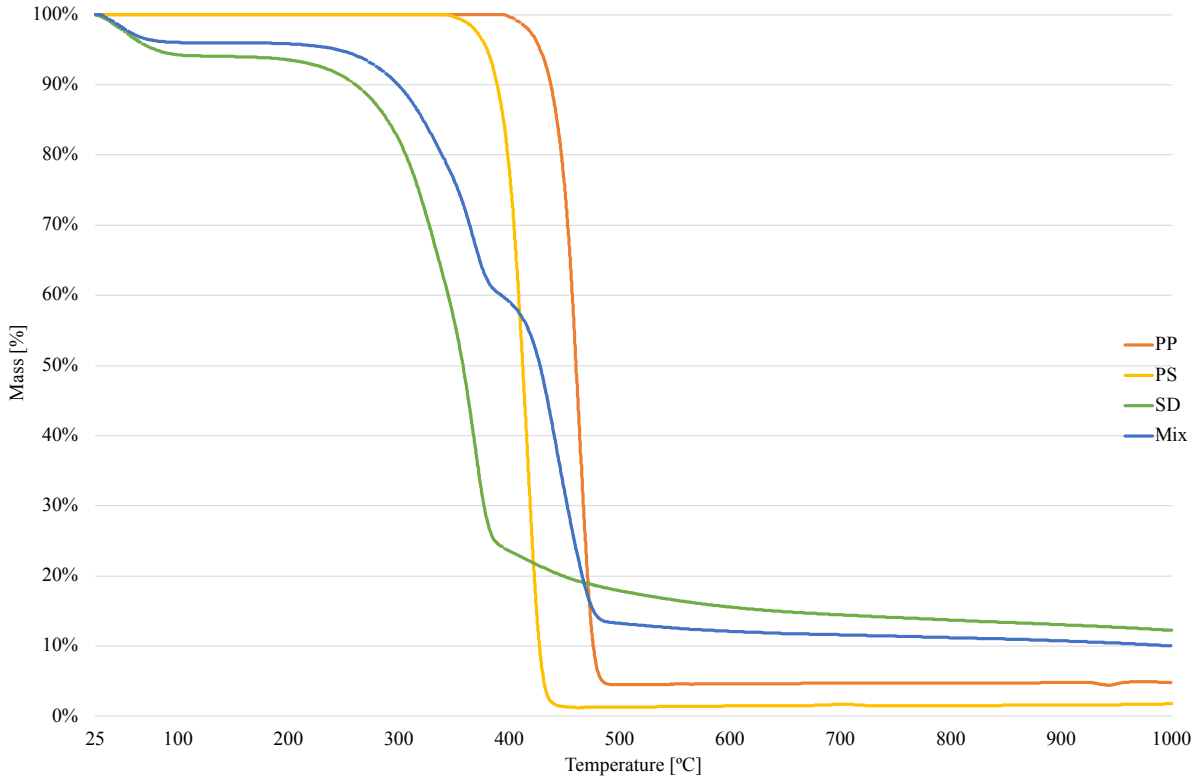

Figure 8.1 - TGA curves of individual samples and mixture

The thermal analysis results are complementary to the results from TGA and are presented in Figure 8.2. Between 100 and 200 ºC, the endothermic peaks indicating moisture evaporation can be noticed for all samples except for PS. In the case of SD this peak is related to the evaporation of strongly bound water. PP showed a pronounced peak, which can be attributed to the melting of the PP fibres without mass loss, which occurs at 170 ºC [37]. The primary decomposition stage for PP starts around 400 ºC, even though changes in specific heat can be observed already at 300 ºC when vaporisation is initiated. By 500 ºC, the sample is completely decomposed, and specific heat is reduced to only 0.5 MJ/m^3. At around 250 ºC, slight fluctuations in specific heat can be observed for SD and mixture. Since cellulose, hemicellulose and lignin are decomposed in this range, this is expected. At 500 ºC, the specific heat for SD becomes constant, indicating that the main decomposition phase is completed. Biomass decomposition generally consists of endothermic peaks in the early stages when moisture is evaporated (100-150 ºC) and at the beginning of cellulose and lignin decomposition (320-360 ºC). Slight exothermic reactions are observed between these areas, already reported in the literature [38]. On the other hand, in the case of the mixture, specific heat sharply increases to almost double values before reaching 400 ºC since the plastic components decompose immediately after the SD is carbonised. When comparing the results, it is clear that this sharp

increase is a consequence of PS presence. Individually, PS undergoes significant and intensified changes in a very narrow temperature range where specific heat dramatically fluctuates. Between 400 and 450 ºC, a tremendous increase in specific heat is noticed, with a peak at 431 ºC. Shortly after the decomposition, specific heat drops back to a similar level as the other samples. Finally, it is important to observe that the decomposition of all samples is mainly completed at 500 ºC, which indicates that for the maximised yield of volatiles, there is no need to heat the sample further.

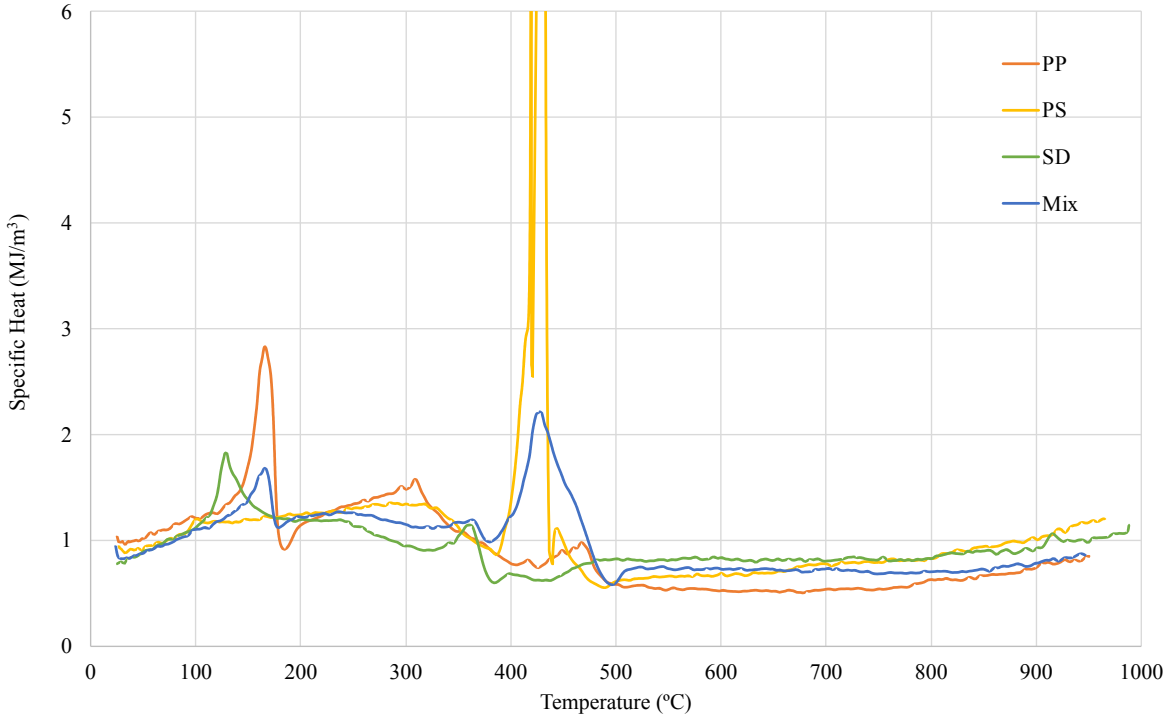

Figure 8.2 - Specific heat of investigated samples

8.3.3. Product yield and synergistic effect

The product yield from the process for individual samples and mixture is given in Figure 8.3. The liquid is the main product for all investigated samples. Sawdust liquid yield is slightly over 50%, with gas accounting for 34% and the remaining 16% being solid residue. High liquid yield is even more expressed for plastics samples, with almost 98% and 76% for PS and PP, respectively. The difference in liquid is primarily due to the difference in gas yield. For PP, around 20% of volatiles are converted to gas, while for PS, this is below 1%. Solid residue for plastics is expectedly low, 5% for PP, and slightly above 1% for PS. The mixture is exceedingly favourable for pyrolysis oil production, with almost 81% share, while the by-products char and gases account for 12% and 7%, respectively.

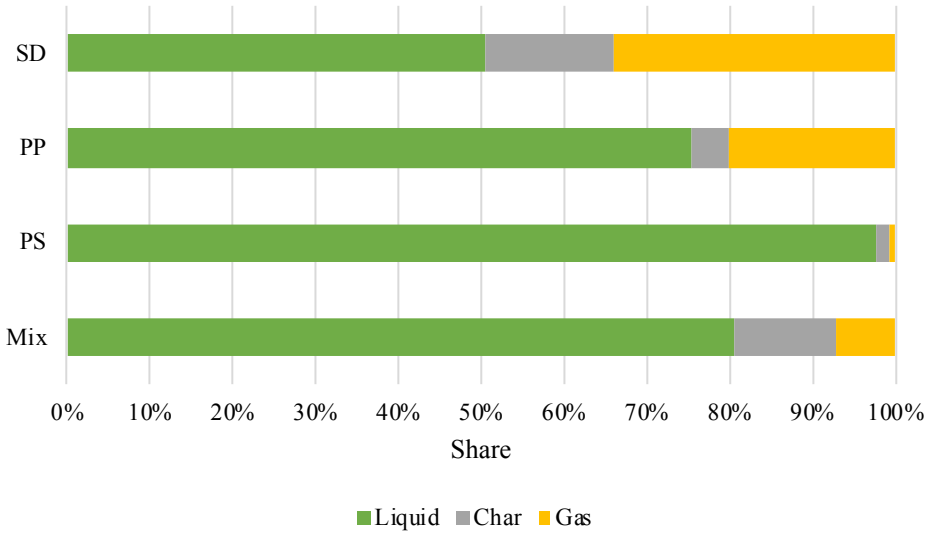

Figure 8.3 - Product yield

The synergistic effect (ΔY) between the biomass and plastics is calculated by subtracting the experimental values (Y_{exp}) from the theoretically calculated ones (Y_{cal}) (Eq. 8.1). Theoretical yield is calculated by multiplying sample share ($W_{SD/PS/PP}$) in the mixture with the fraction yield ($Y_{SD/PS/PP}$) from individual analysis (Eq. 8.2).

$$Y_{cal}=W_{SD}Y_{SD}+W_{PS}Y_{PS}+W_{PP}Y_{PP} \quad \text{Eq. 8.1}$$

$$\Delta Y=Y_{exp}-Y_{cal} \quad \text{Eq. 8.2}$$

Results for the synergistic effect are given in Table 8.2. A high positive synergy of almost 12% is observed for the liquid fraction. This is a positive outcome of the process and feedstock interaction since the aim was to maximise liquid yield. This positive synergy is achieved at the expense of the gaseous fraction, which results is 15% lower than theoretically expected gas yields. This implies that PS is an excellent inhibitor for liquid yield from pyrolysis with similar observations also reported in the literature [15]. The trade-off between liquids and gases often occurs in the co-pyrolysis of biomass with plastics, resulting in liquid favour. Although the synergy level depends on the feedstock type, it is greatly enhanced with PS utilisation. A slight positive synergy of 3% is noted for the char fraction. Similarly, small positive synergy almost always occurs for the char fraction since feedstock interaction inevitably hinders the release of volatiles, resulting in higher than theoretically expected yield.

Table 8.2 – Product yield and synergistic effect

Sample	Liquid fraction			Gas fraction			Solid fraction		
	Theoretical	Exp.	ΔY	Theoretical	Exp.	ΔY	Theoretical	Exp.	ΔY
PS	-	97.8	-	-	0.8	-	-	1.5	-
PP	-	75.5	-	-	19.9	-	-	4.6	-
Sawdust	-	50.4	-	-	34.0	-	-	20.6	-
Mixture	68.5	80.7	12.2	22.2	7.1	-15.1	9.3	12.1	2.8

8.3.4. Pyrolysis oil characterisation

Pyrolysis oil characterisation was conducted for individual samples and their respective mixture. In general, derived pyrolysis oils comprise hundreds of chemical compounds with many present only in traces and cannot be identified by the equipment. Therefore, only compounds with a yield above 0.1% were analysed in this work, and detailed insight is given for the most significant ones. Since the oil composition depends on the temperature, the general comparison based on organic groups was carried out for oils collected at 500 and 600 ºC (Table 8.3.). The main observation regarding the temperature influence relates to the identified number of chemical species with significant yield. With the temperature increment, oil composition becomes more complex due to the degradation of compounds with high carbon numbers to those with lower ones. This is especially evident in the case of plastics-derived oils while observing the hydrocarbon yield (Table 8.4-8.5). It is obvious that higher hydrocarbons are degraded into lighter ones, while most prominent compounds at both temperatures remain the same. In the case of SD-derived oil (Table 8.6), temperature increment greatly influences the selectivity of the compounds since they significantly differ, except for the phenols. Phenols are present at both temperatures, and yield increases with the temperature increment, making the oil composition less complex. In general, biomass-derived oils change their composition quickly, with only slight changes in process conditions, feedstock composition or pre-treatment method [3]. Regarding mixture-derived pyrolysis oil, compositions and temperature behaviour correlate with plastic-derived oils since identified compounds are mostly similar. It should be emphasised that none of the organic compounds identified in SD-derived oil is recognised in the mixture's oil. Nevertheless, various oxygenated compounds, alcohols and acids suggest on the SD's influence on oil composition.

Table 8.3 - Identified organic groups in pyrolysis oils

Temperature [ºC]	Mix		PS		PP		SD	
	500	600	500	600	500	600	500	600
Aromatic hydrocarbons	38.0%	32.1%	72.0%	74.6%				
Cyclic hydrocarbons	28.4%	30.3%	0.2%	0.4%	36.8%	34.4%	3.0%	3.5%
Sulfoxides			1.7%	0.3%			1.1%	3.5%
Alcohols	10.8%	12.4%			38.3%	35.4%	9.1%	1.6%
Linear hydrocarbons	5.1%	4.6%	1.4%	4.8%	10.8%	11.3%		
Ester/Acid	0.7%	3.6%					1.8%	1.4%
PAHs	3.6%	2.6%	20.5%	18.0%				2.3%
Other oxygenated compounds	1.4%	1.4%			5.2%	6.4%	5.4%	0.3%
N_2-containing compounds	0.9%	0.7%					33.5%	2.5%
Silanes					1.2%	0.8%		
Polysaccharides							1.4%	
Phenols							32.4%	71.8%
Ketones							5.4%	3.7%
Furans							0.6%	0.1%

Pyrolysis oil derived from PS has similar compounds identified at both temperatures, even though their yields might differ [15]. Identified compounds given in Table 8.4 are very often found in PS-derived oils with a significant share, making oil composition relatively homogeneous, especially when compared to biooils. As can be seen, obtained products are mostly aromatic hydrocarbons with the addition of 1,2,3,4-tetrahydro-2-phenyl naphthalene (2-phenyl tetralin) as PAH. These six compounds are responsible for almost 92% of oil composition, with styrene accounting for more than half. It should be emphasised that the presence of aromatics is welcomed in fuel composition but to a limited extent. On the other hand, PAHs are not welcomed due to their adverse effects on human health.

Table 8.4 - PS-derived oil composition

Compound	Formula	Share [%]	
		500 ºC	600 ºC
Styrene	C_8H_8	43.7%	51.2%
Naphthalene, 1,2,3,4-tetrahydro-2-phenyl-	$C_{16}H_{16}$	20.3%	17.9%
benzene, 1,1',1"-[5-methyl-1-pentene-1,3,5-triyl]tris-	$C_{24}H_{24}$	24.2%	17.3%
Benzene, 1,1'-(1,3-propanediyl)bis-	$C_{15}H_{16}$	1.3%	3.4%
.alpha.-Methylstyrene	C_9H_{10}	0.6%	2.0%
Ethylbenzene	C_8H_{10}	0.1%	1.0%

PP-derived oil expresses the most complex structure of all investigated samples. Obtained compounds are mostly linear or cyclic hydrocarbons, similar to conventional fuels (Table 8.5). Nevertheless, the compound with the highest share is 2-hexyl-1-decanol, branched alcohol

often used in polymer and lubricant synthesis as softener [39]. It is interesting to notice the presence of silane compounds in oil composition, indicating the presence of inorganic additives in raw materials [35].

Table 8.5 - PP-derived oil composition

Compound	Formula	Share [%]	
		500 ºC	600 ºC
1-Decanol, 2-hexyl-	$C_{16}H_{34}O$	28.7%	26.5%
Cyclohexane, 1,2,3,4,5,6-hexaethyl-	$C_{18}H_{36}$	19.8%	13.0%
3-Heptene, 2,6-dimethyl-	C_9H_{18}	8.0%	6.3%
Cyclododecanemethanol	$C_{13}H_{26}O$	5.0%	5.8%
1R,2c,3t,4t-Tetramethyl-cyclohexane	$C_{10}H_{20}$	3.0%	5.0%
Cyclooctane, 1-methyl-3-propyl-	$C_{12}H_{24}$	1.9%	4.3%
(2,4,6-Trimethylcyclohexyl) methanol	$C_{10}H_{20}O$	3.5%	3.1%
Cyclopentane, 1-butyl-2-propyl-	$C_{12}H_{24}$	4.4%	2.7%
Cyclopropane, 1-butyl-1-methyl-2-propyl-	$C_{11}H_{22}$		2.7%
1,7-Dimethyl-4-(1-methylethyl) cyclodecane	$C_{15}H_{30}$	2.7%	2.2%

Especially complex is the composition of biomass-derived oils or bio-oils due to their heterogeneity and general structural differences in biomass, which often results in the inability to predict product yield. Furthermore, the high share of oxygenated compounds, like phenols, alcohols, ketones, acids and similar, results in thermal instability and limited exploitation properties (i.e. lower heating value) [40]. In this case, phenols are the most abundant organic group from bio-oil analysis accounting for 70% of the total identified compounds (Table 8.6). Phenols are often found in bio-oil composition, even though their presence in fuel is not beneficial due to their high corrosive potential [41].

Table 8.6 - SD-derived oil composition

Compound	Formula	Share [%]	
		500 ºC	600 ºC
2-Methoxy-5-methylphenol	$C_8H_{10}O_2$	14.6%	26.3%
Phenol, 2-methoxy-	$C_7H_8O_2$	6.0%	19.5%
Phenol, 4-ethyl-2-methoxy-	$C_9H_{12}O_2$	5.2%	14.5%
Phenol, 2-methoxy-4-(1-propenyl)-	$C_{10}H_{12}O_2$	5.8%	4.3%
Pyrolo(3,2-d)pyrimidin-2,4(1h,3h)-dione	$C_6H_5N_3O_2$		3.5%
Phenol, 2-methoxy-4-propyl-	$C_{10}H_{14}O_2$		3.4%
2-Isopropyl-10-methylphenanthrene	$C_{18}H_{18}$		2.3%
Phenol, 3,4-dimethyl-	$C_8H_{10}O$	0.3%	2.1%
2-propanone, 1-(4-hydroxy-3-methoxyphenyl)	$C_{10}H_{12}O_3$		1.9%
Diphenyl sulfide	$C_{12}H_{10}S$	1.1%	1.8%

Most significant compounds identified in the mixture-derived oil are summarised in Table 8.7. It is interesting to notice that oil is almost exclusively composed of the compounds identified in plastic oil, while none of the compounds from SD oil is detected in the mixture. Nevertheless, the presence of oxygenated compounds (carbonic acid) is not eliminated, even though it is significantly reduced. Aromatic (32%) and cyclic hydrocarbons (30.3%) are the major constituents accounting for almost 62% of the total composition. Styrene is the major compound with a 20% yield at 600 ºC. This is more than halved compared to individual PS pyrolysis and can be considered a good outcome since the share of aromatics in the fuel composition should be limited. The secondary compound with significant yield is 1-propene, 3-(2-cyclopentenyl)-2-methyl-1,1-diphenyl, responsible for 14.6% of oil composition, belonging to the group of cyclic hydrocarbons. Even more, the yield of polycyclic aromatic hydrocarbons (2-phenyl tetralin) is reduced eight times compared to PS-derived oil to only 2%. Furthermore, a significant share of alcohol is also noticed (12.4%), probably from PP, since individual SD yields only 1.6%. It is interesting to observe the yield of 1-decanol, 2-hexyl-, the main constituent of PP-derived oil (26.5%). In the case of the mixture, its share is only 2.4%, which means that PP interaction with PS and SD completely changes the compound's selectivity and the yield of alcohols, which is reduced three times compared to individual PP-derived oil. Alcohols as oxygenated compounds are also not preferred in fuel composition; therefore, this can also be considered a positive outcome of co-pyrolysis. Cyclic and linear hydrocarbons, which compose almost half of the PP oil, are also found with 16.4% and 4.6%, respectively. Their presence in fuels is welcomed and should be increased if possible due to their high heating value and mostly smoke-free combustion process that does not cause problems to engine equipment [42]. The most significant positive outcome of the process is the complete removal of phenolic compounds, which are the main constituent of SD oil, since they have strong corrosiveness potential and, as oxygenated compounds, reduce fuel heating value.

Table 8.7 - Mix-derived oil composition

Compound	Formula	Share [%]	
		500 ºC	600 ºC
Styrene	C_8H_8	29.2%	20.2%
1-propene, 3-(2-cyclopentenyl)-2-methyl-1,1-diphenyl	$C_{21}H_{22}$	19.3%	14.6%
2-Isopropyl-5-methyl-1-heptanol	$C_{11}H_{24}O$	6.6%	7.1%
1R,2c,3t,4t-Tetramethyl-cyclohexane	$C_{10}H_{20}$	4.1%	5.8%
Benzene, 1,3-dimethyl-	C_8H_{10}	2.8%	3.6%
Benzene, 1,1'-(1,3-propanediyl)bis-	$C_{15}H_{16}$	2.5%	3.5%
.alpha.-Methylstyrene	C_9H_{10}	2.1%	2.6%
1-Decanol, 2-hexyl-	$C_{16}H_{34}O$	1.7%	2.4%
Cyclohexane, 1,2,3,5-tetraisopropyl-	$C_{18}H_{36}$		2.4%
Naphthalene, 1,2,3,4-tetrahydro-2-phenyl-	$C_{16}H_{16}$	3.6%	2.2%
Carbonic acid, eicosyl vinyl ester	$C_{23}H_{44}O_3$		2.0%
3-Heptene, 2,6-dimethyl-	C_9H_{18}	1.8%	1.7%
1,7-Dimethyl-4-(1-methylethyl)cyclodecane	$C_{15}H_{30}$		1.7%
Cyclohexane, 1,2,3,4,5,6-hexaethyl-	$C_{18}H_{36}$	2.0%	1.2%

8.3.5. Gas analysis

Gas yield from the individual samples varies significantly in terms of cumulative volumetric yields and composition. Gases started to evolve slightly below 500 ºC, with the maximum amount noted at 1000 ºC. The highest yield of 974 ml/g is observed for SD at 1000 ºC (Figure 8.4). If the co-pyrolysis temperature is 600 ºC, the gas yield would be around 450 ml/g. PP also yields a significant amount of gases, which is also observed in the literature [20]. At 600 ºC, 183 ml/g of gases is collected, further increasing to almost 500 ml/g at 1000 ºC. The high gas yield from these two samples shows that most volatiles are converted to non-condensable gases, which might comprise liquid yield. On the other hand, the gas yield from PS is almost negligible. At 600 ºC, gases account for less than 10 ml/g, while at 1000 ºC, only 27 ml/g is collected. Consequently, this shows that pyrolysis can convert volatiles from PS to valuable liquids, as preferred. Even though SD and PP compose 75% of the mix, the gas yield of the mixture is several times lower than their individual analyses. At 600 ºC, only 47 ml/g of gases are evolved, which is further increased to 135 ml/g at 1000 ºC. This implies that feedstock interaction and the introduction of PS greatly influence volatile conversion and favour liquid yield at the expense of gases.

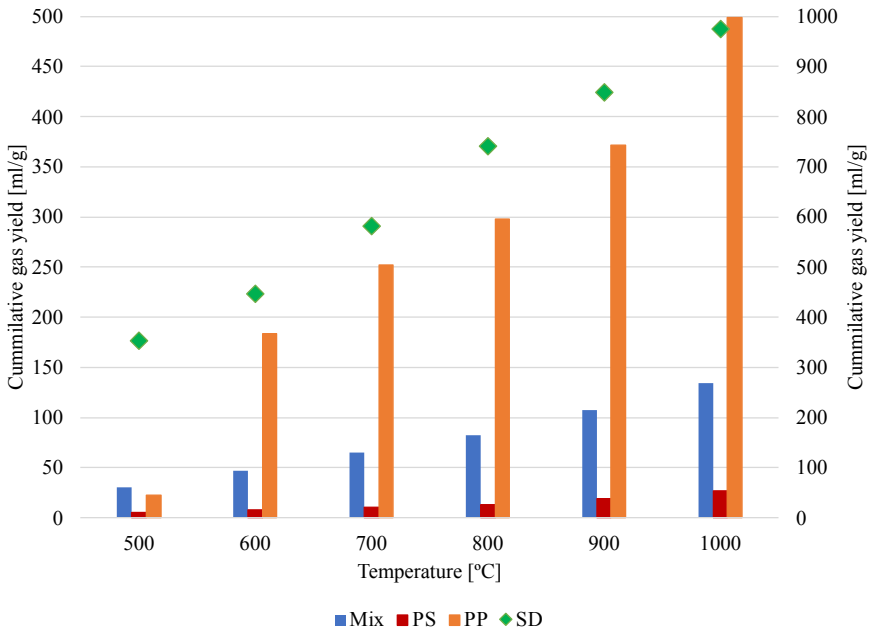

Figure 8.4 - Cumulative gas yield

The gas composition differs among the investigated samples. At 600 ºC, the pyrolysis gas from sawdust is composed mainly of carbon monoxide (CO) and carbon dioxide (CO_2), combined accounting for 83% of volume share (Figure 8.5a). The rest is comprised of methane (13%), hydrogen (2%), and higher hydrocarbons (2%). With the further temperature increment, the share of CO and CO_2 declines while the percentage of hydrogen notably increases. At the final temperature of 1000 ºC, gas is composed of CO (31%), CO_2 (25%), and CH_4 (13%), while hydrogen accounts for almost 30%. Ethane and ethylene are present with a nearly negligible 2% combined.

A significantly different composition is observed for PP (Figure 8.5b). At 600 ºC, a representative amount of gases is collected, composed of light hydrocarbons (89%). The combined yield of CO and CO_2 is almost negligible throughout the process, ranging between an initial 6% and 13% at the final temperature. At the final temperature, a significant share of light hydrocarbons is converted to methane (32%) and hydrogen (24%). Nevertheless, the percentage of hydrocarbons is still respective, with 17% noted for ethane and 14% for ethylene. Since PS generally yields a small amount of gases, its composition is not of great interest. At 600 ºC, the gas yield is below 10 ml/g, with hydrogen (32%) and methane (24%) as the main constituents (Figure 8.5c). With further temperature increments, the share of hydrogen is significantly increasing at the expense of light hydrocarbon gases. At a final temperature of 1000 ºC, it accounts for almost 70% of the total gas yield. For quantitative comparison, at 1000 ºC, hydrogen yield is approximately at the same levels as in the case of SD at 600 ºC.

Finally, the composition of the gases from mixtures expresses similar trends to individual SD sample (Figure 8.5d). At 600 ºC, CO and CO_2 account for 84% of gas composition. Methane brings an additional 11%, while the rest are hydrogen and hydrocarbons. With temperature increment, the share of hydrogen increases at the expense of hydrocarbons, but also because of tar cracking at high temperatures. At 1000 ºC, hydrogen is the principal constituent of the gas composition with 32%, followed by CO_2 (31%) and CO (29%). The share of methane is reduced to only 6%, while ethane and ethylene are responsible for 1% each.

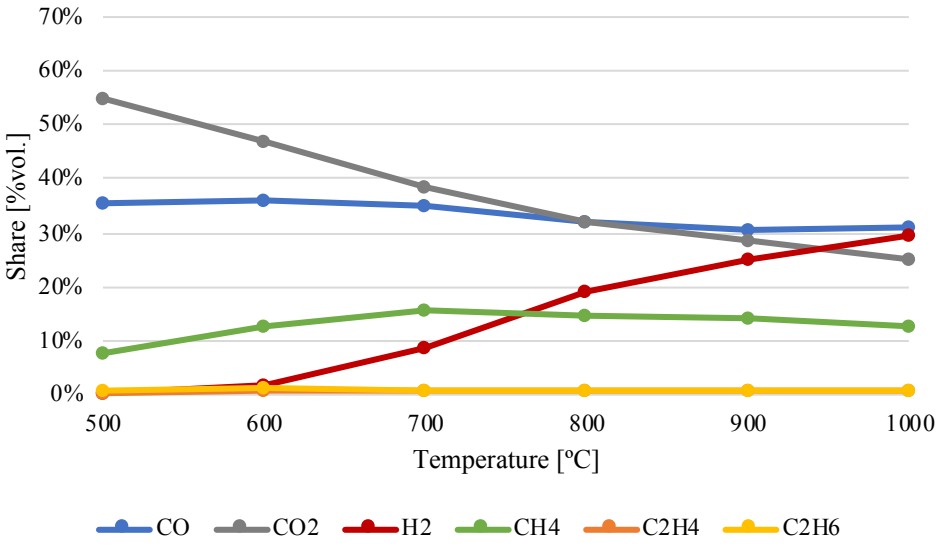

a) Sawdust

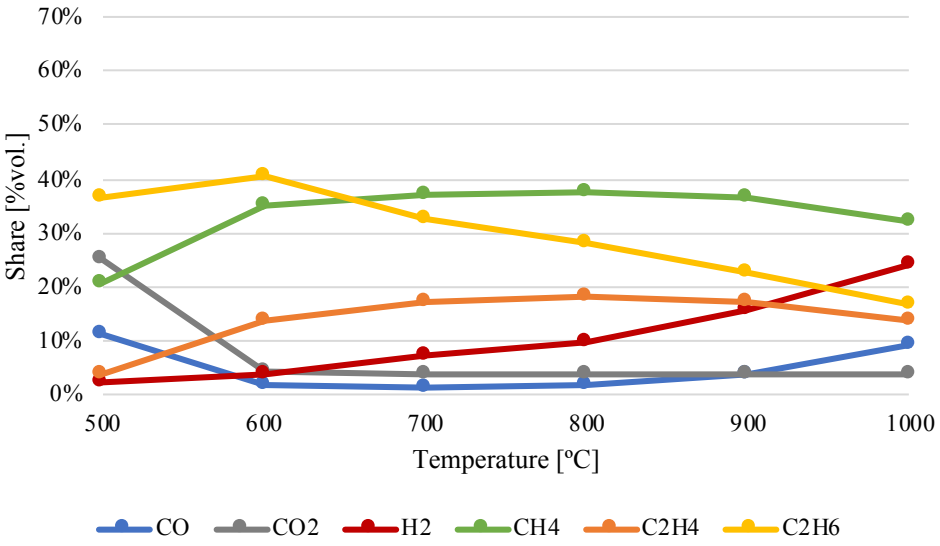

b) PP

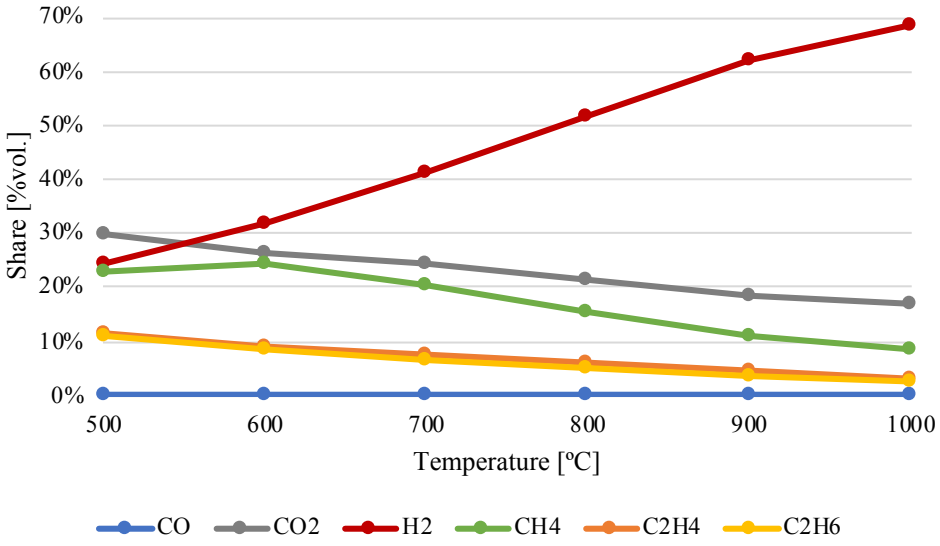

c) PS

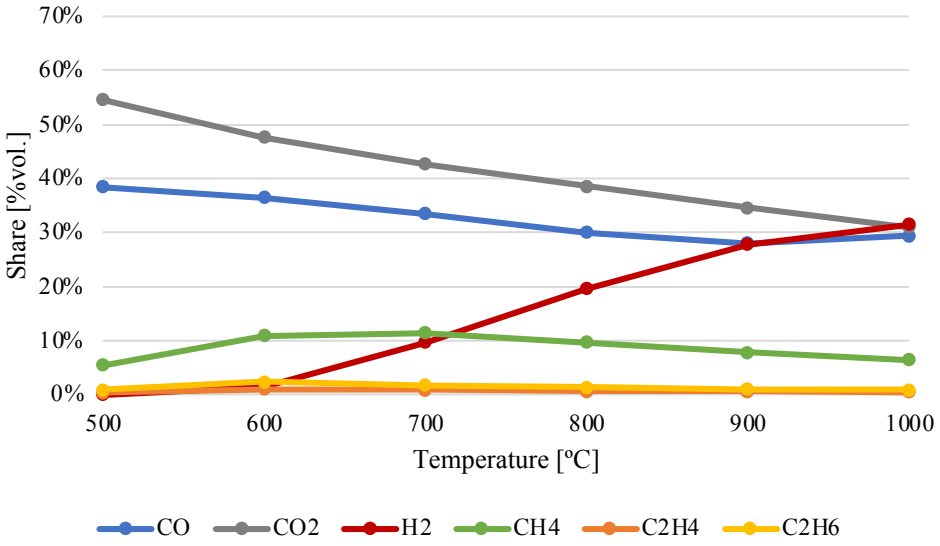

d) Mixture

Figure 8.5 - Composition of obtained pyrolysis gases

8.3.6. Char analysis

Before conducting experiments, FTIR spectra were obtained for selected untreated samples to confirm their identity and compare with commercial spectra to identify possible differences which might impact results. All results for raw and charred samples at 600 and 1000 ºC are plotted in Figure 8.6. Results from plastic samples correlate with commercial spectra from the internal database and the literature [43-44]. In the case of PP (Figure 8.6a), asymmetric and symmetric stretching of methyl (CH_3) and methylene (CH_2) groups are observed. Stretching of methyl groups occurs at 2956 and 2875 cm^{-1}, while methylene stretching can be observed at 2921 and 2836 cm^{-1}. The existence of four peaks in that area suggests the presence of both groups [43]. Symmetrical bending of the CH_3 group is noted again at 1452 cm^{-1}, followed by

the umbrella mode at 1375 cm^{-1}. Finally, three peaks at 1166, 973 and 840 cm^{-1} that are often used to confirm PP structure are also identified and they can be due to the wagging or rocking of C-H and CH_3 groups. In addition, a significant peak is noted at 1016 cm^{-1} and compared with the internal databases. An identical peak is found in the software database for PP mixed with 20% talc, indicating the possible presence of inorganic compounds.

The identification of PS structure (Figure 8.6b) also shows excellent correspondence with the literature [45]. Stretching of aromatic C-H (3059 and 3023 cm^{-1}) and methylene groups (2923 and 2854 cm^{-1}) is first observed. Having peaks above and below 3000 cm^{-1} indicates the presence of saturated and unsaturated carbons. Further presence of aromatics is proven by the peaks in the area between 1600 and 1450 cm^{-1}, with a particular focus on 1600 cm^{-1}, which corresponds to benzene ring mode. Moreover, peaks at 748 (aromatic out-of-plan C-H bend) and 694 cm^{-1} (aromatic ring bend) can be used to identify monosubstituted benzene rings. In conjunction with the evenly distributed benzene fingers between 2000 and 1600 cm^{-1}, these two peaks confirm the presence of monosubstituted benzene rings.

Analysis of SD spectra showed that the sample contains various oxygenated organic groups but also aromatics (Figure 8.6c). Intensive O-H bending is observed between 3400 and 3000 cm^{-1}, indicating the presence of alcohols, phenols and acids. Because of methyl and methylene groups, C-H stretching occurs between 2970 and 2850 cm^{-1}. A strong peak is again noted at 1727 cm^{-1} due to C=O stretching. This stretching might be due to the presence of esters, ketones, aldehydes or acids. Benzene ring stretching vibrations are observed at 1600 and 1506 cm^{-1}. The peak at 1423 cm^{-1} corresponds with the C-H group, probably due to cellulose bending. Significant stretching and bending overlap occurs between 1360 and 1263 cm^{-1}, suggesting the presence of the OH group, lignin and polysaccharides. Additional deformation of C-H and C-O groups is observed at 1153 cm^{-1}. Finally, significant deformations, typical for pine wood, are found between 1054 and 1024 cm^{-1}, which, combined with the peak at 1727 cm^{-1}, confirms the substantial presence of esters [46].

Finally, the analysis of mixture spectra expresses the combination of organic groups identified for individual samples (Figure 8.6d). Therefore, strong stretching of O-H groups is observed in the range between 3500-3000 cm^{-1}, similar to the SD sample. The methylene group is observed at 2915 cm^{-1} and identified in all samples. The presence of aromatics is confirmed by the peaks at 1600 and 1509 cm^{-1}, found in individual PS and SD. The peak at 1450 cm^{-1} is identified in all investigated samples and corresponds to the symmetrical bending of methylene. Another stretching, similar to the SD sample, occurs at 1025 cm^{-1}, indicating the C-O-C

deformations. Finally, several peaks are identified below 750 cm^{-1}, like for PS and PP samples, probably indicating the presence of aromatics.

Spectra analysis of char samples collected from 600 and 1000 ºC is important to determine which organic groups remain in the solid residue. It should be emphasised that char yield from plastics is minimal. Therefore, most of the volatiles are expected to be converted into liquid and gases, and only a minor share remains in the solid residue. In the case of PP char from 600 ºC, few peaks can be identified, starting at 2956 cm^{-1} with the stretching of a methyl group, reported for a raw sample as well. Furthermore, intense stretching can be observed at 1016 cm^{-1} again, corresponding to the inorganic group with silica content. It should be mentioned that the peak at 671 cm^{-1}, also found in PP's spectra with talc, suggests the presence of the inorganics once again. Temperature increment to 1000 ºC completely degrades the sample and ensures that most organics are converted into volatiles. Between 1070 and 850 cm^{-1}, the rocking of remaining C-H bonds is noted.

PS completely degrades almost without solid residue, and char traces can be collected from the tube wall and the FTIR spectra for the char collected for both temperatures corresponds to that of a solid carbon.

Analysis of char fraction from SD is the most important due to the highest yield of solid residue. Compared to the raw sample, there are no peaks above 1600 cm^{-1} in the case of char from 600 or 1000 ºC, implying complete conversion of oxygenated compounds into volatiles at this range. In the case of char from 600 ºC, notable bending is noted at 1573 cm^{-1} indicating the presence of aromatic hydrocarbons and benzene rings. Similar to the raw sample at 1157 cm^{-1}, deformations of C-H and C-O bonds are noted, suggesting presence of lignin compounds [5]. This can be confirmed when observing spectra from 1000 ºC, where this peak is not seen. The 600 ºC is sufficient to degrade cellulose and hemicellulose, but some of the lignin component remains. Only further temperature increments can completely degrade biomass so that no specific organic group can be identified. It should be mentioned that several additional peaks can be seen in char spectra from 600 ºC in the range between 865-500 cm^{-1}, corresponding most probably to hydrocarbons.

Analysis of mixture char shows similar observations. At 600 ºC, most compounds are degraded and converted into volatiles. Slight bending of aromatic rings can be seen at 1575 cm^{-1}. Similar to individual PP sample, intense stretching occurs at 1018 cm^{-1}. The peak absorbance is pronouncedly lower than individual PP since the share of PP in the mixture is only 25%. Even though this peak seems to be the most prominent in char at 600 ºC. Moreover, similar to individual SD at 600 ºC, several peaks are observed between 867-670 cm^{-1},

suggesting the presence of hydrocarbons. Finally, in the case of mixtures char from 1000 ºC, the vast majority of organic compounds are completely degraded and there are almost no clear peaks to identify the remaining compounds. The only pronounced peak is at 1070 cm^{-1}, representing the deformations in C-O-C bonds.

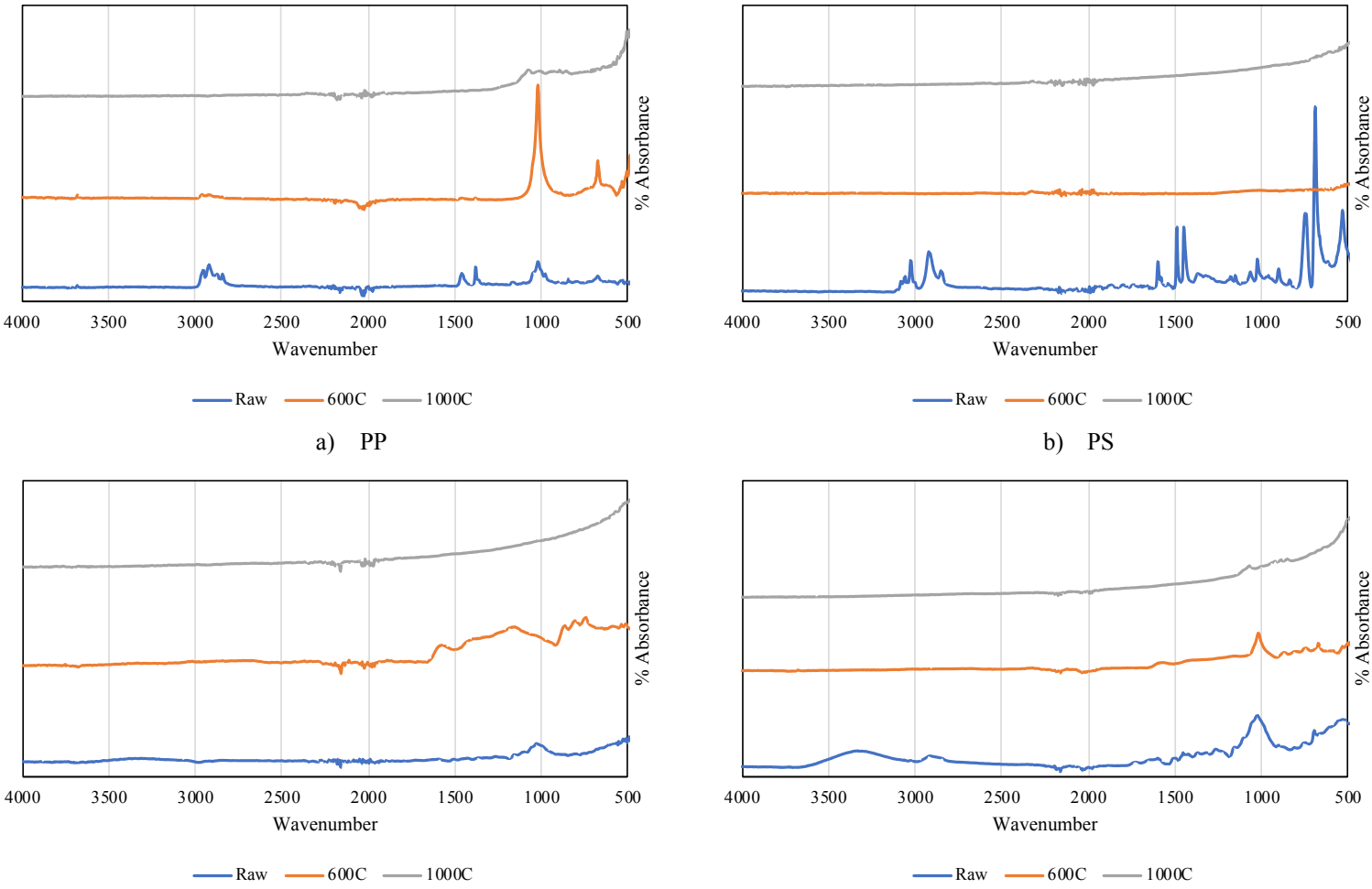

a) PP b) PS

c) SD d) Mix

Figure 8.6 - FTIR spectra from investigated raw and charred samples

8.4. Discussion

The results obtained in this work were further compared to related studies from the literature to draw conclusions from a critical perspective. Suriapparao et al. [47] investigated the co-pyrolysis of PS and PP with different types of biomass, including mixed wood sawdust. Results from the ultimate and proximate analysis show similarities, as well as product yield for SD and PS, while in the case of PP main difference is in the oil yield. This study reports almost 15% higher oil yield, which is unsurprising since the PP can be produced in various forms depending on the application. Regarding the mixtures with biomass-plastic ratio 1:1, oil yield was 60% in the PS case, with a notable gas share of 27%. In the case of PP-SD, oil yield was

only 30%, with almost 54% of gases. PS-derived oils were mostly composed of monoaromatics and polycyclic aromatic hydrocarbons. On the other hand, PP oils were composed of aliphatics, PAHs, and various oxygenated compounds with a lower share. The low oil yield for PP and rubberwood seed co-pyrolysis was also reported in a study by Izzatie et al. [35], with only 37% noted at 550 ºC. Simultaneously, the gas yield was between 40-70% in the temperature range of 450-600 ºC. Nguyen et al. [48] co-pyrolysed PS and pine SD showing a great reduction of oxygenated and acetic compounds with a simultaneous increase in heating value. Nevertheless, the used temperature of 500 ºC seems to be slightly too low due to higher char yield. The reduction of oxygenated compounds with only a slight introduction of PS to mixed wood SD was also confirmed in a study by Stančin et al. [15]. Furthermore, this study shows that only 25% of PS in the mixture will greatly enhance aromatic selectivity. Nisar et al. [34] showed that the polymers recovered from mixed waste should be pre-treated to avoid a higher yield of oxygenated compounds, especially acids. Finally, Li et al. [20] investigated the gasification potential of PS and PP, obtaining very limited gas yield without using CO_2 as a gasification agent. This suggests that PS and PP might be more appropriate for pyrolysis than gasification.

8.5. Conclusion

The co-pyrolysis of three different types of feedstocks, including biomass and plastics, demonstrates the potential for alternative fuel production from these waste resources. Selected waste materials: sawdust, PS and PP show great potential for high liquid yield production due to the high volatile and low ash contents. Furthermore, PS acts as a catalyst for liquid yield since an almost negligible amount of char and gases collected from individual analysis reflects in a beneficial outcome of the mixture pyrolysis, where the gas yield was greatly reduced in favour of the liquids.

The chemical composition of obtained pyrolysis oil from the mixture showed that the selected ratio gives the desired outcome of the identified compounds. The introduction of PS greatly helps in achieving oil homogeneity, simultaneously giving moderate aromatic content in the acceptable range for conventional fuels. On the other hand, the presence of PP helps in selectivity toward linear and cyclic hydrocarbons, which are the main constituents of traditional fuels. Finally, the presence of plastics reduces the oxygenated content of bio-oils, even though feedstock should be pre-treated before pyrolysis to minimise the possibility of acid yield.

Since PS is the primary driver for liquid yield, it also allows better prediction of oil composition as most identified compounds in the mixture will be of PS origin. The selected

25% of PS is sufficient to promote aromatic yield while remaining in the acceptable range for further fuel utilisation. The share of PP content could be increased to increase the yield of linear or cyclic hydrocarbons with lower carbon numbers.

Analysis of process by-products shows that obtained gas composition and charred residue could be further utilised for electricity and heat production as substitutes for fossil fuels, even though their yield accounts for only 20%. Hydrogen, CO and CO_2 are the main gaseous products, primarily derived from sawdust and PP. Collected char consists of inorganics from PP and various hydrocarbon groups, probably derived from sawdust.

The synergistic effect shows that feedstock interaction will promote liquid over a gaseous fraction. The synergy level depends on the mixture composition, and gas yield could be higher with higher content of sawdust, but also PP. In the case of solid residue, synergy level will always have slightly positive values, but with 50% of plastics content, this will mostly stay below 5%. This observation could be very useful for the future development of a prediction model for the product yield from co-pyrolysis.

References

[1] H. Stančin, H. Mikulčić, X. Wang, and N. Duić, "A review on alternative fuels in future energy system," *Renewable and Sustainable Energy Reviews*, vol. 128, 2020, doi: 10.1016/j.rser.2020.109927.

[2] M. Gholizadeh, X. Hu, and Q. Liu, "A mini review of the specialties of the bio-oils produced from pyrolysis of 20 different biomasses," *Renewable and Sustainable Energy Reviews*, vol. 114. Elsevier Ltd, Oct. 01, 2019. doi: 10.1016/j.rser.2019.109313.

[3] X. Chen, Q. Che, S. Li, Z. Liu, H. Yang, Y. Chen, X. Wang, J. Shao, and H. Chen, "Recent developments in lignocellulosic biomass catalytic fast pyrolysis: Strategies for the optimization of bio-oil quality and yield," *Fuel Processing Technology*, vol. 196. Elsevier B.V., Dec. 15, 2019. doi: 10.1016/j.fuproc.2019.106180.

[4] P. Liu, Y. Wang, Z. Zhou, H. Yuan, and T. Zheng, "Gas fuel production derived from pine sawdust pyrolysis catalyzed on alumina," *Asia-Pacific Journal of Chemical Engineering*, vol. 15, no. 4, Jul. 2020, doi: 10.1002/apj.2456.

[5] H. Yang, R. Yan, H. Chen, D. H. Lee, and C. Zheng, "Characteristics of hemicellulose, cellulose and lignin pyrolysis," *Fuel*, vol. 86, no. 12–13, pp. 1781–1788, Aug. 2007, doi: 10.1016/j.fuel.2006.12.013.

[6] L. Esquiaqui, S. D. F. de Oliveira Miranda Santos, and C. M. L. Ugaya, "A systematic review of densified biomass products life cycle assessments," *International Journal of*

Environmental Science and Technology, pp. 1–24, Jan. 2023, doi: 10.1007/S13762-022-04752-1/TABLES/3.

[7] R. Musule, J. Bonales-Revuelta, T. H. Mwampamba, R. M. Gallardo-Alvarez, O. Masera, and C. A. García, "Life Cycle Assessment of Forest-Derived Solid Biofuels: a Systematic Review of the Literature," *Bioenergy Res*, vol. 15, no. 4, pp. 1711–1732, Dec. 2022, doi: 10.1007/S12155-021-10346-5.

[8] V. Sharma, A. Kalam Hossain, G. Griffiths, G. Duraisamy, A. Krishnasamy, V. Ravikrishnan, and J. Ricardo Sodré, "Plastic waste to liquid fuel: A review of technologies, applications, and challenges," *Sustainable Energy Technologies and Assessments*, vol. 53, Oct. 2022, doi: 10.1016/j.seta.2022.102651.

[9] G. Özsin and A. E. Pütün, "A comparative study on co-pyrolysis of lignocellulosic biomass with polyethylene terephthalate, polystyrene, and polyvinyl chloride: Synergistic effects and product characteristics," *J Clean Prod*, vol. 205, pp. 1127–1138, Dec. 2018, doi: 10.1016/j.jclepro.2018.09.134.

[10] N. Singh, D. Hui, R. Singh, I. P. S. Ahuja, L. Feo, and F. Fraternali, "Recycling of plastic solid waste: A state of art review and future applications," *Compos B Eng*, vol. 115, pp. 409–422, Apr. 2017, doi: 10.1016/J.COMPOSITESB.2016.09.013.

[11] R. Hossain, M. T. Islam, A. Ghose, and V. Sahajwalla, "Full circle: Challenges and prospects for plastic waste management in Australia to achieve circular economy," *J Clean Prod*, vol. 368, Sep. 2022, doi: 10.1016/J.JCLEPRO.2022.133127.

[12] H. Stančin, M. Šafář, J. Růžičková, H. Mikulčić, H. Raclavská, X. Wang, and N. Duić, "Influence of plastic content on synergistic effect and bio-oil quality from the co-pyrolysis of waste rigid polyurethane foam and sawdust mixture," *Renew Energy*, vol. 196, pp. 1218–1228, Aug. 2022, doi: 10.1016/J.RENENE.2022.07.047.

[13] H. Jeswani, C. Krüger, M. Russ, M. Horlacher, F. Antony, S. Hann, and A. Azapagic, "Life cycle environmental impacts of chemical recycling via pyrolysis of mixed plastic waste in comparison with mechanical recycling and energy recovery," *Science of the Total Environment*, vol. 769, May 2021, doi: 10.1016/j.scitotenv.2020.144483.

[14] J. Uebe, Z. Kryzevicius, R. Majauskiene, M. Dulevicius, L. Kosychova, and A. Zukauskaite, "Use of polypropylene pyrolysis oil in alternative fuel production," *Waste Management and Research*, vol. 40, no. 8, pp. 1220–1230, Aug. 2022, doi: 10.1177/0734242X211068243.

[15] H. Stančin, M. Šafář, J. Růžičková, H. Mikulčić, H. Raclavská, X. Wang, and N. Duić, "Co-pyrolysis and synergistic effect analysis of biomass sawdust and polystyrene

mixtures for production of high-quality bio-oils," *Process Safety and Environmental Protection*, vol. 145, pp. 1–11, Jan. 2021, doi: 10.1016/j.psep.2020.07.023.

[16] J. Hamilton, Y. Sadat, M. Dwyer, P. Ghali, and B. Khandelwal, "Thermal stability and impact of alternative fuels," *Aviation Fuels*, pp. 149–218, Jan. 2021, doi: 10.1016/B978-0-12-818314-4.00003-0.

[17] X. Zhang, H. Lei, S. Chen, and J. Wu, "Catalytic co-pyrolysis of lignocellulosic biomass with polymers: A critical review," *Green Chemistry*, vol. 18, no. 15. Royal Society of Chemistry, pp. 4145–4169, 2016. doi: 10.1039/c6gc00911e.

[18] F. Abnisa and W. M. A. Wan Daud, "A review on co-pyrolysis of biomass: An optional technique to obtain a high-grade pyrolysis oil," *Energy Convers Manag*, vol. 87, pp. 71–85, Nov. 2014, doi: 10.1016/j.enconman.2014.07.007.

[19] H. Hassan, J. K. Lim, and B. H. Hameed, "Recent progress on biomass co-pyrolysis conversion into high-quality bio-oil," *Bioresource Technology*, vol. 221. Elsevier Ltd, pp. 645–655, Dec. 01, 2016. doi: 10.1016/j.biortech.2016.09.026.

[20] J. Li, X. Ye, K. G. Burra, W. Lu, Z. Wang, X. Liu, and A. K. Gupta, "Synergistic effects during co-pyrolysis and co-gasification of polypropylene and polystyrene," *Appl Energy*, vol. 336, Apr. 2023, doi: 10.1016/j.apenergy.2023.120750.

[21] N. Déparrois, P. Singh, K. G. Burra, and A. K. Gupta, "Syngas production from co-pyrolysis and co-gasification of polystyrene and paper with CO2," *Appl Energy*, vol. 246, pp. 1–10, Jul. 2019, doi: 10.1016/j.apenergy.2019.04.013.

[22] R. K. Mishra, S. M. Chistie, S. U. Naik, and P. Kumar, "Thermocatalytic co-pyrolysis of waste biomass and plastics: Studies of physicochemical properties, kinetics behaviour, and characterization of liquid product," *Journal of the Energy Institute*, vol. 105, pp. 192–202, Dec. 2022, doi: 10.1016/j.joei.2022.09.003.

[23] S. Y. Oh and J. I. Sohn, "Energy recovery and waste treatment using the co-pyrolysis of biomass waste and polymer," *Waste Management and Research*, vol. 40, no. 11, pp. 1637–1644, Nov. 2022, doi: 10.1177/0734242X221087845.

[24] X. Jin, J. H. Lee, and J. W. Choi, "Catalytic co-pyrolysis of woody biomass with waste plastics: Effects of HZSM-5 and pyrolysis temperature on producing high-value pyrolytic products and reducing wax formation," *Energy*, vol. 239, Jan. 2022, doi: 10.1016/j.energy.2021.121739.

[25] K. R. G. Burra, X. Liu, Z. Wang, J. Li, D. Che, and A. K. Gupta, "Quantifying the sources of synergistic effects in co-pyrolysis of pinewood and polystyrene," *Appl Energy*, vol. 302, Nov. 2021, doi: 10.1016/j.apenergy.2021.117562.

[26] “Macquarie University - Elemental Microanalysis Service.” https://www.mq.edu.au/research/research-centres-groups-and-facilities/secure-planet/facilities/chemical-analysis-facility/elemental-microanalysis-service (accessed Feb. 24, 2023).

[27] “ISO - ISO 562:1981 - Hard coal and coke — Determination of volatile matter content.” https://www.iso.org/standard/4652.html (accessed Feb. 22, 2023).

[28] “ASTM D 2867 : 2004 Standard Test Methods for Moisture in Activate.” https://infostore.saiglobal.com/en-us/standards/astm-d-2867-2004-143767_saig_astm_astm_319038/ (accessed Feb. 22, 2023).

[29] “ASTM D2866 : Standard Test Method for Total Ash Content of Activated Carbon.” https://global.ihs.com/doc_detail.cfm?document_name=ASTM%20D2866&item_s_key=00017015 (accessed Feb. 22, 2023).

[30] V. Strezov, J. A. Lucas, and L. Strezov, “Computer aided thermal analysis,” *J Therm Anal Calorim*, vol. 72, no. 3, pp. 907–918, Nov. 2004, doi: 10.1023/A:1025030618161.

[31] R. Xiao, W. Yang, X. Cong, K. Dong, J. Xu, D. Wang, and X. Yang, “Thermogravimetric analysis and reaction kinetics of lignocellulosic biomass pyrolysis,” *Energy*, vol. 201, Jun. 2020, doi: 10.1016/j.energy.2020.117537.

[32] A. v. Bridgwater, D. Meier, and D. Radlein, “An overview of fast pyrolysis of biomass,” *Org Geochem*, vol. 30, no. 12, pp. 1479–1493, Dec. 1999, doi: 10.1016/S0146-6380(99)00120-5.

[33] K. G. Burra and A. K. Gupta, “Kinetics of synergistic effects in co-pyrolysis of biomass with plastic wastes,” *Appl Energy*, vol. 220, pp. 408–418, Jun. 2018, doi: 10.1016/j.apenergy.2018.03.117.

[34] J. Nisar, G. Ali, A. Shah, M. Iqbal, R. A. Khan, Sirajuddin, F. Anwar, R. Ullah, and M. S. Akhter, “Fuel production from waste polystyrene via pyrolysis: Kinetics and products distribution,” *Waste Management*, vol. 88, pp. 236–247, Apr. 2019, doi: 10.1016/j.wasman.2019.03.035.

[35] N. I. Izzatie, M. H. Basha, Y. Uemura, M. S. M. Hashim, M. Afendi, and M. A. F. Mazlan, “Co-pyrolysis of rubberwood sawdust (RWS) and polypropylene (PP) in a fixed bed pyrolyzer,” *Journal of Mechanical Engineering and Sciences*, vol. 13, no. 1, pp. 4636–4647, Mar. 2019, doi: 10.15282/jmes.13.1.2019.20.0390.

[36] S. v. Vassilev, D. Baxter, L. K. Andersen, and C. G. Vassileva, “An overview of the chemical composition of biomass,” *Fuel*, vol. 89, no. 5, pp. 913–933, May 2010, doi: 10.1016/J.FUEL.2009.10.022.

[37] "Polypropylene Fibre Preventing the Occurrence of Spalling | Encyclopedia MDPI." https://encyclopedia.pub/item/revision/d9eafe60d0601e96dfd689f8ccd5bf7b (accessed Feb. 22, 2023).

[38] V. Strezov, B. Moghtaderi, and J. A. Lucas, "THERMAL STUDY OF DECOMPOSITION OF SELECTED BIOMASS SAMPLES," 2003.

[39] "2-Hexyldecanol Market Size, Share, Demand & Forecast | FMI." https://www.futuremarketinsights.com/reports/2-hexyldecanol-market (accessed Mar. 06, 2023).

[40] P. Brassard, S. Godbout, and V. Raghavan, "Pyrolysis in auger reactors for biochar and bio-oil production: A review," *Biosystems Engineering*, vol. 161. Academic Press, pp. 80–92, Sep. 01, 2017. doi: 10.1016/j.biosystemseng.2017.06.020.

[41] X. Hu and M. Gholizadeh, *Biomass pyrolysis: A review of the process development and challenges from initial researches up to the commercialisation stage*, vol. 39. Elsevier B.V. and Science Press, 2019. doi: 10.1016/j.jechem.2019.01.024.

[42] Hendrawati, A. R. Liandi, M. Solehah, M. H. Setyono, I. Aziz, and Y. D. I. Siregar, "Pyrolysis of PP and HDPE from plastic packaging waste into liquid hydrocarbons using natural zeolite Lampung as a catalyst," *Case Studies in Chemical and Environmental Engineering*, vol. 7, Jun. 2023, doi: 10.1016/j.cscee.2022.100290.

[43] B. C. Smith, "The infrared spectra of polymers III: Hydrocarbon polymers," *Spectroscopy (Santa Monica)*, vol. 36, no. 11, pp. 22–25, Nov. 2021, doi: 10.56530/SPECTROSCOPY.MH7872Q7.

[44] J. Fang, L. Zhang, D. Sutton, X. Wang, and T. Lin, "Needleless melt-electrospinning of polypropylene nanofibres," *J Nanomater*, vol. 2012, 2012, doi: 10.1155/2012/382639.

[45] M. A. Peltzer and C. Simoneau, "Report of an Interlaboratory Comparison from the European Reference Laboratory for Food Contact Materials: ILC002 2013 – Identification of Polymeric Materials," , 2013. doi: 10.2788/6233.

[46] B. Esteves, A. V. Marques, I. Domingos, and H. Pereira, "Chemical changes of heat treated pine and eucalypt wood monitored by ftir," *Maderas: Ciencia y Tecnologia*, vol. 15, no. 2, pp. 245–258, Aug. 2013, doi: 10.4067/S0718-221X2013005000020.

[47] D. v. Suriapparao, B. Boruah, D. Raja, and R. Vinu, "Microwave assisted co-pyrolysis of biomasses with polypropylene and polystyrene for high quality bio-oil production," *Fuel Processing Technology*, vol. 175, pp. 64–75, Jun. 2018, doi: 10.1016/j.fuproc.2018.02.019.

[48] Q. van Nguyen, Y. S. Choi, S. K. Choi, Y. W. Jeong, and Y. S. Kwon, “Improvement of bio-crude oil properties via co-pyrolysis of pine sawdust and waste polystyrene foam,” *J Environ Manage*, vol. 237, pp. 24–29, May 2019, doi: 10.1016/j.jenvman.2019.02.039.

PAPER 7

Journal of Cleaner Production 414 (2023) 137676

Contents lists available at ScienceDirect

Journal of Cleaner Production

journal homepage: www.elsevier.com/locate/jclepro

Life cycle assessment of alternative fuel production by co-pyrolysis of waste biomass and plastics

Hrvoje Stančin [a,b], Vladimir Strezov [a], Hrvoje Mikulčić [b,*]

[a] School of Natural Sciences, Faculty of Science and Engineering, Macquarie University, Sydney, 2109, NSW, Australia
[b] University of Zagreb, Faculty of Mechanical Engineering and Naval Architecture, Croatia

ARTICLE INFO

Handling Editor: Cecilia Maria Villas Bôas de Almeida

Keywords:
Co-pyrolysis
Waste plastic
Biomass
Life cycle assessment
Environmental impact

ABSTRACT

In the scope of energy transition and overall decarbonisation, various alternative fuels are investigated as potential substitutes for conventional fossil fuels. Co-pyrolysis has emerged as a potential solution for production of alternative fuels, while dealing with waste management issues, due to its ability to process different feedstocks. Biomass-derived fuels, with all their constraints, are already used on a commercial scale. Simultaneously, significant efforts are given to scale up fuel production from the thermal treatment of waste plastics. The fuel must be produced sustainably with minimal environmental impacts to be considered an alternative. This study presents the life cycle assessment (LCA) of waste biomass and plastic materials, co-pyrolysed with an aim to produce pyrolysis oil that could be used as a petroleum substitute. Moreover, the environmental impacts from the co-pyrolysis are compared to incineration and landfilling, which are today mostly used to deal with end-of-life plastics. The LCA is carried out in openLCA software using ReCiPe Midpoint 2016, and Environmental footprint methods. Results show that co-pyrolysis mostly reduces emissions associated with environmental impacts, even though this greatly depends on the treatment method used to divert the feedstock. Furthermore, most process emissions are associated with electricity consumption, therefore, integration of plastic processing with renewable energy sources can further reduce the environmental impacts. Finally, the products derived from the process should be of high quality with minimal after-treatment requirements to effectively substitute fossil fuels.

1. Introduction

Climate change presents a major challenge nowadays, raising the need for immediate action and energy transition. Increased production of electricity from renewables, electrification of transport and industrial processes, and various alternative fuels are expected to replace fossil fuels and contribute to overall decarbonisation (Stančin et al., 2020). Biofuels were marked as the most promising alternative due to their carbon neutrality. Nevertheless, they still have limitations in technological viability, and lately, practices of the current biofuel production have raised several sustainability considerations (Wang et al., 2015b). Even though emissions released in the utilisation stage can be considered neutral, increased deforestation and land use can significantly negatively impact the environment. Moreover, biofuel production has environmental impacts, especially evident in the pre-treatment stage, specifically from the drying process (Iribarren et al., 2012).

On the other hand, waste plastics cause tremendous environmental burdens and threaten human health and the environment. Current end-of-life treatment methods are either based on incineration (42%) or landfilling (23%), while mechanical recycling accounts for about 34% (Plastics - the Facts, 2021). Lately, co-pyrolysis has emerged as a potential solution to prevail drawbacks of biofuel production while simultaneously tackling waste management problems of plastic materials. Pyrolysis oil cannot be used directly and requires purification and refining to meet conventional fuel standards. Fuel production from co-pyrolysis requires significant energy and material input, resulting in various environmental pollutant emissions. Therefore, to quantify the benefits of the production procedure, it is necessary to carry out a life cycle assessment (LCA) and determine the environmental impacts.

LCA has been carried out for various biomass and plastic feedstock thermal treatment methods. Even though, it is often hard to compare the results since different system boundaries, functional units, or impact assessment methods are applied. Global warming potential (GWP) expressed in kg CO_2 eq. is the only impact category common across all studies, which is also dependent on the functional unit and system model. Gahane et al. (2022) conducted an in-depth review of LCA for

* Corresponding author.
E-mail addresses: hrvoje.stancin@fsb.hr (H. Stančin), vladimir.strezov@mq.edu.au (V. Strezov), hrvoje.mikulcic@fsb.hr (H. Mikulčić).

https://doi.org/10.1016/j.jclepro.2023.137676
Received 26 January 2023; Received in revised form 16 May 2023; Accepted 31 May 2023
Available online 1 June 2023

biomass pyrolysis. The review considered various types of biomass feedstock, sources of electricity for the process, pre-treatment methods, and utilisation. The study concluded that biofuel production and utilisation emissions are lower than fossil fuels; therefore, biomass should be considered a feasible alternative. Osman et al. (2021) carried out a detailed review of biomass LCA, concluding that both production routes, thermochemical and biochemical, come with environmental burdens. In addition, the review showed that most of the studies focused on assessing a particular part of the production stage, while overall assessment from cultivation to end use is missing. Fan et al. (2011) compared the biofuel production process from three different sources. The lowest emissions are associated if the pyrolysis oil is produced from waste wood since it enters the system free of burdens from harvesting and cultivation processes. Nevertheless, due to the lower product density, waste wood comes with higher collection and transportation impacts. Overall results showed that pyrolysis oil could save between 77 and 99% of GHG emissions if used as a fossil fuel substitute. Pyrolysis of agricultural waste was marked as a promising route to produce biofuels, especially since it greatly outperforms other alternatives like incineration (Alcazar-Ruiz et al., 2022). On the other hand, Vienescu et al. (2018) emphasised that emissions could be three times higher in the case when poor synthetic fuel quality is produced compared to conventional fossil fuels.

Antelava et al. (2019) conducted a detailed review of LCA studies for plastic end-of-life treatment to compare the environmental benefits of different waste management methods. The main problem with plastic LCA of waste management practices is associated with the uncertainty of product quality, consequently, its processing properties. Therefore, even though mechanical recycling is the preferred option, the quality of recyclate often constrains the replacement potential of virgin material. This was also confirmed in the study by Martín-Lara et al. (2022), where it was found that environmental impacts and threats to human health are higher due to the requirements to wash and dry waste feedstock. In case when high-quality recyclate is obtained, environmental benefits are significant, as in the study by Papo and Corona (2022). Additionally, they emphasised the need for feedstock pre-sorting to mono-fractions since that allows the control of product quality. Jeswani et al. (2021) studied the LCA of chemical recycling for mixed plastic waste (MPW) from a waste and product perspective. Pyrolysis as a chemical recycling method was found to have about 50% lower GWP than energy recovery from incineration. Still, the rest of the impact categories, such as acidification and eutrophication, perform worse. Some studies (Demetrious and Crossin, 2019; Eriksson and Finnveden, 2009) found that landfilling of MPW might be a better option for thermal treatment from the perspective of GWP but worse for the rest of the impact categories. Mechanical recycling often shows better environmental impact compared to other treatment methods. However, the quality of recyclate must be almost 80% of virgin material to be considered an adequate replacement (Lazarevic et al., 2010).

The utilisation of pyrolysis oil in internal combustion engines has a promising perspective to reduce overall GWP, NO_X, and CO emissions. Furthermore, the formation of particulate matter and unburned hydrocarbons are reduced if optimal combustion conditions are maintained (Roque et al., 2023). Similar observation was confirmed in the study by Puricelli et al. (2022), even though it should be emphasised that electric vehicles are still outperforming alternative fuels in terms of environmental impacts.

There is a limited number of studies focusing on the LCA of co-pyrolysis of two different feedstock. In fact, only Neha et al. (2022) carried out an assessment which is solely focused on co-pyrolysis as a waste treatment method. In their study, food waste and low-density polyethylene (LDPE) were co-pyrolysed, concluding that pyrolysis outperforms landfilling or open dumping several times in terms of GWP. Since food waste contains high moisture feedstock (>70%), the drying requirements are significant, accounting for 57% of total energy demand, which can negatively impact sustainability of the process. The energy required to drive pyrolysis is also energy-intensive and responsible for an additional 33% of total energy consumption. Biomass drying and pyrolysis are the two main contributors to the environmental impacts of the co-pyrolysis process.

This study presents the LCA of waste plastic and biomass materials used in the co-pyrolysis process. The proposed method aims to maximise the liquid fraction yield as the product of interest. The composition of the investigated mixture consists of 50% pine sawdust (SD) and 50% waste plastics, equally divided between polystyrene (PS) and polypropylene (PP). Environmental impacts are assessed for the overall process and pre-processing activities. Compared to similar studies, this work brings extensive, in-depth analysis of several most prominent environmental impacts rather than just focusing on GWP. In addition, sawdust as an abundant waste product is assessed for the first time from the perspective of co-pyrolysis utilisation. Finally, analysis was performed from the perspective of input (feedstock) and output (product) flows to provide a better insight into their influence on the environmental impacts. Individual analysis of input flows opens the possibility to evaluate feedstock burdens and credits, consequently determining their applicability for pyrolysis. On the other hand, individual analysis of output flows suggests which product yields should be prioritised to reduce the environmental impacts of proposed procedure.

2. Materials and methods

The investigated types of plastic are selected since they have low recycling potential, while based on experimental investigations and literature, it was found that they could yield compounds preferred in fuel composition. In the case of PP, these are linear hydrocarbons (Uebe et al., 2022), while aromatics are obtained from PS (Stančin et al., 2021). In the case of polyethylene terephthalate (PET) (Stegmann et al., 2023) and high-density polyethylene (HDPE) (J. Zhang et al., 2023), mechanical recycling is widely used with quite a good recovery rate, therefore, it should be preferred over thermochemical conversion. In the case of polyvinyl chloride (PVC) (Ephraim et al., 2018) and polyurethanes (PU) (Stančin et al., 2022), obtained products are not in line with fuel requirements, and therefore such feedstock requires different approaches and utilisation pathways.

2.1. Goal and scope

The system boundaries are set from feedstock collection in the form of waste materials to the production of pyrolysis oil as the final step. This implies that oil refining and upgrading are not considered, and no credits or burdens are assessed for oil utilisation. As the main product, pyrolysis oil is assessed with all environmental impacts, while credits are received for producing by-products that can substitute fossil fuels elsewhere. Synthetic gas (syngas) is used internally to provide heat, while char is sent to the market as a coal substitute. The functional unit used for impact assessment is 1 t of the pyrolysis oil produced. The model of the proposed system is given in Fig. 1.

As shown, co-pyrolysis is preceded by several processes related to feedstock transport and pre-treatment. Input waste flows are free of production or cultivation burdens, but there are environmental impacts derived from their collection. Biomass, preferably in waste forms like sawdust or shavings, is collected and transported from the sawmill or source of origin to a hypothetical co-pyrolysis plant, where it is dried and shredded to a particle size below 2 mm. The plastic stream starts with waste collection in the form of mixed plastic waste transported to the separation plant. MPW is further separated on monomer fractions where non-recyclable components are diverted from landfilling or incineration to a pyrolysis plant. Before mixing with sawdust, plastic is shredded to the same particle size to ensure the homogeneity of the mixture. The prepared mixture is then introduced to the pyrolysis reactor and heated to 600 °C under an inert atmosphere, where liquid, gaseous and solid charred products are obtained.

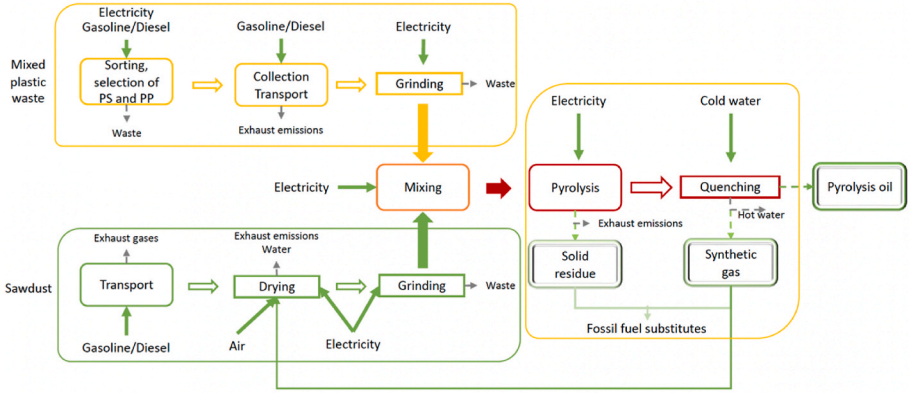

Fig. 1. The proposed model for the co-pyrolysis process.

In the scope of the work, three scenarios are considered based on the current waste management methods used to deal with end-of-life plastic waste. This implies that mechanical recycling is not considered, and pyrolysis is evaluated as an alternative to incineration or landfilling. Each scenario represents a specific country: S1 - Germany, S2 - Croatia and S3 - Australia, but the results are comparable to other countries with the same end-of-life treatment methods. Table 1 summarises the assessed scenarios alongside waste management methods currently used to deal with waste plastics. The values for S1 and S2 scenarios are taken from the ecoinvent database (Home - Ecoinvent), while for the S3 are taken from national strategic documents (Pickin et al., 2020; Schandl H et al., 2020) due to the lack of data in the database. As shown, the S1 scenario is vastly dominated by incineration, while S2 and S3 scenarios are based on landfilling with the difference if they are sanitary or unsanitary. Open dump, in the case of S3, represents a waste plastic leakage to the environment based on a study carried out by Black et al. (2020).

2.2. Impact assessment

OpenLCA 1.11 (Ciroth, 2007). is used to carry out impact assessment using the ReCiPe Midpoint 2016 (H) method. Additionally, to test the model's robustness, an Environmental footprint (EF) analysis is carried out as well. As a functional unit, the 1 t of pyrolysis oil is assessed using the consequential approach. This implies that the environmental impacts present the comparison between pyrolysis and incineration or landfilling from the perspective of waste materials utilisation. The initial sawdust input to produce 1t of pyrolysis oil for the base scenarios (S1–S3) is 817 kg, while the initial input for plastic feedstock is 710 kg, equally divided between PS and PP. For the sensitivity analysis scenarios (S6–S7), where oil yield is lower than expected, to produce 1t of pyrolysis oil, initial input for sawdust is increased to 1632 kg, while initial input for plastics is increased to total of 1420 kg, where each type of plastic accounts for 50% of mass.

As mentioned above, the system boundaries are cutting off further oil upgrading and usage, therefore, potential burdens are not assessed. Altogether 18 impact categories are assessed, of which nine are widely discussed. The rest of the impact categories are briefly mentioned since their impact is primarily neutral. The global warming potential (GWP) expressed in kg CO_2 eq. is used to compare the results with similar studies. The rest of discussed categories include human carcinogenic toxicity (HTC), human non-carcinogenic toxicity (HTNC), freshwater ecotoxicity (FET), marine ecotoxicity (MET), terrestrial ecotoxicity (TET), all expressed in kg 1,4-DCB. Additionally, fossil resource scarcity (FRS) in kg oil eq., acidification potential (AP) in SO_2 eq., and fine particulate matter formation expressed in kg $PM_{2.5}$ eq. are briefly discussed.

Table 1
Analysed scenarios with waste plastic end-of-life treatment methods.

Scenario	S1 DE	S2 HR	S3 AU
Treatment method	[%]		
Incineration	99	1	1
Sanitary landfill	0.5	27	80
Unsanitary landfill	–	70	10
Open burning	0.5	2	–
Open dump	–	–	9

2.3. Inventory data

The ecoinvent 3.8 database with a consequential approach is used in this work to design the product system (Ecoinvent v3.8 - Ecoinvent). Additional literature is consulted for further information about specific consumptions and flows for processes inside the system. An overview of used database flows and service providers is presented in Supplementary Table S1. Furthermore, in Table S2, the electricity mixes for considered scenarios are given, while Table S3 presents the detailed flows with input values for each pre-treatment and pyrolysis process.

2.3.1. Transport

The distance for the mixed plastic waste collection is taken from the database and assumed to vary between 50 and 100 km, depending on the country. Separated plastic is transported to a pyrolysis plant within 100 km. Sawdust is collected from a sawmill or similar forestry production site and transported to a pyrolysis plant within the same distance as the separated plastic. The considered type of transport is a truck with EURO 6 emissions standard for both feedstocks.

2.3.2. Feedstock pre-treatment

The plastic separation plant is powered by electricity, which consumes 69 kWh per tonne of mixed waste plastic processed (Jeswani et al., 2021). Separation plant efficiency is 90%, based on BASF case study analysis (Russ et al., 2020). The same case study analysis assumes that there is no need for plastic washing and drying for pyrolysis, and a similar approach is taken in this study as well. The waste from separation is further sent to the market for waste plastic, where different end-of-life treatment methods are applied, depending on the country. Electricity consumption for plastic shredding is 30 kWh/t (Chen et al., 2019), with 97% efficiency.

Sawdust pre-treatment starts with drying. During the transport and storage of biomass, natural drying is assumed to reduce moisture from 50 to slightly below 35% (Del Giudice et al., 2019). Pyrolysis requires moisture content below 10%, so the difference needs to be removed by drying (Y. Zhang et al., 2014). Rotary dryer requires 1.64 GJ of heat per tonne of water removed with additional electricity consumption of 5 kWh per tonne of biomass processed (Haque and Somerville, 2013).

Electricity requirements for grinding vary depending on the type of biomass and particle size. In this process, 33 kWh/t is assumed (Lan et al., 2020) with an efficiency of 97% (Brassard et al., 2021). Waste from both feedstock grinding is collected and sent to the national market for incinerating or landfilling.

2.3.3. Pyrolysis

The shear mixer is used for mixing purposes before pyrolysis, with an average consumption of 20 kWh/m^3 (Mixers Specific Power Consumption). Electricity consumption for pyrolysis reactors differs in the literature between 400 and 550 kWh per tonne of pyrolysis oil produced. For this case, 500 kWh per tonne of pyrolysis oil is considered based on previous studies (Gahane et al., 2022; Vienescu et al., 2018; Zheng et al., 2022). Nitrogen is used as a carrier gas (Brassard et al., 2017), while water for quenching and condensation of volatiles (Salvi et al., 2021).

2.3.4. Synthetic gas combustion

Synthetic gas is used internally to provide heat for sawdust drying. The input flows are based on a similar process found in the literature (Ayer and Dias, 2018; Jones et al., 2009). The synthetic gas composition is obtained experimentally. Air consumption and process emissions (water and CO_2) are based on combustion stoichiometry which was additionally calculated.

2.3.5. By-products markets

Char residue from the process is sent to the market for coal as a lignite substitute. Besides, the produced char could be used as fertiliser or for water remediation purposes (Osman et al., 2022). Additionally, a surplus of synthetic gas not used for drying is also sent to the market for synthetic gas as a substitute for biomass gasification. In both cases, credits are given to the pyrolysis process.

2.4. Experimental conditions

Before carrying out LCA, an experimental investigation was conducted to determine the yield and distribution of the pyrolysis products. Obtained results are used in the final stage of LCA, where 1 t of the mixture is introduced to co-pyrolysis, while the product output is based on experimental results. The co-pyrolysis is conducted on a mixture of 50% sawdust (radiata pine), 25% waste PS previously used for the CD case, and 25% waste PP used for different packaging purposes. The sample is heated up from room temperature to 600 °C in an infrared packed bed furnace with a heating rate of 10 °C/min (Strezov et al., 2008). The gases are analysed using the Agilent 490 Micro GC analyser with helium as a carrier gas, while the liquid is collected at the end of the tube and diluted with dichloromethane.

3. Results

3.1. Experimental results

Experimental results showed that at the end of the pyrolysis process, the solid residue or char was only 13% of the initial mass. The gas yield was calculated on a He-free basis, accounting for 7% of the obtained products. Finally, the share of liquid fraction is 80%, calculated by the difference between initial mass and the sum of solid and gas yields. Results are summarised in the supplementary material (Table S4).

3.2. Environmental impact assessment of the proposed co-pyrolysis system model

Global warming potential is one of the most important categories when discussing environmental impacts. As shown in Table 2, the greatest savings of CO_2 eq. are in the case of scenario S1 (−574 kg CO_2 eq.). At the same time, S2 and S3 have almost identical values and positive contributions to this impact category (~400 kg CO_2 eq.). The reason behind the GWP reduction in scenario S1 is due to avoided incineration of waste plastics, which would emit emissions into the air. In the case of S2 and S3 scenarios, waste streams are mostly diverted from sanitary and unsanitary landfills, and credits for this are considerably lower compared to S1. In such cases, received credits are insufficient to compensate for the rest of the process burdens, and overall values are positive.

Table 2
Summary of environmental impact assessment category.

Impact category	Reference unit	S1 DE	S2 HR	S3 AU
Global warming potential	kg CO_2 eq.	−547.0	408.5	394.9
Freshwater ecotoxicity	kg 1,4-DCB eq.	−9.9	−80.1	−84.1
Terrestrial ecotoxicity		2410.2	3823.3	3762.7
Human carcinogenic toxicity		99.8	30.6	40.3
Human non-carcinogenic toxicity		814.3	−2862.9	−2498.0
Marine ecotoxicity		−23.3	−115.9	−122.4
Fossil resource scarcity	kg oil eq.	270.9	153.5	109.2
Fine particulate matter formation	kg $PM_{2.5}$ eq.	3.2	0.5	0.5
Freshwater eutrophication	kg P eq.	1.2	−0.3	−0.1
Marine eutrophication	kg N eq.	0.1	−0.2	−0.1
Terrestrial acidification	kg SO_2 eq.	6.2	1.3	1.3
Ozone formation, Human health	kg NOx eq.	2.9	0.9	0.9
Ozone formation, Terrestrial ecosystems		3.0	0.9	1.0
Ionizing radiation	kBq Co-60 eq.	62.3	13.1	13.7
Land use	m^2a crop eq.	1001.3	700.5	674.2
Mineral resource scarcity	kg Cu eq.	2.1	1.8	1.6
Stratospheric ozone depletion	kg CFC11 eq.	0.0	0.0	0.0
Water consumption	m^3	189.3	158.0	157.0

In order to test the robustness of the analysis, for the main three scenarios (S1–S3), an environmental footprint (EF) assessment is also carried out (detailed results are given in Supplementary Table S5). Since there are differences in used units to evaluate the environmental impacts, a comparison between the two used methods can only be made to some extent. Consequently, the obtained values from the analysis differ as well. Most interesting is to observe the GWP, where differences between ReCiPe and EF methods are barely visible. More precisely, the S1 difference is below 4 kg CO2, while almost the same values are observed in the case of S2 and S3 for both methods. The rest of the impact categories have different units used; therefore, obtained values vary greatly, even though the trends are very similar to the ReCiPe method. Following categories are having similar trends between considered scenarios: acidification potential, eutrophication potential, human carcinogenic toxicity, particulate matter formation, mineral resource scarcity, and water consumption. Nevertheless, significant differences are observed for freshwater ecotoxicity which express negative values for all scenarios in case of ReCiPe method, while from EF assessment obtained values are significant and positive. This implies that two considered methods assess this category completely different reducing the results reliability. Similar is noticed for human non-carcinogenic toxicity. In the case of ReCiPe method, avoided landfilling brings environmental credits to the process, while avoided incineration comes with burdens. If EF method is used, all three scenarios are causing negative environmental burdens, even though obtained values are pronouncedly low.

Results of the toxicity impact categories expressed in kg 1,4-DCB eq. significantly differ between the three considered cases. The proposed process reduces freshwater and marine ecotoxicity, especially when the waste is diverted from landfills (S2–S3). The credits received for avoided landfilling are several times higher than for avoided incineration. In the case of freshwater toxicity, avoided emissions are around 80 kg 1,4-DCB eq. for scenarios S2–S3, compared to 10 kg 1,4-DCB eq. in the case of S1. Credits are even higher in the case of marine toxicity, with savings of

more than 115 kg 1,4-DCB eq. for S2–S3, while only 23 kg of emissions is prevented for S1. Some credits are received for char fraction sent to market, around 11 and 8 kg 1,4-DCB eq. for marine and freshwater ecotoxicity, respectively.

Human carcinogenic toxicity impact (HTC) is mainly associated with the sawdust drying process and the combustion of synthetic gas to provide heat. Emissions are not directly related to the combustion itself but to the background process for delivering air for the combustion (27.03 kg 1,4-DCB eq). Similarly, water used for cooling comes with substantial burdens, but most are associated with the distribution network development rather than the pyrolysis process. The HTC is higher in the case of S1 (99.8 kg 1,4-DCB eq.) compared to other scenarios (30.6 and 40.3 for S2 and S3, respectively). This is because avoided incineration requires higher input of fossil fuels to compensate for lost electricity and heat production. Increased demand for fossil fuels consequently requires more mining operations, resulting in rising environmental burdens. Char fraction, which can be sent to market as a lignite substitute, saves around 15% of the emissions related to HTC.

Human non-carcinogenic toxicity shows the most significant differences between scenarios. The S2 and S3 scenarios show a remarkable reduction of emissions associated with HTNC, 2862.9 and 2498 kg 1,4-DCB eq. On the other hand, for the S1 scenario, the process generates significant emissions (814 kg 1,4-DCB eq.) For all scenarios, around 300 kg 1,4 DCB eq. is saved since char is used as a coal substitute which prevents mining operations. Additional credits of 37 kg 1,4-DCB eq. are associated with synthetic gas sent to market.

Terrestrial ecotoxicity (TET) is the category with the highest impact in terms of absolute values. There are several reasons behind these. Firstly, when comparing the results between scenarios, it is noticeable that the treatment methods play an essential role. Avoided incineration brings tremendously higher credits than avoided landfilling, especially in the case of waste PP. Avoided waste plastic landfilling also brings some credits, but not nearly enough to compensate for process burdens. Moreover, significant burdens associated with TET come from sawdust stream flows and feedstock transport to the processing unit. Almost 2000 kg 1,4-DCB eq. is related to the drying process with burdens associated with the production of compression equipment used for air supply. Furthermore, sawdust is heavily burdened with emissions related to various processing techniques like slab, siding, chopping, suction and similar. Finally, significant emissions come from the transport sector due to break wear emissions of copper and antimony to the air. This is the only impact category where the transport sector plays a significant role in environmental impacts.

Regarding fossil resource scarcity, all scenarios generate environmental burdens. Nevertheless, it should be emphasised again that produced pyrolysis oil could substitute conventional naphtha, which would get significant credits, which are still not given in this case due to system boundaries. In general, most of the burdens in this category come from the consumption of fossil fuels to produce the electricity required for the process. In the case of S1, avoided incineration requires higher input of other fuels to satisfy heat and electricity production, therefore, burdens are even higher in this case (270.9, compared to 153.5 and 109.2 kg oil eq. for S2 and S3). About 33 kg of oil eq. is saved for sending the char to the coal market.

The process has a minor or neutral environmental impact for the rest of the impact categories. For terrestrial acidification, it can be observed how avoided incineration increases SO_2 eq. emissions since higher fossil fuel inputs are required to produce electricity and heat. Land use and water consumption have a notable impact. Land use is associated with forestry activities, unrelated to the pyrolysis itself, but it is present here as a background process for acquiring sawdust. Even though system boundaries are set up at feedstock acquisition as the first step, some background processes are inevitable when using a consequential approach. Water used for cooling and condensing volatiles also has a significant impact. Still, this parameter would greatly depend on the cooling system, which is closely related to the reactor design and, as such, may vary greatly.

3.3. Global warming potential of pre-treatment processes

Fig. 2 presents the global warming potential for each process preceding pyrolysis. Environmental impacts from waste streams present cumulative credits or burdens gained through the pre-treatment process for each feedstock separately. They merge into a single flow in the mixing process, which is then subjected to pyrolysis in the next step.

It can be seen from Fig. 2 that the diversion of plastic waste from current waste treatment methods, like incineration or landfilling, brings immediate GWP credit to the proposed process. As already discussed, avoiding incineration is beneficial for reducing GWP due to avoiding direct emissions of CO_2 to the air. Therefore, emissions savings are several times higher in the case of S1, compared to S2 and S3, where pyrolysis prevents methane leakage from landfills. On the other hand, sawdust utilisation comes with burdens associated with forestry and post-processing actions. The sawdust pre-treatment increases GWP until the grinding stage with the same rate for all analysed scenarios. Nevertheless, in the grinding step, a slight reduction is noticed in the case of S1, while a small increment occurs for the rest. This depends on the treatment method for dust collected at this stage, but the overall impact is limited since grinding is considered efficient, with minimal losses. Nevertheless, it should be mentioned that sawdust initially comes with a very low GWP of only 34 kg CO_2 eq., confirming the hypothesis about its carbon neutrality. Before mixing, when all pre-treatment methods are performed, the GWP of the sawdust stream is between 141 and a maximum of 175 kg CO_2 eq. for S1 and S2, respectively.

After the mixing stage, the S1 scenario negatively contributes to GWP, while S2 and S3 express positive values. The primary reason for this is because credits for using waste plastics are insufficient to cover the burdens from the sawdust side. Furthermore, the electricity mix used to power up the process plays an important role, and electricity consumption is the primary source of environmental burdens associated directly with pyrolysis.

Environmental impacts from electricity are associated with emissions directly emitted to the environment from power plants and the background processes required to produce equipment. Electricity consumption is several times lower for pre-treatment processes compared to pyrolysis itself. Consequently, GWP associated with electricity consumption is several times higher in the case of pyrolysis than for the rest of the processes together. The GWP from electricity consumption varies between very low 67 kg CO_2 eq. for S1 to high values in the case of S3 and S2 with 272 and 334 kg CO_2 eq., respectively. All emissions from the electricity sector are based on ecoinvent electricity mixes for selected countries using consequential system modelling. Plastic separation accounts for approximately 7% of the emissions associated with GWP. Sawdust drying with the combustion of synthetic gas has negligible electricity consumption. Sawdust and plastic grinding processes together contribute to additional 6–7% kg CO_2 eq. Mixing has only slightly higher values, accounting for about 8%, while the remaining 77% of the emissions associated with electricity consumption come from pyrolysis and reactor heating. The results are summarised in Fig. 3. The rest of the impact categories have a similar share of emissions for the pre-treatment processes.

Feedstock transport, for both SD and plastics, brings some burdens to the process. Since the transport distance and market are assumed to be the same for all scenarios (S1–S3), values do not differentiate between them. Global warming potentials for this process are 14 and 11 kg CO_2 eq. for SD and plastics, respectively. Slightly higher values in the case of the SD are due to the significant moisture content, which is later removed with the drying process. Nevertheless, mass loss in the drying stage indicates that the initial feedstock requirement is higher for the sawdust stream than the plastic, resulting in higher transport emissions.

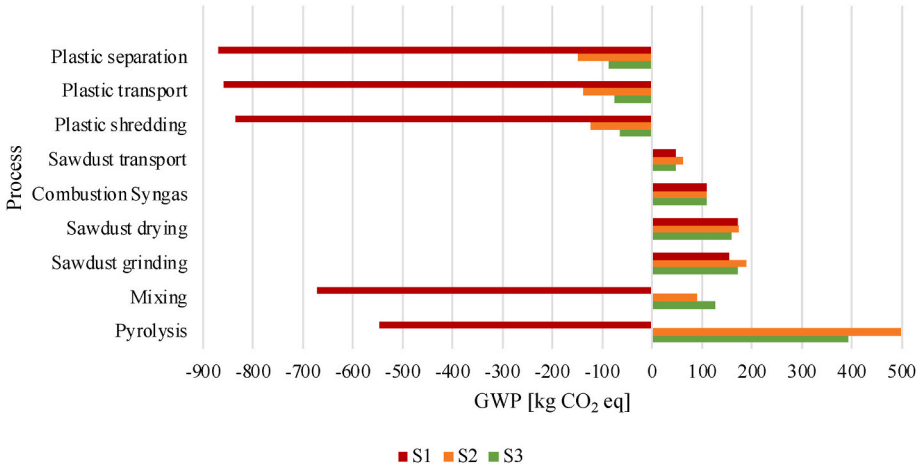

Fig. 2. Global warming potential of separate processes.

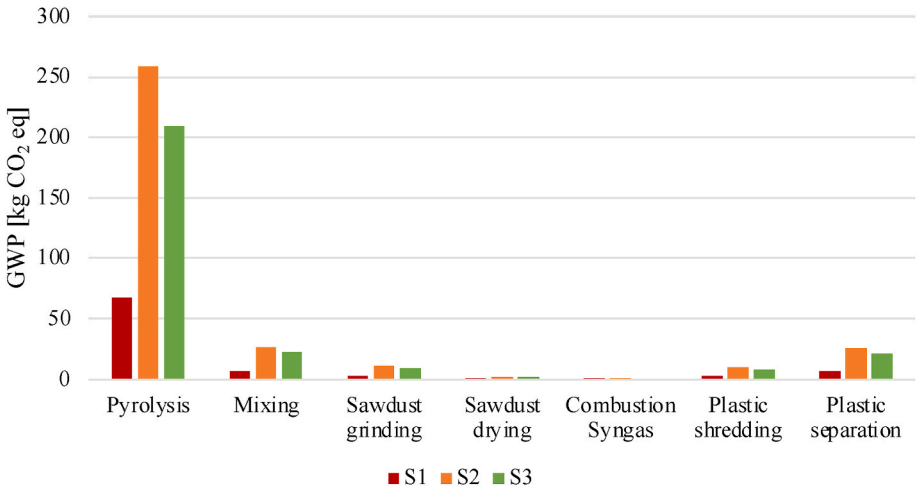

Fig. 3. Global warming potential associated with electricity consumption.

3.4. Waste flow analysis

Plastic consists of two separate waste streams for PS and PP. Their utilisation in pyrolysis comes with either credits or burdens, depending on which treatment methods they are diverted from. Simultaneously, waste sawdust comes to the process with burdens. Nevertheless, these burdens are several times lower than the plastic counterparts for most impact categories, implying that plastics utilisation in the process is the major source or sink of the emissions.

Global warming potential is significantly reduced by using both PP and PS in all scenarios (Fig. 4). The biggest savings are achieved for avoided incineration (S1) of waste PS and PP with −541 and −410 kg CO_2 eq., respectively. A comparison of scenarios S2 and S3 shows that diverting waste plastics from unsanitary landfills brings slightly bigger credits than sanitary ones. Once again, more considerable savings are achieved for waste PS. On the other hand, sawdust positively impacts this category due to the background processes related to forestry activities, and emissions are about 48 kg CO_2 eq. Treatment of plastic impurities from separation and grinding increases GWP, especially if treated by incineration. In general, dust from biomass grinding has a negligible impact on all categories.

Regarding human toxicity categories, the results are quite the opposite (Fig. 5), and the biggest differences are observed in S1. The main source of carcinogenic emissions from the incineration of plastics is chromium VI emissions into the water. Chromium VI, or hexavalent

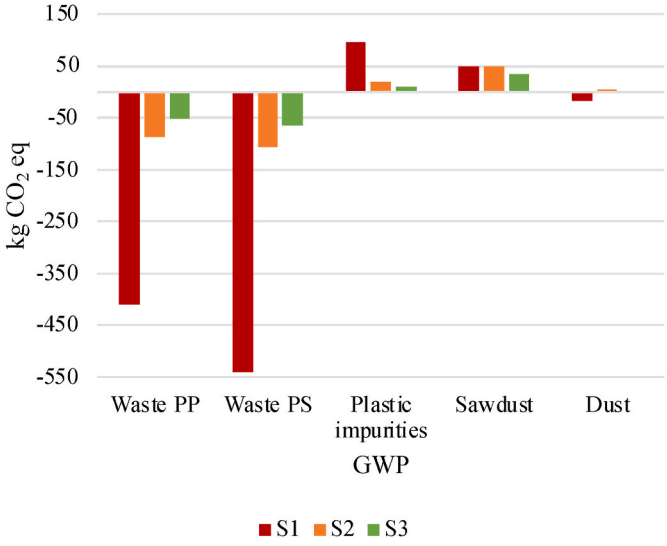

Fig. 4. Global warming potential of waste flows.

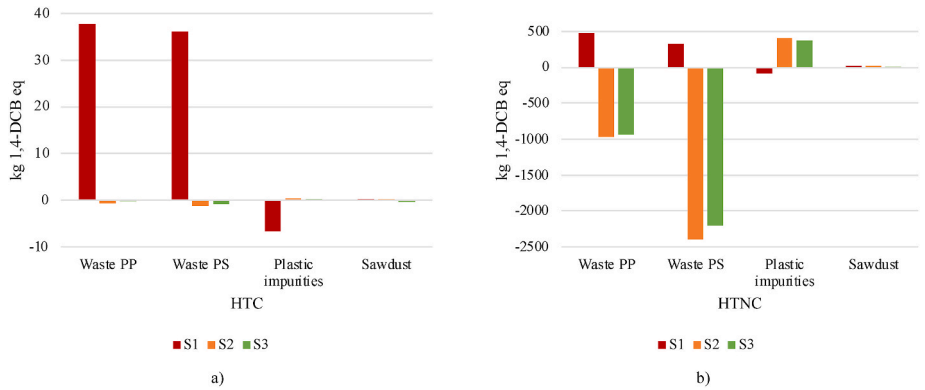

Fig. 5. Human carcinogenic toxicity (a) and non-carcinogenic toxicity (b).

chromium, is used as a pigment in the ink, dyes, paints and plastics. In Fig. 5a, waste PP has a slightly bigger impact than waste PS, even though values are very similar at 37.8 and 36.1 kg 1,4-DCB eq., respectively. Treatment of plastic impurities in S1 by incineration brings some credits (6.6 kg 1,4-DCB eq.). Landfilling, either sanitary or unsanitary, negatively impacts the carcinogenic toxicity impact category. In both S2 and S3 cases, diverting the plastic wastes from landfills brings negligible credits to the process of only 1 kg avoided 1,4-DCB eq. emissions. In this case, emissions are primarily associated with arsenic and chromium leaking into the groundwater.

Sawdust does not have a visible impact on human toxicity categories. The carcinogenic toxicity impact is 0.2 kg 1,4-DCB eq., while around 21 kg 1,4-DCB eq. is noted in the case of non-carcinogenic toxicity. Nevertheless, in Fig. 5b, it can be seen that the non-carcinogenic toxicity potential for waste plastics, associated with zinc and vanadium emission to the water, is enormous. This is especially evident in the case of waste PS, in which utilisation brings substantial credits for pyrolysis. The highest emissions savings are achieved in S2, where ~2400 kg 1,4-DCB eq. is saved, compared to 2200 kg 1,4-DCB eq. in S3. The utilisation of waste PP in pyrolysis instead of landfilling brings notable savings of 969

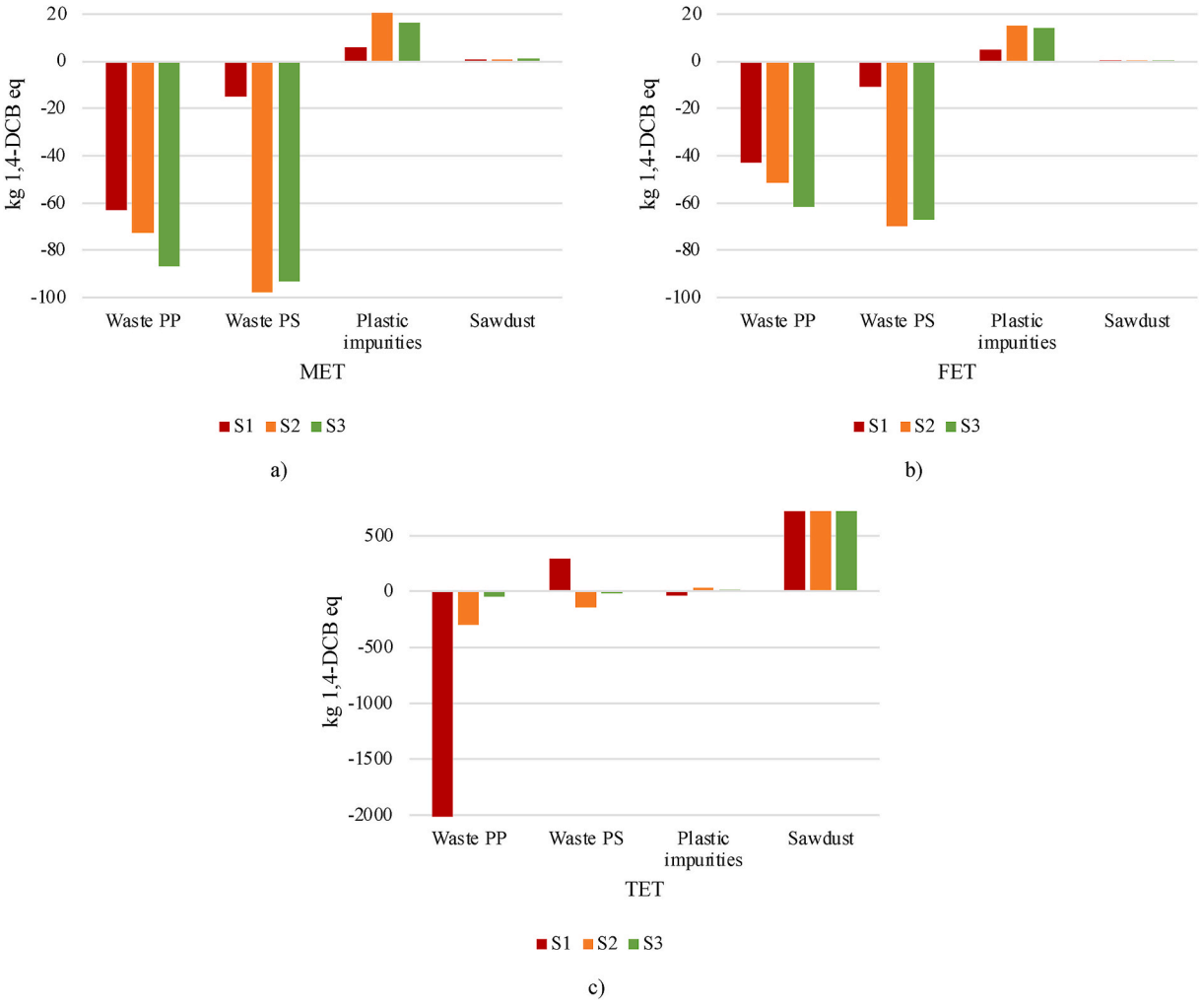

Fig. 6. Ecotoxicity impact categories marine (a), freshwater (b), terrestrial (c).

and 930 kg 1,4-DCB eq., for S2 and S3, respectively. Nevertheless, incineration might be better than pyrolysis regarding HTNC emissions (Fig. 5b). For the S1, emissions associated with using waste PS and PP are 479 and 328 kg 1,4-DCB eq., respectively. From plastic impurities treatment, it can be seen that incineration reduces non-carcinogenic toxicity slightly better than pyrolysis, while landfilling increases emissions drastically (~400 kg 1,4-DCB eq.).

Ecotoxicity categories presented in Fig. 6 are primarily associated with zinc emissions to the air. For the waste PP, vanadium is also emitted. Zinc is used as a heat stabilizer in plastic production, as a coating material in the metal industry, in rubber production and other applications. This is important because zinc emissions are found almost in all processes, from waste treatment and electricity production to feedstock transport.

The same trends and similar values are obtained for the marine (Fig. 6a) and freshwater (Fig. 6b) ecotoxicities. For MET, diverting waste PP from current treatment methods to pyrolysis saves between 63 and 87 kg 1,4-DCB eq. On the other hand, diverting waste PS from incineration brings only slight credits to the process (15 kg 1,4-DCB eq.), but diverting waste PS from landfills brings tremendous credits of almost 100 kg 1,4-DCB eq. for scenarios S2 and S3. Treatment of plastic impurities from separation and grinding burdens the process, especially if waste is landfilled (S2–S3).

Regarding the FET, waste PP saves between 43 and 62 kg 1,4-DCB eq., while waste PS brings an additional 10 and 70 kg 1,4-DCB eq. Similarly to MET, avoided landfilling brings bigger credits than avoided incineration. Sawdust has a negligible impact on these two ecotoxicity categories.

Terrestrial ecotoxicity shows different values and trends between the analysed scenarios and the other two ecotoxicity categories. In Fig. 6c, obtained values for waste PP greatly differ. In S1, more than 2000 kg 1,4-DCB eq. is saved if waste PP is pyrolysed rather than incinerated. Compared to unsanitary (S2) and sanitary (S3) landfilling, pyrolysis saves almost 300 and 40 kg 1,4-DCB eq., respectively. All these savings are achieved due to the prevented emissions of vanadium into the air. Simultaneously, the impacts of waste PS show even more interesting results. For the S1, waste PS does not reduce emissions but increases for almost 300 kg 1,4-DCB eq. If unsanitary landfilling is prevented, about 136 kg 1,4-DCB eq. are saved, while only 17 kg of emissions is prevented in the case of sanitary landfilling. Landfill emissions from waste PS are due to the release of mercury in the air, while vanadium and, to a lower extent, cadmium is responsible for PP emissions. When it comes to sawdust, tremendous emissions of 722 kg of 1,4-DCB eq. are observed (Fig. 6c). High contributions come from the slab and siding process, but the market for transport is the most significant generator of emissions. Biomass feedstock is generally transported several times between chopping and final processing, which requires continuous usage of transport services, resulting in zinc and antimony emissions from break-wearing to the air. This category is similar to the analysed scenarios since they use the same transport markets. This is the only environmental impact category where sawdust impacts exceed waste plastics.

The fossil resource scarcity impact category should be carefully observed. Pyrolysis seems to have a remarkable negative impact on this category in the case of the S1 scenario, with almost 240 kg oil eq. required (Fig. 7). This is since avoided incineration of waste PP and PS demands higher input of hard coal and lignite to compensate for heat and electricity production. For the S2 and S3 scenarios, energy recovery as a treatment method is not considered. Therefore, credits for waste streams are almost insignificant. From the rest of the impact categories, acidification potential is only significant in S1 due to increased coal consumption as a substitute for waste plastics. Emissions are 3.3 and 2.8 kg SO_2 eq., for PS and PP, respectively. Potential for particulate matter formation is only visible for S1, where around 3.3 kg of $PM_{2.5}$ eq. are observed if waste is diverted from incineration to pyrolysis.

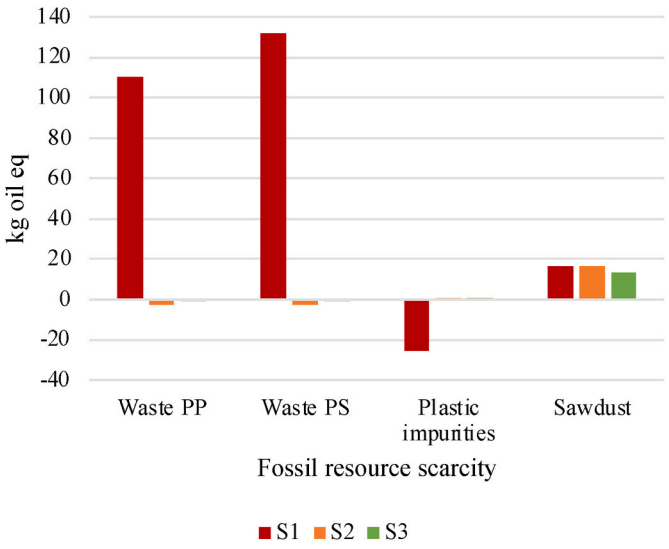

Fig. 7. Fossil resource scarcity.

3.5. Sensitivity analysis

Additional scenarios are built to carry out sensitivity analysis. Varying parameters were electricity mix and product yield. Results are presented in percent of changes to allow easier orientation and are summarised in Fig. 8. Results are presented only for the most significant impact categories.

3.5.1. Electricity mix

Two additional scenarios are made to investigate the electricity mix influence and the potential emission reductions by powering the process entirely with renewables. Scenarios S4 and S5 represent the variation of scenarios S1 and S3. All flows are kept the same, except the electricity, where the market group for electricity is wholly substituted by electricity production from a solar tower power plant of 20 MW. In the case of S4, the provider is selected for the rest of the world, while for S5 provider is dedicated to Australia. For scenario S4, analysed impact categories show emission reductions of up to 10% compared to S1. The limited impact is because, in S1, 76% of electricity already comes from renewable wind production. Marine and freshwater ecotoxicity express almost 100 and 200% reduction, respectively. On the other hand, GWP is reduced by only 10%, or an additional 60 kg CO_2 eq., and avoided emissions are now more than 600 kg CO_2 eq. It is worth mentioning that TET is reduced by almost 25% but still accounts for 1780 kg 1,4-DCB eq.

In the Australian case, the emission reduction is much more pronounced. In S5, solar energy needs to substitute almost 70% of fossil fuels, primarily natural gas and coal, compared to the electricity mix in S3. Since a high share of fossil fuels is substituted, emissions are more significantly reduced. The most considerable emission reductions are achieved in fossil resource scarcity (68%) and GWP (61%), even though the overall GWP of the process is still positive with ~155 kg CO_2 eq. Notable reductions are also seen in AP by 41% to only 0.8 kg SO_2 eq. and HTC, where the decrease is 25% from 40.3 to 30.3 kg 1,4-DCB eq. The rest of the impact categories have emission reductions of around 10%.

For both scenarios, the introduction of solar energy reduced the environmental impacts. In case when fossil fuels are substituted (S5), the reduction can be large. Solar energy can bring only small further savings if the electricity mix already consists of a high share of renewables, like wind in S4.

3.5.2. Product yield

Two additional scenarios, S6 and S7, are also created here, representing the variation of S1 and S3. In these cases, it was assumed that

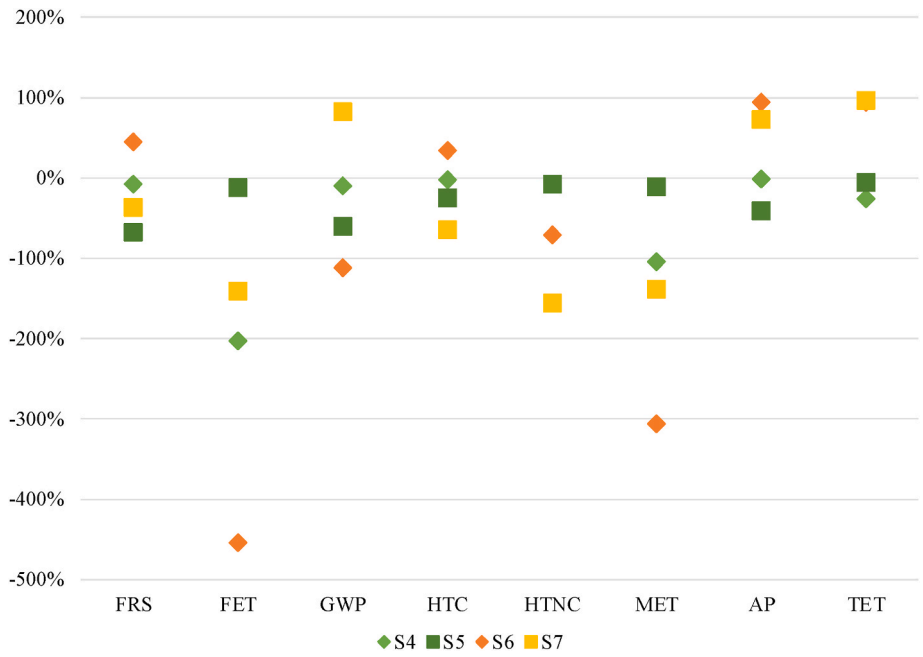

Fig. 8. Results of sensitivity analysis for considered scenarios.

pyrolysis oil yield was halved to only 403 kg, while new masses for char and gas fractions are 367 and 230 kg, respectively. The new mass of char and syngas fraction is calculated by the difference and maintaining the same ratio between them. Since the yield of products depends on process conditions and feedstock quality, it is assumed that due to some impurities or feedstock composition, the yield of products might vary, also affecting the environmental impacts. Fig. 8 shows that product variation has more influence on environmental impacts than the electricity mix. The low liquid yield would cause a 100% increase in GWP for S7, while a more than 100% reduction occurs for S6. The increment or reduction of GWP should be observed from the perspective of FU, which is 1 t of pyrolysis oil, and energy sources used to produce required electricity. When oil yield is lower than expected, this implies that more feedstock is initially required to meet production goals, which is 1 t of pyrolysis oil. For the S6, this leads to greater diversion of waste plastics from incineration, directly reducing released CO_2 emissions and GWP. On the other hand, in the case of S7, waste materials are diverted from landfills, and only slight credits are received for their utilisation in the process from the perspective of GWP. This suggests that low oil yield increases demand for initial feedstock, but since received credits are low, they are not sufficient to compensate for emissions released during the electricity production to power up the process. Besides, in the case of S6, the wind is the main energy source used for electricity production, while natural gas and coal dominate the electricity mix for S7. Energy from wind comes with very low CO_2 emissions, while combustion of natural gas and coal are among the greatest contributors to GWP. Significant reduction is noticed in the case of TET for both scenarios. This results from a substantial char fraction sent to market as a coal substitute, reducing the need for background mine operations. In general, high char yield is beneficial in reducing the demand for coal and associated emissions with coal mining. If credits were given to pyrolysis oil for substituting petroleum products in the first place, a change in yield would likely result in worsened environmental impacts.

3.6. Comparison with other studies

Comparison of the data with other studies is challenging for several reasons, such as different impact assessment methods, inventory data, system models and boundaries. Other studies often deal with either biomass or plastics pyrolysis, and obtained values are hardly comparable. Nevertheless, Table 3 summarises the results from relatable studies to the presented work. It should be emphasised that all studies have multiple scenarios considered, so the given values present a possible emissions range. Results are presented in kg CO_2 eq. per functional unit used in the study. In our research, to obtain 1 t of pyrolysis oil, around 0.75 t of waste PS and PP is pyrolysed. The GWP from this study is mostly lower compared to others. There are multiple reasons for this, as already mentioned. First of all, upgrading the pyrolysis oil is not considered in this study, therefore, these emissions are not taken into account. Even more, Vienescu et al. (2018) investigated biomass pyrolysis, which implies that there are no credits received for avoided incineration of plastic waste. On the other hand, Iribarren et al. (2012) assessed the substitution of conventional fuel with pyrolysis-produced fuel, meaning that significant credits are received for avoided petroleum extraction activities. Furthermore, besides the difference in FU between this study and (Demetrious and Crossin, 2019; Gear et al., 2018; Jeswani et al., 2021; Neha et al., 2022; Wang et al., 2015a), the type of feedstock also differs. This implies that product distribution differs as well, affecting the credits received for each product. For example, Demetrious and Crossin (2019) focused on syngas production, which has a very low heating value between 0.48 and 2.23 MJ/kg. Gear et al. (2018) indicated that the composition of mixed plastic waste varies, affecting the product yield and quality. For this reason, emissions can vary between low and high levels. Wang et al. (2015a) investigated pyrolysis of municipal solid waste, which gives very poor product quality, therefore, the received credits are pronouncedly lower.

Table 3
Comparison with other studies.

Study	GWP (kg CO_2 eq)	FU
This study	−547–408	1 t of pyrolysis oil
Vienescu et al. (2018)	2000–6000	1 t of upgraded fuel
Jeswani et al. (2021)	238–739	1 t of MPW
Iribarren et al. (2012)	−255 - (−178)	1 t of gasoline blend
Demetrious and Crossin (2019)	1870	1 t of MPW
Wang et al. (2015a)	1250	1 t of MSW
Neha et al. (2022)	389	1 t of food waste
Gear et al. (2018)	460–1570	1 t of MPW

4. Conclusion

The LCA carried out in this work shows for the first time the environmental impacts of the co-pyrolysis of biomass and plastic feedstocks. Since the emissions associated with each feedstock are significantly different, co-pyrolysis is shown that is beneficial not just from the perspective of product quality but also from an environmental point of view. The utilisation of plastics brings significant credits to the process, which would not exist if only biomass was pyrolysed. At the same time, the neutral environmental impact of biomass in some categories reduces the overall impact, which would be significant if only plastics were pyrolysed. The main findings of the work are the following:

- Co-pyrolysis is a better option than incineration in terms of GWP, freshwater and marine ecotoxicities. At the same time, it performs much worse in terms of human carcinogenic and non-carcinogenic toxicities, terrestrial ecotoxicity, fossil resource scarcity and acidification potential.
- Co-pyrolysis significantly outperforms landfilling in human non-carcinogenic toxicity and freshwater and marine ecotoxicities, while it has a slightly beneficial impact on eutrophication potential. Nevertheless, emissions associated with GWP are several times higher, as well as terrestrial ecotoxicity, fossil resource scarcity and human carcinogenic toxicity impact.
- Pyrolysis consumes the most electricity and accounts for 77% of emissions associated with GWP. Sawdust drying emits significant emissions associated with terrestrial ecotoxicity due to the systems requirements for syngas combustion.
- Plastic separation plays an important role in keeping product yield at a constant rate and similar quality, therefore, it should always be carried out as a pre-treatment process. Using waste PS brings more credit to the process than waste PP, especially if diverted from landfills. On the other hand, sawdust comes with burdens associated with its collection and is most pronounced for terrestrial ecotoxicity.
- Sensitivity analysis showed that solar energy for electricity production could greatly reduce environmental impacts if used as a substitute for fossil fuels. In contrast, a limited impact can be achieved if the electricity mix is already comprised of renewables. Furthermore, environmental impacts change greatly if the pyrolysis oil yield is halved compared to the expected one. This is especially visible for freshwater and marine ecotoxicity, where emissions reduction is tremendous due to the substitution of coal with char. Human non-carcinogenic toxicity emissions and eutrophication potential are also reduced in both cases. On the other hand, GWP is reduced if waste is diverted from incineration but increased if landfilling is avoided.
- Since the objective of the research was to produce pyrolysis oil, the main limitation of the study can be considered the lack of impact assessment from oil upgrading and final utilisation in internal combustion engines. Nevertheless, the environmental impacts from the oil upgrading come with significant uncertainties regarding the exhaust emissions. Assuming generic values and emissions can lead to unreliable results and wrong conclusions. Therefore, for the future work it is necessary to broaden system boundaries and encompass the emissions from upgrading and final consumption of derived pyrolysis oil based on measured data. This will give the full overview of the process's environmental impacts and suitability for large-scale deployment.

CRediT authorship contribution statement

Hrvoje Stančin: Writing – original draft, Conceptualization, Methodology, Investigation. **Vladimir Strezov:** Conceptualization, Resources, Supervision, Writing – review & editing. **Hrvoje Mikulčić:** Writing – review & editing, Supervision, Project administration.

Declaration of competing interest

The authors declare that they have no known competing financial interests or personal relationships that could have appeared to influence the work reported in this paper.

Data availability

Data has been used from literature. All references are given.

Abbreviations

AP	Acidification potential
FET	Freshwater ecotoxicity
FRS	Fossil resource scarcity
FU	Functional unit
GHG	Greenhouse gasses
GPW	Global warming potential
HTC	Human carcinogenic toxicity
HTNC	Human non-carcinogenic toxicity
LCA	Life cycle assessment
MET	Marine ecotoxicity
MPW	Mixed plastic waste
PP	Polypropylene
PS	Polystyrene
SD	Sawdust
TET	Terrestrial ecotoxicity

Appendix A. Supplementary data

Supplementary data to this article can be found online at https://doi.org/10.1016/j.jclepro.2023.137676.

References

Alcazar-Ruiz, A., Ortiz, M.L., Dorado, F., Sanchez-Silva, L., 2022. Gasification versus fast pyrolysis bio-oil production: a life cycle assessment. J. Clean. Prod. 336, 130373 https://doi.org/10.1016/J.JCLEPRO.2022.130373.

Antelava, A., Damilos, S., Hafeez, S., Manos, G., Al-Salem, S.M., Sharma, B.K., Kohli, K., Constantinou, A., 2019. Plastic solid waste (PSW) in the context of life cycle assessment (LCA) and sustainable management. Environ. Manag. 64 (2), 230–244. https://doi.org/10.1007/s00267-019-01178-3.

Ayer, N.W., Dias, G., 2018. Supplying renewable energy for Canadian cement production: life cycle assessment of bioenergy from forest harvest residues using mobile fast pyrolysis units. J. Clean. Prod. 175, 237–250. https://doi.org/10.1016/j.jclepro.2017.12.040.

Black, S., Harwood, K., Lees, S., Kuhanandan, K., Clements, J., Dickson, K., Mijer, P., le Miere, L., Guo, J., Kheng, D., Rathod, V., Lees, K., 2020. PLASTIC REVOLUTION to REALITY A Roadmap to Halve Australia's Single-Use Plastic Litter 2020. www.wwf.org.au.

Brassard, P., Godbout, S., Hamelin, L., 2021. Framework for consequential life cycle assessment of pyrolysis biorefineries: a case study for the conversion of primary forestry residues. Renew. Sustain. Energy Rev. 138 https://doi.org/10.1016/j.rser.2020.110549.

Brassard, P., Godbout, S., Raghavan, V., 2017. Pyrolysis in auger reactors for biochar and bio-oil production: a review. In: Biosystems Engineering, vol. 161. Academic Press, pp. 80–92. https://doi.org/10.1016/j.biosystemseng.2017.06.020.

Chen, Y., Cui, Z., Cui, X., Liu, W., Wang, X., Li, X.X., Li, S., 2019. Life cycle assessment of end-of-life treatments of waste plastics in China. Resour. Conserv. Recycl. 146, 348–357. https://doi.org/10.1016/j.resconrec.2019.03.011.

Ciroth, A., 2007. ICT for environment in life cycle applications openLCA - a new open source software for Life Cycle Assessment. Int. J. Life Cycle Assess. 12 (4), 209–210. https://doi.org/10.1065/LCA2007.06.337.

Del Giudice, A., Acampora, A., Santangelo, E., Pari, L., Bergonzoli, S., Guerriero, E., Petracchini, F., Torre, M., Paolini, V., Gallucci, F., 2019. Wood chip drying through the using of a mobile rotary dryer. Energies 12 (9). https://doi.org/10.3390/en12091590.

Demetrious, A., Crossin, E., 2019. Life cycle assessment of paper and plastic packaging waste in landfill, incineration, and gasification-pyrolysis. J. Mater. Cycles Waste Manag. 21 (4), 850–860. https://doi.org/10.1007/S10163-019-00842-4/TABLES/7 ecoinvent v3.8 - ecoinvent. (n.d.). https://ecoinvent.org/the-ecoinvent-database/data-releases/ecoinvent-3-8/. Retrieved January 2, 2023, from.

Ephraim, A., Pham Minh, D., Lebonnois, D., Peregrina, C., Sharrock, P., Nzihou, A., 2018. Co-pyrolysis of wood and plastics: influence of plastic type and content on product

yield, gas composition and quality. Fuel 231, 110–117. https://doi.org/10.1016/J.FUEL.2018.04.140.
Eriksson, O., Finnveden, O., 2009. Plastic Waste as a Fuel-CO 2-neutral or Not? https://doi.org/10.1039/b908135f.
Fan, J., Kalnes, T.N., Alward, M., Klinger, J., Sadehvandi, A., Shonnard, D.R., 2011. Life cycle assessment of electricity generation using fast pyrolysis bio-oil. Renew. Energy 36 (2), 632–641. https://doi.org/10.1016/j.renene.2010.06.045.
Gahane, D., Biswal, D., Mandavgane, S.A., 2022. Life cycle assessment of biomass pyrolysis. In Bioenergy Research 15 (3), 1387–1406. https://doi.org/10.1007/s12155-022-10390-9. Springer.
Gear, M., Sadhukhan, J., Thorpe, R., Clift, R., Seville, J., Keast, M., 2018. A life cycle assessment data analysis toolkit for the design of novel processes – a case study for a thermal cracking process for mixed plastic waste. J. Clean. Prod. 180, 735–747. https://doi.org/10.1016/J.JCLEPRO.2018.01.015.
Haque, N., Somerville, M., 2013. Techno-economic and environmental evaluation of biomass dryer. Procedia Eng. 56, 650–655. https://doi.org/10.1016/j.proeng.2013.03.173.
Home - ecoinvent (n.d.). Retrieved January 2, 2023, from. https://ecoinvent.org/.
Iribarren, D., Peters, J.F., Dufour, J., 2012. Life cycle assessment of transportation fuels from biomass pyrolysis. Fuel 97, 812–821. https://doi.org/10.1016/j.fuel.2012.02.053.
Jeswani, H., Krüger, C., Russ, M., Horlacher, M., Antony, F., Hann, S., Azapagic, A., 2021. Life Cycle Environmental Impacts of Chemical Recycling via Pyrolysis of Mixed Plastic Waste in Comparison with Mechanical Recycling and Energy Recovery, vol. 769. Science of the Total Environment. https://doi.org/10.1016/j.scitotenv.2020.144483.
Jones, S.B., Valkenburt, C., Walton, C.W., Elliott, D.C., Holladay, J.E., Stevens, D.J., Kinchin, C., Czernik, S., 2009. Production of Gasoline and Diesel from Biomass via Fast Pyrolysis, Hydrotreating and Hydrocracking: A Design Case. https://doi.org/10.2172/950728.
Lan, K., Ou, L., Park, S., Kelley, S.S., Yao, Y., 2020. Life cycle analysis of decentralized preprocessing systems for fast pyrolysis biorefineries with blended feedstocks in the southeastern United States. Energy Technol. 8 (11), 1900850 https://doi.org/10.1002/ENTE.201900850.
Lazarevic, D., Aoustin, E., Buclet, N., Brandt, N., 2010. Plastic waste management in the context of a European recycling society: comparing results and uncertainties in a life cycle perspective. Resour. Conserv. Recycl. 55 (2), 246–259. https://doi.org/10.1016/J.RESCONREC.2010.09.014.
Martín-Lara, M.A., Moreno, J.A., Garcia-Garcia, G., Arjandas, S., Calero, M., 2022. Life cycle assessment of mechanical recycling of post-consumer polyethylene flexible films based on a real case in Spain. J. Clean. Prod. 365, 132625 https://doi.org/10.1016/J.JCLEPRO.2022.132625.
Mixers specific power consumption (powder mixing) - common mixers power requirements (n.d.). Retrieved December 28, 2022, from. https://powderprocess.net/Mixing/Power_Consumption.html.
Neha, S., Prasanna Kumar Ramesh, K., Remya, N., 2022. Techno-economic analysis and life cycle assessment of microwave co-pyrolysis of food waste and low-density polyethylene. Sustain. Energy Technol. Assessments 52. https://doi.org/10.1016/j.seta.2022.102356.
Osman, A.I., Elgarahy, A.M., Mehta, N., Al-Muhtaseb, A.H., Al-Fatesh, A.S., Rooney, D. W., 2022. Facile synthesis and life cycle assessment of highly active magnetic sorbent composite derived from mixed plastic and biomass waste for water remediation. ACS Sustain. Chem. Eng. 10 (37), 12433–12447. https://doi.org/10.1021/ACSSUSCHEMENG.2C04095/ASSET/IMAGES/MEDIUM/SC2C04095_M015.GIF.
Osman, A.I., Mehta, N., Elgarahy, A.M., Al-Hinai, A., Al-Muhtaseb, A.H., Rooney, D.W., 2021. Conversion of biomass to biofuels and life cycle assessment: a review. Environ. Chem. Lett. 19 (6), 4075–4118. https://doi.org/10.1007/S10311-021-01273-0, 2021 19:6.
Papo, M., Corona, B., 2022. Life cycle sustainability assessment of non-beverage bottles made of recycled High Density Polyethylene. J. Clean. Prod. 378, 134442 https://doi.org/10.1016/J.JCLEPRO.2022.134442.
Pickin, J., Wardle, C., O'farrell, K., Nyunt, P., Donovan, S., Grant, B., 2020. Final National Waste Report 2020.
Plastics - the Facts, 2021. Plastics europe (n.d.). Retrieved January 8, 2023, from. https://plasticseurope.org/knowledge-hub/plastics-the-facts-2021/.
Puricelli, S., Costa, D., Rigamonti, L., Cardellini, G., Casadei, S., Koroma, M.S., Messagie, M., Grosso, M., 2022. Life Cycle Assessment of innovative fuel blends for passenger cars with a spark-ignition engine: a comparative approach. J. Clean. Prod. 378, 134535 https://doi.org/10.1016/J.JCLEPRO.2022.134535.
Roque, L.F.A., da Costa, R.B.R., de Souza, T.A.Z., Coronado, C.J.R., Pinto, G.M., Cintra, A.J.A., Raats, O.O., Oliveira, B.M., Frez, G.V., Alves, L.F.R., 2023. Experimental analysis and life cycle assessment of green diesel (HVO) in dual-fuel operation with bioethanol. J. Clean. Prod. 389, 135989 https://doi.org/10.1016/J.JCLEPRO.2023.135989.
Russ, M., Gonzalez, M., Horlacher, M., Shonfield, P., Deimling, S., 2020. Evaluation of Pyrolysis with LCA-3 Case Studies.
Salvi, B.L., Soni, T., Jindal, S., Panwar, N.L., 2021. Design improvement and experimental study on shell and tube condenser for bio-oil recovery from fast pyrolysis of wheat straw biomass. SN Appl. Sci. 3 (2) https://doi.org/10.1007/s42452-021-04165-8.
Schandl, H., King, S., Walton, A., Kaksonen, A.H., Tapsuwan, S., Baynes, T.M., 2020. Circular Economy Roadmap for Plastics, Glass, Paper and Tyres. CSIRO, Australia.
Stančin, H., Mikulčić, H., Wang, X., Duić, N., 2020. A review on alternative fuels in future energy system. Renew. Sustain. Energy Rev. 128 https://doi.org/10.1016/j.rser.2020.109927.
Stančin, H., Šafář, M., Růžičková, J., Mikulčić, H., Raclavská, H., Wang, X., Duić, N., 2021. Co-pyrolysis and synergistic effect analysis of biomass sawdust and polystyrene mixtures for production of high-quality bio-oils. Process Saf. Environ. Protect. 145, 1–11. https://doi.org/10.1016/j.psep.2020.07.023.
Stančin, H., Šafář, M., Růžičková, J., Mikulčić, H., Raclavská, H., Wang, X., Duić, N., 2022. Influence of plastic content on synergistic effect and bio-oil quality from the co-pyrolysis of waste rigid polyurethane foam and sawdust mixture. Renew. Energy 196, 1218–1228. https://doi.org/10.1016/J.RENENE.2022.07.047.
Stegmann, P., Gerritse, T., Shen, L., Londo, M., Puente, Á., Junginger, M., 2023. The global warming potential and the material utility of PET and bio-based PEF bottles over multiple recycling trips. J. Clean. Prod. 395 https://doi.org/10.1016/J.JCLEPRO.2023.136426.
Strezov, V., Evans, T.J., Hayman, C., 2008. Thermal conversion of elephant grass (Pennisetum purpureum Schum) to bio-gas, bio-oil and charcoal. Bioresour. Technol. 99 (17), 8394–8399. https://doi.org/10.1016/J.BIORTECH.2008.02.039.
Uebe, J., Kryzevicius, Z., Majauskiene, R., Dulevicius, M., Kosychova, L., Zukauskaite, A., 2022. Use of polypropylene pyrolysis oil in alternative fuel production. Waste Manag. Res. 40 (8), 1220–1230. https://doi.org/10.1177/0734242X211068243.
Vienescu, D.N., Wang, J., Le Gresley, A., Nixon, J.D., 2018. A life cycle assessment of options for producing synthetic fuel via pyrolysis. Bioresour. Technol. 249, 626–634. https://doi.org/10.1016/j.biortech.2017.10.069.
Wang, H., Wang, L., Shahbazi, A., 2015a. Life cycle assessment of fast pyrolysis of municipal solid waste in North Carolina of USA. J. Clean. Prod. 87 (1), 130–138. https://doi.org/10.1016/j.jclepro.2014.09.011.
Wang, H., Wang, L., Shahbazi, A., 2015b. Life cycle assessment of five vegetable oils. J. Clean. Prod. 87 (1), 511–519. https://doi.org/10.1016/j.jclepro.2014.09.011.
Zhang, J., Hirschberg, V., Rodrigue, D., 2023. Blending recycled high-density polyethylene HDPE (rHDPE) with virgin (vHDPE) as an effective approach to improve the mechanical properties. Recycling 8 (1). https://doi.org/10.3390/RECYCLING8010002.
Zhang, Y., Hu, G., Meyer, T., Kong, S.-C., Jarboe, L., Raman, R., 2014. Development of Integrated Assessment Platform for Biofuels Production via Fast Pyrolysis and Upgrading Pathway.
Zheng, X., Zhong, Z., Zhang, B., Du, H., Wang, W., Li, Q., 2022. Environmental impact comparison of wheat straw fast pyrolysis systems with different hydrogen production processes based on life cycle assessment. Waste Manag. Res. 40 (6), 654–664. https://doi.org/10.1177/0734242X211045004.